Sarcoma

Osteosarcoma: Lessons Learned and Future Avenues

Guest Editors: Ajay Puri, Norman Jaffe, Peter Choong, and Hans Gelderblom

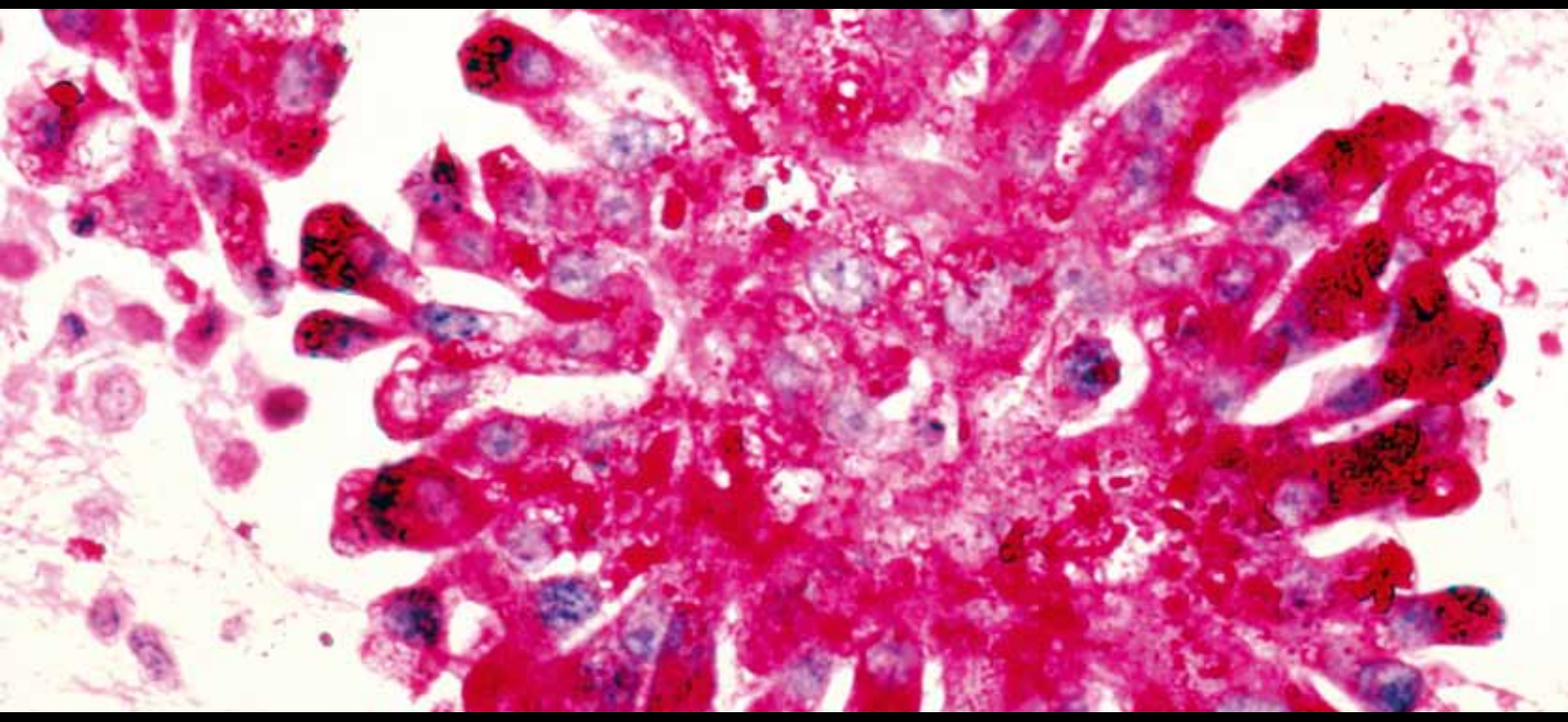

Osteosarcoma: Lessons Learned and Future Avenues

Sarcoma

Osteosarcoma: Lessons Learned and Future Avenues

Guest Editors: Ajay Puri, Norman Jaffe, Peter Choong, and Hans Gelderblom

Editorial Board

Contents

Hindawi Publishing Corporation
Sarcoma
Volume 2013, Article ID 641687, 2 pages
http://dx.doi.org/10.1155/2013/641687

Editorial

Osteosarcoma: Lessons Learned and Future Avenues

Ajay Puri,[1] Norman Jaffe,[2] and Hans Gelderblom[3]

[1] *Department of Surgical Oncology, Tata Memorial Hospital, Mumbai 400012, India*
[2] *Children's Cancer Hospital, University of Texas MD Anderson Cancer Center, Houston, TX 77030, USA*
[3] *Department of Clinical Oncology, Leiden University Medical Center, Albinusdreef 2, 2300 RC Leiden, The Netherlands*

Correspondence should be addressed to Hans Gelderblom; a.j.gelderblom@lumc.nl

Received 28 July 2013; Accepted 28 July 2013

Osteosarcoma is the most common malignant bone tumor in men. The incidence peaks around puberty, with a broader and lower peak after 60 years of age. Risk factors are (pubertal) growth, genetic factors, Paget's disease, and prior radiotherapy. More than 90% of tumors are of high grade, and their prognosis, even without metastasis at presentation, remains dismal in up to 30–45% of cases despite great improvements due to the introduction of chemotherapy some decades ago.

The contribution "*Osteosarcoma: evolution of treatment paradigms*" to this osteosarcoma special issue is truly unique as it describes the history of systemic treatment from first hand, as the first author N. Jaffe coauthored the first studies on the dramatic improvement of long-term survival from 10–15% to 55–70% due to addition of multiagent chemotherapy. This magnitude of improvement has never been observed in other solid tumors, with the exception of germ cell tumors and some childhood cancers such as rhabdomyosarcoma and Ewing's sarcoma. However, these percentages have not further improved over the last decades, and new therapies are needed urgently to cure the remaining one-third of patients and increase the chances for patients with metastatic disease. The authors describe the design of the current EURAMOS study. Meanwhile, the first results of the PEG interferon randomization in the good responder arm were presented at the 2013 annual meeting of the American Society of Clinical Oncology [1]. From the 2260 included patients, 1034 had a good pathological response to preoperative chemotherapy. Of these patients 715, were randomized to either PEG interferon or observation. Only 76% of the patients randomized to interferon started treatment, mainly due to refusal. The event-free survival (primary endpoint) was not statistically improved in the interferon arm, although the results may have been influenced by the low randomization and high treatment refusal rate. Definite results and results of the poor responder randomization are pending. The study has proven that a worldwide platform for potential practice changing rapidly accruing randomized phase III studies is feasible in this rare disease and therefore should be used in the future.

The Birmingham experience with low-grade conventional osteosarcoma (LGCO), a rare (1.2%) and difficult to diagnose variant of osteosarcoma, is also part of this special issue. The diagnosis of LGCO is challenging due to the relatively nonspecific radiological and histological findings. Since treatment of LGCO is so different compared to a benign lesion as well as to high-grade osteosarcoma, accurate diagnosis is essential. The authors therefore advise that any difficult or nondiagnostic biopsies of solitary bone lesions should be referred to a specialist (bone) tumor unit for a second opinion: a conclusion that we fully agree with and should be part of all guidelines.

N. Federman et al. describe a novel osteosarcoma-associated cell surface antigen, ALCAM. The authors created an anti-ALCAM-hybrid polymerized liposomal nanoparticle immunoconjugate (α-AL-HPLN) to specifically target osteosarcoma cells and deliver a cytotoxic agent such as doxorubicin. If feasible in clinical practice, these α-AL-HPLNs are a promising new strategy to specifically deliver cytotoxic agents in osteosarcoma. A similar approach recently took place in breast cancer where the antibody-drug conjugate trastuzumab-DM1 (T-DM1) was designed to combine the biological activity of trastuzumab with the targeted delivery of a highly potent chemotherapeutic agent to

HER2-overexpressing breast cancer cells. The success of the approach in breast cancer underlines the promise of α-AL-HPLN in osteosarcoma.

Y. Suehara et al. focus on proteomics to provide protein expression profiles of osteosarcoma that can be used to develop novel diagnostic and therapeutic biomarkers as well as to understand its biology. The authors provide a brief description of the methodology as well as examples of the recent proteomic studies that have generated new information regarding osteosarcomas. This approach should lead the way to predictive and prognostic information as well as necessary new drug targets in order to bring the necessary further improvement of our therapeutic strategies in osteosarcoma.

M. M. Hagleitner et al. show us a single center experience with osteosarcoma patients under the age of 20. In this retrospective series, improvement in toxicity and outcome was observed over the past 30 years that was attributed to improved supportive care allowing the intended full-dose chemotherapy regimen to be given. It is very well possible that improved experience due to centralization may also have added to this effect.

S. Piperdi et al. present a preclinical evaluation of the role of β-catenin in osteosarcoma development thought to originate from the mesenchymal stem cell. Despite fostering osteogenic differentiation, β-catenin does not induce the malignant features and tumorigenicity conveyed by oncogenic H-RAS when introduced into partly transformed mesenchymal stem cells. Despite this observation, C. H. Lin et al. show, using *in vivo* and *in vitro* studies, that Dickkopf-3 protein (Dkk-3) transfected 143B cells inhibited tumorigenesis and metastasis in an orthotopic xenograft model of OS. As Dkk-3 is known to inhibit the canonical Wnt/β-catenin pathway and its expression has been shown to be downregulated in osteosarcoma cell lines, we must realize that a delicate interplay of this pathway is present in osteosarcoma and requires further understanding before it can be targeted in the clinic.

In the paper by R. Muff et al., forty-eight common genes that are differentially expressed in metastatic cell lines compared to parental cells were identified. This subset of metastasis relevant genes in osteoblastic osteosarcoma overlapped only minimally with differentially expressed genes in the other four preosteoblast or nonosteoblastic cell line systems. These studies add to the microarray studies that were performed in the clinical research setting [2].

X. Mu et al. present a preclinical rationale for m-TOR inhibition for the treatment and prevention of osteosarcoma metastases. A phase II study including osteosarcoma patients was promising [3]. However, the Sarcoma mUltiCenter Clinical Evaluation of the Efficacy of riDaforolimus (SUCCEED) trial did not lead to registration of maintenance mTOR-targeted therapy in metastatic (osteo)sarcoma as the FDA rejected the application in May 2012 [4]. Maybe earlier treatment in nonmetastatic patients or combination treatment or patient selection based on prospectively collected biomarkers may lead the way to future clinical use.

In our opinion, the holy grail towards further survival benefit in osteosarcoma is thorough preclinical studies leading to new targets and biomarkers, followed by properly designed studies that can be performed rapidly in international collaboration of bone centers. This osteosarcoma issue of Sarcoma is just a tiny step in this process that will need perseverance.

Ajay Puri
Norman Jaffe
Hans Gelderblom

References

[1] S. S. Bielack, S. Smeland, J. Whelan et al., "MAP plus maintenance pegylated interferon α-2b (MAPIfn) versus MAP alone in patients with resectable high-grade osteosarcoma and good histologic response to preoperative MAP: First results of the EURAMOS-1 "good response" randomization," *Journal of Clinical Oncology*, vol. 31, Article ID LBA10504, 2013.

[2] A.-M. Cleton-Jansen, J. K. Anninga, I. H. Briaire-De Bruijn et al., "Profiling of high-grade central osteosarcoma and its putative progenitor cells identifies tumourigenic pathways," *British Journal of Cancer*, vol. 101, no. 11, pp. 1909–1918, 2009.

[3] S. P. Chawla, A. P. Staddon, L. H. Baker et al., "Phase II study of the mammalian target of rapamycin inhibitor ridaforolimus in patients with advanced bone and soft tissue sarcomas," *Journal of Clinical Oncology*, vol. 30, no. 1, pp. 78–84, 2012.

[4] G. D. Demetri, S. P. Chawla, I. Ray-Coquard et al., "Results of an international randomized phase III trial of the mammalian target of rapamycin inhibitor ridaforolimus to control metastatic sarcoma in patients after benefit from prior chemotherapy," *Journal of Clinical Oncology*, vol. 31, no. 19, pp. 2485–2492, 2013.

Hindawi Publishing Corporation
Sarcoma
Volume 2013, Article ID 203531, 7 pages
http://dx.doi.org/10.1155/2013/203531

Review Article

Osteosarcoma: Evolution of Treatment Paradigms

Norman Jaffe,[1] Ajay Puri,[2] and Hans Gelderblom[3]

[1] *Children's Cancer Hospital, University of Texas M.D Anderson Cancer Center, Houston, TX 77030, USA*
[2] *Department of Surgical Oncology, Tata Memorial Hospital, Mumbai, India*
[3] *Department of Clinical Oncology, Leiden University Medical Center, Albinusdreef 2, 2300RC Leiden, The Netherlands*

Correspondence should be addressed to Norman Jaffe; njaffe@mdanderson.org

Received 31 January 2013; Accepted 20 April 2013

Academic Editor: Peter Choong

This paper reviews the contribution of chemotherapy in the conquest of osteosarcoma. It discusses how the treatment of osteosarcoma has evolved over the last five decades, resulting in a more than fivefold increase in survival. Though the initial improvements in survival were dramatic, essentially there has been no change in the outlook for this disease over the past 30 years. The paper also highlights the necessity of a multidisciplinary approach to combat this disease and stresses the need to explore newer treatment agents in order to build on the lessons learnt from the past while striving to achieve greater levels of success.

1. Introduction

Bone cancers are rare in humans. In 2009, it is estimated that 2570 new cases of bone sarcomas were diagnosed in the United States [1]. Osteosarcoma is the most common. The term "osteosarcoma" as opposed to "osteogenic sarcoma" is preferred by the World Health Organization (WHO). The eponym was introduced by Boyer in 1805 [2]. In 1879, Gross published a paper entitled "Sarcoma of the Long Bone Based upon a Study of One Hundred and Sixty-five Cases" [3]. Most, if not all the tumors, were probably osteosarcoma. He advocated treatment by early amputation. The outcome was dismal; nonetheless it was accepted as the "standard" of treatment.

In the course of the ensuing one and a half century, osteosarcoma became established as a distinct pathological and radiological entity with no change in the "standard" of therapy. The survival rate was less than 10%; in rare publications, it occasionally rose to 20%. The dismal survival was due to the biological behavior of the malignancy: pulmonary micrometastases were present in at least 80% of patients at diagnosis. These metastases were not visible on conventional imaging studies. However, they surfaced 8–12 months after amputation and were responsible for the patient's demise within 12 to 24 months of their appearance. Osteosarcoma therefore had to be considered a systemic disease with systemic therapy required for cure. Until the mid-20th century, no such therapy was available.

2. Radiation Therapy

In view of the poor prognosis with primary surgical ablation, Sir Stanford Cade a British Surgeon Radiotherapist in 1931 advocated radiation therapy to treat the primary tumor [4]. Following completion of therapy (6000 rad over six weeks) the patient was observed for the possible emergence of pulmonary metastases for 6–9 months; if metastases failed to appear, an elective amputation was performed. The intent was to avoid "futile mutilation" in a patient destined to die. It was also postulated that, in some patients, effective radiation with optimum local control might also avert amputation. A similar approach was employed by Ferguson at the Sloan Kettering Memorial Cancer Center in New York [5]. The strategy failed to meet its objectives. Tumor dissemination from a nonamputated limb remained a constant threat and failure of local control produced severe pain and protracted morbidity eventually requiring amputation for palliation in most patients. Cade in summarizing the prevailing treatment at a meeting for osteosarcoma concluded "Gentlemen if you operate they die, if you do not operate they die just the same; this meeting should be concluded with prayers."

Radiation therapy was also administered to the lungs by the Mayo Clinic [6]. There was little effect on the long-term survival.

3. Immunotherapy

A glimmer of hope emerged from preliminary studies in immunotherapy advocated by Marcove et al. [7] and Neff and Enneking [8] as therapy for destruction of the systemic micrometastases; however long-term results were disappointing. Fudenberg presented the preliminary results with Transfer Factor but it did not gain wide acceptance [9]. Strander et al. published the initial results with interferon [10]. This biological agent was also utilized by Swedish investigators and appeared to hold some promise. It is currently a component of the EURAMOS investigative study (vide infra).

4. Chemotherapy

The discovery of chemotherapeutic agents which were active in osteosarcoma was a milestone in attempts to find a cure. This occurred in the 1960s after a few disappointing experiences. Nitrogen mustard had been administered concurrently with radiation therapy for treatment of the primary tumor (Dana Farber Institute, formerly the Children's Cancer Foundation, (NJ unpublished data)); it failed to prevent the emergence of overt pulmonary metastases. Similarly, regimens utilizing combinations of Nitrogen Mustard, Mitomycin C and Vincristine yielded minimal responses and were abandoned [11] However, an early report by Pinkel indicated possible activity with oral cyclophosphamide [12].

4.1. Compadri Regimens. "Conpadri" is an acronym for the combination of cyclophosphamide, Oncovin, vincristine (Oncovin), doxorubicin (Adriamycin), and L-phenylalanine mustard. With the addition of methotrexate the acronym changed to "Compadri." It was developed by Sutow in the early 1960s [13]. L-phenylalanine mustard was shown to have mild antitumor effects. Temporary regressions in 10%–43% of patients were reported [14]. It was therefore administered as adjuvant therapy to nonmetastatic patients after surgical ablation of the primary tumor. A disease-free survival of 14% was attained [15]. In 1969, the combination of vincristine, actinomycin D (Dactinomycin), and cyclophosphamide (VAC) was investigated as adjuvant therapy for rhabdomyosarcoma and also found to be effective in osteosarcoma [16]. It was administered in an intensive "pulse" schedule based upon the understanding that cyclophosphamide was more effective when utilized in this manner. Twelve osteosarcoma patients were treated yielding a 33% disease-free survival. This laid the cornerstone for the construction of the "Conpadri/Compadri" regimens. With the demonstration that doxorubicin was highly effective in osteosarcoma (see below), Sutow substituted doxorubicin for actinomycin D [13].

The Compadri regimens constituted the first rational attempt to employ combination chemotherapy for patients as adjuvant postoperative chemotherapy. They comprised agents with different mechanisms of action and minimal overlapping toxicity. Compadri I–III yielded a 41% 18 + month disease-free survival [17].

4.2. High Dose Methorexate. High dose methotrexate was a major weapon in the armamentarium of treatment for osteosarcoma. It demonstrated that the disease was indeed responsive to chemotherapy; it also ignited tremendous controversy. No other agent was subjected to similar criticism. It was the only drug among the effective agents which was subjected to a comparative trial of efficacy with another agent (cisplatin) [18].

Methotrexate was discovered by Farber et al. in the 1940s and was a pivotal agent for the cure of childhood leukemia and lymphoma [19]. It acts by depriving the cell of folates which is essential for the formation of DNA. The antidote is leucovorin which can reverse its activity and abort and treat toxicity. Except for osteosarcoma, there are no reports of its efficacy in childhood solid tumors.

A novel strategy to increase the efficacy of methotrexate in leukemia was devised by Abraham Goldin. He administered large (toxic) doses of the drug to leukemia bearing mice and after a defined period "rescued" them with leucovorin [20]. Toxicity was aborted and cure was achieved. The regimen was investigated by Djerassi et al. in childhood lymphoma and leukemia and found to be safe and effective [21].

Farber held a weekly tumor board conference at the Dana Farber Cancer Institute. Djerassi was invited to present his data on methotrexate/leucovorin at one of the meetings; the presentation was novel and intriguing and well received. In view of the absence of any known effective chemotherapeutic agent in osteosarcoma, NJ requested permission from Farber to investigate the regimen in this disease. During this period (the 1960s), therapeutic research was in its infancy and Institutional Review Boards and Surveillance Committees had not been formally mandated or established. Permission to conduct investigations was generally obtained from senior investigators, consultants, or directors or was decided by consensus among attending physicians. Permission was granted by Farber for the regimen to be administered to a patient who had developed pulmonary metastases six months after a hemipelvectomy. The potential side effects were outlined and consent for treatment from the parent was obtained. Complete disappearance of the metastases was achieved! The result was published [22].

The scientific community was kept abreast of the efficacy and potential toxicity of high dose methotrexate through follow-up investigations: toxicity was low and acceptable although an occasional death was reported from renal failure, hepatic failure, or superimposed infection from myelosuppression [23, 24]. The incidence of toxicity was subsequently reduced by assays that measured serum methotrexate levels (permitting construction of a methotrexate decay curve) and improved expertise, familiarity with the drug regimen, accumulating knowledge in its administration, and methods to treat and abort toxicity [25].

Methotrexate with leucovorin was also found to be nonmyelosuppressive and could be combined safely with other agents. When administered preoperatively, generally in

preparation for limb salvage, and postoperatively as adjuvant therapy, survival was escalated to 60%–75% [26]. In addition with multimodal intervention comprising the possible administration of alternate agents and surgical resection to remove local recurrence and persistent or recurrent metastases, survival was escalated by an additional 10%–15% [27]. The discovery of effective chemotherapy was instrumental in implementing aggressive surgical sustained attacks (principally thoracotomies) to ablate recurrent and persistent tumor.

A major point of contention to the introduction and use of methotrexate was the report that the improved survival alleged to have occurred with methotrexate had been derived by comparison with survival in historical controls as opposed to concurrent controls [28–30]. The argument was bolstered by a concurrent control trial by the Mayo Clinic comparing methotrexate and leucovorin and amputation versus amputation only. There was apparently no improvement from the administration of methotrexate [31]. The above criticism was addressed by demonstrating that there had been no change in survival in several publications over the past half century, principally in reports published in the 1960s and 1970s [32, 33]. Eventually a two-arm randomized trial, MIOS, was launched utilizing concurrent controls: surgical ablation and chemotherapy were employed in one arm and surgical ablation only in the other "control" arm. Chemotherapy comprised methotrexate in combination with other agents [34]. Surgical ablation and combination chemotherapy therapy yielded a 65% survival whereas survival in the control arm (surgery only) was superimposable on historical controls, 5%! The result was repeated in a second similar, almost parallel running, trial conducted by Eilber et al. [35]. The outcome of the MIOS investigation and the contentious nature of the prevailing atmosphere were addressed by NJ in a letter to the New England Journal of Medicine [36] and the Eilber study in an editorial by Holland in the Journal of Clinical Oncology [37]. Numerous publications followed attesting to the efficacy of chemotherapy in osteosarcoma.

Forty years after the appearance of the first report of treatment with high dose methotrexate with leucovorum rescue in osteosarcoma an editorial in the Journal of Clinical Oncology reiterated the efficacy of the agent [38]. Among the references cited was a publication that *"non-methotrexate based therapy was a major poor prognostic factor"* for survival (NJ author emphasis) [39]. Of note also was a separate publication that three patients were cured without surgical resection of the primary tumor. They were treated with chemotherapy comprising high dose methotrexate, doxorubicin, and cisplatin. One patient achieved an initial response exclusively with methotrexate [40].

4.3. Doxorubicin. Doxorubicin was shown to be active in osteosarcoma in the 1960s [41, 42]. It constitutes the major component of the Compadri and other regimens utilized in osteosarcoma [17, 43, 44]. It acts by intercalating into DNA and inducing topoisomerase II-mediated single- and double-strand breaks. When administered alone or in combination with decarbazine and other agents it produced responses in 30%–40% of patients with a variety of cancers including patients with pulmonary metastases. It also potentiates the action of radiation therapy. Extravasation of the drug may cause ulceration. However its major toxic effect is cardiac failure; the total cumulative dose is generally limited to 300 mg/m^2 in children under 6 years and 450 mg/m^2 in adults. It is employed as combination therapy in pre- and postoperative regimens.

4.4. Cisplatin. Cisplatin was first used in the treatment of osteosarcoma in the 1970s. It exerts its cytotoxic effect by platination of DNA. It has been administered by the intravenous and intra-arterial routes. Intravenously it produced a 30%–60% response in patients with metastatic disease. The response rate via the intra-arterial route is 60%–90% [45–48]. The intra-arterial route was introduced in an attempt to enhance the efficacy of therapy when it was surmised that alternate modes of therapy would possibly be helpful in advancing treatment of the disease. This route achieves higher local cytotoxic and concurrently effective systemic concentrations [48]. The angiogram utilized for intra-arterial administration was useful for assessing response by its effect on tumor neovascularity and stain. Unfortunately the intra-arterial route is labor intensive and generally requires conscious sedation or general anesthesia. Its use is therefore generally limited to selective circumstances. It was considered extremely useful in treating pathological fractures and in assessing a *rapid* response and the efficacy of treatment. Similar responses were achieved with intravenous cisplatin in combination with other agents and hence this approach has generally replaced the administration of intra-arterial cisplatin.

4.5. Oxazaphosphorines. Cyclophosphamide and ifosfamide were the two major alkylating agents used in the treatment of osteosarcoma. They require hepatic microsomes for activation. They were often used in combination with etoposide. The discovery of MESNA to prevent hemorrhagic cystitis permitted their administration in high doses. Response rates of 10%–40% have been reported [49–51]. The response rates can often be escalated by increasing the dose. The agents are not cross-resistant and therefore not mutually exclusive; responses may be achieved with the alternate agent if relapse has occurred with one agent. The drugs are used in preoperative and postoperative regimens, generally in combination with other agents.

5. Chemotherapy and Biological Agents

In an effort to identify new agents, a biological compound muramyl tripeptide phosphatidyl ethanolamine encapsulated in liposome (L-MTP-PE) was investigated. It was combined with chemotherapy in a 2×2 randomized factorial trial by the Children's Oncology Group [52]. It was administered after surgical resection of the primary tumor treated initially with neoadjuvant chemotherapy: cisplatin, doxorubicin, and high dose methotrexate. One-half of the patients were also randomly assigned to receive ifosfamide. In a second randomization they were assigned to receive L-MTP-PE

after definitive surgical resection of the primary tumor. The addition of ifosfamide did not improve the outcome. The addition of the biological compound improved event free survival but did not meet the conventional test for statistical significance ($P = 0.08$) nor for a significant improvement in overall survival (78% versus 70%; $P = 0.3$). The role of L-MTP-PE in the United States remains under discussion; it is available by request on a compassionate Investigational New Drug (IND) application It has been accepted for use in Europe, but in the European ESMO guidelines no consensus could be reached on its use and more prospective research was advised before it could be generally accepted by the experts. L-MTP-PE was further addressed in subsequent communications [53]. Additional acceptance in other centers followed without alteration of its status in the United States.

6. Neoadjuvant Therapy

Preoperative agents administered to treat the primary tumor to determine their potential use as postoperative treatment are designated "neoadjuvant therapy" a term introduced by Emil Frei III in discussing a presentation by Gerry Rosen at an American Society of Clinical Oncology (ASCO) meeting in the 1980s. Initially, the concept and rationale for administration of neoadjuvant chemotherapy were met with some resistance. However it appeared that the strategy could confer several local and systemic advantages: it could serve as an *in vivo/in vitro* trial for the selection of the postoperative agents as adjuvant therapy if a good response was obtained with the preoperative treatment; alternatively if ineffective, alternative agents would be introduced. Necrosis > 90% attained with preoperative chemotherapy is considered a good prognostic factor, whereas necrosis < 90% would be an indication for a possible change in the regimen.

Most studies currently advocate the deployment of neoadjuvant therapy. However several preliminary reports suggest that the results in long follow-up are similar in either circumstance. To address the controversy an international cooperative study, EURAMOS, has been formed to test the neoadjuvant hypothesis and other aspects of osteosarcoma [54]. The aim is to determine with greater confidence the potential for adding additional chemotherapeutic agents in order to improve outcome in patients whose tumors demonstrate a poor histological response to preoperative chemotherapy. In addition to that, the added value of interferon in good responders is being investigated. It is possible that the study may provide insight into biological and other variants which may impact response. This could provide information for construction of protocols for personalized treatment with chemotherapy. This is considered to be the new paradigm for treatment of the future.

Preoperative chemotherapy in EURAMOS comprises methotrexate, adriamycin, and cisplatin (MAP). Two different questions have then been posed for patients with either good or poor histological response: Favorable histological response (<10% viable tumor): patients receive the same agents administered preoperatively. They are also randomly assigned to receive additional therapy with pegylated interferon alpha-2b. Unfavorable histological response (10%–100%) viable tumor: patients randomly assigned to receive the same preoperative chemotherapy postoperatively plus or minus ifosfamide/etoposide.

7. Management of the Primary Tumor

Optimum treatment for osteosarcoma demands a multidisciplinary strategy. While the effective and judicious application of chemotherapy has substantially changed the prognosis, it must be accompanied by appropriate local control to achieve cure. Surgical ablation of the diseased bone with oncologically safe margins is the best means of local control. For decades amputation and ablative surgery were widely practiced in an attempt to remove the tumor with safe margins and the least chance of local relapse. The advent of better imaging modalities, more effective chemotherapy, a better understanding of anatomy with continuous refinement in surgical techniques, and advances in prosthesis design and materials have all played a part in increasing the incidence of limb preserving surgery in osteosarcoma [55, 56]. From an era where amputation was the only option to the current day function preserving resections and complex reconstructions has been a major advance.

While the number of limb salvage surgeries undertaken for malignant bone tumors of the extremity has increased, the principles that govern surgical resection of bone tumors remain unchanged. The surgeon must ensure adequate resection of involved bone and soft tissue so as to minimize the chance of local recurrence. If after achieving this goal he is still able to preserve adequate function of the limb after reconstruction, then the patient is a suitable candidate for limb salvage. At no stage must adequate disease clearance be compromised in an attempt to achieve limb salvage.

Kawaguchi's concept of "barrier effects" helped surgeons better understand evaluation of margins of resection [57]. Though conventionally quantitative parameters were used to define resection margins Kawaguchi converted anatomical structures (any tissue that has resistance against tumor invasion like muscle fascia, joint capsule, tendon, tendon sheath, epineurium, vascular sheath, and cartilage) into definitive thickness of normal tissue and classified them as either a thick barrier or a thin barrier. For purposes of margin evaluation a thick barrier was equivalent of 3 cm thickness of normal tissue, a thin barrier was considered to be 2 cm, and joint cartilage 5 cm. By considering barrier effects translated into concrete distance equivalents, oncologically safe surgery can be planned at sites where barriers exist by using margins less than those mandated by true physical distance.

The advent of computer-assisted tumor surgery (CATS) in malignant bone tumors has increased the accuracy of intended bone resection and may be beneficial in resection and reconstruction of pelvic, sacral, and difficult joint-preserving tumor surgery [58]. It provides a useful tool in achieving a better balance between disease resection and preservation of function in anatomically challenging locations.

There are a variety of reconstruction options after excision of osteosarcoma. Metallic prostheses (megaprostheses) which span the resection gap and allow for movement of the joint form the mainstay in limb salvage surgery for reconstruction after tumor resection, providing both mobility and stability. Biological means of reconstruction using autografts, allografts, and reimplantation of sterilized tumor bone (after autoclaving/pasteurization/irradiation) offer an attractive alternative option in certain scenarios.

Though not the first choice for local control in these lesions, the advent of newer techniques of delivery has resulted in radiation playing an increasing role in unresectable lesions or after incomplete resection. Proton therapy and carbon ion radiotherapy have demonstrated acceptable local control and a survival advantage with acceptable morbidity in the management of unresectable or incompletely resected osteosarcoma [59, 60]. Use of other nonconventional modalities for local control like microwave induced hyperthermia and high intensity focused ultrasound have also shown promising results [61, 62]. These techniques may thus eventually have the potential to be utilized as one of the components of limb sparing options in patients with malignant bone tumors.

8. The Future

Despite the current impasse in an inability to improve survival, the future for patients afflicted with cancer appears to hold exciting possibilities for further advancement. Such advances will probably accrue with the introduction of personalized medical care based upon molecular diagnoses of individual tumors. Advances in diagnostic procedures particularly imaging studies will probably improve the ability for more accurate staging and possibly contribute to better identification of subtle metastases. Molecular diagnostic procedures and identification of tumors permitting more specific therapy are currently in use in several tumors and may possibly be extended to osteosarcoma in the forseeable future. Ultimately these advances are also predicated on the discovery of new chemotherapeutic agents and alternate mechanisms of therapy.

9. Summary

With the introduction of effective chemotherapeutic agents during the 1960s–1980s cure in osteosarcoma was escalated from <10% to 60%–75%. Approximately 80% of patients are currently considered eligible for limb salvage. While major advances have been achieved with chemotherapy, the results have been stagnant over the past thirty to forty years. New types of chemotherapy and new modes of treatment are urgently required. The EURAMOS study is currently designed to explore new avenues of investigation. It particularly includes an assessment of the utility of neoadjuvant treatment. Possibly the discovery of new biological variants and other factors may prove useful in designing personalized therapy for the future. Realistic new targets must be identified utilizing lessons from the past to achieve new levels of success.

References

[1] A. Jemal, R. Siegel, E. Ward, Y. Hao, J. Xu, and M. J. Thun, "Cancer statistics, 2009," *CA Cancer Journal for Clinicians*, vol. 59, no. 4, pp. 225–249, 2009.

[2] A. Boyer, *The Lectures Boyer Upon Disease of the Bone*, James Humphreys, Philadelphia, Pa, USA, 1805.

[3] S. W. Gross, "Sarcoma of the long bones: based on a study of one hundred sixty five cases," *The American Journal of the Medical Sciences*, pp. 8338–8377, 1879.

[4] S. Cade, "Osteogenic sarcoma; a study based on 133 patients," *Journal of the Royal College of Surgeons of Edinburgh*, vol. 1, no. 2, pp. 79–111, 1955.

[5] A. B. Ferguson, "Treatment of osteosarcoma," *The Journal of Bone & Joint Surgery*, vol. 22, pp. 92–96, 1940.

[6] G. T. Rab, J. C. Ivins, and D. S. Childs, "Elective whole lung irradiation in the treatment of osteogenic sarcoma," *Cancer*, vol. 38, no. 2, pp. 939–942, 1976.

[7] R. C. Marcove, V. Miké, A. G. Huvos, C. M. Southam, and A. G. Levin, "Vaccine trials for osteogenic sarcoma. A preliminary report," *Ca-A Cancer Journal for Clinicians*, vol. 23, no. 2, pp. 74–80, 1973.

[8] J. R. Neff and W. F. Enneking, "Adoptive immunotherapy in primary osteosarcoma: an interim report," *Journal of Bone and Joint Surgery A*, vol. 57, no. 2, pp. 145–148, 1975.

[9] H. H. Fudenberg, "Dialyzable transfer factor in the treatment of human osteosarcoma: an analytic review," *Annals of the New York Academy of Sciences*, vol. 277, pp. 545–557, 1976.

[10] H. Strander, K. Cantell, P. A. Jakobsson, U. Nilsonne, and G. Soderberg, "Exogenous interferon therapy.of osteogenic sarcoma," *Acta Orthopaedica Scandinavica*, vol. 45, pp. 958–959.

[11] N. Jaffe, D. Traggis, and C. Enriquez, "Evaluation of a combination of mitomycin C (NSC-26980), phenylalanine mustard (NSC-14210), and vincristine (NSC-67574) in the treatment of osteogenic sarcoma," *Cancer Chemotherapy Reports*, vol. 55, no. 2, pp. 189–191, 1971.

[12] D. Pinkel, "Cyclophosphamide in children with cancer," *Cancer*, vol. 15, pp. 42–49, 1962.

[13] W. W. Sutow, "Combination chemotherapy with adriamycin (NSC 123127) in primary treatment of osteogenic sarcoma (Part III)," *Cancer Chemotherapy Reports*, vol. 6, no. 2, pp. 315–317, 1975.

[14] M. P. Sullivan, W. W. Sutow, and G. Taylor, "L-Phenylalanine mustard as a treatment for metastatic osteogenic sarcoma in children," *The Journal of Pediatrics*, vol. 63, no. 2, pp. 227–237, 1963.

[15] W. W. Sutow, M. P. Sullivan, and D. J. Fernbach, "Adjuvant chemotherapy in primary treatment of osteogenic sarcoma. A southwest oncology group study," *Cancer*, vol. 36, no. 5, pp. 1598–1602, 1975.

[16] W. W. Sutow, M. P. Sullivan, J. R. Wilbur, and A. Cangir, "Study of adjuvant chemotherapy in osteogenic sarcoma," *Journal of Clinical Pharmacology*, vol. 15, no. 7, pp. 530–533, 1975.

[17] J. Herson, W. W. Sutow, and K. Elder, "Adjuvant chemotherapy in nonmetastatic osteosarcoma: a Southwest Oncology Group study," *Medical and Pediatric Oncology*, vol. 8, no. 4, pp. 343–352, 1980.

[18] E. C. van Dalen, J. W. van As, and B. de Camargo, "Methotrexate for high-grade osteosarcoma in children and young adults," *Cochrane Database of Systematic Reviews*, vol. 5, Article ID CD006325, 2011.

[19] S. Farber, L. K. Diamond, R. D. Mercer, R. F. Sylvester Jr., and J. A. Wolff, "Temporary remissions in children in acute leukemia prodiced by folic acid antagonist 4-aminopteroyl-glutamic acid (aminopterin)," *The New England Journal of Medicine*, vol. 238, pp. 787–793, 1946.

[20] A. Goldin, N. Mantel, S. W. Greenhouse, J. M. Venditti, and S. R. Humphreys, "Effect of delayed administration of Citrocorin factor on the antileukemic effectiveness of aminopterin in mice," *Cancer Research*, vol. 14, pp. 43–48, 1954.

[21] I. Djerassi, E. Abir, G. L. Royer Jr., and C. L. Treat, "Long term remission in childhood acute leukemia: use of infrequent infusions of methotrexate: supportive roles of platelet transfusions and citrovorium factor," *Clinical Pediatrics*, vol. 5, pp. 502–509, 1966.

[22] N. Jaffe, "Recent advances in the chemotherapy of metastatic osteogenic sarcoma," *Cancer*, vol. 30, no. 6, pp. 1627–1631, 1972.

[23] N. Jaffe, "Progress report on high dose methotrexate (NSC 740) with citrovorum. Rescue in the treatment of metastatic bone tumors," *Cancer Chemotherapy Reports*, vol. 58, no. 2, pp. 275–280, 1974.

[24] N. Jaffe and D. Traggis, "Toxicity of high dose methotrexate (NSC 740) and citrovorum factor (NSC 3590) in osteogenic sarcoma," *Cancer Chemotherapy Reports*, vol. 6, no. 1, pp. 31–36, 1975.

[25] N. Jaffe, "Antifolate rescue use of high-dose methotrexate and citrovorum factor," in *Advances in Chemotherapy*, A. Rossowsky, Ed., pp. 11–141, Marcel Decker, New York, NY, USA, 1979.

[26] A. M. Goorin, M. Delorey, and R. D. Gelber, "Dana-Farber Cancer Institute/The Children's Hospital adjuvant chemotherapy trials for osteosarcoma: three sequential studies," *Cancer Treatment Symposia*, vol. 3, pp. 155–159, 1985.

[27] M. T. Harting, M. L. Blakely, N. Jaffe et al., "Long-term survival after aggressive resection of pulmonary metastases among children and adolescents with osteosarcoma," *Journal of Pediatric Surgery*, vol. 41, no. 1, pp. 194–199, 2006.

[28] S. K. Carter, "Adjuvant chemotherapy in osteogenic sarcoma: the triumph that isn't?" *Journal of Clinical Oncology*, vol. 2, no. 3, pp. 147–148, 1984.

[29] W. F. Taylor, J. C. Ivins, and D. J. Pritchard, "Trends and variability in survival among patients with osteosarcoma: a 7-year update," *Mayo Clinic Proceedings*, vol. 60, no. 2, pp. 91–104, 1985.

[30] K. M. McCarten, N. Jaffe, and J. A. Kirkpatrick, "The changing radiographic appearance of osteogenic sarcoma," *Annales de Radiologie Medecine Nucleaire*, vol. 23, no. 3, pp. 203–208, 1980.

[31] J. H. Edmonson, S. J. Green, and J. C. Ivins, "A controlled pilot study of high-dose methotrexate as postsurgical adjuvant treatment for primary osteosarcoma," *Journal of Clinical Oncology*, vol. 2, no. 3, pp. 152–156, 1984.

[32] M. A. Friedman and S. K. Carter, "The therapy of osteogenic sarcoma: current status and thoughts for the future," *Journal of Surgical Oncology*, vol. 4, no. 5, pp. 482–510, 1972.

[33] N. Jaffe, E. Frei III, D. Traggis, and Y. Bishop, "Adjuvant methotrexate and citrovorum factor treatment of osteogenic sarcoma," *The New England Journal of Medicine*, vol. 291, no. 19, pp. 994–997, 1974.

[34] M. P. Link, A. M. Goorin, and A. W. Miser, "The effect of adjuvant chemotherapy on relapse-free survival in patients with osteosarcoma of the extremity," *The New England Journal of Medicine*, vol. 314, no. 25, pp. 1600–1606, 1986.

[35] F. Eilber, A. Giuliano, J. Eckardt, K. Patterson, S. Moseley, and J. Goodnight, "Adjuvant chemotherapy for osteosarcoma: a randomized prospective trial," *Journal of Clinical Oncology*, vol. 5, no. 1, pp. 21–26, 1987.

[36] N. Jaffe, "Osteosarcoma," in *The New England Journal of Medicine*, vol. 314, p. 1513, 1986.

[37] J. F. Holland, "Adjuvant chemotherapy of osteosarcoma: no runs, no hits, two men left on base," *Journal of Clinical Oncology*, vol. 5, no. 1, pp. 4–6, 1987.

[38] N. Jaffe and R. Gorlick, "High-dose methotrexate in osteosarcoma: let the questions surcease—time for final acceptance," *Journal of Clinical Oncology*, vol. 26, no. 27, pp. 4365–4366, 2008.

[39] M. S. Kim, W. H. Cho, W. S. Song, S. Y. Lee, and D. G. Jeon, "Time depenancy of prognostic factors in patients with stage II osteosarcomas," *Clinical Orthopaedics and Related Research*, vol. 463, pp. 157–165, 2007.

[40] N. Jaffe, H. Carrasco, K. Raymond, A. Ayala, and F. Eftekhari, "Can cure in patients with osteosarcoma be achieved exclusively with chemotherapy and abrogation of surgery?" *Cancer*, vol. 95, no. 10, pp. 2202–2210, 2002.

[41] G. Bonadonna, S. Monfardini, M. De Lena, F. Fossati-Bellani, and G. Beretta, "Phase I and preliminary phase II evaluation of Adriamycin (NSC/123/21)," *Cancer Research*, vol. 30, pp. 2572–2582, 1970.

[42] E. Middleman, J. Luce, and E. Frei 3rd. E., "Clinical trials with adriamycin," *Cancer*, vol. 28, no. 4, pp. 844–850, 1971.

[43] E. P. Cortes, J. F. Holland, and J. Jaw Wang, "Amputation and adriamycin in primary osteosarcoma," *The New England Journal of Medicine*, vol. 291, no. 19, pp. 998–1000, 1974.

[44] M. A. Smith, R. S. Ungerleider, M. E. Horowitz, and R. Simon, "Influence of doxorubicin dose intensity on response and outcome for patients with osteogenic sarcoma and Ewing's sarcoma," *Journal of the National Cancer Institute*, vol. 83, no. 20, pp. 1460–1470, 1991.

[45] E. Baum, L. Greenberg, and P. Gaynon, "Use of Cis-platinum diammine dichloride (CPDD) in osteogenic sarcoma (OS) in children," *Proceedings of the American Association for Cancer Research*, vol. 19, abstract C-315, article 385, 1978.

[46] R. Nitschke, K. A. Starling, T. Vats, and H. Bryan, "Cis-diamminedichloroplatinum (NSC-119875) in childhood malignancies: a southwest oncology group study," *Medical and Pediatric Oncology*, vol. 4, no. 2, pp. 127–132, 1978.

[47] V. P. Chuang, S. Wallace, and R. S. Benjamin, "Multimodal approach to osteosarcoma: emphasis on intra-arterial cis-diamminedichloroplatinum II and limb preservation," *Cardiovas Intervent Radiol*, vol. 4, pp. 229–235, 1981.

[48] N. Jaffe, J. Knapp, and V. P. Chuang, "Osteosarcoma: intra-arterial treatment of the primary tumor with cis-diamminedichloroplatinum II (CDP). Angiographic, pathologic, and pharmacologic studies," *Cancer*, vol. 51, no. 3, pp. 402–407, 1983.

[49] K. H. Antman, D. Montella, C. Rosenbaum, and M. Schwen, "Phase II trial of ifosfamide with mesna in previously treated metastatic sarcoma," *Cancer Treatment Reports*, vol. 69, no. 5, pp. 499–504, 1985.

[50] N. Grana, J. Graham-Pole, W. Cassano et al., "Etoposide (VP-16) infusion plus Cyclophosphamide (CY) pulses: an effective combination for refractory cancer," *Proceedings of the American Society of Clinical Oncology*, vol. 8, article 300, 1989.

[51] M. B. Harris, A. B. Cantor, A. M. Goorin et al., "Treatment of osteosarcoma with ifosfamide: comparison of response in pediatric patients with recurrent disease versus patients previously untreated: a Pediatric Oncology Group Study," *Medical and Pediatric Oncology*, vol. 24, no. 2, pp. 87–92, 1995.

[52] P. A. Meyers, C. L. Schwartz, M. Krailo et al., "Osteosarcoma: a randomized, prospective trial of the addition of ifosfamide and/or muramyl tripeptide to cisplatin, doxorubicin, and high-dose methotrexate," *Journal of Clinical Oncology*, vol. 23, no. 9, pp. 2004–2011, 2005.

[53] P. A. Meyers, C. L. Schwartz, M. D. Krailo et al., "Osteosarcoma: the addition of muramyl tripeptide to chemotherapy improves overall survival—a report from the Children's Oncology Group," *Journal of Clinical Oncology*, vol. 26, no. 4, pp. 633–638, 2008.

[54] The European and American Osteosarcoma Study Group, "The EURAMOS I Trial," 2006, http://www.euramos.org.

[55] M. A. Simon, M. A. Aschliman, N. Thomas, and H. J. Mankin, "Limb-salvage treatment versus amputation for osteosarcoma of the distal end of the femur," *Journal of Bone and Joint Surgery A*, vol. 68, no. 9, pp. 1331–1337, 1986.

[56] D. C. Allison, S. C. Carney, E. R. Ahlmann et al., "A meta-analysis of osteosarcoma outcomes in the modern medical era," *Sarcoma*, vol. 2012, Article ID 704872, 10 pages, 2012.

[57] N. Kawaguchi, A. R. Ahmed, S. Matsumoto, J. Manabe, and Y. Matsushita, "The concept of curative margin in surgery for bone and soft tissue sarcoma," *Clinical Orthopaedics and Related Research*, no. 419, pp. 165–172, 2004.

[58] K. C. Wong and S. M. Kumta, "Computer-assisted tumor surgery in malignant bone tumors," *Clinical Orthopaedics and Related Research*, vol. 471, no. 3, pp. 750–761, 2012.

[59] I. F. Ciernik, A. Niemierko, D. C. Harmon et al., "Proton-based radiotherapy for unresectable or incompletely resected osteosarcoma," *Cancer*, vol. 117–119, pp. 4522–4530, 2011.

[60] A. Matsunobu, R. Imai, T. Kamada et al., "Impact of carbon ion radiotherapy for unresectable osteosarcoma of the trunk," *Cancer*, vol. 118, no. 18, pp. 4555–4563, 2012.

[61] Y. C. Hu, J. T. Ji, and D. X. Lun, "Intraoperative microwave inactivation in-situ of malignant tumors in the scapula," *Orthopaedic Surgery*, vol. 4, pp. 229–235, 2011.

[62] W. Chen, H. Zhu, L. Zhang et al., "Primary bone malignancy: effective treatment with high-intensity focused ultrasound ablation," *Radiology*, vol. 255, no. 3, pp. 967–978, 2010.

Hindawi Publishing Corporation
Sarcoma
Volume 2013, Article ID 480713, 11 pages
http://dx.doi.org/10.1155/2013/480713

Research Article

Rapamycin Inhibits ALDH Activity, Resistance to Oxidative Stress, and Metastatic Potential in Murine Osteosarcoma Cells

Xiaodong Mu,[1] Christian Isaac,[1,2] Trevor Schott,[1,2] Johnny Huard,[1,2] and Kurt Weiss[1,2]

[1] *Stem Cell Research Center, University of Pittsburgh School of Medicine, Bridgeside Point II, 450 Technology Drive, Pittsburgh, PA 15219, USA*
[2] *Department of Orthopaedic Surgery, University of Pittsburgh School of Medicine, Bridgeside Point II, 450 Technology Drive, Pittsburgh, PA 15219, USA*

Correspondence should be addressed to Kurt Weiss; weisskr@upmc.edu

Received 13 September 2012; Revised 4 December 2012; Accepted 22 December 2012

Academic Editor: Norman Jaffe

Osteosarcoma (OS) is the most common primary malignancy of bone. Mortality is determined by the presence of metastatic disease, but little is known regarding the biochemical events that drive metastases. Two murine OS cell lines, K7M2 and K12, are related but differ significantly in their metastatic potentials: K7M2 is highly metastatic whereas K12 displays much less metastatic potential. Using this experimental system, the mammalian target of rapamycin (mTOR) pathway has been implicated in OS metastasis. We also discovered that aldehyde dehydrogenase (ALDH, a stem cell marker) activity is higher in K7M2 cells than K12 cells. Rapamycin treatment reduces the expression and enzymatic activity of ALDH in K7M2 cells. ALDH inhibition renders these cells more susceptible to apoptotic death when exposed to oxidative stress. Furthermore, rapamycin treatment reduces bone morphogenetic protein-2 (BMP2) and vascular endothelial growth factor (VEGF) gene expression and inhibits K7M2 proliferation, migration, and invasion *in vitro*. Inhibition of ALDH with disulfiram correlated with decreased mTOR expression and activity. In conclusion, we provide evidence for interaction between mTOR activity, ALDH activity, and metastatic potential in murine OS cells. Our work suggests that mTOR and ALDH are therapeutic targets for the treatment and prevention of OS metastasis.

1. Introduction

Osteosarcoma (OS), the most common primary malignancy of bone, usually occurs in the long bones during childhood and adolescence at sites of rapid bone turnover [1–3]. Despite pre- and postoperative chemotherapy and wide surgical resection of the tumor, overall survival for patients without radiographically detectable metastases is only 65–70% [1, 2, 4, 5, 8]. The prognosis for patients with detectable metastases at the time of diagnosis is particularly poor, ranging from 15 to 30% [1, 7, 8]. It is thus the presence of pulmonary metastatic disease that ultimately determines OS mortality [9]. However, little is known about the biochemical signaling pathways that drive the progression of metastases and the molecular biology of OS remains poorly understood. As a result, we have yet to develop therapeutic strategies that specifically target metastatic disease.

The mammalian target of rapamycin (mTOR) is a highly conserved serine/threonine kinase, and as its name implies, mTOR activity is specifically inhibited by the drug rapamycin [10–13]. Rapamycin is an antimicrobial agent produced by *Streptomyces hygroscopius* that also exhibits potent immunosuppressive and antitumor properties, likely due to its ability to arrest the cell cycle in G1-phase [14]. mTOR signaling regulates a number of critical cellular processes including cellular growth, metabolism, and aging via an extraordinarily complex intercellular signaling network [15, 16]. Dysregulation of this mTOR signaling network can participate in a variety of human disease processes including cancer [17].

In mammals, mTOR associates with the proteins Raptor or Rictor to form mTOR complexes 1 and 2 (mTORC1 and 2), respectively. mTORC1 activity is sensitive to rapamycin, whereas mTORC2 is not [18, 19]. The best characterized

substrates of mTORC1 are p70 ribosomal protein S6 kinase (S6 K1) and the eukaryotic initiation factor 4E-binding protein 1 (4E-BP1), through which mTOR activity can regulate protein synthesis and cell growth [17]. A role for rapamycin-sensitive and rapamycin-insensitive mTOR signaling in cell motility and cancer metastasis is evolving but our current understanding is limited [14]. It is, however, widely recognized that mTOR signaling plays a critical role in protein synthesis, cell proliferation, growth, and survival [10, 20–22]. Dysregulated mTOR signaling is found in a variety of human cancers including hematologic, lung, breast, liver, pancreas, renal, skin, and gastrointestinal tract neoplasms [17]. In addition, it was recently discovered that mTOR signaling is activated in human osteosarcoma and correlates with surgical stage, metastasis, and disease-free survival [23]. The primary goal of this study was to investigate the role of mTOR signaling in OS metastasis and mTOR inhibition with rapamycin.

K7M2 and K12 are related murine OS cell populations derived from the same spontaneously-occurring OS in a Balb-C mouse. K7M2 cells are highly metastatic to the lungs and were clonally derived from the much less metastatic K12 cells [24]. K7M2 and K12 cells are thus very similar genetically but differ significantly in their metastatic potentials. As such, they represent excellent tools for determining critical biochemical pathways in OS metastasis. It has been reported that mTOR signaling activity is enhanced in K7M2 cells compared to K12 cells [25]. Here we report that mTOR signaling in K7M2 cells is associated with higher aldehyde dehydrogenase (ALDH, a cancer stem cell marker) activity, increased resistance to oxidative stress, increased proliferation, migration, and invasion, and higher bone morphogenetic protein (BMP2) and vascular endothelial growth factor (VEGF) expression than in the less metastatic K12 cells. All of these metastatic phenotypes were reversed with rapamycin treatment. Interestingly, we also report that ALDH inhibition with disulfiram is correlated with decreased mTOR activity and causes morphological alterations to K7M2 cells. This study provides evidence that the mTOR pathway promotes ALDH activity and metastatic potential in OS cells. We conclude that mTOR and ALDH are potential therapeutic targets in the treatment and prevention of OS metastasis.

2. Materials and Methods

2.1. Cell Culture and Rapamycin Treatment. K7M2 cells and K12 cells were cultured with proliferation medium (PM; DMEM with 10% FBS and 5% penicillin and streptomycin). For mTORC1 inhibition of K7M2 cells, rapamycin (Sigma) was dissolved in DMSO (10 mM) and diluted 1 : 1000 in proliferation medium to a working concentration of 10 μM. K7M2 cells were seeded in 12-well plastic plates at 5,000 cells per well, and 1 mL treatment medium containing rapamycin was added to each well. 1 mL of medium containing the same amount of DMSO served as control treatment. Treatment medium was refreshed each day and cells were treated for 2 to 4 days.

2.2. Fluorescence-Activated Cell Sorting (FACS) Analysis of ALDH Activity and Sorting of Cells. The Aldelfluor Kit (STEMCELL Technologies) was used to determine ALDH enzymatic activity. Cultured K7M2 cells and K12 cells, with or without rapamycin treatment (10 μM for 48 hrs), were resuspended in Aldefluor buffer (1×10^6 cells/mL) and incubated at 37°C according to the manufacturer's instructions. Cells were washed in Aldefluor buffer and maintained in 4°C throughout the cell sorting process. ALDH activity was assessed using the FL1 channel of a BD FACSAria Cell Sorting System and FACSDiva software (version 6.1.2; Becton, Dickinson and Company, San Jose, CA). Collected cells were sorted with fluorescence-activated cell sorting (FACS), according to their fluorescence intensity, which corresponds to their ALDH activity levels, as well as low side scatter (SCC^{lo}). ALDH-high cells and ALDH-low cells were separately harvested and cultured.

2.3. Cell Proliferation Assay. K7M2 and K12 cells were plated at 1000 cells per well in a 12-well plate and cultured in PM. A time-lapsed microscopic live-cell imaging (LCI) system (Automated Cell, Inc.) was used to take images of cells per each field of view at 15 minute intervals for 4 days. The approximate population doubling time (PDT) as determined as follows: 2^n = cell number at harvest time/cell number initially plated; "n" refers to the number of doublings during the period of cell culture (96 hrs), thus PDT = 96 hrs/n.

2.4. Cell Survival Assay after Exposure to Oxidative Stress. The antioxidant capacities of K7M2 (unsorted, ALDH-high, and ALDH-low fraction) and K12 cells cultured in 12-well plastic plates were compared by exposure to oxidative stress (250 μM H_2O_2 in PM) for 6 hrs. Also, to test the role of mTOR inhibition on the antioxidant capacity of K7M2 cells, K7M2 cells were pretreated with rapamycin (10 μM) for 48 hrs prior to exposure to oxidative stress (0, 250, or 500 μM H_2O_2 in PM) conditions for 6 hours. Propidium iodide (PI) was added to the medium (1 μg/mL) and apoptotic cells were identified with positive PI staining.

2.5. In Vitro Single Cell Migration Assay. An automated time-lapsed microscopy system (Biorad) was used to track the single cell migration on plastic surface. Cells were observed at 15 minute increments over 96 hours, the composite images were analyzed, the tracks of migration of 10 preselected single cells were monitored for each cell group, and cell velocities were calculated.

2.6. Cell In Vitro Invasion Assay. *In vitro* invasion capacity of K7M2 cells with or without rapamycin treatment, as well as ALDH-high and ALDH-low fractions of untreated K7M2 cells, was assessed using a real-time cell invasion and migration (RT-CIM) assay system (ACEA Biosciences, Inc.), with a 16-well trans-well plate (CIM-plate 16, Roche Diagnostics GmbH). The surface of the wells in the upper chamber was coated with Matrigel (BD BioSciences, Bedford, MA USA) of different concentrations (2.5%, 5%, and 10%). Serum-containing medium (10% FBS) was added to the wells

Table 1: Primer Sequences.

Gene	Primer sequence	Band size (bp)
GAPDH	Forward: TCCATGACAACTTTGGCATTG	103
	Reverse: TCACGCCACAGCTTTCCA	
BMP2	Forward: TCTTCCGGGAACAGATACAGG	126
	Reverse: TGGTGTCCAATAGTCTGGTCA	
BMP4	Forward: ATTCCTGGTAACCGAATGCTG	89
	Reverse: CCGGTCTCAGGTATCAAACTAGC	
VEGF	Forward: GCCAGACAGGGTTGCCATAC	108
	Reverse: GGAGTGGGATGGATGATGTCAG	
c-Myc	Forward: TGACCTAACTCGAGGAGGAGCTGGAATC	170
	Reverse: AAGTTTGAGGCAGTTAAAATTATGGCTGAAGC	
ALDH	Forward: GACAGGCTTTCCAGATTGGCTC	142
	Reverse: AAGACTTTCCCACCATTGAGTGC	
mTOR	Forward: CAGTTCGCCAGTGGACTGAAG	130
	Reverse: GCTGGTCATAGAAGCGAGTAGAC	

of the lower chamber. Cells (4×10^4 per well) in serum-free medium were seeded in the upper chamber. The migration of the cells through the Matrigel was monitored by the system every 15 minutes for 24 hours. Data analysis was carried out using RTCA Software 1.2 supplied with the instrument.

2.7. Semiquantitative Reverse Transcription Polymerase Chain Reaction (RT-PCR). Total RNA was extracted from the cells using the RNeasy plus mini kit (Qiagen) and cDNA was generated using the iScript cDNA Synthesis kit (Bio-Rad). The sense and antisense primers for RT-PCR and their product sizes are found in Table 1. The cycling parameters used for all reactions were as follows: 94°C for 5 minutes; 30 cycles of the following: denature for 45 seconds at 95°C, anneal for 30 seconds (53°C–56°C), and extend for 45 seconds at 72°C. RT-PCR was performed using a Bio-Rad MyiQ thermal cycler (Bio-Rad). GAPDH served as a control gene, and the expression of target genes was normalized to the expression of GAPDH. Gradient dilution (1 : 1, 1 : 2, and 1 : 4) of RNA samples from different cell groups was compared respectively to verify the quantitative difference of gene expression. RT-PCR analysis was performed using ImageJ software (version 1.32j, National Institutes of Health, Bethesda, MD) where the integrated density (product of the area and the mean gray value) of bands was calculated. All molecular bands were normalized to GAPDH.

2.8. Actin Staining. Organization of actin in ALDH-high, ALDH-low, and disulfiram treated cells was assessed using the phalloidin conjugated with Alexa Fluor 488 (Invitrogen). Populations of ALDH-high and ALDH-low cells were plated on to 12 well plates (50,000 cells/plate) and grown overnight in proliferation medium. The following day, the plates were washed twice with PBS, fixed in 3.7% formaldehyde solution for 10 minutes at room temperature, and washed two more times with PBS. The cells were then permeabilized in 0.1% Trition X-100 for 20 minutes and washed again with PBS. For each well a staining solution of 5 μL of methanolic stock solution phalloidin with 200 μL PBS and 1% BSA was added. The staining solution was kept in the wells for 20 minutes, and then the wells were washed again with PBS. This made the actin appear green under a fluorescence microscope. The nucleus was stained by adding 300 μL of 300 nM DAPI to wells for 5 minutes and then rising twice with PBS. This made the nucleus appear blue under a fluorescence microscope.

2.9. Disulfiram Treatment. Disulfiram is an ALDH inhibitor that has been used to treat alcoholism by blocking the enzymatic conversion of ethanol to acetic acid. In this study it was used to determine the effect of blocking ALDH in K7M2 cells vis-à-vis mTOR activity and cell morphology. ALDH-high and ALDH-low cells were plated and left to grow for approximately 2 hours before adding the disulfiram. A concentration of 250 nM was found to be the high nontoxic concentration able to be used on the cells.

2.10. mTOR Immunostaining. In order to determine the relative expression of mTOR in disulfiram-treated versus untreated cells, the cells were incubated with p-4E-BP1 (a rabbit antibody to mTOR). After a period of 2 hours, the cells were rinsed and then incubated with a fluorescent anti-rabbit antibody for one hour. The cells were then treated with DAPI as described earlier in order to visualize the nuclei. Pictures were then taken with a fluorescence microscope.

2.11. Statistical Analysis. At least three samples obtained from each subject were pooled for statistical analysis of all results from this study, and the results are expressed as a mean ± SD. The differences between two means were considered to be statistically significant if P value was <0.05. A Student's t-test was used to determine statistically significant differences between two means.

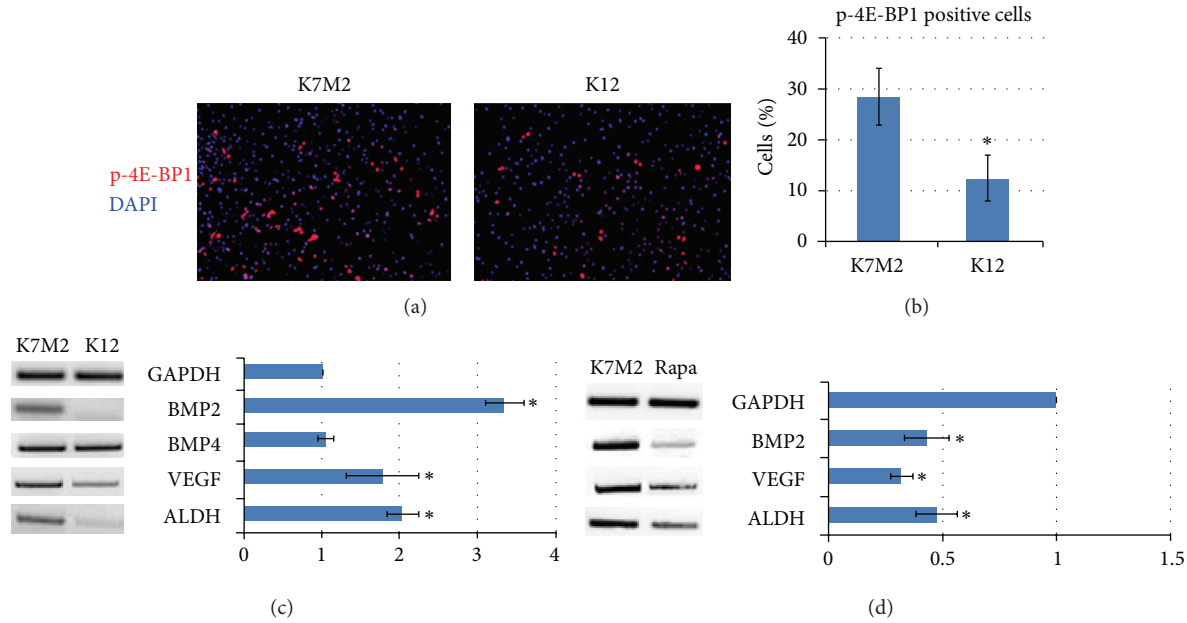

Figure 1: Phospho-4E-BP1 levels and rapamycin-sensitive gene expression in murine OS cells. (a) Immunofluorescence analysis of K7M2 and K12 cells depicting phospho-4E-BP1 (p-4E-BP1) counterstained with DAPI. (b) Quantitative analysis of p-4E-BP1 staining comparing the percentage of positive K7M2 and K12 cells. (c) RT-PCR was performed on cellular RNA extracted from K7M2 and K12 cells in order to quantitate the relative expression of BMP2, BMP4, VEGF, and ALDH-1A1. GAPDH serves as a loading control. (d) RT-PCR was performed on cellular RNA extracted from K7M2 cells treated with rapamycin or DMSO only (K7M2) in order to quantitate the relative expression of BMP2, VEGF, and ALDH-1A1 in the presence of mTORC1 kinase inhibition. Again, GAPDH serves as a loading control. Asterisks (∗) indicate statistically significant differences ($P < 0.05$).

3. Results

3.1. Rapamycin Inhibits BMP2, VEGF, and ALDH-1A1 Gene Expression in K7M2 Cells. K7M2 cells are known to exhibit greater mTORC1 kinase activity [25]. In order to confirm elevated mTORC1 kinase activity in our K7M2 cells we compared the amount of its phosphorylated substrate, phospho-4E-BP1 (p-4E-BP1), in K7M2 and K12 cells by immunofluorescence using a phosphospecific antibody (anti-phospho-threonine-37/46). Figure 1(a) shows a representative image of fixed K7M2 and K12 cell populations processed for p-4E-BP1 and DAPI immunofluorescence. Consistent with published results [25], we observed a greater than twofold increase in p-4E-BP1 immunofluorescence in K7M2 cultures compared to K12 cultures (Figure 1(b)), suggestive of elevated mTORC1 kinase activity in the more metastatic K7M2 cells.

ALDH activity, a "cancer stem cell marker," is found in a variety of human cancers and has been associated with metastasis, drug resistance, and a poor prognosis [26–30]. In order to investigate the role of mTORC1 activity in the regulation of ALDH in K7M2 cells we first performed reverse transcription polymerase chain reaction (RT-PCR) using RNA extracted from K7M2 and K12 cells treated with rapamycin or DMSO control. We have previously shown that BMP2 and VEGF expressions are upregulated in K7M2 cells compared to K12 cells [31]. Therefore, we analyzed the expression of BMP2, BMP4, and VEGF, in addition to ALDH-1A1 expression. GAPDH served as a loading control. Figure 1(c) shows the upregulation of these genes, except BMP4, in K7M2 cells compared to K12 cells, in the absence of rapamycin. After the addition of rapamycin to the media, we observed a significant down-regulation of BMP2, VEGF, and ALDH-1A1 mRNA transcripts of K7M2 cells (Figure 1(d)).

3.2. Rapamycin Treatment Reduces ALDH Activity and Sensitizes K7M2 Cells to Oxidative Stress. In order to further investigate the effect of rapamycin on ALDH we performed fluorescence-associated cell sorting (FACS) analysis to quantitate the percentage of cells with ALDH activity. Consistent with our RT-PCR results, we observed a threefold increase in the percentage of K7M2 cells with ALDH activity (23.1 ± 3.5% versus 7.4 ± 2.7%) compared to K12 cells (Figure 2(a)). However, after rapamycin treatment, the percentage of K7M2 cells with ALDH activity reduced significantly, compared to DMSO control group, and approached a level of activity more comparable to the less metastatic K12 cells (Figure 2(b)).

After observing that rapamycin effectively reduced ALDH-1A1 expression and ALDH activity in K7M2 cells, we next wanted to investigate the effect of rapamycin treatment on K7M2 resistance to oxidative stress because the activity of ALDH in cancer may function to neutralize oxidative stress and provide chemoresistance [32, 33]. We tested resistance to oxidative stress using H_2O_2 treatment. Apoptosis was monitored by nuclear inclusion of propidium iodide (PI). Figure 2(c) contains representative images of K7M2 cells and K12 cells treated with or without H_2O_2. After treatment with H_2O_2, the large majority (>85%) of

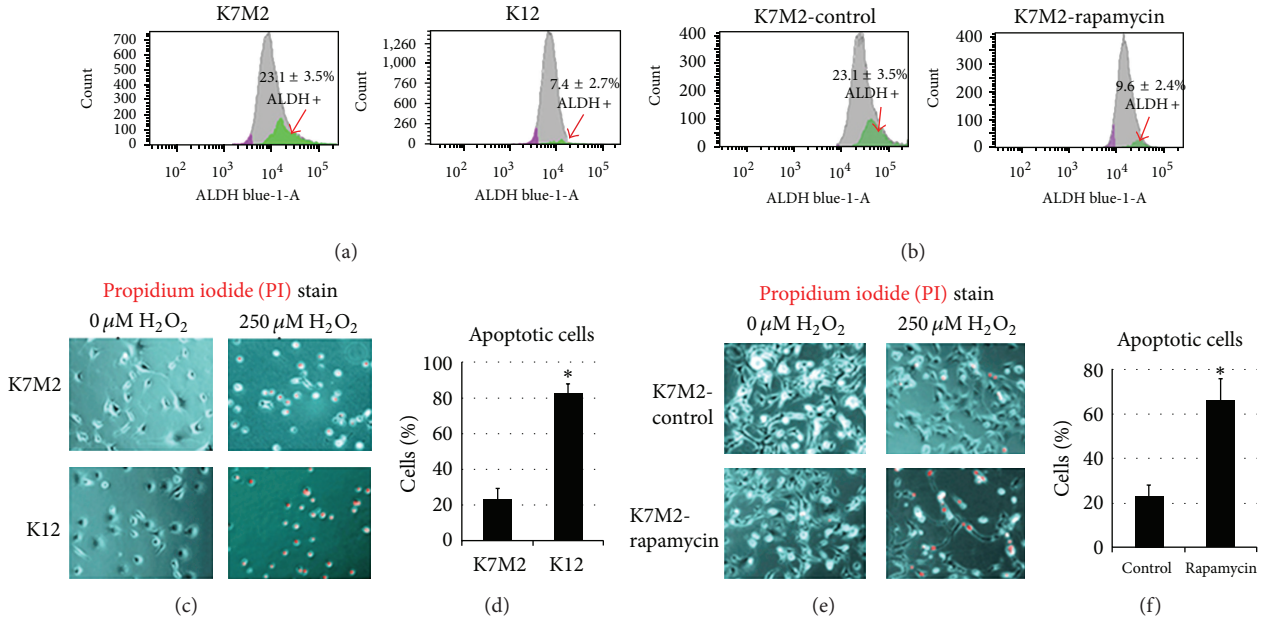

FIGURE 2: Rapamycin treatment reduces ALDH activity and sensitizes K7M2 cells to oxidative stress. (a) ALDH activity was detected in K7M2 and K12 cells using FACS analysis and the relative amount of cells positive for ALDH is shown for each cell population. (b) K7M2 cells were treated with rapamycin or DMSO only (control) and analyzed by FACS as in (a). (c) K7M2 and K12 cells were treated with or without H_2O_2 (250 μM) and apoptosis was detected using PI staining. (d) A quantitative analysis of (c) illustrating the percentage of apoptotic cells after H_2O_2 treatment compared to untreated controls. (e) K7M2 cells were treated with or without H_2O_2, in the presence or absence (DMSO only control) of rapamycin, and apoptotic cells were detected as in (c). (f) A quantitative analysis of (e) illustrating the percentage of apoptotic cells after H_2O_2 compared to untreated controls. Asterisks (∗) indicate statistically significant differences ($P < 0.05$).

K12 cells underwent apoptosis as indicated by PI inclusion, whereas most of the K7M2 cells maintained viability (>65%) as indicated by nuclear exclusion of PI (Figure 2(d)). Therefore, K7M2 cells are more resistant to oxidative stress from H_2O_2 exposure than K12 cells. In order to test if this resistance to H_2O_2 was related to mTORC1 or ALDH activity we repeated these experiments on K7M2 cells in the presence or absence of rapamycin, and 0 μM or 250 μM of H_2O_2. Representative images are shown in Figure 2(e). We observed an increased sensitivity to H_2O_2 with rapamycin treatment as rapamycin caused a threefold increase in apoptosis (Figure 2(f)). Rapamycin alone is not proapoptotic in this assay, as rapamycin in the absence of H_2O_2 did not increase the frequency of PI nuclear inclusion in K7M2 cells.

3.3. Rapamycin Treatment Reduces K7M2 Cell Proliferation. We analyzed K7M2 cell proliferation with and without rapamycin treatment because rapamycin has been shown to induce a G1-arrest in many tumor cell lines including osteosarcoma [10, 34]. After four days of culture in the presence or absence of rapamycin, K7M2 cells cultured in the presence of rapamycin appeared less dense on the culture dishes (Figure 3(a)). We then determined the population doubling time (PDT) of K7M2 and K12 cells with or without rapamycin treatment, over a culture period of 4 days (Figures 3(b) and 3(c)). It showed that PDT of both K7M2 and K12 was increased by rapamycin treatment, while its effect on K7M2 cells is more profound than that of K12 cells.

3.4. Rapamycin Treatment Reduces K7M2 Cell Migration and Invasion. K7M2 cells display much greater metastatic potential *in vivo* compared to K12 cells [24]. Consistent with this enhanced metastatic ability, we performed an *in vitro* tracking cell migration assay and observed more migratory activity in K7M2 cells compared to K12 cells and both K7M2 and K12 migration was sensitive to rapamycin (Figure 4(a)). We then determined the velocity of cell migration in this assay and the results are similar and displayed in Figure 4(b). Lastly, we evaluated the invasion capacity of K7M2 and K12 cells in 2.5% Matrigel and found that K7M2 cells have much stronger invasion capacity than K12 cells (data not shown). Furthermore, it was found that rapamycin greatly reduces K7M2 cell invasion in this assay (Figure 4(c)).

3.5. ALDH-High K7M2 Cells Have Greater Invasiveness, Morphologic Changes, Resistance to Oxidative Stress, and Expression of Oncogenic Factors Than ALDH-Low K7M2 Cells. K7M2 cells have been sorted according to the differential ALDH activity. The sorted populations of ALDH-high and ALDH-low K7M2 cells have been expanded *in vitro* (Figure 5(a)). *In vitro* invasion assay with 2.5% Matrigel demonstrated that ALDH-high K7M2 cells have much higher invasion capacity compared to ALDH-low K7M2 cells (Figure 5(b)). ALDH-high K7M2 cells were found to

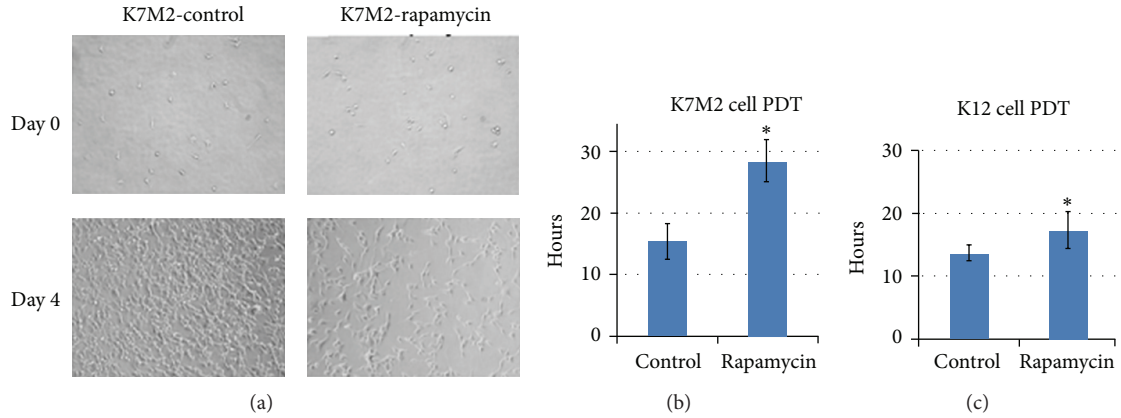

FIGURE 3: Rapamycin treatment reduces K7M2 cell proliferation. (a) K7M2 cells were cultured with media containing 10 μM rapamycin or DMSO only (control) for four days. Representative images of cell density at the beginning and end of treatment are shown. (b) A quantitative analysis of (a) to determine the population doubling time (PDT) of K7M2 cells in rapamycin-treated and control groups (DMSO only). (c) A quantitative analysis determining the population doubling time (PDT) of K12 cells in rapamycin-treated and control groups (DMSO only). Asterisks (∗) indicate statistically significant differences ($P < 0.05$).

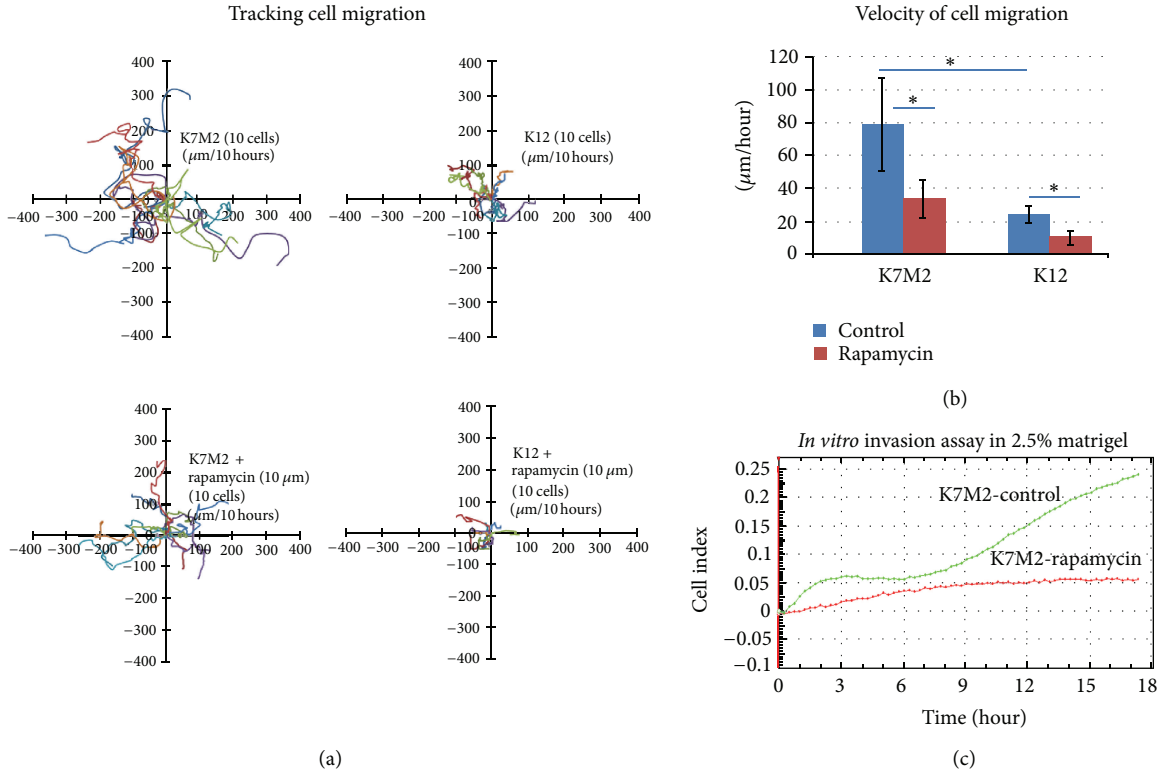

FIGURE 4: OS cell migration and invasion is sensitive to rapamycin treatment. (a) K7M2 and K12 cell migration was tracked in the presence or absence (DMSO only control) of rapamycin (10 μM) and the data obtained is displayed. (b) The velocity of cell migration was determined in each group in (a) and the results are displayed. (c) K7M2 cell invasion through a 2.5% Matrigel was monitored for 18 hours in the presence or absence (DMSO only) of 10 μM rapamycin. Asterisks (∗) indicate statistically significant differences ($P < 0.05$).

be more spread out and irregular in shape than ALDH-low K7M2 cells. They also displayed characteristics of typical motile behavior such as more organized structure of actin and the presence of filopodia (Figure 5(c)). Certain types of filopodia have been associated with increased invasiveness and metastasis rate [35]. Antioxidative stress assay showed that ALDH-high K7M2 cells are more resistant to the treatment of hydrogen peroxide, compared to

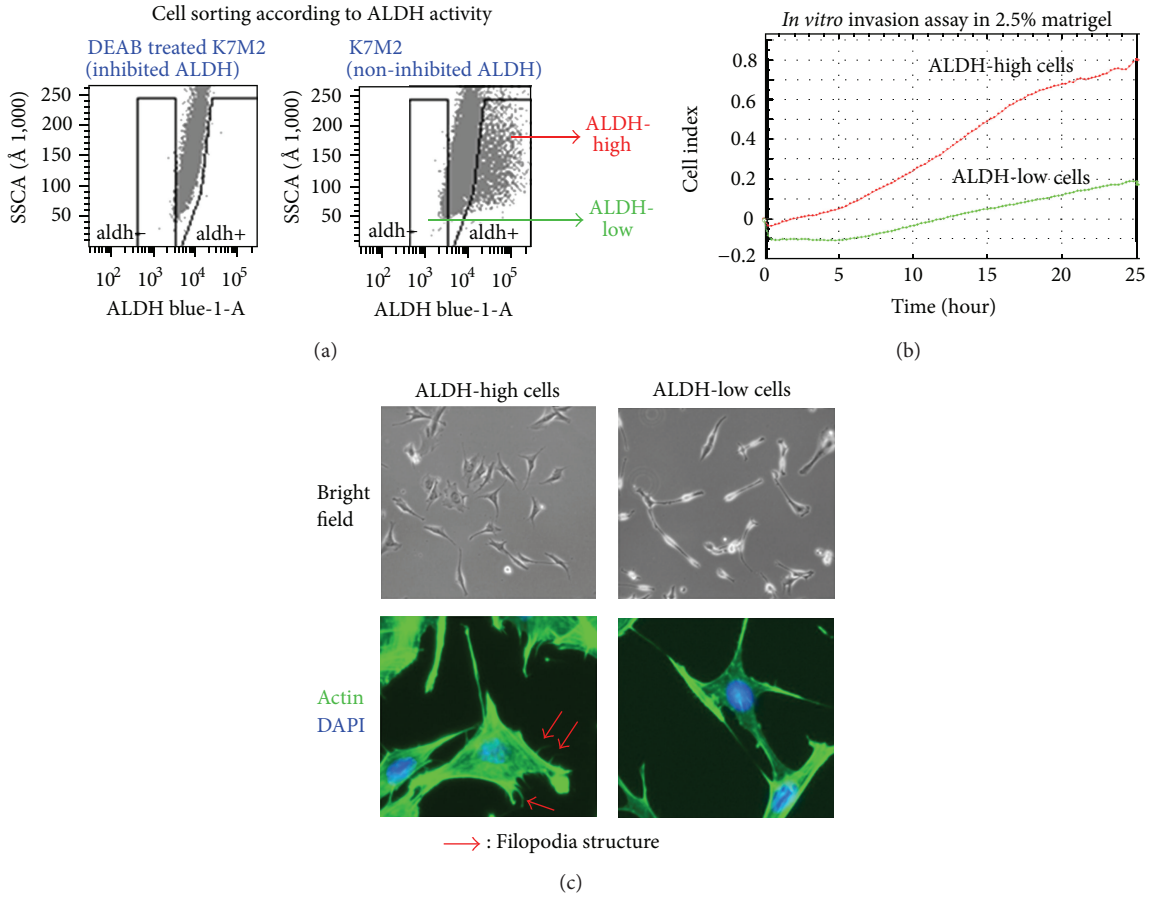

Figure 5: Cell sorting of K7M2 cells via ALDH activity and differential features of ALDH-high cells and ALDH-low cells. (a) K7M2 cells were suspended in Aldefluor buffer and sorted according to their fluorescence. Cells were treated with DEAB to block ALDH fluorescence, and cells were deemed ALDH-high if their fluorescence was higher than that of the DEAB-treated controls. Cells were deemed ALDH-low if their fluorescence was lower than that of the DEAB-treated controls. (b) ALDH-high and ALDH-low K7M2 cell invasion was tracked over a period of 24 hours and the data obtained is displayed. The ALDH-high cells displayed a much higher invasion potential, with more fraction of cells invading through the matrigel (2.5%). (c) Under bright field microscopy and under fluorescent microscopy (after staining for actin (green) and nucleic acids (blue)) ALDH-high K7M2 cells displayed more filopodia than ALDH-low cells. Also the ALDH-high cells were more irregularly shaped and were more pleomorphic than ALDH-low K7M2 cells.

ALDH-low K7M2 cells (Figure 2). RT-PCR also showed that ALDH-high cells had a higher expression of mTOR and c-Myc.

3.6. ALDH-High K7M2 Cells Treated with an ALDH-Inhibitor (Disulfiram) Show Reduced ALDH Activity, Oncogene Expression, and Morphologic Alterations. ALDH-high cells treated with disulfiram were verified to show a much reduced ALDH activity (data not shown). ALDH-high cells treated with disulfiram were found to have a lower expression of mTOR and c-Myc than untreated ALDH-high cells as shown via RT-PCR (Figure 6(a)). Treated cells also displayed less mTOR activity as shown via immunostaining with phosphpo-4E-BP1 (Figure 6(b)). Finally, the addition of disulfiram altered the cells' morphologies: they appeared much more like ALDH-low cells than untreated ALDH-high cells. There were much fewer filapodia, and the cells appeared much more uniform in shape (Figure 6(c)).

4. Discussion

K7M2 murine OS cells are highly metastatic to the lungs and were clonally derived from the less metastatic K12 OS cells [24]. Thus, the K7M2 and K12 cell lines are very similar genetically but differ significantly in their metastatic phenotypes and represent excellent tools for determining the critical biochemical pathways of OS metastasis. Here we report that, in comparison with K12 cells, K7M2 cells feature "rapamycin-sensitive" mTOR signaling which promotes cellular behaviors associated with metastasis, including higher ALDH activity, increased resistance to oxidative stress, proliferation, migration, invasion, and upregulation of BMP2 and VEGF expression. These results imply that mTORC1 activity may contribute to the enhanced metastatic potential of K7M2 cells.

There are several limitations to this study not the least of which is that all of our experiments were performed *in vitro*. Additionally, all of our experiments, and therefore our

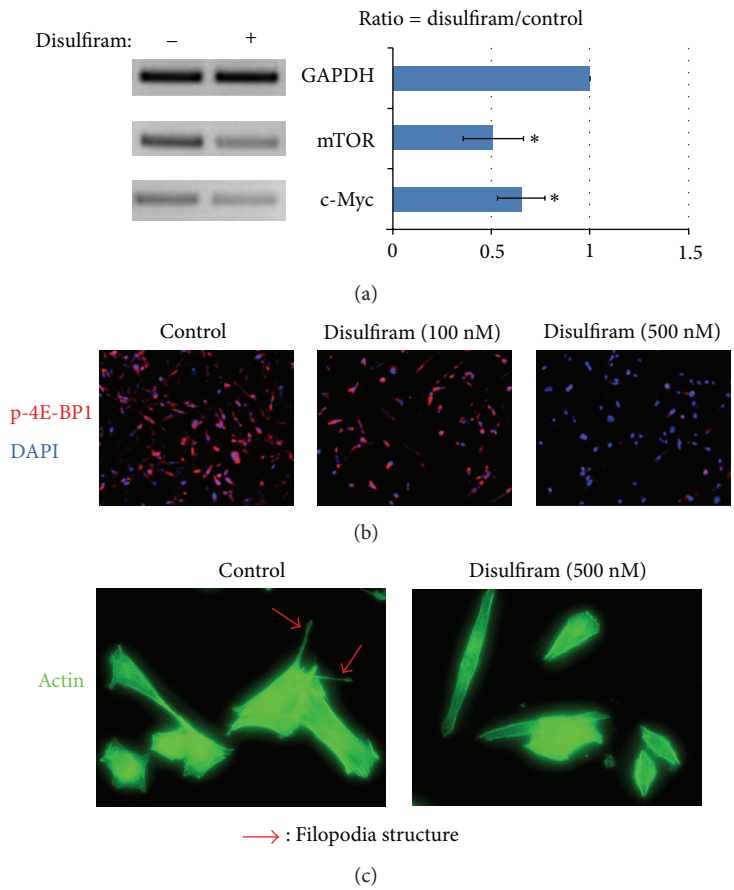

Figure 6: Inhibition of ALDH with disulfiram inhibits metastatic properties of ALDH-high K7M2 cells. (a) Disulfiram (250 nM) was added to ALDH-high K7M2 cells and the cells were cultured for at least 24 hours in 10% FBS growth medium. RT-PCR was used to determine gene expression differences as a result of this treatment, with GADPH used as a control. Both mTOR and c-Myc expression were reduced as a result of the treatment with disulfiram. (b) Immunostaining with phospho-4E-BP1 (a mouse anti-mTOR antibody) was done to confirm that treatment with disulfiram reduced expression of mTOR As the concentration of disulfiram was increased (0 nm, 100 nm and 500 nm) cells displayed progressively less mTOR expression. (c) Morphologic differences after treatment with disulfriam were also present, with disulfiram treated cells (stained for actin) appearing less pleomorphic and with fewer filopodia.

conclusions, are based entirely on the study of two murine cell lines. Although the observations reported above are interesting, care must be taken not to overstate these data. Fortunately, the metastatic phenotypes of K7M2 and K12 cells have been well-characterized in previous studies, including the effect of rapamycin treatment on K7M2 metastasis [24, 36]. We believe that our conclusions are sound, but future studies evaluating ALDH and mTOR activity in other OS cell lines and *in vivo* will be essential to validate these observations.

A role for mTOR signaling in osteosarcoma metastasis is slowly evolving. Human osteosarcoma tissue samples have stained positive for mTOR signaling and this has been correlated with surgical stage, metastasis pattern, and disease-free survival [23]. Our current understanding of the molecular biology remains limited. It has been shown in K7M2 cells that Ezrin (a plasma membrane to actin cytoskeleton linker protein) expression is upregulated compared to K12 cells, and that dynamic regulation of Ezrin activity via phosphorylation is required for metastasis to occur in a mouse xenograft model. It appears that Ezrin must be turned "on" and "off" in order to regulate cellular metabolism and protect K7M2 OS cells against stress after early arrival in the lungs. Furthermore, Ezrin, phosphatidylinositol-3-kinase (PI3K), and AKT are each associated with phosphorylation of S6K1 and 4E-BP1. Interestingly, Ezrin-associated phosphorylation of S6K1 and 4E-BP1 is sensitive to rapamycin, suggesting that these phosphorylation events depend on the mTORC1 kinase complex [25, 37].

mTOR signaling can regulate cell motility through mTORC1 and mTORC2-dependent kinase activity. Here we show that rapamycin can inhibit K7M2 cell migration *in vitro*, presumably by blocking mTORC1 activity. The regulation of cell motility by mTORC1 is most likely to be the mechanism that influences cell migration. Both mTORC1/S6K1 and mTORC1/4E-BP1 pathways are known to regulate cell motility. S6K1 participates in the phosphorylation of the focal adhesion proteins and F-actin reorganization in order to modulate cell motility but little is known about the manner in which 4E-BP1 regulates this process [14]. Thus,

rapamycin treatment could block migration by interfering with mTORC1-mediated cell motility but would potentially leave mTORC2 unchecked and free to regulate cell motility via control of the actin cytoskeleton through activation of the Rho GTPases [14].

ALDH activity has been identified as a "cancer stem cell" (CSC) marker in multiple neoplasms and has been associated with metastasis and a poor prognosis, but such a role has yet to be established in osteosarcoma [26–30]. The CSC hypothesis predicts that if certain genetic alterations occur in the right context, and within a more primitive cell, then a cancer-initiating cell is born that retains all the qualities of stem cells including self-renewal, proliferation, differentiation, resistance to drugs, stress, apoptosis, and the capacity to migrate, invade, and induce angiogenesis [38]. Our results show that ALDH-high OS cells display a significantly greater metastatic phenotype than ALDH-low cells. Although the relationship between CSCs and metastasis has not been clearly elucidated, it has been demonstrated that the number of metastatic cancer colonies correlates with the frequency of CSCs in the primary tissue. Furthermore, CSC subpopulations display a higher potential for invasiveness than subpopulations of nonstem tumor cells [39].

In this study, we observed that K7M2 cells exhibit higher levels of ALDH activity and this is dependent on mTORC1 activity as indicated by treatment with rapamycin. Furthermore, we showed that K7M2 cells, in comparison to K12 cells, are more resistant to oxidative stress caused by H_2O_2 treatment. The activity of ALDH in cancer may function to neutralize oxidative stress and provide chemoresistance, and thus upregulation of ALDH activity by mTOR may be one mechanism that confers resistance to oxidative stress in K7M2 cells [32, 33]. Alternatively, disulfiram, an ALDH inhibitor, has been shown to reduce the invasiveness of U2OS cells and the expression of matrix metalloproteinases, raising the possibility that ALDH activity may have a more direct role in tumor invasion [28]. However, the mechanisms for disulfiram's effects on U2OS invasion remain unclear.

In terms of stem cell regulation, an integral role for mTOR signaling in the proliferation and self-renewal of embryonic stem cells (ESCs) has been implicated. Loss of mTOR activity in human ESCs impairs pluripotency, blocks proliferation, and enhances mesoderm and endoderm activities [40]. The repression of developmental genes through mTOR signaling is thought to maintain pluripotency. Differentiation induces an "anabolic switch" and an increase in protein synthesis and protein content coincide with cell fate determination. Specifically, mTOR, and 4E-BP1 may function to regulate global and selective protein synthesis during self-renewal and differentiation [41]. Therefore, mTORC1 kinase activity may serve a similar role in the regulation of osteosarcoma stem cell proliferation and self-renewal.

Indeed, the ability of mTOR to promote proliferation without differentiation has been demonstrated in the literature. Many studies have shown that rapamycin treatment induces a G1-arrest in various cell lines, including osteosarcoma [10, 34], and here we have shown that rapamycin has a similar effect on K7M2 OS cells. This G1-arrest is likely to occur through the down-regulation of cyclin D1 as was previously shown in human OS cells by Gazitt et al. [42]. mTOR activity has also been shown to block differentiation as rapamycin treatment can enhance osteoblast differentiation [43]. Although an OS cancer stem cell has not been identified to date, evidence is accumulating that suggests this discovery is merely a matter of time [44]. If an OS cancer stem cell exists, we suspect that mTOR and ALDH activity play pivotal roles in the maintenance of this subpopulation of cancer cells.

Here we also demonstrated that BMP2 and VEGF expression in K7M2 cells is reduced by rapamycin treatment. Previously we had shown that BMP2 and VEGF expression is upregulated in K7M2 cells compared to K12 cells [31]. Furthermore, treatment with the BMP antagonist Noggin caused decreased motility, altered morphology, and increased cell death in K7M2 cells. It is also known that BMP2 is activated through hypoxia/AKT/mTOR/HIFα pathway in osteoblasts [45]. VEGF, on the other hand, is a potent inducer of neovascularization whose activity is thought to be an absolute requirement for tumor growth and metastasis [46]. Consistent with the present study, rapamycin has been shown to reduce VEGF production and inhibit angiogenesis in mice *in vivo* [47]. Therefore, down-regulation of BMP2 and VEGF (by mTORC1 inhibition) may each contribute to alter the metastatic behavior of K7M2 cells. Both BMP2 and VEGF may prove to be therapeutic targets in the treatment of OS metastasis. *In vivo* studies are essential to investigate the role of these secreted proteins in OS metastatic biology.

Our results show that ALDH inhibition via disulfiram actually decreased mTOR activity. This implies that under certain circumstances, mTOR activity may be regulated by ALDH. This has profound implications as mTOR activity is important in many cancers and is downstream of important tumor suppressors and oncogenes that are frequently mutated in human cancers [17]. Our work supports an oncogenic role for mTORC1 activity in osteosarcoma and provides evidence to link mTOR signaling, ALDH activity, and metastatic behavior. To our knowledge the present study is the first to implicate mTOR in the regulation of ALDH activity. Given our data and other evidence that exists to implicate mTOR and ALDH function in CSCs, we suspect that if an OS stem cell exists, mTOR and ALDH may be important for its proliferation, self-renewal, drug resistance, cell survival, and metastasis. The search for surface markers of OS cells has been long and disappointing, but ALDH may represent great promise as an OS stem cell surface marker. At this point in time we cannot be certain of the mechanisms by which ALDH and mTOR interact. Future investigations are required to further delineate the roles and relationships of mTOR, ALDH, and OS cancer stem cells.

In conclusion, mTOR signaling is upregulated in highly metastatic K7M2 OS cells. This upregulation is associated with increased ALDH expression and activity, resistance to oxidative stress, greater proliferation, migration, and invasion, and higher BMP2 and VEGF expression. This work implicates rapamycin and its analogs as potential agents in the treatment and prevention of OS metastasis. It also suggests a relationship between mTOR and ALDH. ALDH may, in its own right, represent a possible marker and therapeutic target of OS cell metastatic potential.

Conflict of Interests

The coauthor, J. Huard, receives remuneration for consulting and royalties from Cook Myosite Inc. The corresponding author, K. Weiss, is on the scientific advisory board of Eleison Pharmaceuticals. The remaining authors have no conflict of interests to disclose.

Acknowledgments

The authors wish to acknowledge the generous support of the Pittsburgh Foundation and the Houy family in loving memory of Jon Houy. The flow cytometry work was made possible by Lynda Guzik at the McGowan Institute for Regenerative Medicine, University of Pittsburgh, Pittsburgh, PA, USA.

References

[1] S. S. Bielack, B. Kempf-Bielack, G. Delling et al., "Prognostic factors in high-grade osteosarcoma of the extremities or trunk: an analysis of 1,702 patients treated on neoadjuvant cooperative osteosarcoma study group protocols," *Journal of Clinical Oncology*, vol. 20, no. 3, pp. 776–790, 2002.

[2] D. Carrle and S. S. Bielack, "Current strategies of chemotherapy in osteosarcoma," *International Orthopaedics*, vol. 30, no. 6, pp. 445–451, 2006.

[3] J. B. Hayden and B. H. Hoang, "Osteosarcoma: basic science and clinical implications," *Orthopedic Clinics of North America*, vol. 37, no. 1, pp. 1–7, 2006.

[4] S. Ferrari, S. Smeland, M. Mercuri et al., "Neoadjuvant chemotherapy with high-dose ifosfamide, high-dose methotrexate, cisplatin, and doxorubicin for patients with localized osteosarcoma of the extremity: a joint study by the italian and Scandinavian Sarcoma Groups," *Journal of Clinical Oncology*, vol. 23, no. 34, pp. 8845–8852, 2005.

[5] P. J. Messerschmitt, R. M. Garcia, F. W. Abdul-Karim, E. M. Greenfield, and P. J. Getty, "Osteosarcoma," *Journal of the American Academy of Orthopaedic Surgeons*, vol. 17, no. 8, pp. 515–527, 2009.

[6] K. Vo, B. Amarasinghe, K. Washington, A. Gonzalez, J. Berlin, and T. P. Dang, "Targeting notch pathway enhances rapamycin antitumor activity in pancreas cancers through PTEN phosphorylation," *Molecular Cancer*, vol. 10, article 138, 2011.

[7] P. A. Meyers, C. L. Schwartz, M. Krailo et al., "Osteosarcoma: a randomized, prospective trial of the addition of ifosfamide and/or muramyl tripeptide to cisplatin, doxorubicin, and high-dose methotrexate," *Journal of Clinical Oncology*, vol. 23, no. 9, pp. 2004–2011, 2005.

[8] P. A. Meyers, C. L. Schwartz, M. D. Krailo et al., "Osteosarcoma: the addition of muramyl tripeptide to chemotherapy improves overall survival—a report from the children's oncology group," *Journal of Clinical Oncology*, vol. 26, no. 4, pp. 633–638, 2008.

[9] P. A. Meyers and R. Gorlick, "Osteosarcoma," *Pediatric Clinics of North America*, vol. 44, no. 4, pp. 973–989, 1997.

[10] E. J. Brown, M. W. Albers, T. B. Shin et al., "A mammalian protein targeted by G1-arresting rapamycin-receptor complex," *Nature*, vol. 369, no. 6483, pp. 756–758, 1994.

[11] M. I. Chiu, H. Katz, and V. Berlin, "RAPT1, a mammalian homolog of yeast Tor, interacts with the FKBP12/rapamycin complex," *Proceedings of the National Academy of Sciences of the United States of America*, vol. 91, no. 26, pp. 12574–12578, 1994.

[12] D. M. Sabatini, H. Erdjument-Bromage, M. Lui, P. Tempst, and S. H. Snyder, "RAFT1: a mammalian protein that binds to FKBP12 in a rapamycin-dependent fashion and is homologous to yeast TORs," *Cell*, vol. 78, no. 1, pp. 35–43, 1994.

[13] C. J. Sabers, M. M. Martin, G. J. Brunn et al., "Isolation of a protein target of the FKBP12-rapamycin complex in mammalian cells," *The Journal of Biological Chemistry*, vol. 270, no. 2, pp. 815–822, 1995.

[14] H. Zhou and S. Huang, "MTOR signaling in cancer cell motility and tumor metastasis," *Critical Reviews in Eukaryotic Gene Expression*, vol. 20, no. 1, pp. 1–16, 2010.

[15] S. Wullschleger, R. Loewith, and M. N. Hall, "TOR signaling in growth and metabolism," *Cell*, vol. 124, no. 3, pp. 471–484, 2006.

[16] R. Zoncu, A. Efeyan, and D. M. Sabatini, "MTOR: from growth signal integration to cancer, diabetes and ageing," *Nature Reviews Molecular Cell Biology*, vol. 12, no. 1, pp. 21–35, 2011.

[17] E. Dazert and M. N. Hall, "mTOR signaling in disease," *Current Opinion in Cell Biology*, vol. 23, pp. 744–755, 2011.

[18] E. Jacinto, R. Loewith, A. Schmidt et al., "Mammalian TOR complex 2 controls the actin cytoskeleton and is rapamycin insensitive," *Nature Cell Biology*, vol. 6, no. 11, pp. 1122–1128, 2004.

[19] R. Loewith, E. Jacinto, S. Wullschleger et al., "Two TOR complexes, only one of which is rapamycin sensitive, have distinct roles in cell growth control," *Molecular Cell*, vol. 10, no. 3, pp. 457–468, 2002.

[20] M. F. Crouch, "Regulation of thrombin-induced stress fibre formation in Swiss 3T3 cells by the 70-kDa S6 kinase," *Biochemical and Biophysical Research Communications*, vol. 233, no. 1, pp. 193–199, 1997.

[21] A. Dufner and G. Thomas, "Ribosomal S6 kinase signaling and the control of translation," *Experimental Cell Research*, vol. 253, no. 1, pp. 100–109, 1999.

[22] S. Ferrari, H. R. Bandi, J. Hofsteenge, B. M. Bussian, and G. Thomas, "Mitogen-activated 70K S6 kinase. Identification of in vitro 40 S ribosomal S6 phosphorylation sites," *The Journal of Biological Chemistry*, vol. 266, no. 33, pp. 22770–22775, 1991.

[23] Q. Zhou, Z. Deng, Y. Zhu, H. Long, S. Zhang, and J. Zhao, "mTOR/p70S6K signal transduction pathway contributes to osteosarcoma progression and patients' prognosis," *Medical Oncology*, vol. 27, no. 4, pp. 1239–1245, 2010.

[24] C. Khanna, J. Prehn, C. Yeung, J. Caylor, M. Tsokos, and L. Helman, "An orthotopic model of murine osteosarcoma with clonally related variants differing in pulmonary metastatic potential," *Clinical and Experimental Metastasis*, vol. 18, no. 3, pp. 261–271, 2000.

[25] X. Wan, A. Mendoza, C. Khanna, and L. J. Helman, "Rapamycin inhibits ezrin-mediated metastatic behavior in a murine model of osteosarcoma," *Cancer Research*, vol. 65, no. 6, pp. 2406–2411, 2005.

[26] E. Charafe-Jauffret, C. Ginestier, F. Iovino et al., "Aldehyde dehydrogenase 1-positive cancer stem cells mediate metastasis and poor clinical outcome in inflammatory breast cancer," *Clinical Cancer Research*, vol. 16, no. 1, pp. 45–55, 2010.

[27] A. M. S. Cheung, T. S. K. Wan, J. C. K. Leung et al., "Aldehyde dehydrogenase activity in leukemic blasts defines a subgroup of acute myeloid leukemia with adverse prognosis and superior NOD/SCID engrafting potential," *Leukemia*, vol. 21, no. 7, pp. 1423–1430, 2007.

[28] H. J. Cho, T. S. Lee, J. B. Park et al., "Disulfiram suppresses invasive ability of osteosarcoma cells via the inhibition of MMP-2 and MMP-9 expression," *Journal of Biochemistry and Molecular Biology*, vol. 40, no. 6, pp. 1069–1076, 2007.

[29] K. Honoki, H. Fujii, A. Kubo et al., "Possible involvement of stem-like populations with elevated ALDH1 in sarcomas for chemotherapeutic drug resistance," *Oncology Reports*, vol. 24, no. 2, pp. 501–505, 2010.

[30] E. H. Huang, M. J. Hynes, T. Zhang et al., "Aldehyde dehydrogenase 1 is a marker for normal and malignant human colonic stem cells (SC) and tracks SC overpopulation during colon tumorigenesis," *Cancer Research*, vol. 69, no. 8, pp. 3382–3389, 2009.

[31] K. R. Weiss, G. M. Cooper, J. A. Jadlowiec, R. L. McGough III, and J. Huard, "VEGF and BMP expression in mouse osteosarcoma cells," *Clinical Orthopaedics and Related Research*, vol. 450, pp. 111–117, 2006.

[32] M. Magni, S. Shammah, R. Schiró, W. Mellado, R. Dalla-Favera, and A. M. Gianni, "Induction of cyclophosphamide-resistance by aldehyde-dehydrogenase gene transfer," *Blood*, vol. 87, no. 3, pp. 1097–1103, 1996.

[33] J. E. Russo and J. Hilton, "Characterization of cytosolic aldehyde dehydrogenase from cyclophosphamide resistant L1210 cells," *Cancer Research*, vol. 48, no. 11, pp. 2963–2968, 1988.

[34] M. W. Albers, R. T. Williams, E. J. Brown, A. Tanaka, F. L. Hall, and S. L. Schreiber, "FKBP-rapamycin inhibits a cyclin-dependent kinase activity and a cyclin D1-Cdk association in early G1 of an osteosarcoma cell line," *The Journal of Biological Chemistry*, vol. 268, no. 30, pp. 22825–22829, 1993.

[35] L. M. Machesky, "Lamellipodia and filopodia in metastasis and invasion," *FEBS Letters*, vol. 582, no. 14, pp. 2102–2111, 2008.

[36] C. Khanna, J. Khan, P. Nguyen et al., "Metastasis-associated differences in gene expression in a murine model of osteosarcoma," *Cancer Research*, vol. 61, no. 9, pp. 3750–3759, 2001.

[37] L. Ren, S. H. Hong, Q. R. Chen et al., "Dysregulation of ezrin phosphorylation prevents metastasis and alters cellular metabolism in osteosarcoma," *Cancer Research*, vol. 72, pp. 1001–1012, 2012.

[38] M. S. Wicha, S. Liu, and G. Dontu, "Cancer stem cells: an old idea—a paradigm shift," *Cancer Research*, vol. 66, no. 4, pp. 1883–1890, 2006.

[39] Y. Y. Hu, M. H. Zheng, R. Zhang, Y. M. Liang, and H. Han, "Notch signaling pathway and cancer metastasis," *Advances in Experimental Medicine and Biology*, vol. 727, pp. 186–198, 2012.

[40] J. Zhou, P. Su, L. Wang et al., "mTOR supports long-term self-renewal and suppresses mesoderm and endoderm activities of human embryonic stem cells," *Proceedings of the National Academy of Sciences of the United States of America*, vol. 106, no. 19, pp. 7840–7845, 2009.

[41] P. Sampath, D. K. Pritchard, L. Pabon et al., "A hierarchical network controls protein translation during murine rmbryonic stem cell self-renewal and differentiation," *Cell Stem Cell*, vol. 2, no. 5, pp. 448–460, 2008.

[42] Y. Gazitt, V. Kolaparthi, K. Moncada, C. Thomas, and J. Freeman, "Targeted therapy of human osteosarcoma with 17AAG or rapamycin: characterization of induced apoptosis and inhibition of mTOR and Akt/MAPK/Wnt pathways," *International Journal of Oncology*, vol. 34, no. 2, pp. 551–561, 2009.

[43] T. Ogawa, M. Tokuda, K. Tomizawa et al., "Osteoblastic differentiation is enhanced by rapamycin in rat osteoblast-like osteosarcoma (ROS 17/2.8) cells," *Biochemical and Biophysical Research Communications*, vol. 249, no. 1, pp. 226–230, 1998.

[44] C. P. Gibbs Jr., P. P. Levings, and S. C. Ghivizzani, "Evidence for the osteosarcoma stem cell," *Current Orthopaedic Practice*, vol. 22, pp. 322–326, 2011.

[45] W. P. Tseng, S. N. Yang, C. H. Lai, and C. H. Tang, "Hypoxia induces BMP-2 expression via ILK, Akt, mTOR, and HIF-1 pathways in osteoblasts," *Journal of Cellular Physiology*, vol. 223, no. 3, pp. 810–818, 2010.

[46] L. M. Ellis and D. J. Hicklin, "VEGF-targeted therapy: mechanisms of anti-tumour activity," *Nature Reviews Cancer*, vol. 8, no. 8, pp. 579–591, 2008.

[47] M. Guba, P. Von Breitenbuch, M. Steinbauer et al., "Rapamycin inhibits primary and metastatic tumor growth by antiangiogenesis: involvement of vascular endothelial growth factor," *Nature Medicine*, vol. 8, no. 2, pp. 128–135, 2002.

Hindawi Publishing Corporation
Sarcoma
Volume 2013, Article ID 147541, 11 pages
http://dx.doi.org/10.1155/2013/147541

Research Article

Dkk-3, a Secreted Wnt Antagonist, Suppresses Tumorigenic Potential and Pulmonary Metastasis in Osteosarcoma

Carol H. Lin,[1,2] Yi Guo,[2] Samia Ghaffar,[2] Peter McQueen,[2] Jonathan Pourmorady,[2] Alexander Christ,[2] Kevin Rooney,[2] Tao Ji,[2] Ramez Eskander,[3] Xiaolin Zi,[4,5] and Bang H. Hoang[2,6]

[1] *Department of Oncology, CHOC Children's Hospital, 455 South Main Street, Orange, CA 92868, USA*
[2] *Department of Orthopaedic Surgery, University of California, Irvine, 101 The City Drive South, Orange, CA 92868, USA*
[3] *Department of Obstetrics and Gynecology, University of California, Irvine, 101 The City Drive South, Building 56, Suite 260, Orange, CA 92868, USA*
[4] *Department of Urology, University of California, Irvine, 101 The City Drive South, Building 55, Suite 302, Orange, CA 92868, USA*
[5] *Department of Pharmaceutical Sciences, University of California, Irvine, 101 The City Drive South, Orange, CA 92868, USA*
[6] *Department of Orthopaedic Surgery and Chao Family Comprehensive Cancer Center, University of California, Irvine, 101 The City Drive South, Orange, CA 92868, USA*

Correspondence should be addressed to Bang H. Hoang; bhhoang@uci.edu

Received 7 July 2012; Revised 10 December 2012; Accepted 16 December 2012

Academic Editor: H. Gelderblom

Osteosarcoma (OS) is the most common primary bone malignancy with a high propensity for local invasion and distant metastasis. Despite current multidisciplinary treatments, there has not been a drastic change in overall prognosis within the past 2 decades. Dickkopf-3 protein (Dkk-3/REIC) has been known to inhibit canonical Wnt/β-catenin pathway, and its expression has been shown to be downregulated in OS cell lines. Using *in vivo* and *in vitro* studies, we demonstrated that Dkk-3-transfected 143B cells inhibited tumorigenesis and metastasis in an orthotopic xenograft model of OS. Inoculation of Dkk-3-transfected 143B cell lines into nude mice showed significant decreased tumor growth and less metastatic pulmonary nodules (88.7%) compared to the control vector. *In vitro* experiments examining cellular motility and viability demonstrated less anchorage-independent growth and decreased cellular motility for Dkk-3-transfected 143B and SaOS2 cell lines compared to the control vector. Downstream expressions of Met, MAPK, ALK, and S1004A were also downregulated in Dkk-3-transfected SaOS2 cells, suggesting the ability of Dkk-3 to inhibit tumorigenic potential of OS. Together, these data suggest that Dkk-3 has a negative impact on the progression of osteosarcoma. Reexpressing Dkk-3 in Dkk-3-deficient OS tumors may prove to be of benefit as a preventive or therapeutic strategy.

1. Introduction

Osteosarcoma (OS) is the most common primary bone malignancy diagnosed in children and adolescents. With the current multidisciplinary treatments, 60–70% of patients with localized disease survive [1]. According to the Children's Oncology Group (COG) protocol for localized disease, standard therapy consists of neoadjuvant chemotherapy, including doxorubicin, cisplatin, and high-dose methotrexate, followed by surgical resection. After surgical intervention, adjuvant chemotherapy is given, dependent upon the degree of necrosis. Good responders to neoadjuvant therapy will show < 10% viable tumor and will be randomized to continue with adjuvant therapy. According to the European and American Osteosarcoma 1 Trial (EURAMOS 1), the five-year survival for good responders is 75–80% compared to poor responders who face survival percentages of 45–55%. Prognostic factors for OS include tumor site and size, primary metastases, response to chemotherapy and surgical remission [2, 3]. Osteosarcoma has a high tendency for local invasion and early metastasis. Unfortunately, with metastatic disease, the rate of 5-year overall survival is greatly reduced to 20–30%,

and the 5-year event-free survival for patients with relapse is only 20% [4, 5]. Metastasis occurs primarily to the pulmonary fields. Even though there is no initial evidence of metastasis from baseline chest CT scans, it is thought that there are micrometastasis, creating further difficulties in treating this malignant process. Despite aggressive efforts to treat, the outcome of patients with OS has not significantly improved during the past two decades. This creates an opportunity for more effective targeted therapies.

The canonical Wnt/β-catenin signaling pathway has been shown to control multiple cellular processes, including cellular proliferation, cell fate determination, and differentiation in numerous developmental stages, from embryogenesis to adult tissue homeostasis [6–9]. Given the power of this central mediator, inhibition of Wnt/β-catenin signaling is a key potential strategy for cancer therapy. Our previous study on Dickkopf 3 (Dkk-3, also known as reduced expression in immortalized cells (REIC)) showed its ability to inhibit invasion and motility of OS cells via modulation of the Wnt-β-catenin pathway. We showed that Dkk-3 downregulates β-catenin nuclear translocation in osteosarcoma cells resulting in inhibition of downstream Wnt-mediated lymphoid enhancer factor/TCF activation [10].

The Dickkopf family comprises of four secretory proteins, Dkk-1, Dkk-2, Dkk-3, and Dkk-4. Human Dkk-1 inhibits Wnt signaling pathway (well known for its roles in embryogenesis and cancer) by binding to the transmembrane receptors (Lipoprotein receptor-related protein-5 and -6 (LRP5, LRP6) [11]. The secretory protein REIC/Dkk-3 mechanism of action for inhibiting Wnt signaling pathway is currently unknown, but its expression has been shown to be downregulated in various cancer cell lines, including prostate, renal, liver, pancreas, cervical, lung, melanoma, glioma, testicular, colon, and even osteosarcoma cancer cells [10–20].

Our previous data showed that Dkk-3 inhibited *in vitro* invasion and motility of OS cell line SaOS2 by modulating the Wnt/β-Catenin pathway. Transfection of Dkk-3 and dominant-negative *LRP5* into SaOS-2 cells significantly reduced the invasion capacity and motility [10]. In this study, we continued to focus on the effects of Dkk-3 *in vitro* and *in vivo* to assess its ability to decrease tumor progression in osteosarcoma and elucidated the potential molecular mechanism.

2. Materials and Methods

2.1. Cell Lines, Compounds, Reagents, and Plasmids. Human OS cell lines 143B, 143.98.2, SaOS-2, MNNG-HOS, MG-63, and U2-OS (American Type Culture Collection), SaOS-LM7 (a gift from Dr. Eugenie Kleinerman, MD Anderson Cancer Center, Houston, TX, USA), and OS160 (a gift from Richard Gorlick, Albert Einstein College of Medicine, Bronx, NY, USA) were maintained in MEM-Alpha medium supplemented with 10% fetal bovine serum (FBS). Normal human osteoblasts (NHOSTs) were obtained from Cambrex Bio Science and maintained in Osteoblast Growth Media (Lonza). All cells were maintained in a 37°C incubator with humidified atmosphere of 5% CO_2. *PcDNA3.1* Directional TOPO Expression vector was obtained from Invitrogen. Dkk-3 clone was constructed as previously described [10]. Antibodies against β-actin was from Santa Cruz Biotechnology, Inc. (Santa Cruz, CA, USA). Thymidine, 3-(4,5-dimethylthiazol-2-yl)-2,5-diphenyltetrazolium bromide (MTT) and propidium iodide were obtained from Sigma (Saint Louis, MO, USA). RNAzol B was purchased from Tel-Test (Friendswood, TX), and the Reverse Transcription System kit was from Applied Biosystems (Carlsbad, CA, USA).

2.2. MTT Assay. 143B OS cells were plated at a density of 2×10^4 cells per well in 24-well culture plates in 500 μL of growth medium containing 10% FBS. After 24 hours, the cells were transfected with either PcDNA control or various colonies of Dkk-3. Following transfection, at 72 hours, 500 uL of MTT solution (final concentration of 1 mg/mL) was added to each well and incubated at 37°C for 1.5 hours. Once MTT solution was removed, 500 uL of dissolve buffer (4% 1 M HCl, 96% Isopropanol) was added, and plates were gently shaken for 5 minutes to dissolve the crystals. Cell viability was assessed by measuring the absorbance at 570 nm from a 96-well plate microplate reader (Bio-Rad, Hercules, CA, USA). Dose response curves for cell viability were generated as a percentage of vehicle-treated control.

2.3. Stable Transfection. 143B and SaOS-2 cells were plated at 1.6×10^5 per 100 mm dish. Once confluency reached 60%, cultures were transfected with *PcDNA3.1* or Dkk-3 using FuGENE 6 (Roche) according to the manufacturer's instructions. Once transfected, stable clones were selected with G418 (800 μg/mL) starting at 48 hours after transfection and assayed for transgene expression via Western blot and real-time reverse transcription PCR (RT-PCR). Pooled transfectants were propagated and maintained in MEM-alpha with 10% FBS and 500 μg/mL G418.

2.4. Transient Transfection. 143B and SaOS-2 cells were plated at 1.0×10^5 per 100 mm dish. After reaching 80–90% confluency, both cell lines were transfected with PcDNA3.1 (Invitrogen) or Dkk-3 (Addgene) plasmids using Lipofectamine 2000 (Invitrogen) according to the manufacturer's instructions. Transfectants were maintained in MEM-alpha with 10% FBS and 1% penicillin/streptomycin for 48 h prior to cell extraction.

2.5. Western Blot Analysis. Cell extracts from transfected 143B and SaOS-2 cells with either PcDNA3.1 or Dkk-3 were prepared in RIPA lysis buffer containing protease inhibitors (Sigma, St. Louis, MO, USA). Cell lysates were centrifuged at 12,000 RPM for 15 minutes and the supernatant was collected. Clarified protein lysates (50 μg) were electrophoretically resolved (90 minutes at 100 Volts) on denaturing 10–12% sodium dodecyl sulfate-polyacrylamide gel electrophoresis (SDS-PAGE). They were transferred to a nitrocellulose membrane (GE Healthcare, Piscataway, NJ, USA). Following blotting for 1 hour with 5% nonfat dry

milk (Bio-Rad, Hercules, CA, USA) in TBST (10 mM Tris-HCL, pH 8.0, 150 nM NaCl, and 0.05% Tween-20), membranes were probed with primary antibodies and incubated overnight at 4°C. After washing twice with TBST for 5 minutes each, membranes were incubated for 1.5 hours at room temperature with secondary antibodies and visualized using the SuperSignal West Pico Chemiluminescent Substrate (Pierce). For loading control, the membrane used in initial Western blot was placed in Restore Western blotting Stripping Buffer (Thermo Scientific) for 15 minutes to remove the primary and secondary antibodies. After washing with water for 5 minutes and blocking with 5% milk for 1 hour, the membrane was probed with β-actin antibody (Santa Cruz Biotechnology).

2.6. Real-Time Reverse Transcription-Polymerase Chain Reaction (RT-PCR). After transfecting 143B and SaOS-2 with PcDNA3.1 or Dkk-3, total RNA was isolated using the TRIzol reagent (Invitrogen, Carlsbad, CA, USA). Using a high-capacity cDNA reverse transcription kit, cDNA was synthesized from 2 μg of total RNA. The sequences of the primers are as follows: Dkk-3, forward: 5′-ctgtgtgtctggggtcactg-3′; reverse: 5′-gctctagctcccaggtgatg-3′. PCR condition was as follows: 45 cycles of 30s at 95°C, 30s at 58°C, and 60s at 72°C. Relative fold change in mRNA expression compared with control was calculated using the comparative C_t method, where C_t is the cycle number at which fluorescence first exceeds the threshold. C_t values were obtained by subtracting the values of β-actin C_t from the target gene C_t. Gene-specific primer sequences are available upon request. The specificity of amplification products was verified by agarose gel electrophoresis and melting curve analysis.

2.7. Immunohistochemistry Analysis of MMP-2. Paraffin-embedded osteosarcoma tissue specimens from pulmonary metastatic nodules of mice inoculated with Dkk-3-transfected 143B OS were available for immunohistochemical analysis. Four micrometer sections were deparaffinized in xylene and rehydrated in graded alcohol. Antigen retrieval was performed using 10 mM sodium citrate (pH 6.0) in a water bath at 95°C for 15 minutes. Slides were incubated with a rabbit polyclonal anti-MMP-2 antibody (Santa Cruz, CA, USA) at 1 : 300 dilution for 12 hr at RT using a humidified chamber. Slides were then incubated with a biotinylated anti-rabbit secondary antibody (Santa Cruz, CA, USA) at 1 : 200 dilution for 1 hr. Staining was visualized with diaminobenzidine using the Vectastain Elite Kit (Vector Lab, Burlingame, CA, USA) according to the manufacturer's instructions. Slides were counterstained with hematoxylin and photographed using a light microscope.

2.8. Soft Agar Colony Formation Assay. Soft agar colony formation assays were performed for 143B OS cells using six-well plates. Each well contained 2 mL of 0.8% agar in complete medium as the bottom layer, 1 mL of 0.35% agar in complete medium with 6,000 cells as the feeder layer, and 1 mL complete medium as the top layer. Cultures were maintained under standard culture conditions. The number of colonies was determined with an inverted phase-contrast microscope at ×100 magnification. A group of > 10 cells was counted as a colony. 14 days after the wells were seeded, mean number of colonies from 4 independent wells was calculated.

2.9. Wound Healing Assay. Motility was assessed with a scratch assay to measure two-dimensional cellular movement. For *in vitro* scratch assays, transfected 143B cells (PcDNA, Dkk-3) were seeded and grown in 24-well plates at a density of 1×10^5 cells/well in growth medium until they reached a confluence of ~90%. A scratch was made through each well using a sterile pipette tip. The monolayer was washed with a migration assay buffer consisting of serum-free medium plus 0.1% bovine serum albumin. The cells were monitored under the microscope (magnification ×10) for 0- and 12-hour time points after wounding. Images of cells were captured at the same position before and after incubation to assess the repair process. The experiment was repeated thrice.

2.10. Zymogram Assay. To determine the proenzyme and active form of MMP-2 and MMP-9, zymogram assay was done as previously described [21]. In brief, the condition medium was collected from Dkk-3-transfected 143B cells and control cells, and concentrated 20x using centricon (Millipore). Fifteen microliters of concentrated condition medium was separated by electrophoresis in 0.1% gelatin-impregnated gel (Bio-Rad). After getting renatured at room temperature for 1 hour in zymogram renature buffer, the gel was incubated overnight at 37°C in the zymogram development buffer (Bio-Rad). The gel was then stained with Coomassie Blue and destained according to the manufacturer's protocols (Bio-Rad). Gelatinolytic activity was visualized as clear bands on the gel.

2.11. Luciferase Reporter Assays for Wnt Inhibition. 143B cells were plated in a six-well plate at a density of 1.0×10^5 per well and incubated overnight. The cells were transiently cotransfected with 1.5 ug of TOPFLASH luciferase reporter plasmid (Upstate Biotechnology) and 1.5 ug of Dkk-3 (Addgene) or control PcDNA (Invitrogen) plasmids. Transfection was performed using Lipofectamine 2000 (Invitrogen) according to the manufacturer's protocol. After 48 h, cells were lysed with Glo Lysis Buffer (Promega) and luciferase activity was measured using the Bright-Glo Luciferase Assay System (Promega).

2.12. In Vivo Tumorigenesis and Metastasis Model. 4-week-old male *nu/nu* nude mice (Taconic) were housed in pathogen-free conditions. The animal protocol was approved by the Institutional Animal Care Utilization Committee. Once Dkk-3-transfected and vector-control-transfected 143B cells were grown to near confluence, they were resuspended in 0.03 mL of PBS (1×10^7 cells/mL PBS) and injected percutaneously into the tibia of anesthetized nude mice. Tumor size was measured every 3 days using a caliper. The tumor volume was calculated by the formula $1/6\ \pi\ ab^2$ (π = 3.14; a is the long axis, and b is the short axis of the tumor).

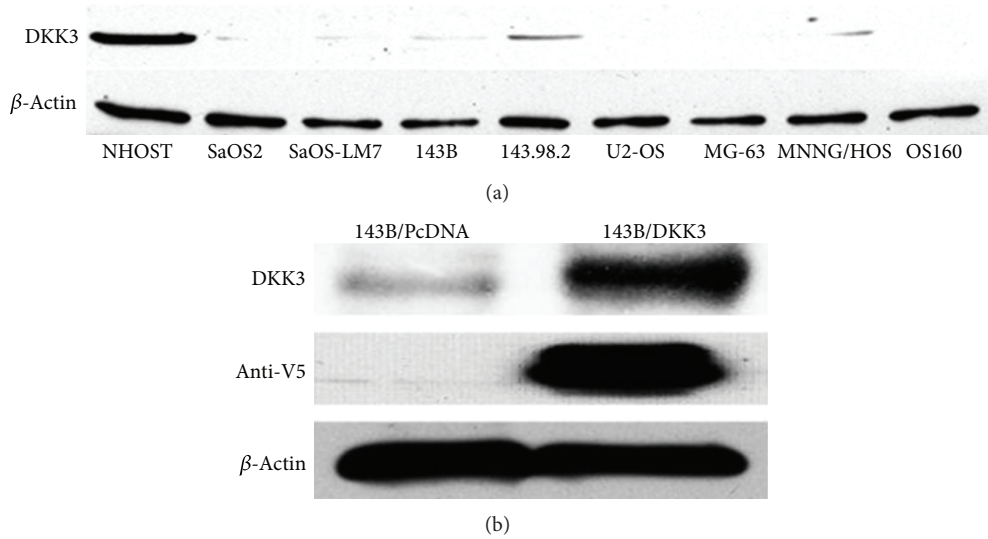

Figure 1: Dkk-3 protein expression of human osteoblast and OS cell lines and Dkk-3 transfected 143B cells. (a) Comparing expression of Dkk-3 in human osteoblast (NHOST) to 8 osteosarcoma cell lines (SaOS-2, SaOS-LM7, 143B, 143.98.2, US-OS, MG-63, MNNG/HOS, and OS160) via Western blot analysis using an anti-Dkk-3 antibody. All osteosarcoma cell types showed reduced expression of Dkk-3. (b) Ectopic expression of Dkk-3 in transfected 143B cells was confirmed by Western blot using an anti-V5 antibody. Dkk-3 is overexpressed in Dkk-3 transfected cells compared to PcDNA control vector.

Growth curves were plotted with the mean tumor volume ± SEM from 10 animals in each group. 21 days after injection, the animals were sacrificed according to the Institutional Animal Care Utilization Committee protocol. The tumors were harvested, measured, weighed, and fixed in 10% formalin. Wet tumor weight of each animal was calculated as mean weight ± SD from 10 animals in each group. Lungs were harvested and fixed in Bouin's solution. The number of surface lung metastatic nodules was counted, and the mean number of lung nodules was compared between the two groups. Microscopic lung metastases were visualized on 5 μm paraffin-embedded sections stained with H&E.

2.13. Statistical Analysis. Comparisons of cell viabilities between treated and control cell lines, number of colonies, fold change in levels of mRNA, and tumor weight were conducted using Student's t-test. For tumor growth experiments, repeated measures ANOVA was used to examine the differences in tumor volume among different time points and transfection-time interactions. Additional posttest was done to examine the differences in tumor volume between vector control and Dkk-3 transfection at each time point by conservative Bonferroni method. All statistical tests were 2 sided. Data was presented as a mean ± standard errors (SEs), and the level of significance was set at a P value < 0.05.

3. Results

3.1. Transfected Dkk-3/REIC Suppresses Tumor Growth in Nude Mice and Inhibits Pulmonary Metastasis. Given the *in vitro* data supporting reduced expression of Dkk-3 in various malignant cell lines, we wanted to examine the *in vivo* effect of transfected Dkk-3 of OS cells on nude mice. 143B osteosarcoma cell line was utilized given its propensity to grow quickly and metastasize to the pulmonary fields. As seen in other cancer cell lines [11–14, 16, 22], Dkk-3 protein expression was downregulated with varying degree in all osteosarcoma cell lines (Figure 1(a)). Out of 8 OS cell lines (SaOS-2, SaOS-LM7, 143B, 143.98.2, U2-OS, MG-63, MNNG/HOS, and OS160), the 3 which showed the least expression were U2-OS, MG-63, and OS160. The human osteoblast (NHOST) in comparison showed definite greater protein expression of Dkk-3.

Initially, we confirmed successful transfection of Dkk-3 into 143B cells by western blotting of the V5-tagged Dkk-3 protein using an anti-V5 antibody (Invitrogen; Figure 1(b)). Dkk-3-transfected and vector control-transfected 143B cells (equally resuspended in 0.03 mL of PBS to obtain 1×10^7 cells/mL PBS) were injected percutaneously into the tibia of anesthetized nude mice and tumor size was measured every 3 days. In comparison to the control vector, the Dkk-3-transfected 143B cells showed significant slower tumor growth rate ($P < 0.05$) (Figure 2(a)). After 21 days, animals were sacrificed and tumors harvested, and Dkk-3-transfected tumors were substantially smaller compared to the control (Figure 2(b)). These results suggest that overexpression of Dkk-3 inhibits tumorigenesis.

Given the propensity of osteosarcoma cells to metastasize to the pulmonary fields, lungs were harvested to analyze metastatic lesions. Gross anatomy of lung fields showed significantly higher number of nodules for the vector control-transfected 143B cells compared to the Dkk-3-transfected cells (Figure 2(c)). The Dkk-3-transfected 143B cell line formed 88.7% fewer lung nodules compared to the control (Student's t-test; $P \leq 0.01$) (Figure 2(d)). Histologic

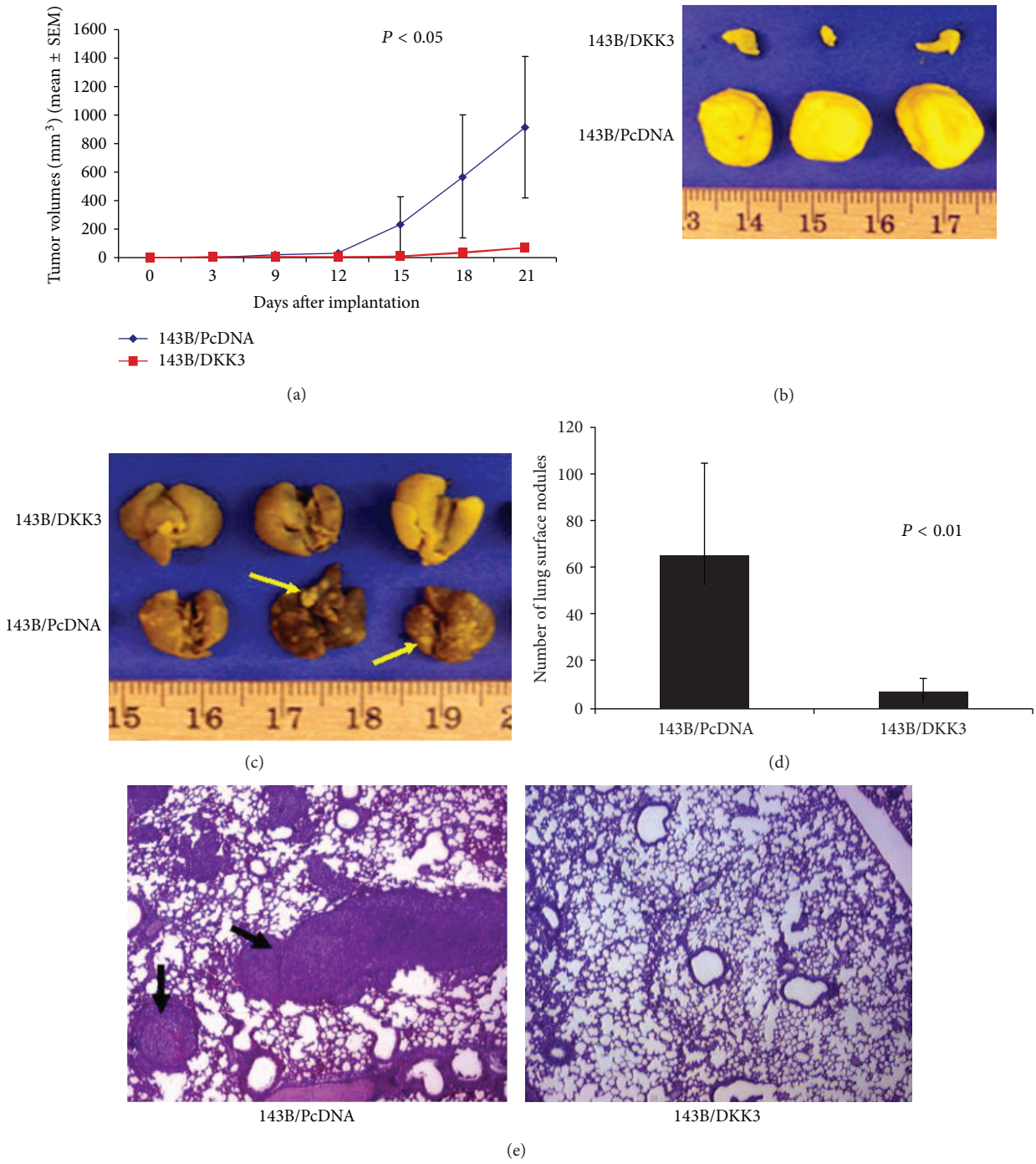

FIGURE 2: *In vivo*, Dkk-3 inhibits tumor growth in nude mice and decreases pulmonary metastasis in an orthotopic osteosarcoma mouse model. Transfected 143B cells (1×10^7) with either PcDNA (control) or Dkk-3 were injected percutaneously into the tibia of anesthetized nude mice. (a) Tumor growth curve after implantation of tumor cells. Tumor size was measured every 3 days using a caliper and volume calculated (points reflect mean tumor volume), each group contained 10 mice; bars, SEM. (b) Harvested tumor tissue. Tumors were harvested 21 days after inoculation. (c) Lungs were harvested from mice injected with transfected control (PcDNA) and Dkk-3-143B OS cells. Arrows point to surface lung nodules. (d) Surface pulmonary nodules were counted under a dissecting microscope. Columns represent mean number of pulmonary surface nodules from 10 mice in each group; bars, SEM. (e) Immunohistochemical H&E staining (×40 magnification) of lung sections from mice inoculated with either transfected vector control or Dkk-3-143B OS cells. Arrows represent lung metastatic nodules.

examination also substantiated smaller pulmonary nodules from the Dkk-3-transfected cells compared to the control-transfected cells (Figure 2(e)). These results show the remarkable inhibitory effects of Dkk-3 on pulmonary metastasis.

3.2. Dkk-3 Inhibits Motility, Anchorage-Independent Growth, and Cellular Viability. Given the results of our *in vivo* experiments, eliciting the potential molecular mechanism of Dkk-3 would be helpful in future gene targeting therapy. Cellular motility assay is an *in vitro* surrogate for assessing metastatic potential. Figure 3(a) demonstrated the difference in cellular motility of Dkk-3-transfected 143B cells compared to the control. After 12 hours of incubation after wounding, it was clear that Dkk-3-transfected 143B cells had significant slower cellular motility compared to the control-transfected cells.

Besides cellular motility, metastatic cancer cells also have the ability to proliferate independently of both external and internal signals that normally restrain growth. Soft agar colony formation assay was used to monitor anchorage-independent cellular growth. Figures 3(b) and 3(c) validated Dkk-3's ability to inhibit anchorage-independent growth. Dkk-3-transfected 143B cells formed 87.6% less colonies than the vector control cells ($P < 0.05$). These results confirm that Dkk-3 expression deters tumorigenesis in 143B cells.

Along with inhibiting cellular motility and anchorage-independent growth, Dkk-3-transfected OS cells also showed a decrease cell viability compared to the control vector. MTT assay at 72 hours showed a 49.6% decrease in cell viability for Dkk-3-transfected OS cells ($P < 0.001$) (Figure 3(d)). Furthermore, to assess the inhibition of canonical Wnt activity by Dkk-3, LEF-1/TCF4 transcriptional activity was examined with TOPFLASH luciferase reporter assay for Dkk-3-transfected 143B cells and PcDNA vector control. Compared with controls, Dkk-3 reduced LEF-1/TCF4 transcriptional activity significantly (Figure 3(e), Student's t-test; $P < 0.05$). These results support Dkk-3 inhibits canonical Wnt activity in 143B OS cells.

3.3. Dkk-3 Downregulates Matrix Metalloproteinase-2 and -9 Activities (MMP-2, MMP-9). We next examined the effect of Dkk-3 expression on matrix metalloproteinase (MMP) activities. Proteins of the MMP family are involved in the breakdown of extracellular matrix (ECM) in normal physiological processes as well as malignant processes, and its expression has been known to be regulated by Wnt signaling [23]. Besides ECM degradation, they also contribute significantly to tumor invasion and metastasis. Many studies have demonstrated a correlation between the overexpression of MMP with poor prognosis of various cancers, including osteosarcoma [24]. Based on these findings, we examined the effect of Dkk-3 expression on MMP-2 and MMP-9 activities. Zymography showed that ectopic expression of Dkk-3-transfected SaOS-2 cells resulted in decreased activities in both MMP-2 and MMP-9 compared to the vector control (Figure 4(a)). In addition, MMP-2 expression was also reduced by immunohistochemical analysis of pulmonary tissue from mice injected with Dkk-3/143B cells. Compared to Dkk-3 transfected tumors, pulmonary metastatic nodules from control tumors showed more intense staining of MMP-2 (Figure 4(b)).

3.4. Dkk-3 Inhibits the Epithelial-Mesenchymal Transition and Transcriptional Factors, Decreasing Tumorigenesis and Cellular Motility/Migration. Epithelial-mesenchymal transition (EMT) is a process characterized by loss of cell adhesion and increased cell mobility. EMT may be essential for numerous developmental processes including mesoderm and neural tube formation and tumorigenesis. Cells that are involved with EMT are known to lose cell adhesion and acquire expression of mesenchymal components, which ultimately aid in cellular motility and migration. This process has been shown in various human cancers, including breast, ovarian, esophagus, gastric, colon, endometrial and synovial sarcoma [25]. E-cadherin, an essential component of cell-cell junction, is normally downregulated during EMT. In our study, overexpression of Dkk-3 led to a reversal of the EMT in SaOS-2 cells, with upregulation of epithelial markers (E-cadherin, Keratin 8, and Keratin 18) by Western blot analysis and of E-cadherin by real-time RT-PCR (1585 fold upregulation, $P < 0.01$) (Figure 5(a)). On the contrary, mesenchymal markers (N-cadherin, fibronectin) were downregulated in Dkk-3-transfected SaOS-2 cell lines. The expression of N-cadherin mRNA in Dkk-3-transfected SaOS-2 cells was markedly reduced ($P < 0.01$), and Western blot analysis revealed N-cadherin and fibronectin were greatly reduced in Dkk-3-transfected cells (Figure 5(b)). Immunofluorescent staining also suggested a greater epithelial phenotype for Dkk-3-transfected cells. Compared to control vector, Dkk-3-transfected SaOS-2 cells showed greater immunofluorescent staining for E-cadherin compared to N-cadherin (Figure 5(c)). These data further support the role of Dkk-3 in modulating EMT in OS cell lines.

Several regulators of EMT are Wnt-responsive transcriptional repressors (Snail, Slug, and Twist) that have been shown to promote cancer progression and metastasis [25–28]. Figure 5(d) shows markedly decreased mRNA expression of Snail, Twist, and Slug in the Dkk-3-transfected SaOS-2 cells by 77.2%, 95.6%, and 99.8%, respectively ($P < 0.01$). Similarly, protein expression of these repressors is also reduced in Dkk-3-transfected cells compared to vector control cells (Figure 5(d)). This evidence suggests that in OS cells, Dkk-3 promotes a reversal of the EMT and down-regulation of transcriptional factors: Snail, Twist, and Slug.

3.5. Dkk-3 Downregulates S100A4, c-Met, and Phosphorylated MAPK and AKT. S100A4 is a member of the S100 family of calcium-binding proteins known to be involved in tumor metastasis [29]. S100A4 has been associated with enhanced metastatic potential, although the exact underlying mechanism is still unknown. Knockdown of S100A4 has been shown to decrease cell migration, tumorigenesis, and metastasis of OS [30, 31]. In our study, Western blot analysis showed that Dkk-3 overexpression was associated with down-regulation of S100A4 protein (Figure 6(a)), consistent with a reduction in metastatic potential.

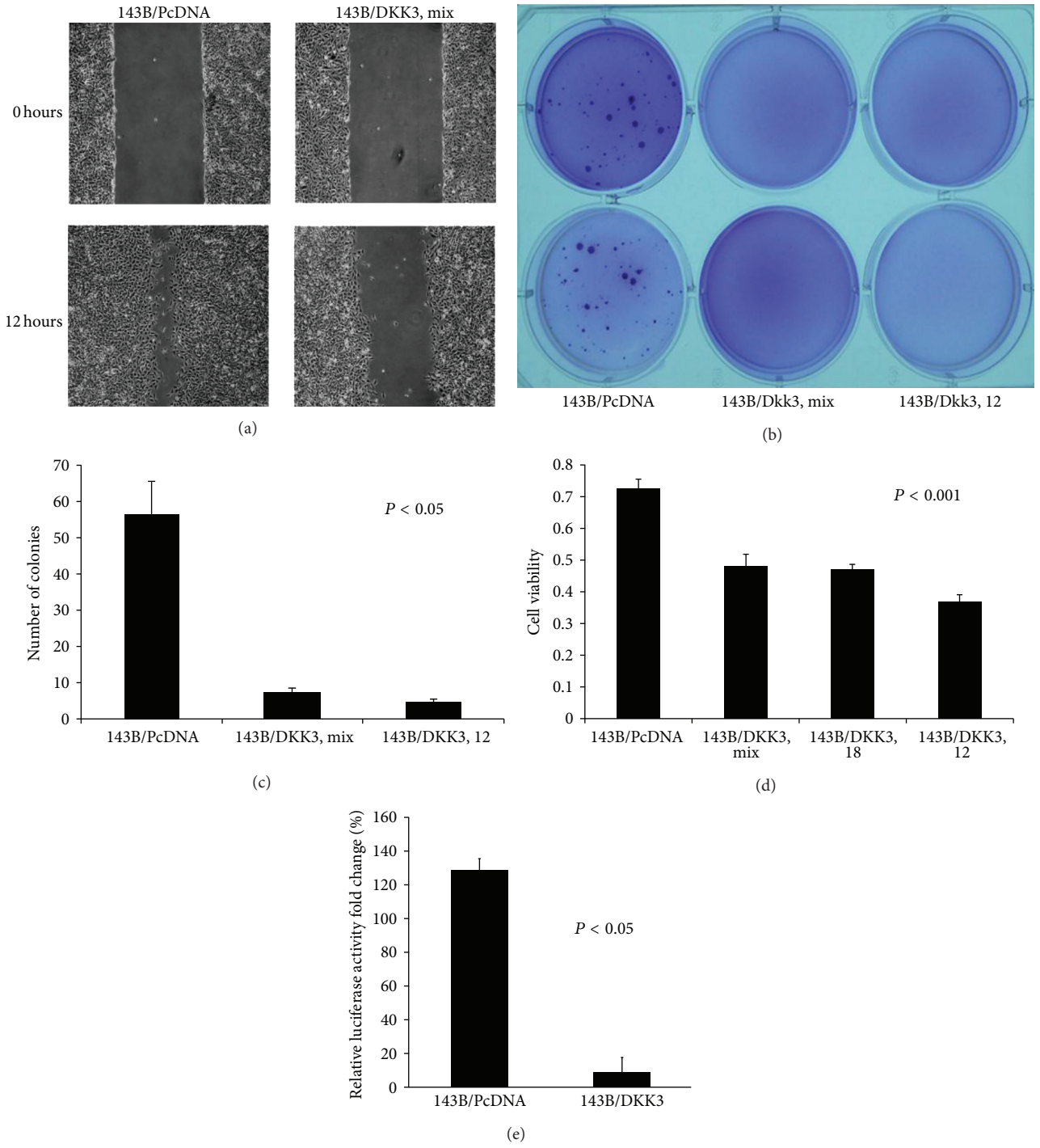

Figure 3: Dkk-3 inhibits cellular motility, anchorage-independent growth in soft agar and cellular viability. (a) Wound assay—photographs of scratch wounds at 0 and 12 hours after wounds were made. After 12 hours of incubation, under the fluorescence microscope, the Dkk-3-143B-transfected OS cells showed less migratory effect compared to the control vector. (b) and (c), Anchorage-independent colony formation assay showed decreased amount of colonies formed by Dkk-3-143B-transfected OS cells (both mixture of all Dkk-3 cells and a single Dkk-3 no. 12 plate) compared to transfected vector control 143B cells. (b) Photograph of soft agar colonies at 18 d after cell seeding. (c) Columns—mean number of colonies; bars—SEM. (d) MTT assay at 72 hours showed less cell viability for Dkk-3-transfected 143B cells (mix, individual cell plates nos. 12 and 18) compared to control vector. Experiments were replicated thrice. (e) Dkk-3-transfected 143B OS cells reduced TCF4 transcriptional activity compared with vector control transfection of 143B cells.

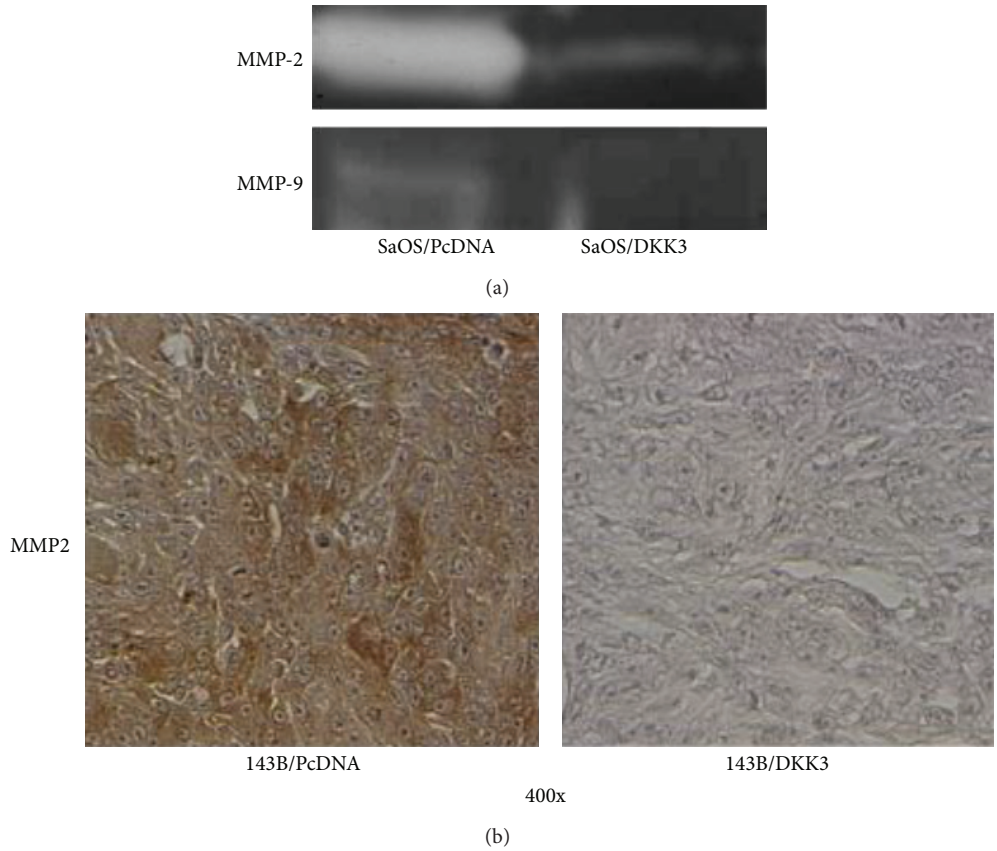

Figure 4: Dkk-3 deters invasive capacity of OS cells via downregulation of MMP-2 and -9 activities. (a) Gelatinolytic activities of MMP-2 and MMP-9 for Dkk-3-transfected SaOS-2 OS cells compared to vector control were evaluated by zymographic analysis. (b) Representative photographs of immunohistochemical detection of MMP-2 of pulmonary metastatic nodules in inoculated mice with Dkk-3-transfected-143B OS; magnification 400x.

In addition to S100A4, c-Met and its downstream kinases (MAPK and AKT) were also examined in Dkk-3-transfected cells. Met is a known protooncogene that encodes the hepatocyte growth factor (HGF) receptor. Met activation also results in activation of MAP kinase and AKT in OS cell lines, leading to increased proliferation and motility [32]. Compared to the control vector, Dkk-3-transfected SaOS-2 cells showed decreased protein expression of c-Met and its downstream effectors phosphorylated MAPK and AKT (Figure 6(b)), further suggesting the role of Dkk-3 as an inhibitor of tumorigenesis and metastasis.

4. Discussion

In the present study, Dkk-3 expression was downregulated in several OS cell lines. Overexpression of Dkk-3 in OS cell line SaOS-2 led to upregulation of epithelial markers (E-cadherin, Keratin-8 and -18) and down-regulation of mesenchymal makers (N-cadherin and fibronectin), suggesting a reversal of the EMT. Furthermore, Dkk-3 expression resulted in decreased cell motility as well as reduced tumor growth and pulmonary metastasis in an orthotopic xenograft model of OS. These cellular changes are associated with reduced activities of MMP-2 and MMP-9 as well as a decrease in oncogenic c-Met, phosphorylated MAPK and AKT, and reduced expression of metastasis-associated proteins S100A4, Slug, and Twist.

The Wnt/β-catenin pathway has been known to play a major role in multiple cancers, including osteosarcoma. By investigating key factors which enable this pathway for tumorigenesis, the hope is to create a more targeted approach that helps to improve prognosis of OS patients. Dkk-3/REIC expression has been shown to be downregulated in multiple cancer cell lines although its exact oncogenic suppressive mechanism is still unknown. We have previously shown that human OS cell lines express several Wnt ligand and frizzled receptor combinations, suggesting an autocrine mechanism of Wnt activation in OS [33]. Furthermore, we have reported that Dkk-3 inhibits cellular invasion and motility by modulating the Wnt/β-catenin pathway [10]. In the present study, through *in vivo* and *in vitro* analyses, we have demonstrated that Dkk-3 has the potential capacity to inhibit tumorigenesis and metastatic properties, at least in a subset of OS tumors. Using stably transfected OS cell lines, we were able to inject these cells orthotopically into nude mice to create a clinically relevant animal model of OS and to examine both local tumor growth as well as pulmonary metastasis from the primary

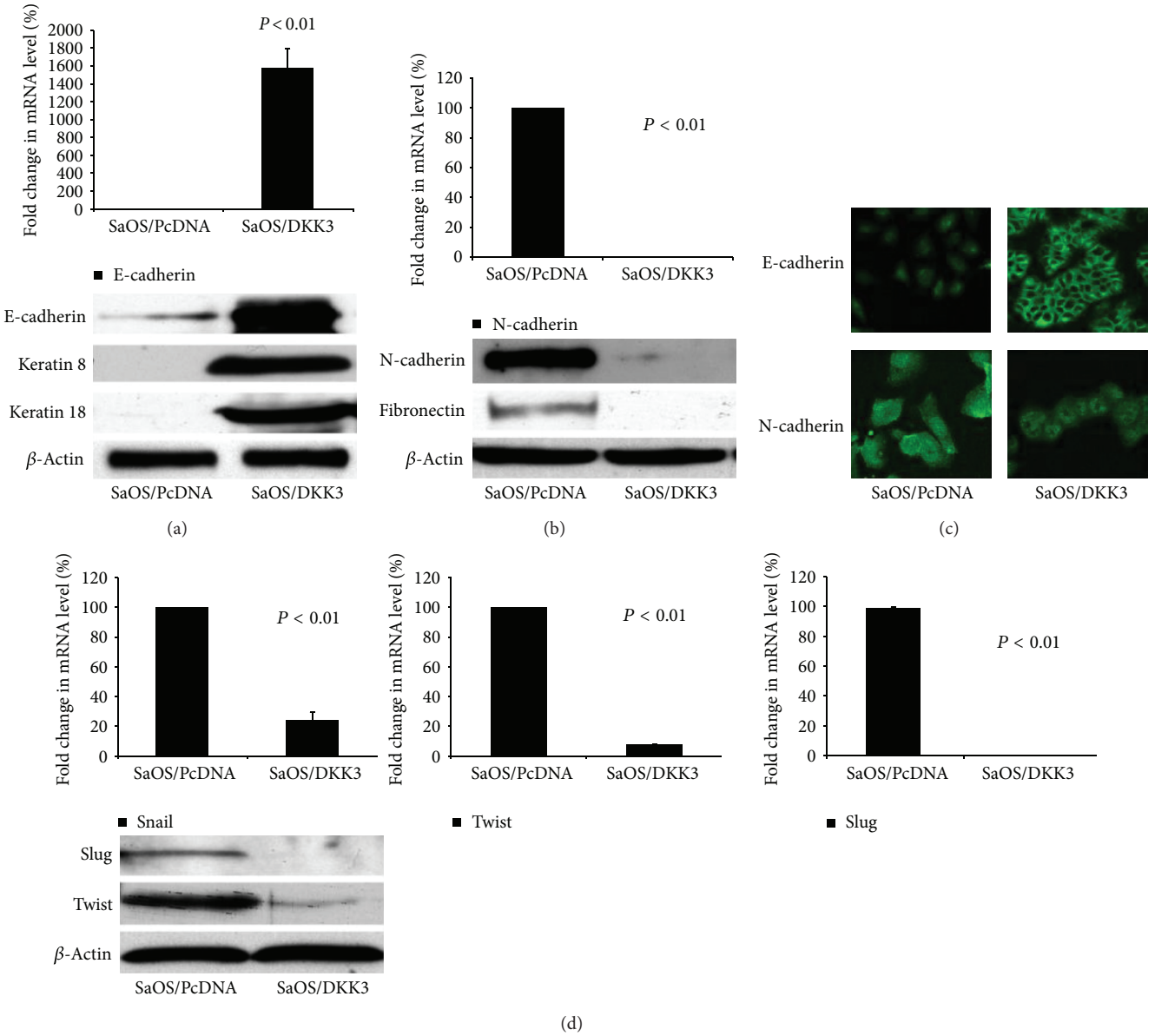

Figure 5: Dkk-3 inhibits epithelial-mesenchymal transitions and transcriptional factors, decreasing tumorigenesis and cellular motility/migration. (a) EMT-related marker, E-cadherin (epithelial marker) expression for Dkk-3-transfected SaOS-2 OS cells compared to control vector was determined by real-time RT-PCR. Columns, mean from 3 independent experiments; bars, SE. Western blot analysis showing expression of E-cadherin along with other epithelial markers, including Keratin 8, Keratin 18 for both subsets. Beta actin utilized as housekeeping gene. (b) EMT-related markers, N-cadherin (mesenchymal marker) fold changes in mRNA level comparing SaOS-2 OS control to Dkk-3-transfected SaOS-2 OS cells. Columns, mean from 3 independent experiments; bars, SE. Western blot analysis of mesenchymal markers (N-cadherin, fibronectin) for both subsets. (c) Immunofluorescent microscopy of N-cadherin and E-cadherin staining in transfected SaOS-2 OS cells; magnification 400x. (d) Real-time RT-PCR of transcription factors (Snail, Twist, and Slug) in transfected SaOS-2 OS cells; columns, mean from 3 independent experiments; bars, SE. Western blot analysis of Snail, Slug, and Twist in transfected SaOS-2 OS cells.

site. Consistent with our *in vitro* experiments, Dkk-3 demonstrates a remarkable suppressive effect on tumor growth. Furthermore, we observed pulmonary metastatic nodules that were present in much lower levels in mice injected with Dkk-3 transfected cells. These findings strongly suggest that targeting Dkk-3 for antitumorigenic and antimetastatic purposes should be investigated further.

S100A4 and c-Met have been shown to be a key prognostic marker in multiple cancers. *In vivo* experiments have shown evidence of S100A4 direct involvement in tumor progression and metastasis [29]. In our study, down-regulation of S100A4 in Dkk-3-transfected OS cells is consistent with the observation that Dkk-3 can suppress cellular invasion and motility. Not only is oncogenic c-Met expression decreased

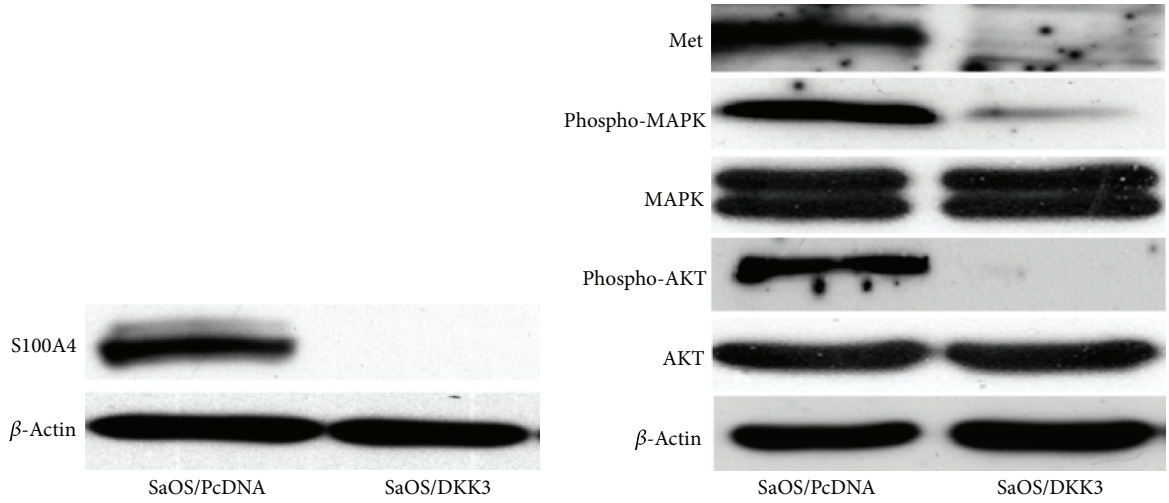

Figure 6: Dkk-3 modulates S100A4, Met, and downstream phosphorylated MAPK and AKT. (a) and (b) Western blot analysis demonstrating expressions of S100A4, Met, and phosphorylated/non-phosphorylated MAPK and AKT in Dkk-3 and control vector transfected SaOS-2 cells.

in Dkk-3-transfected OS cells, but its downstream activation of MAPK and AKT is similarly downregulated. These results show a strong correlation between Dkk-3 and antitumor and antimetastatic effects.

5. Conclusions

Despite current therapies using intensive neoadjuvant/adjuvant chemotherapy and wide surgical resection, we still have not made a significant impact in the prognosis of metastatic osteosarcoma. Multiple canonical and noncanonical Wnt/β-catenin pathway inhibitors and agonists are being explored for potential gene targeting therapies. Our results, both *in vitro* and *in vivo*, are intriguing and certainly suggest an important role for Dkk-3 in the pathobiology of human OS. The mechanisms of action of Dkk-3 are likely to involve multiple important oncogenic pathways and processes (i.e., S100A4, Met, MMPs, and EMT) and their complex interactions. Reexpressing Dkk-3 in Dkk-3-deficient OS can potentially prove to be of benefit as a preventive or therapeutic strategy.

Acknowledgments

B. H. Hoang received Grant support from NIH CA-116003, Chao Family Comprehensive Cancer Center, American Cancer Society, and Orthopaedic Research and Education Foundation. X. Zi is supported by NIH Grants CA129793 and CA122558, and the Neil Chamberlain Urological Cancer Research Fund. The authors thank Dr. Eugenie Kleinerman (MD Anderson Cancer Center) for the SaOS-LM7 cell line.

References

[1] G. Bacci, S. Ferrari, F. Bertoni et al., "Long-term outcome for patients with nonmetastatic osteosarcoma of the extremity treated at the istituto ortopedico rizzoli according to the istituto ortopedico rizzoli/osteosarcoma-2 protocol: an updated report," *Journal of Clinical Oncology*, vol. 18, no. 24, pp. 4016–4027, 2000.

[2] S. S. Bielack, B. Kempf-Bielack, G. Delling et al., "Prognostic factors in high-grade osteosarcoma of the extremities or trunk: an analysis of 1,702 patients treated on neoadjuvant cooperative osteosarcoma study group protocols," *Journal of Clinical Oncology*, vol. 20, no. 3, pp. 776–790, 2002.

[3] L. Kager, A. Zoubek, U. Pötschger et al., "Primary metastatic osteosarcoma: presentation and outcome of patients treated on neoadjuvant cooperative osteosarcoma study group protocols," *Journal of Clinical Oncology*, vol. 21, no. 10, pp. 2011–2018, 2003.

[4] V. Mialou, T. Philip, C. Kalifa et al., "Metastatic osteosarcoma at diagnosis: prognostic factors and long-term outcome—the French pediatric experience," *Cancer*, vol. 104, no. 5, pp. 1100–1109, 2005.

[5] J. B. Hayden and B. H. Hoang, "Osteosarcoma: basic science and clinical implications," *Orthopedic Clinics of North America*, vol. 37, no. 1, pp. 1–7, 2006.

[6] B. T. MacDonald, K. Tamai, and X. He, "Wnt/β-catenin signaling: components, mechanisms, and diseases," *Developmental Cell*, vol. 17, no. 1, pp. 9–26, 2009.

[7] R. T. Moon, "Wnt/beta-catenin pathway," *Science's STKE*, vol. 2005, no. 271, article cm1, 2005.

[8] C. Jamieson, M. Sharma, and B. R. Henderson, "Wnt signaling from membrane to nucleus: beta-catenin caught in a loop," *The International Journal of Biochemistry & Cell Biology*, vol. 44, no. 6, pp. 847–850, 2012.

[9] H. H. Luu, R. Zhang, R. C. Haydon et al., "Wnt/β-catenin signaling pathway as novel cancer drug targets," *Current Cancer Drug Targets*, vol. 4, no. 8, pp. 653–671, 2004.

[10] B. H. Hoang, T. Kubo, J. H. Healey et al., "Dickkopf 3 inhibits invasion and motility of saos-2 osteosarcoma cells by modulating the Wnt-β-catenin pathway," *Cancer Research*, vol. 64, no. 8, pp. 2734–2739, 2004.

[11] S. Y. Hsieh, P. S. Hsieh, C. T. Chiu, and W. Y. Chen, "Dickkopf-3/REIC functions as a suppressor gene of tumor growth," *Oncogene*, vol. 23, no. 57, pp. 9183–9189, 2004.

[12] K. Zhang, M. Watanabe, Y. Kashiwakura et al., "Expression pattern of REIC/Dkk-3 in various cell types and the implications of the soluble form in prostatic acinar development," *International Journal of Oncology*, vol. 37, no. 6, pp. 1495–1501, 2010.

[13] I. L. Jung, J. K. Hyo, C. K. Kug, and G. K. In, "Knockdown of the Dickkopf 3 gene induces apoptosis in a lung adenocarcinoma," *International Journal of Molecular Medicine*, vol. 26, no. 1, pp. 33–38, 2010.

[14] S. Kuphal, S. Lodermeyer, F. Bataille, M. Schuierer, B. H. Hoang, and A. K. Bosserhoff, "Expression of Dickkopf genes is strongly reduced in malignant melanoma," *Oncogene*, vol. 25, no. 36, pp. 5027–5036, 2006.

[15] P. Polakis, "Wnt signaling and cancer," *Genes and Development*, vol. 14, no. 15, pp. 1837–1851, 2000.

[16] Y. Mizobuchi, K. Matsuzaki, K. Kuwayama et al., "REIC/Dkk-3 induces cell death in human malignant glioma," *Neuro-Oncology*, vol. 10, no. 3, pp. 244–253, 2008.

[17] K. Ueno, H. Hirata, S. Majid et al., "Wnt antagonist DICKKOPF-3 (Dkk-3) induces apoptosis in human renal cell carcinoma," *Molecular Carcinogenesis*, vol. 50, no. 6, pp. 449–457, 2011.

[18] C. Zenzmaier, G. Untergasser, M. Hermann, S. Dirnhofer, N. Sampson, and P. Berger, "Dysregulation of Dkk-3 expression in benign and malignant prostatic tissue," *Prostate*, vol. 68, no. 5, pp. 540–547, 2008.

[19] R. Tanimoto, F. Abarzua, M. Sakaguchi et al., "REIC/Dkk-3 as a potential gene therapeutic agent against human testicular cancer," *International Journal of Molecular Medicine*, vol. 19, no. 3, pp. 363–368, 2007.

[20] Z. R. Yang, W. G. Dong, X. F. Lei et al., "Overexpression of Dickkopf-3 induces apoptosis through mitochondrial pathway in human colon cancer," *World Journal of Gastroenterology*, vol. 18, no. 14, pp. 1590–1601, 2012.

[21] Y. Guo, X. Zi, Z. Koontz et al., "Blocking Wnt/LRP5 signaling by a soluble receptor modulates the epithelial to mesenchymal transition and suppresses met and metalloproteinases in osteosarcoma Saos-2 cells," *Journal of Orthopaedic Research*, vol. 25, no. 7, pp. 964–971, 2007.

[22] J. Veeck and E. Dahl, "Targeting the Wnt pathway in cancer: the emerging role of Dickkopf-3," *Biochimica et Biophysica Acta*, vol. 1825, no. 1, pp. 18–28, 2012.

[23] B. Wu, S. P. Crampton, and C. C. W. Hughes, "Wnt Signaling induces matrix metalloproteinase expression and regulates T cell transmigration," *Immunity*, vol. 26, no. 2, pp. 227–239, 2007.

[24] M. Uchibori, Y. Nishida, T. Nagasaka, Y. Yamada, K. Nakanishi, and N. Ishiguro, "Increased expression of membrane-type matrix metalloproteinase-1 is correlated with poor prognosis in patients with osteosarcoma," *International Journal of Oncology*, vol. 28, no. 1, pp. 33–42, 2006.

[25] K. F. Becker, E. Rosivatz, K. Blechschmidt, E. Kremmer, M. Sarbia, and H. Höfler, "Analysis of the E-cadherin repressor snail in primary human cancers," *Cells Tissues Organs*, vol. 185, no. 1–3, pp. 204–212, 2007.

[26] P. McQueen, S. Ghaffar, Y. Guo et al., "The Wnt signaling pathway: implications for therapy in osteosarcoma," *Expert Review of Anticancer Therapy*, vol. 11, no. 8, pp. 1223–1232, 2011.

[27] Y. Kang and J. Massagué, "Epithelial-mesenchymal transitions: twist in development and metastasis," *Cell*, vol. 118, no. 3, pp. 277–279, 2004.

[28] L. R. Howe, O. Watanabe, J. Leonard, and A. M. C. Brown, "Twist is up-regulated in response to Wnt1 and inhibits mouse mammary cell differentiation," *Cancer Research*, vol. 63, no. 8, pp. 1906–1913, 2003.

[29] S. C. Garrett, K. M. Varney, D. J. Weber, and A. R. Bresnick, "S100A4, a mediator of metastasis," *Journal of Biological Chemistry*, vol. 281, no. 2, pp. 677–680, 2006.

[30] M. Fujiwara, T. G. Kashima, A. Kunita et al., "Stable knockdown of S100A4 suppresses cell migration and metastasis of osteosarcoma," *Tumour Biology*, vol. 32, no. 3, pp. 611–622, 2011.

[31] G. Zhang, M. Li, J. Jin et al., "Knockdown of S100A4 decreases tumorigenesis and metastasis in osteosarcoma cells by repression of matrix metalloproteinase-9," *Asian Pacific Journal of Cancer Prevention*, vol. 12, no. 8, pp. 2075–2080, 2011.

[32] N. Coltella, M. C. Manara, V. Cerisano et al., "Role of the MET/HGF receptor in proliferation and invasive behavior of osteosarcoma," *The FASEB Journal*, vol. 17, no. 9, pp. 1162–1164, 2003.

[33] B. H. Hoang, T. Kubo, J. H. Healey et al., "Expression of LDL receptor-related protein 5 (LRP5) as a novel marker for disease progression in high-grade osteosarcoma," *International Journal of Cancer*, vol. 109, no. 1, pp. 106–111, 2004.

Hindawi Publishing Corporation
Sarcoma
Volume 2012, Article ID 636405, 5 pages
doi:10.1155/2012/636405

Clinical Study

Survival Trends and Long-Term Toxicity in Pediatric Patients with Osteosarcoma

Melanie M. Hagleitner,[1] Eveline S. J. M. de Bont,[2] and D. Maroeska W. M. te Loo[1]

[1] *Department of Pediatric Hematology and Oncology, Radboud University Nijmegen Medical Centre, P.O. Box 9101, 6500 HB Nijmegen, The Netherlands*
[2] *Department of Pediatric Hematology and Oncology, University Medical Centre Groningen, University of Groningen, P.O. Box 30.001, 9700 RB Groningen, The Netherlands*

Correspondence should be addressed to Melanie M. Hagleitner, mm.hagleitner@cukz.umcn.nl

Received 4 July 2012; Revised 23 October 2012; Accepted 2 November 2012

Academic Editor: Norman Jaffe

Background. This study was conducted to investigate the clinical characteristics and treatment results of osteosarcoma in pediatric patients during the past 30 years. Trends in survival rates and long-term toxicity were analyzed. *Procedure*. 130 pediatric patients under the age of 20 years with primary localized or metastatic high-grade osteosarcoma were analyzed regarding demographic, treatment-related variables, long-term toxicity, and survival data. *Results*. Comparison of the different time periods of treatment showed that the 5-year OS improved from 58.6% for children diagnosed during 1979–1983 to 78.6% for those diagnosed during 2003–2008 ($P = 0.13$). Interestingly, the basic treatment agents including cisplatin, doxorubicin, and methotrexate remained the same. Treatment reduction due to acute toxicity was less frequent in patients treated in the last era (7.1% versus 24.1% in patients treated in 1979–1983; $P = 0.04$). Furthermore, late cardiac effects and secondary malignancies can become evident many years after treatment. *Conclusion*. We elucidate the prevalence of toxicity to therapy of patients with osteosarcoma over the past 30 years. The overall improvement in survival may in part be attributed to improved supportive care allowing regimens to be administered to best advantage with higher tolerance of chemotherapy and therefore less chemotherapy-related toxicity.

1. Introduction

Osteosarcoma comprises 5% of all pediatric malignancies and is the most common primary bone cancer in children and adolescents. It is a highly aggressive tumor that usually involves the metaphysis of long bones and metastasizes primarily to the lung. Before the 1970s, the prognosis for patients with high-grade osteosarcoma was poor, with long-term survival rates of less than 20% [1]. Advances in adjuvant and neoadjuvant chemotherapy have improved the 5-year disease-free survival to more than 60% [2]. Since then different attempts have been made to further improve prognosis. However, it has been demonstrated that neither dose intensification nor addition of newer agents does improve survival [3–6]. Furthermore, patients that survive experience prolonged periods of rehabilitation after long periods of chemotherapeutic treatment and after often disabling surgery. Although the long-term toxicities have not been assessed completely, cardiotoxicity already emerged as a significant price of cure for survivors of osteosarcoma patients [7]. Monitoring trends in survival and the long term toxicities is essential to enhance current treatment regimens.

To gain more insight in the young patients, as osteosarcoma is predominantly being a disease that affects young patients, we investigate survival trends in this patient group and subsequently analyze the occurrence of long term toxicity over the last three decades.

2. Material and Methods

2.1. Patients. In total 130 pediatric patients were consecutively treated between 1979 and 2008 in two different centers: Radboud University Nijmegen Medical Centre and University Medical Centre Groningen. All patients under

the age of 20 years with newly diagnosed, primary localized, or metastatic high-grade osteosarcoma were evaluated. Complete clinical and pathologic records and appropriate data regarding followup were present. Informed consent was obtained for all patients.

2.2. Treatment. Information from the patients' medical charts about cumulative dosage of treatment, treatment response (good responders defined as <10% vital cells after neoadjuvant therapy), reduction of chemotherapy (defined as >15% reduction of planned chemotherapy), and surgical approach was collected. The overall period was split into subperiods relating to the major changes in protocol (1979–1983, 1984–2002, and 2003–2008). In the first era from 1979–1983 a T10-based multidrug regimen consisting of six cycles of doxorubicin 30 mg/m^2 daily for 2-3 consecutive days, six cycles of cisplatin 120 mg/m^2 administered by repeated 6 hours infusions, 8–12 cycles of high-dose methotrexate 8–12 mg/m^2 with appropriate folinic acid rescue, and 1-2 cycles of BCD was used. From 1984 to 2002 trials with control arm treatment of six cycles of doxorubicin 25 mg/m^2 daily for 3 days in combination with cisplatin 100 mg/m^2 as a continuous infusion were used. The comparison arm consisted of only four doxorubicin/cisplatin courses and additionally 12 courses of high-dose methotrexate 12 mg/m^2 with appropriate folinic acid rescue. In the last era from 2003 to 2008 patients was treated with six cycles of doxorubicine 25 mg/m^2 daily for 3 days, four cycles of cisplatin 120 mg/m^2 as a continuous infusion, and 12 cycles of high-dose methotrexate 8–12 g/m^2 with appropriate folinic acid rescue.

2.3. Survival. Overall survival (OS) and disease-free survival (DFS) were estimated using the Kaplan-Meier method [8]. OS was defined as the interval between diagnosis and death from any cause. Patients alive at the date of last followup were censored at that time point. DFS was defined as the interval between diagnosis and disease progression/recurrence. Patients without disease recurrence at the date of last followup were censored at that date. Cox's proportional hazard regression analysis was used to determine significance of differences in survival curves. Confidence intervals were calculated at the 95% level. We evaluated gender, location, stage, treatment, treatment response, and toxicity-induced reduction of chemotherapy as prognostic factors. Associations between outcome and potential predictors were evaluated with the Fisher's exact test for categorical variables. Statistical analysis was performed using SSPS software (version 16.0, SSPS Inc, Chicago, IL, USA).

2.4. Long-Term Toxicities. Long-term toxicities after chemotherapeutic treatment were evaluated regarding development of secondary malignancies, cardiotoxicity, and ototoxicity. The length of time at risk for the secondary malignancy neoplasm (SMN) was calculated from the date of diagnosis of primary osteosarcoma until the date of diagnosis of the second malignancy. The cumulative incidence rate of second malignancies was calculated based on the method of Gray [9]. For the analysis of cardiac toxicity resulting from doxorubicin therapy, we included surviving patients who underwent serial echocardiographic evaluations before, during, and at least one followup echocardiogram after the initial treatment with doxorubicin. An echocardiogram at the end of chemotherapy was recommended annually for 5 years. Data concerning the fractional shortening (FS) value were collected. Cardiac dysfunction was defined as a decrease in FS <28% or a reduction of more than 10% [10]. Hearing loss, a complication of cisplatin was defined according to Brock Criteria [11] (grade 0: <40 dB at all frequencies; grade1: ≥40 dB at 8000 Hz; grade 2: ≥40 dB at 4000 Hz; grade3: ≥40 dB at 2000 Hz; grade 4: ≥40 dB at 1000 Hz). For this analysis only survivors were included with a baseline audiogram and an audiogram at the end of treatment.

3. Results and Discussion

3.1. Patients. The median age at diagnosis was 14.4 years (range from 4.5 to 19.9 years). There were 72 male patients (55.4%; median age: 14.8 years; range from 6.3 to 19.9 years) and 58 female patients (44.6%; median age: 13.9 years; range from 4.5 to 19.1 years). At diagnosis, 29 patients (22.3%) had metastases and in 9 patients (6.6%) the tumor was located in the axial skeleton.

3.2. Survival

3.2.1. Overall Survival. At a followup ranging between 4 and 33 years (median 8.9 years), 51 patients (39%) died. Of all deaths, 45 were directly related to osteosarcoma with 16 deaths due to progressive disease, eight due to local recurrence, and 21 after the development of distant metastases. The development of recurrent disease was predictive of death. Incidence of recurrences was relatively stable after 5 years with only three patients developing disease recurrence more than 5 years after diagnosis. Of the remaining six patients that died, four patients developed a second malignancy which was fatal, and two patients passed away due to anthracycline-induced cardiomyopathy. The 5-year OS of the whole population was 66.9% ± 0.15 the 10-year OS was 64.6% ± 0.23; the 20-year OS was 62.3% ± 0.82. These findings are in concordance with earlier reports in the literature [12, 13]. In total, 60 patients had a followup longer than 5 years, 38 patients were followed for more than 10 years, and a group of 20 patients was followed beyond 20 years. Comparison of the different time periods of treatment showed that the 5-year OS improved from 58.6% for children diagnosed during 1979–1983 to 78.6% for those diagnosed during 2003–2008 ($P = 0.13$; Figure 1). The distribution of known prognostic factors, such as metastatic disease at diagnosis, tumor location and good histologic response to neoadjuvant chemotherapy, was comparable regarding the different time periods (Table 1).

3.2.2. Disease-Free Survival. The 5-year DFS of the whole group was 59.2% ± 0.18. Patients with nonmetastatic osteosarcoma disease showed a DFS of 65.3% versus 37.9% in

Table 1: Distribution of prognostic factors over three decades.

Prognostic factor (N)	1979–1983 $N = 29$	1984–2002 $N = 59$	2003–2008 $N = 42$	P
Metastases at diagnosis	24.1% (7)	25.4% (15)	16.7% (7)	0.58
Tumor in axial skeleton	6.9% (2)	8.5% (5)	4.8% (2)	0.51
Good histologic response	24.1% (7)	23.7% (14)	35.7% (15)	0.55
>15% reduction due to toxicity	24.1% (7)	20.3% (12)	7.1% (3)	0.04

patients with metastases at diagnosis. During the past 3 decades the DFS of patients with metastases increased from 28.6% in 1979–1983, 40.0% in 1984–2002 to 42.9% in 2003–2008. The same trend is seen in patients with bad histologic response to neoadjuvant chemotherapy: 5-year DFS increased from 30.0% in 1979–1983, 57.6% in 1984–2002 to 65.4% in 2003–2008. Comparison of DFS in patients with axial involvement was not possible due to a small group.

3.3. Treatment

3.3.1. Chemotherapeutic Treatment. In the first era, surgical resection was performed after 4 weeks of neoadjuvant chemotherapy, after 1984 resection was performed in the 10th week of induction therapy. Good histologic response to neoadjuvant chemotherapy was observed in 13.3% of patients treated with cisplatin and doxorubicin and in 29.4% of patients additionally treated with methotrexate ($P = 0.083$). Although an increased rate of good histologic responders was seen in the group additionally treated with methotrexate, comparing the regimen arms with and without methotrexate, no evident difference was seen in 5-year OS (HR = 0.75; 95% CI = 0.39–1.27; $P = 0.24$) or 5-year DFS (HR = 0.75; 95% CI = 0.43–1.29; $P = 0.29$). The effect of high-dose methotrexate in the treatment of osteosarcoma is not unambiguously proven in the literature. Several studies have shown a relationship between peak serum concentrations of methotrexate and improved histologic response [14–16]. However, a Cochrane systematic review comparing the effectiveness of methotrexate was unable to make clear conclusions due to the lack of randomized controlled trials using high-dose methotrexate as the only difference between the intervention and control group [17].

3.3.2. Toxicity-Related Treatment Reduction. Chemotherapy was reduced due to severe bone marrow depression ($N = 6$), renal toxicity ($N = 3$), ototoxicity ($N = 3$), cardiotoxicity ($N = 3$), and adverse effects to methotrexate, like methotrexate encephalopathy ($N = 1$) or allergic reactions to methotrexate ($N = 3$). Interestingly, treatment reduction due to acute toxicity is less frequent in patients treated between 2003 and 2008 than in patients treated between 1984 and 1998 and in patients treated between 1979 and 1983 ($P = 0.04$, Table 1).

3.3.3. Surgical Treatment. Analysis of surgical treatment method showed a rise from 26.9% of patients with limb salvage treatment in 1979–1983 to 69% in 2003–2008.

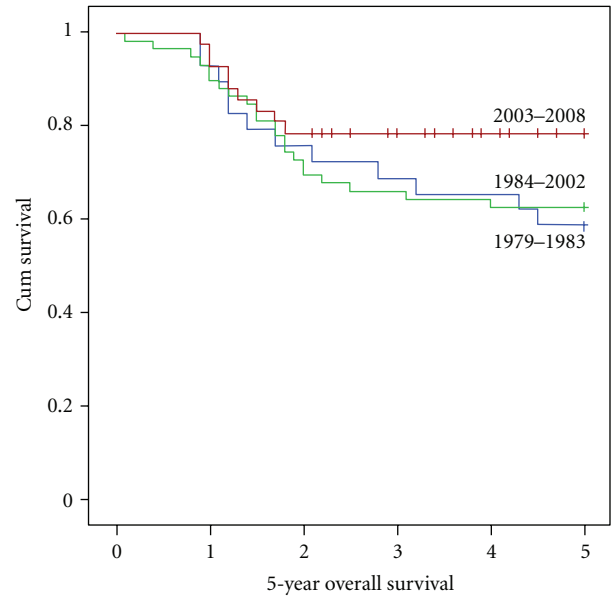

Figure 1: 5-year overall survival in pediatric patients with osteosarcoma over three decades.

The 5-year DFS rates were 57.8% for limb salvage treatment and 66.1% for amputation (HR = 1.35; 95% CI = 0.76–2.39; $P = 0.30$). The advancement of patients with limb salvage treatment could be expected considering that amputation patients might have had more advanced disease. A slightly but not significant improvement of DFS was seen in both surgical methods over the past three decades (data not shown).

3.4. Long-Term Toxicity

3.4.1. Secondary Malignancy Neoplasm. In total, seven patients (5.3%) developed a second malignancy, with a median latency from original diagnosis to second malignancy of 12 years (range 2.4–23 years). Second malignancies were two patients with acute lymphatic leukemia, four patients with breast cancer, and one patient with gastric adenocarcinoma. Of the seven patients who developed secondary malignancy neoplasm (SMN), two patients had a history of Li-Fraumeni syndrome. Both patients developed SMN within 5 years after treatment of osteosarcoma. The 5- and 10-year estimated cumulative SMN incidence rates were 1.5% ± 1.1% and 3.1% ± 1.3%, respectively, which is similar to earlier studies in survivors of osteosarcoma [18, 19].

Overall, the incidence ratio of secondary malignancies in long-term survivors of osteosarcoma is much less compared to other malignancies, for example, Hodgkin disease [20]. However, the cohort has been followed for a median of 8.9 years, and it is likely that with increasing followup, second malignancies will emerge, due to a latency of 10 to 15 years.

3.4.2. Cardiotoxicity. In 46 patients sufficient data concerning baseline and followup echocardiogram was available. No patient had clinically evident cardiac disease before chemotherapy. Before starting therapy with doxorubicin the median FS value was 36%. In 8 patients the FS decreased <28% during therapy, with a median change in the percent FS value of 4% which is in concordance with earlier studies on this subject [21]. The long-term implications of doxorubicin-associated echocardiographic abnormalities are not fully understood, but at least one study suggests that echocardiographic abnormalities are progressive over time [22]. In our cohort, three patients with decreased FS during therapy remained to have cardiac dysfunction after finishing primary treatment. In total, 11 out of 46 patients developed cardiac dysfunction in the followup period. The median frequency of cardiac evaluation in the first five years was three (range: 1–5). The median latency of cardiac effects after finishing primary therapy was 219 days (range: from 30 days to 28.2 years). Six out of 11 patients with cardiac dysfunction experienced symptomatic heart failures, four of them more than 5 years after primary treatment and regular controls. Two patients died of cardiomyopathy and three of metastatic disease, which occurred after the diagnosis of cardiomyopathy. Affected patients were predominantly treated in the first two decades of our study realizing that the last cohort treated might not had enough followup to adequately evaluate this late sequelae. All patients received a mean cumulative doxorubicin dose of 450 mg/m^2.

3.4.3. Ototoxicity. Cisplatin-associated hearing loss develops in the period when cisplatin is administered, and it has already been observed in patients treated with a single dose of 50 mg/m^2 [23]. However, it is unlikely to improve over time, and as even mild hearing loss can have considerable impact on the social-emotional development of a child [24], it is considered to be one of the late effects in the treatment of osteosarcoma patients. Of the 79 survivors in our study, 62 (78.5%) had an audiogram at the end of treatment. Preexisting hearing loss was not reported in one of these patients. Of the 62 survivors with an audiogram, 31 patients (50%) had no hearing loss, 23 patients (37.1%) were Brock grade I, and 7 patients (11.1%) developed severe hearing loss (Brock grades 3 and 4). All patients with severe hearing loss required hearing aids. No difference was seen in cumulative dosage of cisplatin comparing patients with severe hearing loss (cumulative dosage: 407 mg/m^2) versus patients with grade 0,1 or 2 hearing loss (cumulative dosage: 442 mg/m^2, $P = 0.55$). Furthermore, no difference in prevalence of severe ototoxicity was seen between the drug regimens using either 600 mg/m^2 or 480 mg/m^2 cisplatin ($P = 0.25$) or continuous infusion versus repeated 6-hour infusions ($P = 0.76$).

Like other studies in childhood cancer [25] we showed an improved survival of patients with osteosarcoma over the past decades. This improvement is seen in all subgroups irrespective of known prognostic factors like metastases at diagnosis or histological response to neoadjuvant therapy. This increase in childhood cancer survival is often attributed to more effective treatment strategies. However, in our study the treatment agents and dosage basically remained the same over the past 30 years with cumulative doses of doxorubicin 450 mg/m^2, cisplatin 480 or 600 mg/m^2, and high-dose methotrexate 96–144 g/m^2 appropriate to age. Furthermore, there was no difference in method of administration regarding doxorubicin and high-dose methotrexate. Cisplatin was administered as a 6-hour infusion during 1979–1983 in our study and then as continuous infusion. While continuous cisplatin infusions are observed to be considerably ototoxic (Lanvers-Kaminsky PBC 2006 [26]), we found no difference in our study. Therefore, other factors like empiric use of broad spectrum antibiotics in case of neutropenic fever, pain management, antiemetics, nutrition, blood banking, and improved pediatric intensive care might have improved the acceptability of the current treatment. On the other hand, with an increasing number of cancer survivors detection of late effects of osteosarcoma therapy is required. In this study, we show that late cardiac effects and SMN can become evident many years after treatment and can have profound impact on cancer survivors.

In conclusion, these data elucidate the prevalence of toxicity to therapy in children with osteosarcoma. Further studies concerning the management of long-term toxicities are needed to finally improve survival rates in patients with osteosarcoma.

Acknowledgment

This project was supported by a Grant from the Foundation KiKa, Amstelveen, The Netherlands.

References

[1] G. Bacci, P. Picci, S. Ferrari et al., "Primary chemotherap and deleyed surgery for nonmetastatic osteosarcom of the extremities: results in 164 patients preoperatively treates with high doses of methotrexate followed by cisplatin and doxorubin," *Cancer*, vol. 72, pp. 3227–3230, 1993.

[2] S. S. Bielack, D. Carrle, J. Hardes, A. Schuck, and M. Paulussen, "Bone tumors in adolescents and young adults," *Current Treatment Options in Oncology*, vol. 9, no. 1, pp. 67–80, 2008.

[3] M. Eselgrim, H. Grunert, T. Kühne et al., "Dose intensity of chemotherapy for osteosarcoma and outcome in the Cooperative Osteosarcoma Study Group (COSS) trials," *Pediatric Blood and Cancer*, vol. 47, no. 1, pp. 42–50, 2006.

[4] I. J. Lewis, S. Weeden, D. Machin, D. Stark, and A. W. Craft, "Received dose and dose-intensity of chemotherapy and outcome in nonmetastatic extremity osteosarcoma," *Journal of Clinical Oncology*, vol. 18, no. 24, pp. 4028–4037, 2000.

[5] G. Bacci, C. Forni, S. Ferrari et al., "Neoadjuvant chemotherapy for osteosarcoma of the extremity: intensification of

preoperative treatment does not increase the rate of good histologic response to the primary tumor or improve the final outcome," *Journal of Pediatric Hematology/Oncology*, vol. 25, no. 11, pp. 845–853, 2003.

[6] S. Ferrari and E. Palmerini, "Adjuvant and neoadjuvant combination chemotherapy for osteogenic sarcoma," *Current Opinion in Oncology*, vol. 19, no. 4, pp. 341–346, 2007.

[7] G. Bacci, S. Ferrari, F. Bertoni et al., "Long-term outcome for patients with nonmetastatic osteosarcoma of the extremity treated at the Istituto Ortopedico Rizzoli according to the Istituto Ortopedico Rizzoli/osteosarcoma-2 protocol: an updated report," *Journal of Clinical Oncology*, vol. 18, no. 24, pp. 4016–4027, 2000.

[8] E. L. Kaplan and P. Meier, "Nonparametric observations from incomplete observations," *Journal of the American Statistical Association*, vol. 53, pp. 457–481, 1958.

[9] R. J. Gray, "A class of K-sample tests for comparing the cumulative incidence of a competing risk," *The Annals of Statistics*, vol. 16, pp. 1141–1154, 1988.

[10] T. R. Kimball and E. C. Michelfelder, *Echocardiography, in Moss & Adams's 'Heart Disease in Infants, Children, and Adolescents'*, Lippincott Williams & Wilkins, Philadelphia, Pa, USA, 8th edition, 2008.

[11] P. R. Brock, S. C. Bellman, E. C. Yeomans, C. R. Pinkerton, and J. Pritchard, "Cisplatin ototoxicity in children: a practical grading system," *Medical and Pediatric Oncology*, vol. 19, no. 4, pp. 295–300, 1991.

[12] S. S. Bielack, B. Kempf-Bielack, G. Delling et al., "Prognostic factors in high-grade osteosarcoma of the extremities or trunk: an analysis of 1,702 patients treated on neoadjuvant cooperative osteosarcoma study group protocols," *Journal of Clinical Oncology*, vol. 20, no. 3, pp. 776–790, 2002.

[13] R. Nagarajan, A. Kamruzzaman, K. K. Ness et al., "Twenty years of follow-up of survivors of childhood osteosarcoma," *Cancer*, vol. 117, no. 3, pp. 625–634, 2011.

[14] N. Delepine, G. Delepine, C. Jasmin, J. C. Desbois, H. Cornille, and G. Mathe, "Importance of age and methotrexate dosage: prognosis in children and young adults with high-grade osteosarcomas," *Biomedicine and Pharmacotherapy*, vol. 42, no. 4, pp. 257–262, 1988.

[15] G. Bacci, S. Ferrari, N. Delepine et al., "Predictive factors of histologic response to primary chemotherapy in osteosarcoma of the extremity: study of 272 patients preoperatively treated with high-dose methotrexate, doxorubicin, and cisplatin," *Journal of Clinical Oncology*, vol. 16, no. 2, pp. 658–663, 1998.

[16] N. Graf, K. Winkler, M. Betlemovic, N. Fuchs, and U. Bode, "Methotrexate pharmacokinetics and prognosis in osteosarcoma," *Journal of Clinical Oncology*, vol. 12, no. 7, pp. 1443–1451, 1994.

[17] E. C. van Dalen, J. W. van As, and B. de Camargo, "Methotrexate for high-grade osteosarcoma in children and young adults," *Cochrane Database of Systematic Reviews*, vol. 5, Article ID CD006325, 2011.

[18] C. B. Pratt, W. H. Meyer, X. Luo et al., "Second malignant neoplasms occurring in survivors of osteosarcoma," *Cancer*, vol. 80, pp. 960–965, 1997.

[19] L. Aung, R. G. Gorlick, W. Shi et al., "Second malignant neoplasms in long-term survivors of osteosarcoma: Memorial Sloan-Kettering Cancer Center experience," *Cancer*, vol. 95, no. 8, pp. 1728–1734, 2002.

[20] J. P. Neglia, D. L. Friedman, Y. Yasui et al., "Second malignant neoplasms in five-year survivors of childhood cancer: childhood cancer survivor study," *Journal of the National Cancer Institute*, vol. 93, no. 8, pp. 618–629, 2001.

[21] S. E. Lipshultz, S. P. Sanders, A. M. Goorin, J. P. Krischer, S. E. Sallan, and S. D. Colan, "Monitoring for anthracycline cardiotoxicity," *Pediatrics*, vol. 93, no. 3, pp. 433–437, 1994.

[22] L. J. Steinherz, P. G. Steinherz, C. T. C. Tan, G. Heller, and M. L. Murphy, "Cardiac toxicity 4 to 20 years after completing anthracycline therapy," *Journal of the American Medical Association*, vol. 266, no. 12, pp. 1672–1677, 1991.

[23] P. Stavroulaki, N. Apostolopoulos, J. Segas, M. Tsakanikos, and G. Adamopoulos, "Evoked otoacoustic emissions—an approach for monitoring cisplatin induced ototoxicity in children," *International Journal of Pediatric Otorhinolaryngology*, vol. 59, no. 1, pp. 47–57, 2001.

[24] Y. Li, R. B. Womer, and J. H. Silber, "Predicting cisplatin ototoxicity in children: the influence of age and the cumulative dose," *European Journal of Cancer*, vol. 40, no. 16, pp. 2445–2451, 2004.

[25] C. H. Pui, A. J. Gajjar, J. R. Kane et al., "Challenging issues in pediatric oncology," *Nature Reviews Clinical Oncology*, vol. 8, pp. 540–549, 2011.

[26] C. Lanvers-Kaminsky, B. Krefeld, A. G. Dinnesen et al., "Continuous or repeated prolonged cisplatin infusions in children: a prospective study on ototoxicity, platinum concentrations, and standard serum parameters," *Pediatric Blood and Cancer*, vol. 47, no. 2, pp. 183–193, 2006.

Hindawi Publishing Corporation
Sarcoma
Volume 2012, Article ID 425636, 15 pages
doi:10.1155/2012/425636

Review Article

Discovery of Biomarkers for Osteosarcoma by Proteomics Approaches

Yoshiyuki Suehara,[1] Daisuke Kubota,[1,2] Kazutaka Kikuta,[3] Kazuo Kaneko,[1] Akira Kawai,[4] and Tadashi Kondo[2]

[1] *Department of Orthopedic Surgery, Juntendo University School of Medicine, 2-1-1 Hongo, Bunkyo-ku, Tokyo 113-8421, Japan*
[2] *Division of Pharmacoproteomics, National Cancer Center Research Institute, 5-1-1 Tsukiji, Chuo-ku, Tokyo 104-0045, Japan*
[3] *Department of Orthopedic Surgery, Tachikawa Memorial Hospital, 4-2-22 Nishikichou, Tachikawa, Tokyo 190-8531, Japan*
[4] *Division of Musculoskeletal Oncology, National Cancer Center Hospital, 5-1-1 Tsukiji, Chuo-ku, Tokyo 104-0045, Japan*

Correspondence should be addressed to Yoshiyuki Suehara, ysuehara@juntendo.ac.jp

Received 3 July 2012; Accepted 30 August 2012

Academic Editor: Norman Jaffe

Osteosarcomas are the most common malignant bone tumors, and the identification of useful tumor biomarkers and target proteins is required to predict the clinical outcome of patients and therapeutic response as well as to develop novel therapeutic strategies. Global protein expression studies, namely, proteomic studies, can offer important clues to understanding the tumor biology that cannot be obtained by other approaches. These studies, such as two-dimensional gel electrophoresis and mass spectrometry, have provided protein expression profiles of osteosarcoma that can be used to develop novel diagnostic and therapeutic biomarkers, as well as to understand biology of tumor progression and malignancy. In this paper, a brief description of the methodology will be provided followed by a few examples of the recent proteomic studies that have generated new information regarding osteosarcomas.

1. Introduction

Osteosarcoma is the most common, nonhematopoietic, primary malignant bone tumor and most frequently occurs in the second decade, with 60% of patients under the age of 25 years [1]. After the initial diagnosis, patients usually receive multiagent preoperative chemotherapy and surgical resection of the tumor, followed by postoperative chemotherapy. Chemotherapy has improved the cure rate of patients with localized OS from 15%–20% achieved with surgery alone to approximately 70% [1, 2]. The response to preoperative chemotherapy is critical information for patients and the chemosensitive patients are divided into two groups based on the pathological features: the good responder (>90% tumor necrosis) and the poor responder (<90% tumor necrosis) [1, 2]. However, patients who have a poor response to chemotherapy often have a poor outcome and a high risk of developing metastasis compared to patients who have a good response to chemotherapy [1, 2]. Therefore, it is critical to identify proteins associated with chemoresistance as predictive biomarkers and novel theoretical targets in osteosarcomas. Additionally, despite significant progress regarding chemotherapy and improvements in the outcome for patients with localized osteosarcomas, patients who have metastases at diagnosis are not uncommon, and patients with metastases still have poor prognosis [1, 2]. Therefore, the development of a novel focus on the identification of prognostic indicators, and novel therapeutic targets that inhibit biological pathways known to contribute to osteosarcoma growth, are essential.

The use of high-throughput screening approaches, such as array-based comparative genomic hybridization analysis and cDNA microarray technology, allows for the screening of several thousand DNA and mRNA sequences and can identify the genes relevant to the diagnosis and clinical features of tumors [3–13]. These comprehensive studies have identified several genes that may be involved in the development or progression of osteosarcomas, and represent candidate biomarkers and/or drug targets [3–13]. However, in clinical applications, there are currently no specific markers

available for predicting the prognosis and chemosensitivity of osteosarcomas. The identification of these factors could provide not only a new method for stratifying patients and selecting the treatment strategy, but could also provide novel therapeutic targets for osteosarcoma. Global protein expression studies, an approach known as "proteomics," may also be more clinically relevant than genomic studies, since proteins directly regulate the aberrant tumor phenotypes. Moreover, DNA sequencing or measurement of mRNA expression cannot detect posttranslational modifications of proteins that affect their activity, such as phosphorylation, glycosylation, and acetylation, or differences in protein stability, and these factors play important roles in the malignant behavior of tumor cells [14–17]. Furthermore, many lines of evidence have indicated that there is discordance between the mRNA and protein expression [14–17]. Therefore, proteomic studies are becoming critical tools for understanding the biology of tumors, as well as for the identification of biomarkers for various cancers. In addition, the results obtained from proteomic studies are more easily applied to the clinical field, because of the potential use of specific antibodies.

Recent advances in proteomic technology have made it possible to identify disease-related proteins in clinical samples, and extensive efforts are now being made to identify biomarkers of specific cancers that can be used for diagnostic or therapeutic purposes [15, 16, 18–25]. The standard proteomic techniques, such as two-dimensional gel electrophoresis (2DE) and mass spectrometry (MS), have been developing over the past three decades. From the end of the 1990s, through the development of high-throughput platforms, proteomics has become able to allow the simultaneous measurement of multiple protein products and protein modifications. These newlydeveloped technologies provide ways to detect crucial protein expression patterns corresponding to disease progression or responses to treatment and are now considered vital research tools [15, 16, 18–34]. Therefore, proteomic studies can be particularly useful to identify novel biomarkers and therapeutic targets of sarcomas. Our studies have identified some candidate proteins associated with a differential diagnosis [15, 16, 20, 21], prognosis [18, 19, 25], and in predicting the response to chemotherapy [16, 23] in bone and soft-tissue sarcomas. The following section describes how proteomic approaches have been applied to osteosarcoma and reviews many of the articles regarding proteomic studies of osteosarcoma.

We identified approximately 30 papers about proteomic research on osteosarcoma during a search of PubMed (Table 1). In this paper, in order to discuss the contributions of proteomics to the identification of useful clinical biomarkers and targets for human osteosarcomas, we chose the articles that used actual patient samples, such as surgical materials and plasma, rather than information from human cell lines and animal studies (Table 1). In this paper, we briefly discuss the proteomic technologies, especially electrophoresis-based techniques, as well as the identification of biomarkers and novel targets for osteosarcoma identified by proteomic approaches.

2. Proteomic Technologies and Analyses in Sarcomas

Proteomics is the large-scale study of proteins, especially their structures and functions [35]. Technologies used in proteomics research include electrophoresis, mass spectrometric technologies, protein labeling, protein arrays, antibody-based approaches, imaging, and bioinformatics technology. As a result of the recent advances in these technologies, proteomics may provide powerful information for improved biomarker and novel therapeutic target discovery in malignant tumors. In particular, mass spectrometry technologies are now high throughput, allowing for the rapid and accurate identification of thousands of proteins present within a complex tumor specimen. Furthermore, a differential protein expression analysis can be used to compare tumors with normal tissues, and is able to identify a range of protein markers potentially related to the malignant features of tumors [35–37]. Bone and soft tissue sarcomas are relatively rare compared with other malignancies. The development of diagnostic and prognostic modalities, identification of novel therapeutic targets, and understanding of the mechanisms of sarcomagenesis are currently the main research priorities. Therefore, various strategies are now being employed to identify tumor-specific proteins in sarcoma using proteomics technologies.

Based on a search of the PubMed database, electrophoresis, specifically 2D difference gel electrophoresis (2D-DIGE) [15, 16, 19–21, 25, 32, 34, 38] and mass spectrometry, especially matrix-assisted laser desorption ionization mass spectrometry (MALDI MS) [39] and surface-enhanced laser desorption/ionization (SELDI) [26, 33, 40], have mainly been used to obtain protein expression profiles of bone and soft-tissue sarcomas. We briefly summarized both the advantages and disadvantages of main platforms for performing a proteomic analysis (Table 2). In this article, we mainly discuss 2D-DIGE, because this technology is the most commonly used method for obtaining protein expression profiles in proteomic studies of bone and soft tissue tumors [15, 16, 18–21, 25, 26, 32–34, 38–40].

2.1. 2D-DIGE. We routinely employ 2D-DIGE for biomarker identification [15, 16, 18–21, 25, 41, 42]. 2D-DIGE is an advanced variation of 2D-PAGE (two-dimensional polyacrylamide gel electrophoresis) and has the potential to solve many drawbacks of classical 2D-PAGE (Figure 1) [41, 42]. The standard 2D-PAGE technique employs isoelectric separation according to protein charge as a first dimension, coupled with MW resolution by polyacrylamide gel electrophoresis. Our 2D-DIGE method uses DIGE dyes which react with cysteine residues. There are only a few cysteines per protein and the cysteine-reactive dyes are highly soluble zwitterions. Therefore, these dyes are suitable for saturation labeling of all cysteine residues. As a result, the sensitivity for protein detection is improved and enables a successful 2D-PAGE analysis with of even low protein concentrations [41–43], and various studies have demonstrated the successful application of saturation labeling to detect protein differences in scarce samples derived from

Table 1: Overview of protein expression studies using osteosarcoma samples published so far.

Sample type	Sample entity (cases)	Purpose of study	Method	Literature	Study contents
Patient's tissue samples (osteosarcoma, normal bone, and benign tumor)	Osteosarcoma (16)	Chemosensitivity	2D-DIGE	Kawai et al.	Chemosensitivity (poor responder (7) versus good responder (9))
	Osteosarcoma (5) and normal bone (5)	Tumor-specific and malignancy	2D-DIGE	Folio et al.	Tumor-specific proteins (osteosarcoma (5) versus normal bone (5))
	Osteosarcoma (12)	Chemosensitivity	2D-DIGE	Kikuta et al.	Chemosensitivity (poor responder (6) versus good responder (6))
	Osteosarcoma (5), chondroblastoma (2), osteoblastoma (2), and giant cell tumor (1)	Tumor-specific and malignancy	2DE	Li et al.	Tumor-specific proteins (osteosarcoma (5) versus chondroblastoma (2), osteoblastoma (2), and giant cell tumor (1))
Patient's plasma samples (osteosarcoma and benign tumor)	Osteosarcoma (29) and osteoblastoma (20)	Tumor-specific and malignancy	SELDI	Li et al.	Tumor-specific proteins (osteosarcoma (29) versus osteoblastoma (20))
	Osteosarcoma (54)	Chemosensitivity	SELDI	Li et al.	Tumor-specific proteins (poor responder (27) versus good responder (27))
Cell line samples (osteosarcoma cell line versus normal bone or osteoblast cell)	Osteosarcoma cell (1), osteoblastic cell (1)	Tumor-specific and malignancy	2DE	Spreafico et al.	Tumor-specific proteins (SaOS-2 (1) versus osteoblastic cell (1))
	Osteosarcoma cell (3), osteoblastic cell (1)	Tumor-specific and malignancy	2DE	Guo et al.	Tumor-specific proteins (U2OS (1), IOR/OS9 (1) and SaOS-2 (1) versus osteoblastic cell (1))
	Osteosarcoma cell (1), osteoblastic cell (1)	Tumor-specific and malignancy	2DE	Liu et al.	Tumor-specific proteins (SaOS-2 (1) versus osteoblastic cell (1))
	Osteosarcoma cell (1), osteoblastic cell (1)	Tumor-specific and malignancy	iTRAQ	Zhang et al.	Tumor-specific proteins of plasma membrane (MG63 (1) versus osteoblastic cell (1))
	Osteosarcoma cell (1), osteoblastic cell (1)	Tumor-specific and malignancy	2D-DIGE	Hua et al.	Tumor-specific proteins of plasma membrane (MG63 (1) versus osteoblastic cell (1))
Cell line sample (osetosarcoma cell)	Osteosarcoma cell (1)	Tumor specific	2D-DIGE	Niforou et al.	Characteristic proteins of U2OS cell line
Cell line sample (high metastatic osetosarcoma cell versus low metastatic osteosarcoma cell)	Osteosarcoma cell (2)	Metastasis	MALDI and 2D-DIGE	Cates et al.	Proteins corresponding to metastasis (high metastatic osetosarcoma cell (1) versus low metastatic osetosarcoma cell (2))
Cell line sample (drug treatment cell versus nontreatment cell)	Osteosarcoma cell (2)	Drug-sensitivity	2DE	Kang et al.	Drug-sensitivity: Ascochlorin (drug-treatment U2OS (1) versus no-treatment U2OS (1))
	Osteosarcoma cell (2)	Drug-sensitivity	2DE	Chang et al.	Drug-sensitivity: Ascochlorin (drug-treatment USOS (1) versus no-treatment USOS (1))
	Osteosarcoma cell (2)	Drug-sensitivity	2DE	Zhang et al.	Drug-sensitivity: DATS (drug-treatment SaOS2 (1) versus non-treatment SaOS2 (1))
Cell line sample (target inhibition or activation cell versus non-treatment cell)	Osteosarcoma cell (2)	Target related proteins	2D-DIGE	Li et al.	Target-related proteins: E2F1 (E2F1-activated SaOS2 (1) versus non-treatment SaOS2 (1))
	Osteosarcoma cell (4)	Target related proteins	2D-DIGE	Annunen-Rasia et al.	Target-related proteins: (i) OXPHOS, (ii) CI or CV, and (iii) mtDNA (inhibited SaOS2 (1) versus non-treatment SaOS2 (1))

2D-DIGE: 2-dimensional fluorescence difference gel electrophoresis, 2DE: 2-dimensional electrophoresis, MALDI: matrix-assisted laser desorption/ionization, and SELDI: surface-enhanced laser desorption/ionization.

Table 2: Summary of the platforms in proteomic analysis.

	Gel-based methods		Gel free methods		Microarray
	2D gel electrophoresis	2D-DIGE	SELDI and MALDI	LC-MS	Protein array
Advantage	Separation of large number of proteins	Reliable quantification Required small amount of proteins Reproducible Separation of large number of proteins	Automation Required small amount of proteins Possibility of quantification	Automation Required small amount of proteins Possibility of quantification	High-throughput Automation High reproducible Required small amount of proteins Sensitive detection for post translational modification
Disadvantage	Required large amount of proteins Nonautomation Limitation for large and small proteins in directions	Nonautomaition Limitation for large and small proteins in directions	Less reliable in protein direction Less detection of low abundance proteins	Less detection of low abundance proteins	Limitation for the total number of proteins

2D-DIGE: 2-dimensional fluorescence difference gel electrophoresis, SELDI: surface-enhanced laser desorption/ionization, MALDI: matrix-assisted laser desorption/ionization, LC-MS: liquid chromatography mass spectrometry.

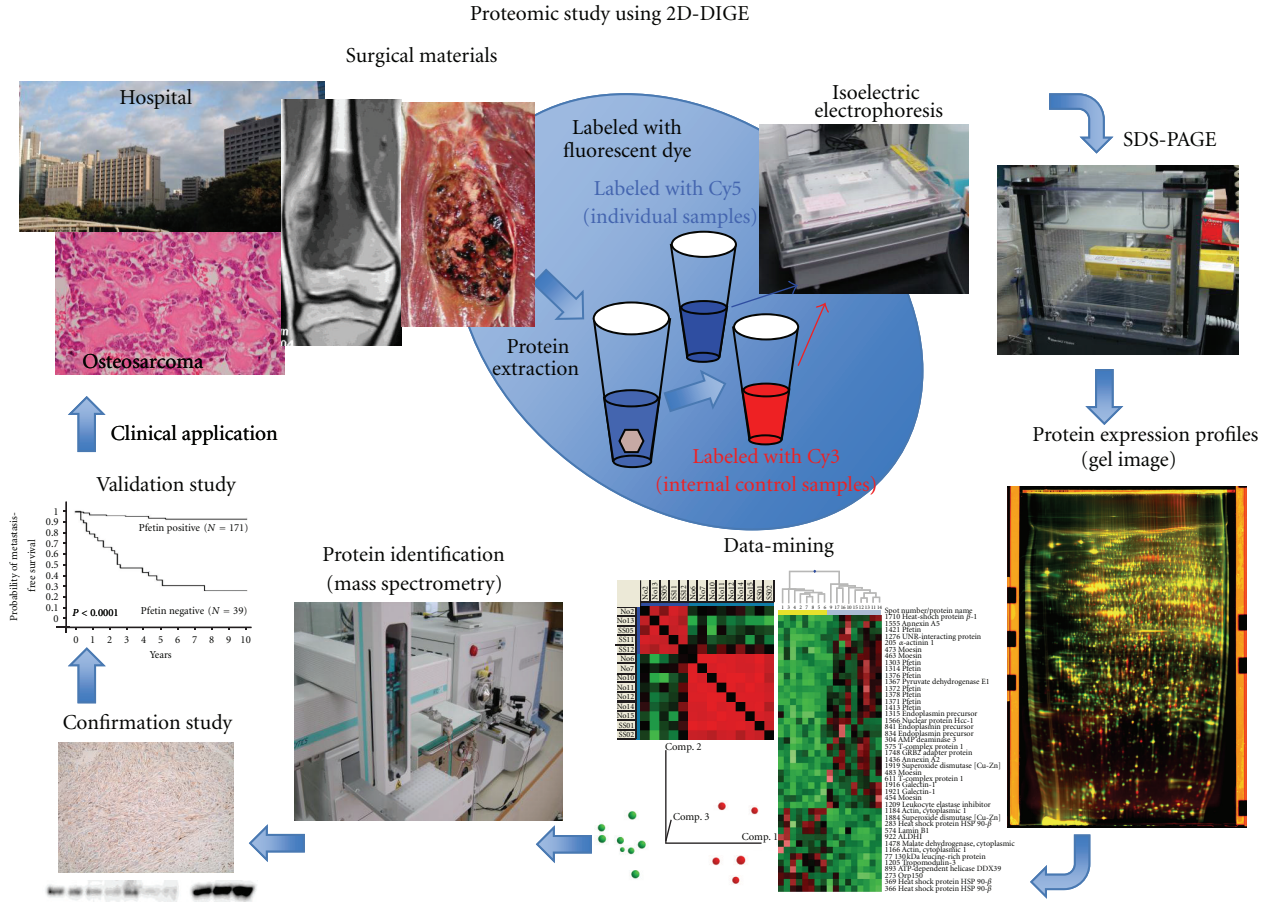

Figure 1: The process for 2D-DIGE-based target identification, confirmation, and validation. Surgical samples are collected from patients with osteosarcoma. Collected samples contain proteins associated with clinical information. All protein samples are labeled with different fluorescent dyes (The internal control sample is a mixture of a small portion of all individual samples labeled by Cy3, and the individual samples are labeled by Cy 5). The protein expression profiles are obtained using 2D-DIGE with highly sensitive fluorescent dyes. The protein expression profiles are analyzed to identify candidate biomarkers through data-mining using the proteomic profiles and clinical data. The protein expression levels are then confirmed by a western blot analysis and/or immunohistochemistry. The biomarker candidates are validated using additional large-variation cohorts to develop them for clinical applications.

1000 to 5000 protein spots. These two DIGE labeling options provide rapid methods for preparing differentially labeled samples for fluorescence-based proteome comparisons [41–43].

Using our 2D-DIGE method, proteins were extracted from surgical specimens, and all protein samples were labeled with different fluorescent dyes before gel electrophoresis (Figure 1) [15, 16, 18–21, 25, 41, 42]. We first created a common internal control sample, which was a mixture of a small portion of all individual samples, and labeled it with a fluorescent dye that is different from the one used to label the individual samples. These differentially labeled internal control and individual samples are then mixed together and separated by both their pH and molecular weight ranges by 2D-PAGE (Figure 1). Laser scanning can be used to obtain the gel images, because all proteins are labeled with fluorescent dye before the gel electrophoresis (Figure 1). By normalizing the 2D image of each individual sample with that of the common internal control sample in the same gels, there is compensation for gel-to-gel variations, and reproducible results can be obtained across multiple gel images. These gel images provide data about protein spots as protein expression profiles. In the data analysis, the protein spots whose intensities are significantly different between the groups examined are identified using the Wilcoxon test, Hierarchical clustering, a principle component analysis, correlation matrix studies, and a support vector analysis using a data-mining software program (Figure 1). Proteins corresponding to the spots of interest are identified by mass spectrometry. Protein identification and differential expression are confirmed by a western-blotting analysis and/or immunohistochemistry using specific antibodies. Finally, in order to identify useful biomarkers and to develop clinical applications, we usually try to verify the value of biomarkers or targets using a large scale validation set which consists of clinical samples by an immunohistochemical analysis (Figure 1).

3. The Identification of Tumor-Specific Biomarkers and Therapeutic Targets in Osteosarcoma

In osteosarcoma, the biology of malignant progression and tumorigenesis are still largely unknown. Therefore, protein and gene expression studies have mainly been used to provide a source of expression profiles and to obtain clues about the causes of osteosarcomas. The identification of tumor-specific biomarkers and therapeutic targets are the most important goals of global protein and gene expression studies. The current gene expression profiling technologies have been used to identify upregulated or downregulated genes associated with tumor progression, or that can be used to predict the malignant potential in osteosarcoma [3–6]. In this section, we mainly describe pertinent proteomic studies that have identified tumor-specific proteins corresponding to tumor progression and that can be used as prognostic biomarkers and therapeutic targets in osteosarcoma using patient materials. Two papers reported comparative proteomic studies using tissue samples; (i) osteosarcoma versus normal bone [32] and (ii) osteosarcoma samples versus benign tumors [34]. Additionally, one paper described a plasma proteomic study comparing osteosarcoma patients' plasma with plasma from patients with benign bone tumors (Table 1) [33].

Folio et al. carried out comparative proteomic studies using five paired samples of osteosarcomas and normal bone to identify the proteins involved in malignant transformation and that were tumor-specific (Table 1) [32]. Additionally, the authors described that they could identify the proteins associated with metastasis and chemoresistance in their study. The five pairs of samples (tumor versus normal bone) were isolated form surgical tissue samples as cell lines. The study detected 56 differentially-expressed protein spots ($P < 0.05$) and 16 proteins were identified as having differences in their relative abundance in osteosarcomas and paired normal bones by nanoliquid chromatography/electrospray ionization tandem mass spectrometry (Nano-LC-ESI-MS/MS). Both alpha-crystallin B chain (*CRYAB*) and ezrin (*EZR*) were confirmed to be differentially expressed using an immunohistochemical analysis and real-time PCR. The confirmation studies revealed that tumor tissues had higher protein expression levels of both *CRYAB* and *EZR* than normal tissues. This study also demonstrated that there were significant differences in the metastasis and recurrence rates between positive and negative samples in terms of both *CRYAB* and *EZR*.

Li et al. conducted a proteomic study of osteosarcoma to identify the specific protein markers of the disease and to improve the understanding of the tumorigenesis and progression of osteosarcoma (Table 1) [34]. Protein samples were extracted from five osteosarcoma tissue samples and five benign bone tumor samples (two osteoblastoma, two chondroblastoma, and one giant cell tumor). The protein expression profiles were acquired by comparing the osteosarcoma profiles with those of benign tumors using 2DE analyses. A total of 30 protein spots ($P < 0.05$) were detected as differentially expressed in this study, and 18 proteins were finally identified by mass spectrometry. These proteins included 12 upregulated proteins (VIM, TUBA1C, ZNF133, EZR, ACTG1, TF, etc.) and six downregulated proteins (ADCY1, ATP5B, TUBB, RCN3, ACTB, and YWHAZ). They confirmed the differences in the protein expression levels of TUBA1C and ZNF133 by the western-blotting and immunohistochemical analyses. The study concluded that these identified proteins might be potential biomarkers for osteosarcomagenesis and might represent novel therapeutic targets for the disease.

Both studies (Folis et al. and Li et al.) identified osteosarcoma-specific proteins, as well as proteins associated with malignant progression and tumorigenesis in bone tumors, especially osteosarcomas [32, 33]. EZR was a common protein identified by both studies (Tables 3(a) and 3(b)). In a cDNA microarray study of osteosarcoma, EZR was also identified as a highly expressed gene in osteosarcomas, and that study suggested that EZR may have an important role in metastasis [5].

Table 3: Summay of protein expression studies using patient's tissue samples of osteosarcoma.

(a)

Protein name	Folio et al. (osteosarcoma versus normal bone)	Li et al. (osteosarcoma versus benign bone tumor)	Kikuta et al. (poor responder versus good responder)
40S ribosomal protein SA	Folio_4 (OS↓)		Kikuta_27 (poor↑)
Alpha-actinin-1			Kikuta_10 (poor↑)
Alpha-enolase			Kikuta_20, Kikuta_21 (poor↑)
Alpha1-antitrypsin		Li_11 (OS↑)	
Actin cytoplasmic 2	Folio_16 (OS↓)		
Actin-beta		Li_14 (OS↓)	
Actin-gamma1		Li_4 (OS↑)	
Adenylate cyclase 1		Li_13 (OS↓)	
Alpha crystallin beta chain	Folio_13 (OS↑)		
Alpha-enolase	Folio_8 (OS↓)		
Annexin A6			Kikuta_1 (poor↑)
ATP synthase mitochondrial F1 complex b polypeptide		Li_16 (OS↓)	
ATP synthase subunit b			Kikuta_39 (poor↓)
C-type lectin domain family 11 member A			Kikuta_4 (poor↑)
Carbonic anhydrase 1			Kikuta_52, Kikuta_54 (poor↓)
Chaperonin containing TCP1		Li_12 (OS↑)	
Clusterin precursor			Kikuta_2 (poor↑)
CNDP dipeptidase 2			Kikuta_17 (poor↑)
Coatomer protein complex		Li_3 (OS↑)	
Collagen alpha-1			Kikuta_55 (poor↓)
Desmoglein-1			Kikuta_46 (poor↓)
Elongation factor 1-gamma			Kikuta_34 (poor↓)
Eukaryotic initiation factor 4A-I			Kikuta_38 (poor↓)
Ezrin	Folio_7 (OS↑)	Li_9 (OS↑)	
Fascin	Folio_12 (OS↓)		
Ferritin light polypeptide		Li_7 (OS↑)	
Haptoglobin-related protein			Kikuta_31, Kikuta_53 (poor↓)
Heat shock 70 kDa protein 1			Kikuta_19 (poor↑)
Heat shock cognate 71 kDa protein	Folio_6 (OS↓)		Kikuta_23, Kikuta_25 (poor↑)
Heat shock protein beta 6	Folio_1 (OS↑)		
Heme binding protein 1	Folio_2 (OS↑)		
Hemoglobin subunit beta			Kikuta_7, 11, 15, 28, 36 (poor↑↓)
Keratin type II cytoskeletal 1			Kikuta_9 (poor↑)
Lamin B2		Li_1 (OS↑)	
Lamin-A/C			Kikuta_29 (poor↑)
LIM and SH3 domain protein 1	Folio_9 (OS↑)		
Lumican			Kikuta_43 (poor↓)
Myosin light chain 6 alkali smooth muscle and nonmuscle		Li_8 (OS↑)	
NADH-ubiquinone oxidoreductase			Kikuta_22 (poor↑)
Nucleophosmin	Folio_5 (OS↓)		
Peroxiredoxin 6	Folio_11 (OS↑)		

(a) Continued.

Protein name	Folio et al. (osteosarcoma versus normal bone)	Li et al. (osteosarcoma versus benign bone tumor)	Kikuta et al. (poor responder versus good responder)
Peroxiredoxin 2			Kikuta_30 (poor↑)
PR65-A isoform			Kikuta_50 (poor↓)
Proteasome activator complex subunit 1			Kikuta_16 (poor↑)
Purine nucleoside phosphorylase			Kikuta_12 (poor↑)
Pyruvate kinase isozymes M1/M2	Folio_14 (OS↓)		
Reticulocalbin 3		Li_17 (OS↓)	Kikuta_13 (poor↑)
Ribose-phosphate pyrophosphokinase II			Kikuta_35 (poor↓)
Septin-11	Folio_15 (OS↑)		
Serum albumin			Kikuta_14, 41, 48 (poor↑↓)
Stress-70 protein			Kikuta_3, 24 (poor↑)
Thioredoxin reductase 1	Folio_10 (OS↑)		
Transferrin		Li_10 (OS↑)	
Trypsin-3 precursor			Kikuta_8, 26, 32 (poor↑↓)
Tubulin alpha-ubiquitous chain			Kikuta_45 (poor↓)
Tubulin beta-2A chain			Kikuta_47 (poor↓)
Tubulin beta-2C chain			Kikuta_37 (poor↓)
Tubulin beta-chain			Kikuta_44 (poor↓)
Tubulin-alpha-1C		Li_6 (OS↑)	
Tubulin-beta		Li_15 (OS↓)	
Tumor protein D54			Kikuta_40, 49 (poor↓)
Tyrosine 3-monooxygenase/tryptophan 5-monooxygenase activation protein		Li_18 (OS↓)	
Ubiquitin carboxyl terminal hydrolase isozyme L1	Folio_3 (OS↑)		
UV excision repair protein RAD23			Kikuta_33, 51 (poor↓)
Vesicle-fusing ATPase			Kikuta_42 (poor↓)
Vimentin		Li_2 (OS↑)	Kikuta_5, 6, 18 (poor↑)
Zinc finger protein 133		Li_5 (OS↑)	

(b)

Protein name	Folio et al. (OS versus normal bone)	Li et al. (OS versus benign tumor)	Kikuta et al. (poor responder versus good responder)
40S ribosomal protein SA	Folio_4 (OS↓)	—	Kikuta_27 (poor↑)
Ezrin	Folio_7 (OS↑)	Li_9 (OS↑)	—
Heat shock cognate 71 kDa protein	Folio_6 (OS↓)	—	Kikuta_25 (poor↑)
Reticulocalbin 3	—	Li_17 (OS↓)	Kikuta_13 (poor↑)
Vimentin	—	Li_2 (OS↑)	Kikuta_5, _6, 18 (poor↑)
PRDX family	Folio_11 (PRDX6) (OS↑)	—	Kikuta_30 (PRDX2) (poor↑)

EZR, an ezrin/radixin/moesin (ERM) family member, is evolutionarily conserved both structurally and functionally [44, 45]. By regulating membrane-cytoskeleton complexes, EZR has critical roles in normal cellular processes such as the maintenance of membrane dynamics, survival, adhesion, motility, cytokinesis, phagocytosis, and integration of membrane transport with signaling pathways [45, 46]. The activation of EZR is mediated by both exposure to PIP2 and phosphorylation of the C-terminal threonine (T567) [44, 47]. The deactivation of EZR is also important for physiologic functions, including the dynamics of actin-rich membrane projections. EZR has been implicated in various steps of the metastatic process, for example, as a conduit for signals between metastasis-associated cell surface molecules and signal transduction components [48].

In osteosarcoma studies, EZR was necessary for metastasis, and a high expression of ezrin was associated with the early development of metastasis [49]. A relationship was

also shown between high expression levels of EZR and a poor outcome in 19 pediatric osteosarcoma patients [49]. In addition, two articles that compared the EZR expression in high- and low-grade human osteosarcoma tumor samples demonstrated a clear correlation between ezrin expression and survival [50, 51]. Furthermore, some studies suggested that EZR phosphorylation is not only present in the early stage of metastasis, but also late in tumor progression, at the leading edge of large metastatsic lesions. More importantly, using dominant-negative mutants, antisense RNA or RNA interference, these experiments demonstrated that EZR overexpression is not only sufficient for metastatic progression, but it is also necessary in these experimental systems [49, 52]. Finally, the suppression of EZR protein expression significantly reduced the metastatic behavior in two murine models and it was also associated with a decreased Akt and mitogen-activated protein kinase (MAPK) activity [49, 52, 53]. These findings suggest that targeting EZR might improve the treatment of osteosarcoma, especially in metastasis cases.

Li et al. conducted a proteomic study to identify a plasma protein signature that was tumor-specific or that corresponded to the malignancy of osteosarcoma using SELDI-MS (Table 1) [33]. The study compared the plasma specimens between 29 patients with osteosarcomas and 20 with osteochondromas. They identified 19 ion peaks which had statistically significant differences in the protein expression levels between the osteosarcoma group and the benign bone tumor group ($P < 0.001$ and false discovery rate, 10%). The statistical analyses detected that there was a significant difference in the expression of one of the proteins (m/z 11 704) in the proteomic signature, which was found to be serum amyloid protein A by PMF. Serum amyloid protein A is highly expressed in the plasma samples of osteosarcoma patients. A Western blotting analysis also confirmed that there were high expression levels of serum amyloid protein A in the plasma of osteosarcoma patients compared to that of osteochondroma patients and normal subjects. That study concluded that the findings based on this plasma proteomic signature might be useful to differentiate malignant bone cancer from benign bone tumors, and also might contribute to early detection of a high-risk osteosarcoma group.

In summary, we believe that these proteins, which are tumor-specific and associated with the malignancy of osteosarcomas, may contribute to understanding the biology of the tumors and may be useful as biomarkers. An analysis of the functions of these proteins and their correlations with osteosarcoma would provide insight into the biology of osteosarcoma and improve the therapeutic management of osteosarcoma patients.

4. The Identification of Biomarkers of Chemosensitivity in Osteosarcoma

The major prognostic factor in patients with localized osteosarcoma is the development of resistance to preoperative chemotherapy. Therefore, the identification of biomarkers of chemosensitivity in osteosarcoma is critical. Some gene expression studies have been conducted to identify genes associated with the chemosensitivity in osteosarcoma [3–6]. In this section, we mainly introduce pertinent proteomic studies that have previously identified markers of the response to chemotherapy in osteosarcoma. We found only two papers, which are our own studies, that have conducted protein expression studies of potential biomarkers of chemosensitivity in osteosarcoma using tissue samples (Table 1) [16, 23]. Another paper described a chemosensitivity study of osteosarcoma using patient plasma samples (Table 1) [26].

In our study, we employed a proteomic approach to identify novel biomarkers of the chemosensitivity of osteosarcoma (Table 1) [23]. We used 12 biopsy samples, including six osteosarcoma samples from patients who were good responders and six osteosarcoma patients who were poor responders, according to the Huvos grading system. The protein expression profiles obtained by 2D-DIGE consisted of 2250 protein spots. We identified 55 protein spots ($P < 0.01$) whose intensity was significantly different between the two groups. Mass spectrometric protein identification demonstrated that these 55 spots corresponded to 38 distinct gene products, including peroxiredoxin 2 (PRDX2). The PRDX2 spots had higher intensity in the poor responder group, and we also confirmed the presence of an increased protein expression of PRDX2 in the poor responder group by a western blot analysis. In order to validate the prediction of chemosensitivity using the markers we identified, we performed a validation study using an additional four osteosarcoma samples, including two samples each from good responders and poor responders by a western blot analysis. The validation study demonstrated that the poor responders had higher PRDX2 expression levels compared to the good responders. We concluded that PRDX2 might be a candidate marker for chemosensitivity in osteosarcoma patients. In our other paper, by Kawai et al., we identified 10 protein spots which were found to be correlated with chemoresistance by 2D-DIGE, but the study did not identify the protein names associated with the spots, so we will not discuss the details of these findings here.

Li et al. conducted a plasma proteomic study to identify proteins that could be used to distinguish good from poor responders in osteosarcoma patients prior to the start of treatment (Table 1) [26]. Their study used two sets of 54 plasma samples that were collected from 27 prechemotherapy osteosarcoma patients and 27 postchemotherapy patients. The pre-chemotherapy samples included 14 good responders and 13 poor responders, and the postchemotherapy samples included 12 good responders and 15 poor responders. The analyses divided the subjects into two classes (consisting of good and poor responders) in both sets of plasma samples. In the post-treatment plasma set, 65 protein peaks were identified as the signature of the chemotherapeutic response. The levels of 29 protein peaks were higher and those of 36 protein peaks were lower in the plasma of poor responders. In the pretreatment plasma set, 56 protein peaks were identified, and the pre-treatment signature demonstrated that 32 and 24 protein peaks in the plasma of the poor responders were expressed at higher and lower levels, respectively, compared to good responders.

These studies identified two plasma proteins, serum amyloid protein A and transthyretin, that appear to be especially sensitive markers. The expression of serum amyloid protein A was significantly higher in the plasma of the good responders, while transthyretin was more highly expressed in poor responders. These protein expression differences were confirmed by a western blot analysis. Both of these proteins are involved in innate immunity based on a protein database search. The authors concluded that the study might lead to the development of a simple blood test that can predict the response to chemotherapy in osteosarcoma patients and suggested that their findings might be corroborated by the notion that boosting the innate immunity in conjunction with chemotherapy leads to better anti-tumor activity, thus improving the overall survival of osteosarcoma patients.

Several reports have described that the histological response to preoperative chemotherapy has provided the most consistent and reliable prognostic indicator [1, 2, 5, 54]. The patients with localized disease whose tumors have undergone more than 90% necrosis have a 5-year survival of approximately 70%, while for those in whom the response falls short of 90%, survival rarely exceeds 40–50% [5, 54]. Furthermore, in comparison studies of osteosarcomas, the sample sets for chemosensitivity (poor responder versus good responder) were strongly correlated with the sets for prognosis (good outcome patients versus poor outcome patients). Therefore, we believe that the identified proteins associated with malignancy are also related to the chemosensitivity of the tumors.

Moreover, in a previous study, we have already discussed a comparison of the protein lists reported in Folio's and Li's studies (see above), with the Folio study examining tumor-specific and/or malignancy-related proteins (osteosarcoma versus normal tissue samples) and the Li study examining tumor malignancy (osteosarcoma versus benign bone tumor) (Table 3(a)). As noted above, we identified that EZR was a common protein identified in both studies (Table 3(b)). In this section, we also reviewed and organized the proteins lists from three papers: (i) Folio et al. reported tumor-specific and/or tumor malignancy-associated proteins (osteosarcoma versus normal tissue), (ii) Li et al. reported tumor malignancy-associated proteins (osteosarcoma versus benign bone tumors) and (iii) Kikuta et al. reported chemosensitivity- and/or tumor malignancy-related proteins (poor responder versus good responder) (Table 3(a)). During a further review of these studies, we found that not only EZR, but also the PRDX family were common proteins in the lists (Table 3(b)), with the study by Kikuta having identified PRDX2 and the Folio study having identified PRDX6 (Table 3(b)).

The PRDX family of proteins show peroxidase activities that degrade hydrogen peroxide (H_2O_2), as well as serving as alkyl hydroperoxides. In human tissues, six members of the family (PRDX1-6) have been identified so far [55]. Several papers have reported that PRDX proteins act as cytoprotective antioxidant enzymes, while PRDX expression was shown to enhance oxidative damage in some cells and tissues [55–60]. Recently, PRDX proteins have received increasing attention in the field of cancer biology. The analyses of cancer samples obtained from patients have revealed that there is increased expression of PRDX in malignancies of various organs and tissues [61–66]. In addition, the upregulation of PRDX proteins (specifically, 1, 2, 4, 5, and 6) may contribute to the resistance of tumors to chemotherapy and radiotherapy [67–73]. In addition, some papers have demonstrated in functional studies of PRDX proteins that they appear to influence the efficacy of cancer therapy not only by supporting the resistance of cancer cells, but also by promoting their invasiveness and metastasis [62, 74]. Therefore, the mechanism(s) underlying these functions of PRDX and information about their expression patterns may be essential for obtaining a better understanding of tumor biology and the development of new treatment strategies for osteosarcoma.

In summary, based on the previous proteomic studies, there are several common proteins that have been identified as corresponding to chemoresistance and/or malignancy. Moreover, these proteins have been reported to be involved in malignancy and/or chemoresistance in other cancers [62, 67–74]. Therefore, these proteins should be major targets for development as diagnostic or prognostic biomarkers, and may also be useful for targeted therapy.

5. Our Experiences with Proteomic Studies of Osteosarcoma

Before the publication of Kikuta's paper, we conducted the 2D-DIGE analyses using 16 OS tissue samples to identify proteins corresponding to chemoresistance (Table 4). We compared nine osteosarcoma samples from good responders with seven osteosarcoma samples from poor responders. However, the sample set included osteosarcoma samples that were collected from elderly patients and from a trunk origin (pelvis), while typical osteosarcomas occur in young patients (<30 years) and in the extremities (Table 4). More importantly, the sample set was mixed, because several chemotherapy protocols, such as HD-MTX and HD-IFM, had been used (Table 4). Although this study identified 41 (of 1465) protein spots that were differentially expressed ($P < 0.05$), there were no statistically significant differences between the two groups of patients (good/poor responders) (Figure 2). On the other hand, Kikuta's study successfully identified 55 of 2250 protein spots ($P < 0.01$) which had statistically significant differences when the good responders and poor responders were compared. One of the keys to the success of the latter study was that Kituta's analyses used typical osteosarcoma samples, which were obtained only from tumors with an origin in an extremity and that were only obtained from young subjects. In addition, this study employed patient samples from only subjects who were treated with HD-IFM-based protocols. We think that the modified study design likely contributed to the successful identification of candidate proteins corresponding to chemosensitivity.

Oteosarcoma is a heterogeneous tumor, the etiology of which is still largely unknown. Three global gene expression studies using cDNA microarrays were conducted to

Table 4: Clinicopathological features of osetosarcoma tissue samples for chemosensitivity study.

Sample name	Age	Gender	Histological subtype	Site	Huvos grading	Preoperation chemotherapy agents	Mstastasis (months)	Followup (months)	Status
Huvos I									
OS03	9	Female	Telangiectatic	Proximal femur	1	MTX, ADR/CDDP	46	54	DOD
OS17	13	Female	Osteoblastic	Proximal tibia	1	HD-MTX	15	51	DOD
OS18	14	Male	Osteoblastic	Proximal tibia	1	HD-MTX, ADR/CDDP	—	73	NED
OS32	19	Male	Osteoblastic	Distal femur	1	HD-MTX, CDDP/ADR,	—	47	NED
OS36	63	Female	Osteoblastic	Metatarsus	1	IFO, CDDP/ADR	—	18	NED
OS41	18	Male	Osteoblastic	Pelvis	1	IFO, CDDP/ADR	At diagnosis	18	DOD
OS47	14	Male	Chondroblastic	Proximal femur	1	IFO, CDDP/ADR	At diagnosis	15	AWD
Huvos III and IV									
OS11	19	Male	Osteoblastic	Distal tibia	3	HD-MTX, ADR/CDDP	18	88	NED
OS25	13	Male	Li-Fraumeni	Distal femur	3	HD-MTX, ADR/CDDP	47	48	DOD
OS27	15	Female	Osteoblastic	Distal femur	3	HD-MTX, IFO, ADR/CDDP	At diagnosis	26	DOD
OS35	19	Female	Fibroblastic	Distal tibia	3	HD-MTX, CDDP/ADR	—	40	NED
OS38	18	Male	Osteoblastic	Distal tibia	3	IFO, CDDP/ADR	—	26	NED
OS48	8	Male	Osteoblastic	Proximal humerus	3	IFO, CDDP/ADR	—	14	NED
OS24	14	Female	Osteoblastic	Distal femur	4	HD-MTX, CDDP/ADR,	—	60	NED
OS28	9	Female	Osteoblastic	Proximal tibia	4	HD-MTX, CDDP/ADR,	6	51	NED
OS39	16	Male	Chondroblastic	Proximal tibia	4	IFO, CDDP/ADR	—	26	NED

Table 5: Clinicopathological features of osetosarcoma tissue samples for prognosis study.

Sample name	Age	Gender	Histological subtype	Site	Huvos grading	Preoperation chemotheapy agents	Mstastasis (months)	Followup (months)	Status
Metastasis within 2 years									
OS07	43	Male	Osteoblastic	Pelvis	2	MTX, ADR/CDDP	6	27	DOD
OS11	19	Male	Osteoblastic	Distal tibia	3	HD-MTX, ADR/CDDP	18	88	NED
OS16	67	Female	Osteoblastic	Distal femur	—	—	19	38	DOD
OS17	13	Female	Osteoblastic	Proximal tibia	1	HD-MTX	15	51	DOD
OS22	61	Male	Osteoblastic	Spine	—	—	5	7	DOD
OS26	19	Male	Osteoblastic	Distal femur	1	HD-MTX, CDDP	19	45	AWD
OS27	15	Female	Osteoblastic	Distal femur	3	HD-MTX, IFO, ADR/CDDP	At diagnosis	26	DOD
OS28	9	Female	Osteoblastic	Proximal tibia	4	HD-MTX, CDDP/ADR,	6	51	NED
OS41	18	Male	Osteoblastic	Pelvis	1	IFO, CDDP/ADR	At diagnosis	18	DOD
OS44	18	Male	Osteoblastic	Distal femur	1	IFO/VP	At diagnosis	3	DOD
OS46	18	Male	Chondroblastic	Distal femur	2	IFO, CDDP/ADR	At diagnosis	17	NED
OS47	14	Male	Chondroblastic	Proximal femur	1	IFO, CDDP/ADR	At diagnosis	15	AWD
No metastasis over 3 years									
OS18	14	Male	Osteoblastic	Proximal tibia	1	HD-MTX, ADR/CDDP	—	73	NED
OS20	12	Male	Osteoblastic	Distal femur	1	HD-MTX, ADR/CDDP, IFO	—	68	NED
OS24	14	Female	Osteoblastic	Distal femur	4	HD-MTX, CDDP/ADR,	—	60	NED
OS32	19	Male	Osteoblastic	Distal femur	1	HD-MTX, CDDP/ADR,	—	47	NED
OS35	19	Female	Fibroblastic	Proximal tibia	3	HD-MTX, CDDP/ADR	—	40	NED

determine genes that were differentially expressed with regard to the response to chemotherapy using osteosarcoma tissue samples. Ochi et al. identified a 60-gene signature predicting the treatment response on the basis of the 23000 cDNA microarray analyses and biopsy samples from 13 osteosarcoma patients. Mintz et al. reported a 104-gene signature associated with histologically evident responses to chemotherapy in osteosarcoma using an Affymetrix chip analysis of 30 pretreatment biopsy specimens. Man et al. described a 45-gene signature using the 9000 cDNA microarray analyses and 20 definitive surgical excision samples of osteosarcoma. However, these gene expression profiles lacked

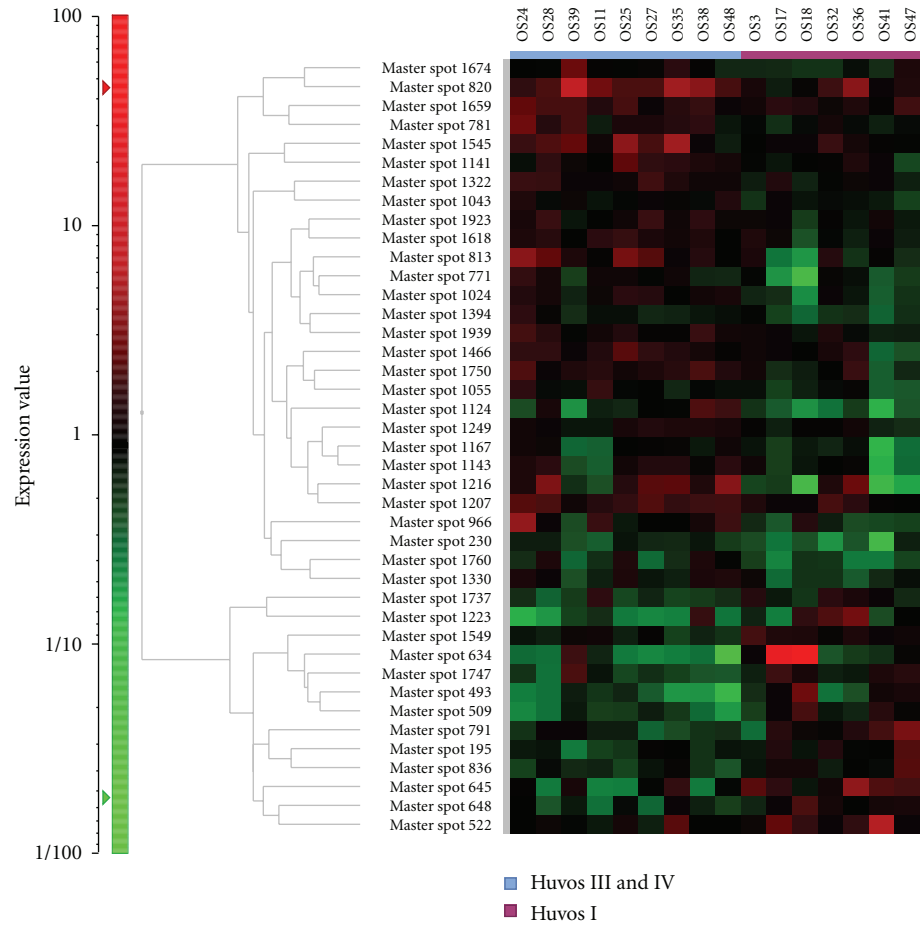

Figure 2: To identify proteins associated with the chemosensitivity of osteosarcoma, we conducted a 2D-DIGE study using osteosarcoma biopsy samples. A hierarchical cluster analysis of 16 osteosarcoma samples demonstrated that there were 41 protein spots that had different levels of intensity between samples. These 41 protein spots were identified from a total of 1465 protein spots ($P < 0.05$). The expected value of this study (from 1465 total protein spots and $P < 0.05$) was >73 protein spots. Therefore, the study design could not acquire a sufficient number of protein spots that had statistically significant differences in the expression levels between samples.

overlapping genes. Some reviews have suggested that the heterogeneity of osteosarcomas might be one of the reasons for the non-overlap [75].

We conducted several proteomic studies using several kinds of surgical tissue samples and were able to identify candidate proteins associated with the prognosis of bone and soft tissue sarcomas, especially GISTs, Ewing sarcomas and synovial sarcomas [18, 19, 25]. Therefore, in our study that was not published, we conducted a proteomic approach to develop prognostic biomarkers for osteosarcoma using 2D-DIGE. In this trial, we used 17 surgical samples and divided the patients into two groups based on their prognosis ((i) the good prognosis group; five osteosarcoma patients who had not developed metastasis over a 3-year period and (ii) a poor prognosis group; 12 osteosarcoma patients who had developed metastasis within 2 years of the initial treatment) (Table 5). We compared the protein expression profiles between the two groups and identified that 72 of 1457 protein spots were differentially expressed ($P < 0.05$). However, these protein spots were not statistically different between the good and poor responder groups (Figure 3). As described above, we hypothesize that the heterogeneity of these osteosarcomas may have been one of the causes of the failure observed in this study.

The three types of tumors examined in our initial sarcoma studies; GISTs, Ewing sarcomas and synovial sarcomas, for which prognostic proteins could be identified in our studies, are associated with translocations or oncoproteins [18, 19, 25]. A general observation of both cDNA microarray- and proteomic-based expression profiling studies of sarcomas is that translocation-associated sarcomas are tightly clustered, whereas complex karyotype sarcomas tend to be less tightly clustered [15, 16, 75–79]. These findings and many reports indicate that translocation or oncoprotein-associated tumors are usually homogeneous tumors. On the other hand, complex karyotype sarcomas are usually heterogeneous tumors [15, 16, 75–79]. Therefore, based on our experiences with sarcoma proteomics, it likely to be more difficult to identify genes or proteins associated with the prognosis and chemosensitivity in heterogeneous tumors,

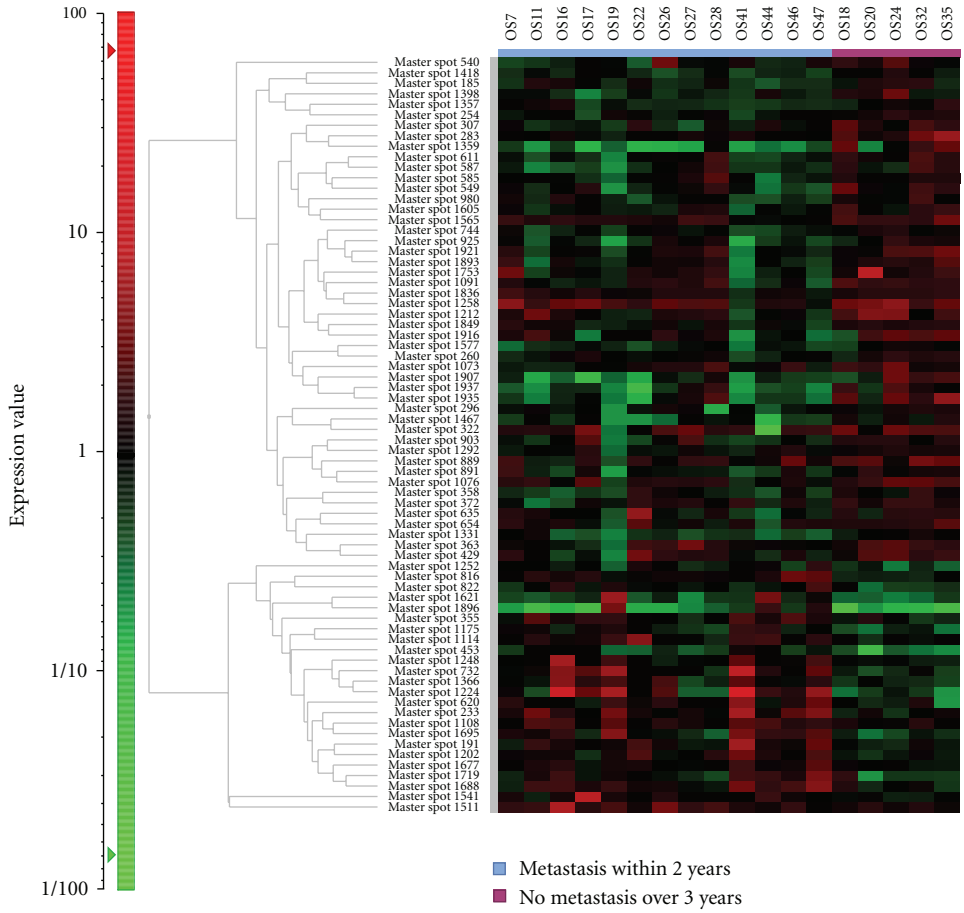

Figure 3: To identify proteins associated with the prognosis and malignant grade of osteosarcoma, we conducted a 2D-DIGE study using osteosarcoma biopsy samples. A hierarchical cluster analysis of 17 osteosarcoma showed that there were 72 protein spots that had different intensity out of a total of 1457 protein spots ($P < 0.05$). The expected value of this study (from 1457 total protein spots and $P < 0.05$) was >73 protein spots. Therefore, the study design also could not obtain a sufficient number of protein spots which had statistically significant differences.

like osteosarcoma, compared to homogenous tumors. Based on our experiences, we believe that it is vitally important to have a good study design which minimizes the noise by avoiding the inclusion of unsuitable samples. This will help to identify real and useful candidate proteins and will facilitate studies of highly heterogeneous tumors, such as osteosarcomas.

6. Conclusion

Several proteomic studies have identified candidate biomarkers relevant to a diagnosis of osteosarcoma, as well as for predicting its level of malignancy and chemosensitivity.

We believe that these proteins are potentially useful biomarkers which may be useful for various clinical applications. However, such proteomic studies have not verified the value of biomarkers in a large validation set by immunohistochemistry or another reliable method. DNA sequencing or measurement of mRNA expression cannot predict the posttranslational modifications of proteins, but proteomic analyses are more directly linked to aberrant tumor phenotypes, and can more accurately reflect the status of tumors. However, compared with cDNA microarray analyses (50,000 probe sets), the sensitivity of the current 2D-DIGE analysis (5000 spots) is still unsatisfactory. In addition, whole-genome sequence tautologies have been developed. Because osteosarcomas are heterogeneous tumors, it is necessary to employ these technologies, such as CGH arrays, cDNA microarrays, whole-genome sequences and 2D-DIGE in combination, so that their individual disadvantages can be overcome, and to identify the most promising and useful biomarkers and molecular targets. These hybrid comprehensive studies consisting of genomics, transcriptomics, and proteomics experiments may provide important, novel clues for understanding the biology of tumors and for revealing biomarkers and therapeutic targets for osteosarcoma.

Conflict of Interests

The corresponding author declares that there is no conflict of interest.

Acknowledgment

This work was supported by a grant from the Japan Society for the Promotion of Science (JSPS), science Grant-in-Aid for Young Scientists B, no. 22791405.

References

[1] C. D. M. Fletcher, K. K. Unni, and F. Mertens, World health organization classification of tumours, pathology and genetics, tumours of soft tissue and bone, 2002.

[2] A. J. Provisor, L. J. Ettinger, J. B. Nachman et al., "Treatment of nonmetastatic osteosarcoma of the extremity with preoperative and postoperative chemotherapy: a report from the children's cancer group," *Journal of Clinical Oncology*, vol. 15, no. 1, pp. 76–84, 1997.

[3] K. Ochi, Y. Daigo, T. Katagiri et al., "Prediction of response to neoadjuvant chemotherapy for osteosarcoma by gene-expression profiles," *International Journal of Oncology*, vol. 24, no. 3, pp. 647–655, 2004.

[4] M. B. Mintz, R. Sowers, K. M. Brown et al., "An expression signature classifies chemotherapy-resistant pediatric osteosarcoma," *Cancer Research*, vol. 65, no. 5, pp. 1748–1754, 2005.

[5] P. Leonard, T. Sharp, S. Henderson et al., "Gene expression array profile of human osteosarcoma," *British Journal of Cancer*, vol. 89, no. 12, pp. 2284–2288, 2003.

[6] T. K. Man, X. Y. Lu, K. Jaeweon et al., "Genome-wide array comparative genomic hybridization analysis reveals distinct amplifications in osteosarcoma," *BMC Cancer*, vol. 4, article 45, 2004.

[7] M. Zielenska, J. Bayani, A. Pandita et al., "Comparative genomic hybridization analysis identifies gains of 1p35~p36 and chromosome 19 in osteosarcoma," *Cancer Genetics and Cytogenetics*, vol. 130, no. 1, pp. 14–21, 2001.

[8] S. dos Santos Aguiar, L. de Jesus Girotto Zambaldi, A. M. dos Santos, W. Pinto Jr., and S. R. Brandalise, "Comparative genomic hybridization analysis of abnormalities in chromosome 21 in childhood osteosarcoma," *Cancer Genetics and Cytogenetics*, vol. 175, no. 1, pp. 35–40, 2007.

[9] C. C. Lau, C. P. Harris, X. Y. Lu et al., "Frequent amplification and rearrangement of chromosomal bands 6p12-p21 and 17p11.2 in osteosarcoma," *Genes Chromosomes and Cancer*, vol. 39, no. 1, pp. 11–21, 2004.

[10] J. Atiye, M. Wolf, S. Kaur et al., "Gene amplifications in osteosarcoma—CGH microarray analysis," *Genes Chromosomes and Cancer*, vol. 42, no. 2, pp. 158–163, 2005.

[11] C. M. Hattinger, G. Reverter-Branchat, D. Remondini et al., "Genomic imbalances associated with methotrexaate resistance in human osteosarcoma cell lines detected by comparative genomic hybridization-based techniques," *European Journal of Cell Biology*, vol. 82, no. 9, pp. 483–493, 2003.

[12] J. A. Squire, J. Pei, P. Marrano et al., "High-resolution mapping of amplifications and deletions in pediatric osteosarcoma by use of CGH analysis of cDNA microarrays," *Genes Chromosomes and Cancer*, vol. 38, no. 3, pp. 215–225, 2003.

[13] G. Lim, J. Karaskova, B. Beheshti et al., "An integrated mBAND and submegabase resolution tiling set (SMRT) CGH array analysis of focal amplification, microdeletions, and ladder structures consistent with breakage-fusion-bridge cycle events in osteosarcoma," *Genes Chromosomes and Cancer*, vol. 42, no. 4, pp. 392–403, 2005.

[14] G. Chen, T. G. Gharib, C. C. Huang et al., "Discordant protein and mRNA expression in lung adenocarcinomas," *Molecular & Cellular Proteomics*, vol. 1, no. 4, pp. 304–313, 2002.

[15] Y. Suehara, T. Kondo, K. Fujii et al., "Proteomic signatures corresponding to histological classification and grading of soft-tissue sarcomas," *Proteomics*, vol. 6, no. 15, pp. 4402–4409, 2006.

[16] A. Kawai, T. Kondo, Y. Suehara, K. Kikuta, and S. Hirohashi, "Global protein-expression analysis of bone and soft tissue sarcomas," *Clinical Orthopaedics and Related Research*, vol. 466, no. 9, pp. 2099–2106, 2008.

[17] S. P. Gygi, Y. Rochon, B. R. Franza, and R. Aebersold, "Correlation between protein and mRNA abundance in yeast," *Molecular and Cellular Biology*, vol. 19, no. 3, pp. 1720–1730, 1999.

[18] Y. Suehara, N. Tochigi, D. Kubota et al., "Secernin-1 as a novel prognostic biomarker candidate of synovial sarcoma revealed by proteomics," *Journal of Proteomics*, vol. 74, no. 6, pp. 829–842, 2011.

[19] Y. Suehara, T. Kondo, K. Seki et al., "Pfetin as a prognostic biomarker of gastrointestinal stromal tumors revealed by proteomics," *Clinical Cancer Research*, vol. 14, no. 6, pp. 1707–1717, 2008.

[20] Y. Suehara, K. Kikuta, R. Nakayama et al., "GST-P1 as a histological biomarker of synovial sarcoma revealed by proteomics," *Proteomics—Clinical Applications*, vol. 3, no. 5, pp. 623–634, 2009.

[21] Y. Suehara, K. Kikuta, R. Nakayama et al., "Anatomic site-specific proteomic signatures of gastrointestinal stromal tumors," *Proteomics—Clinical Applications*, vol. 3, no. 5, pp. 584–596, 2009.

[22] Y. Suehara, "Proteomic analysis of soft tissue sarcoma," *International Journal of Clinical Oncology*, vol. 16, no. 2, pp. 92–100, 2011.

[23] K. Kikuta, N. Tochigi, S. Saito et al., "Peroxiredoxin 2 as a chemotherapy responsiveness biomarker candidate in osteosarcoma revealed by proteomics," *Proteomics—Clinical Applications*, vol. 4, no. 5, pp. 560–567, 2010.

[24] K. Kikuta, D. Kubota, T. Saito et al., "Clinical proteomics identified ATP-dependent RNA helicase DDX39 as a novel biomarker to predict poor prognosis of patients with gastrointestinal stromal tumor," *Journal of Proteomics*, vol. 75, no. 4, pp. 1089–1098.

[25] K. Kikuta, N. Tochigi, T. Shimoda et al., "Nucleophosmin as a candidate prognostic biomarker of ewing's sarcoma revealed by proteomics," *Clinical Cancer Research*, vol. 15, no. 8, pp. 2885–2894, 2009.

[26] Y. Li, T. A. Dang, J. Shen et al., "Plasma proteome predicts chemotherapy response in osteosarcoma patients," *Oncology Reports*, vol. 25, no. 2, pp. 303–314, 2011.

[27] K. Yanagisawa, Y. Shyr, B. J. Xu et al., "Proteomic patterns of tumour subsets in non-small-cell lung cancer," *The Lancet*, vol. 362, no. 9382, pp. 433–439, 2003.

[28] A. A. Alaiya, B. Franzén, A. Hagman et al., "Molecular classification of borderline ovarian tumors using hierarchical cluster analysis of protein expression profiles," *International Journal of Cancer*, vol. 98, no. 6, pp. 895–899, 2002.

[29] M. L. Reyzer, R. L. Caldwell, T. C. Dugger et al., "Early changes in protein expression detected by mass spectrometry predict tumor response to molecular therapeutics," *Cancer Research*, vol. 64, no. 24, pp. 9093–9100, 2004.

[30] J. W. Cui, J. Wang, K. He et al., "Proteomic analysis of human acute leukemia cells: insight into their classification," *Clinical Cancer Research*, vol. 10, no. 20, pp. 6887–6896, 2004.

[31] S. Varambally, J. Yu, B. Laxman et al., "Integrative genomic and proteomic analysis of prostate cancer reveals signatures of metastatic progression," *Cancer Cell*, vol. 8, no. 5, pp. 393–406, 2005.

[32] C. Folio, M. I. Mora, M. Zalacain et al., "Proteomic analysis of chemonaïve pediatric osteosarcomas and corresponding normal bone reveals multiple altered molecular targets," *Journal of Proteome Research*, vol. 8, no. 8, pp. 3882–3888, 2009.

[33] Y. Li, T. A. Dang, J. Shen et al., "Identification of a plasma proteomic signature to distinguish pediatric osteosarcoma from benign osteochondroma," *Proteomics*, vol. 6, no. 11, pp. 3426–3435, 2006.

[34] Y. Li, Q. Liang, Y. Q. Wen et al., "Comparative proteomics analysis of human osteosarcomas and benign tumor of bone," *Cancer Genetics and Cytogenetics*, vol. 198, no. 2, pp. 97–106, 2010.

[35] D. H. Conrad, J. Goyette, and P. S. Thomas, "Proteomics as a method for early detection of cancer: a review of proteomics, exhaled breath condensate, and lung cancer screening," *Journal of General Internal Medicine*, vol. 23, supplement 1, pp. 78–84, 2008.

[36] C. A. Granville and P. A. Dennis, "An overview of lung cancer genomics and proteomics," *American Journal of Respiratory Cell and Molecular Biology*, vol. 32, no. 3, pp. 169–176, 2005.

[37] R. Alessandro, S. Fontana, E. Kohn, and G. de Leo, "Proteomic strategies and their application in cancer research," *Tumori*, vol. 91, no. 6, pp. 447–455, 2005.

[38] T. Takahashi, T. Naka, M. Fujimoto et al., "Aberrant expression of glycosylation in juvenile gastrointestinal stromal tumors," *Proteomics—Clinical Applications*, vol. 2, no. 9, pp. 1246–1254, 2008.

[39] G. E. Holt, H. S. Schwartz, and R. L. Caldwell, "Proteomic profiling in musculoskeletal oncology by MALDI mass spectrometry," *Clinical Orthopaedics and Related Research*, no. 450, pp. 105–110, 2006.

[40] P. A. Fetsch, N. L. Simone, P. K. Bryant-Greenwood et al., "Proteomic evaluation of archival cytologic material using SELDI affinity mass spectrometry: potential for diagnostic applications," *American Journal of Clinical Pathology*, vol. 118, no. 6, pp. 870–876, 2002.

[41] T. Kondo and S. Hirohashi, "Application of highly sensitive fluorescent dyes (CyDye DIGE Fluor saturation dyes) to laser microdissection and two-dimensional difference gel electrophoresis (2D-DIGE) for cancer proteomics," *Nature Protocols*, vol. 1, no. 6, pp. 2940–2956, 2006.

[42] T. Kondo and S. Hirohashi, "Application of 2D-DIGE in cancer proteomics toward personalized medicine," *Methods in Molecular Biology*, vol. 577, pp. 135–154, 2009.

[43] J. S. Minden, S. R. Dowd, H. E. Meyer, and K. Stühler, "Difference gel electrophoresis," *Electrophoresis*, vol. 30, supplement 1, pp. S156–S161, 2009.

[44] B. Fiévet, D. Louvard, and M. Arpin, "ERM proteins in epithelial cell organization and functions," *Biochimica et Biophysica Acta*, vol. 1773, no. 5, pp. 653–660, 2007.

[45] G. Bulut, S. H. Hong, K. Chen et al., "Small molecule inhibitors of ezrin inhibit the invasive phenotype of osteosarcoma cells," *Oncogene*, vol. 31, pp. 269–281, 2012.

[46] A. Bretscher, K. Edwards, and R. G. Fehon, "ERM proteins and merlin: integrators at the cell cortex," *Nature Reviews Molecular Cell Biology*, vol. 3, no. 8, pp. 586–599, 2002.

[47] L. Ren, S. H. Hong, Q. R. Chen et al., "Dysregulation of ezrin phosphorylation prevents metastasis and alters cellular metabolism in osteosarcoma," *Cancer Research*, vol. 72, no. 4, pp. 1001–1012.

[48] S. Tsukita, S. Yonemura, and S. Tsukita, "ERM (ezrin/radixin/moesin) family: from cytoskeleton to signal transduction," *Current Opinion in Cell Biology*, vol. 9, no. 1, pp. 70–75, 1997.

[49] C. Khanna, X. Wan, S. Bose et al., "The membrane-cytoskeleton linker ezrin is necessary for osteosarcoma metastasis," *Nature Medicine*, vol. 10, no. 2, pp. 182–186, 2004.

[50] H. R. Park, R. L. Cabrini, E. S. Araujo, M. L. Paparella, D. Brandizzi, and Y. K. Park, "Expression of ezrin and metastatic tumor antigen in osteosarcomas of the jaw," *Tumori*, vol. 95, no. 1, pp. 81–86, 2009.

[51] H. R. Park, W. W. Jung, P. Bacchini, F. Bertoni, Y. W. Kim, and Y. K. Park, "Ezrin in osteosarcoma: comparison between conventional high-grade and central low-grade osteosarcoma," *Pathology Research and Practice*, vol. 202, no. 7, pp. 509–515, 2006.

[52] C. Di Cristofano, M. Leopizzi, A. Miraglia et al., "Phosphorylated ezrin is located in the nucleus of the osteosarcoma cell," *Modern Pathology*, vol. 23, no. 7, pp. 1012–1020, 2010.

[53] Y. Yu, J. Khan, C. Khanna, L. Helman, P. S. Meltzer, and G. Merlino, "Expression profiling identifies the cytoskeletal organizer ezrin and the developmental homeoprotein Six-1 as key metastatic regulators," *Nature Medicine*, vol. 10, no. 2, pp. 175–181, 2004.

[54] A. M. Davis, R. S. Bell, and P. J. Goodwin, "Prognostic factors in osteosarcoma: a critical review," *Journal of Clinical Oncology*, vol. 12, no. 2, pp. 423–431, 1994.

[55] S. B. Lee, J. N. Ho, S. H. Yoon, G. Y. Kang, S. G. Hwang, and H. D. Um, "Peroxiredoxin 6 promotes lung cancer cell invasion by inducing urokinase-type plasminogen activator via p38 kinase, phosphoinositide 3-kinase, and Akt," *Molecules and Cells*, vol. 28, no. 6, pp. 583–588, 2009.

[56] C. A. Neumann, D. S. Krause, C. V. Carman et al., "Essential role for the peroxiredoxin Prdx1 in erythrocyte antioxidant defence and tumour suppression," *Nature*, vol. 424, no. 6948, pp. 561–565, 2003.

[57] T. H. Lee, S. U. Kim, S. L. Yu et al., "Peroxiredoxin II is essential for sustaining life span of erythrocytes in mice," *Blood*, vol. 101, no. 12, pp. 5033–5038, 2003.

[58] X. Wang, S. A. Phelan, K. Forsman-Semb et al., "Mice with targeted mutation of peroxiredoxin 6 develop normally but are susceptible to oxidative stress," *The Journal of Biological Chemistry*, vol. 278, no. 27, pp. 25179–25190, 2003.

[59] Y. Wang, S. I. Feinstein, and A. B. Fisher, "Peroxiredoxin 6 as an antioxidant enzyme: protection of lung alveolar epithelial type II cells from H2O2-induced oxidative stress," *Journal of Cellular Biochemistry*, vol. 104, no. 4, pp. 1274–1285, 2008.

[60] Y. Wang, S. I. Feinstein, Y. Manevich, Y. S. Ho, and A. B. Fisher, "Peroxiredoxin 6 gene-targeted mice show increased lung injury with paraquat-induced oxidative stress," *Antioxidants and Redox Signaling*, vol. 8, no. 1-2, pp. 229–237, 2006.

[61] S. T. Lehtonen, A. M. Svensk, Y. Soini et al., "Peroxiredoxins, a novel protein family in lung cancer," *International Journal of Cancer*, vol. 111, no. 4, pp. 514–521, 2004.

[62] D. Q. Li, L. Wang, F. Fei et al., "Identification of breast cancer metastasis-associated proteins in an isogenic tumor metastasis model using two-dimensional gel electrophoresis and liquid chromatography-ion trap-mass spectrometry," *Proteomics*, vol. 6, no. 11, pp. 3352–3368, 2006.

[63] P. Karihtala, A. Mäntyniemi, S. W. Kang, V. L. Kinnula, and Y. Soini, "Peroxiredoxins in breast carcinoma," *Clinical Cancer Research*, vol. 9, no. 9, pp. 3418–3424, 2003.

[64] J. B. Lee, S. J. Yun, H. Z. Chae, Y. H. Won, Y. P. Kim, and S. C. Lee, "Expression of peroxiredoxin and thioredoxin in dermatological disorders," *British Journal of Dermatology*, vol. 146, no. 4, pp. 710–712, 2002.

[65] V. L. Kinnula, S. Lehtonen, R. Sormunen et al., "Overexpression of peroxiredoxins I, II, III, V, and VI in malignant mesothelioma," *Journal of Pathology*, vol. 196, no. 3, pp. 316–323, 2002.

[66] T. Yanagawa, T. Ishikawa, T. Ishii et al., "Peroxiredoxin I expression in human thyroid tumors," *Cancer Letters*, vol. 145, no. 1-2, pp. 127–132, 1999.

[67] W. C. Chen, W. H. McBride, K. S. Iwamoto et al., "Induction of radioprotective peroxiredoxin-I by ionizing irradiation," *Journal of Neuroscience Research*, vol. 70, no. 6, pp. 794–798, 2002.

[68] J. H. Kim, P. N. Bogner, N. Ramnath, Y. Park, J. Yu, and Y. M. Park, "Elevated peroxiredoxin 1, but not NF-E2-related factor 2, is an independent prognostic factor for disease recurrence and reduced survival in stage I non-small cell lung cancer," *Clinical Cancer Research*, vol. 13, no. 13, pp. 3875–3882, 2007.

[69] Y. M. Chung, Y. D. Yoo, J. K. Park, Y. T. Kim, and H. J. Kim, "Increased expression of peroxiredoxin II confers resistance to cisplatin," *Anticancer Research*, vol. 21, no. 2, pp. 1129–1133, 2001.

[70] S. H. Park, Y. M. Chung, Y. S. Lee et al., "Antisense of human peroxiredoxin II enhances radiation-induced cell death," *Clinical Cancer Research*, vol. 6, no. 12, pp. 4915–4920, 2000.

[71] L. Smith, K. J. Welham, M. B. Watson, P. J. Drew, M. J. Lind, and L. Cawkwell, "The proteomic analysis of cisplatin resistance in breast cancer cells," *Oncology Research*, vol. 16, no. 11, pp. 497–506, 2007.

[72] A. Kropotov, V. Gogvadze, O. Shupliakov et al., "Peroxiredoxin V is essential for protection against apoptosis in human lung carcinoma cells," *Experimental Cell Research*, vol. 312, no. 15, pp. 2806–2815, 2006.

[73] A. Castagna, P. Antonioli, H. Astner et al., "A proteomic approach to cisplatin resistance in the cervix squamous cell carcinoma cell line A431," *Proteomics*, vol. 4, no. 10, pp. 3246–3267, 2004.

[74] X. Z. Chang, D. Q. Li, Y. F. Hou et al., "Identification of the functional role of peroxiredoxin 6 in the progression of breast cancer," *Breast Cancer Research*, vol. 9, no. 6, article R76, 2007.

[75] T. O. Nielsen, "Microarray analysis of sarcomas," *Advances in Anatomic Pathology*, vol. 13, no. 4, pp. 166–173, 2006.

[76] K. Tschoep, A. Kohlmann, M. Schlemmer, T. Haferlach, and R. D. Issels, "Gene expression profiling in sarcomas," *Critical Reviews in Oncology/Hematology*, vol. 63, no. 2, pp. 111–124, 2007.

[77] T. O. Nielsen, R. B. West, S. C. Linn et al., "Molecular characterisation of soft tissue tumours: a gene expression study," *The Lancet*, vol. 359, no. 9314, pp. 1301–1307, 2002.

[78] C. R. Antonescu, "Molecular profiling in the diagnosis and treatment of high grade sarcomas," *Ultrastructural Pathology*, vol. 32, no. 2, pp. 37–42, 2008.

[79] R. Nakayama, T. Nemoto, H. Takahashi et al., "Gene expression analysis of soft tissue sarcomas: characterization and reclassification of malignant fibrous histiocytoma," *Modern Pathology*, vol. 20, no. 7, pp. 749–759, 2007.

Hindawi Publishing Corporation
Sarcoma
Volume 2012, Article ID 937506, 13 pages
doi:10.1155/2012/937506

Research Article

Genes Regulated in Metastatic Osteosarcoma: Evaluation by Microarray Analysis in Four Human and Two Mouse Cell Line Systems

Roman Muff, Ram Mohan Ram Kumar, Sander M. Botter, Walter Born, and Bruno Fuchs

Laboratory for Orthopedic Research, Balgrist University Hospital, Forchstrasse 340, 8008 Zurich, Switzerland

Correspondence should be addressed to Bruno Fuchs, bfuchs@research.balgrist.ch

Received 6 July 2012; Accepted 7 September 2012

Academic Editor: Norman Jaffe

Osteosarcoma (OS) is a rare bone neoplasm that affects mainly adolescents. It is associated with poor prognosis in case of metastases formation. The search for metastasis predicting markers is therefore imperative to optimize treatment strategies for patients at risk and important for the search of new drugs for the treatment of this devastating disease. Here, we have analyzed by microarray the differential gene expression in four human and two mouse OS cell line systems consisting of parental cell lines with low metastatic potential and derivatives thereof with increased metastatic potential. Using two osteoblastic cell line systems, the most common OS phenotype, we have identified forty-eight common genes that are differentially expressed in metastatic cell lines compared to parental cells. The identified subset of metastasis relevant genes in osteoblastic OS overlapped only minimally with differentially expressed genes in the other four preosteoblast or nonosteoblastic cell line systems. The results imply an OS phenotype specific expression pattern of metastasis regulating proteins and form a basis for further investigation of gene expression profiles in patients' samples combined with survival analysis with the aim to optimize treatment strategies to develop new drugs and to consequently improve the survival of patients with the most common form of osteoblastic OS.

1. Introduction

Osteosarcoma (OS) is a rare but highly malignant neoplasm of bone that affects mainly young patients during the second decade of their lives. The survival of patients with localized disease has been improved by refinement of surgical techniques and by the introduction of neoadjuvant chemotherapy. However, the survival rate of patients that develop metastases remains to be low. The identification of proteins that are involved in OS progression and metastasis is therefore of immediate importance to develop new and improved treatment strategies.

The analysis of differentially expressed genes by microarray, comparing metastatic OS cell lines to parental cell lines with low metastatic potential, should help to identify common pathways or even a set of proteins that regulate OS tumor progression and metastasis. To our knowledge, four human and two mouse OS systems were developed that fulfill this requirement. Human metastatic LM5 and M132 cells were derived from parental SAOS and HUO9 cells, respectively, by *in vivo* selection in mice carried out by repeated tail vein injection of cells isolated from lung metastases [1, 2]. Human metastatic 143B cells were obtained by K-ras transformation of HOS [3] cells and human metastatic M8 cells by *in vitro* subcloning of parental MG63 cells as described [4]. Mouse metastatic LM8 and K7M2 cells were also selected *in vivo* from parental Dunn and K12 cells, respectively [5, 6]. Comparative microarray analyses were performed with HUO9/M132 [7], K12/K7M2 [8], and most recently with SAOS/LM7 and HOS/143B cells [9]. The results obtained in these studies imply that different sets of proteins are differentially expressed in each system and that different signaling pathways are involved in OS tumor progression. These studies identified ezrin as an important player in OS pathogenesis [8, 10].

OS is a heterogeneous disease. Diverse cell types originating from mesenchymal stem cells may be affected by genomic instability during different stages of differentiation

[11, 12]. Histologically, most of the patients present with tumors with an osteoblastic (60–70%) phenotype, followed by chondroblastic and fibroblastic OS (both approximately 10%) [13]. Although there is no evidence for a cell type dependent propensity to form metastases in OS [13], different pathways involved in tumor progression in such diverse cell types appear likely. SAOS and Dunn cells are considered osteoblast-like cells or early osteoblasts as they express high alkaline phosphatase (ALPL) activity, possess parathyroid hormone (PTH) responsiveness, and produce mineralized extracellular matrix upon osteogenic induction *in vitro* ([5, 14], and this study). HUO9 are also described to be osteoblastic [2], but the relatively low ALPL activity observed in this study suggests that they are preosteoblastic. MG63 and K12 are considered fibroblastic [15, 16], and HOS have a mixed type of fibroblastic and epithelial-like morphology.

In this study we analyzed differentially expressed genes by microarray analyses in the four human OS cell line systems SAOS/LM5, HUO9/M132, HOS/143B, and MG63/M8 and the two mouse cell line systems Dunn/LM8 and K12/K7M2. Based on the enrichment of differentially regulated genes in common gene ontology (GO) terms, we identified 48 (17 up- and 31 downregulated) commonly regulated genes in OS metastasis in the two osteoblastic systems (SAOS/LM5 and Dunn/LM8), that were shared only at a limited number in the other four cell line systems. The possible role of some of the identified genes in osteoblastic tumor progression is discussed.

2. Materials and Methods

2.1. Cell Lines and Culture. SAOS (HTB-85), HOS (CRL-1543), and 143B (CRL-8303) cells were obtained from ATCC (Rockville, MD, USA). LM5 cells were kindly provided by E.S. Kleinerman (M.D. Anderson Cancer Center, Houston, TX, USA), HUO9 and HUO9-M132 (M132) cells by M. Tani (National Cancer Center Hospital, Tokyo, Japan), Dunn and LM8 cells by T. Ueda (Osaka University Graduate School of Medicine, Osaka, Japan), MG63 cells by G. Sarkar (Mayo Clinic, Rochester, MN, USA), and MG63-M8 (M8) cells by W. T. Zhu (Tongji Hospital, Huazhong University of Science and Technology, Wuhan, China). K12 and K7M2 cells were obtained from C. Khanna (National Cancer Institute, Bethesda, MD, USA), the former with permission from J. Schmidt (GSF, National Research Center for Environment and Health, Neuherberg, Germany) who established the K12 cells [16]. Cells were cultured in DMEM (4.5 g/L glucose)/F12 (1 : 1) medium supplemented with 10% heat-inactivated FCS in a humidified atmosphere of 5% CO_2. Subconfluent cells were detached with trypsin/EDTA, centrifuged and cell pellets immediately frozen in liquid nitrogen, and stored at −80°C until RNA extraction.

2.2. RNA Extraction, Array Hybridization, and Analysis. Total RNA was isolated from frozen cell pellets of individual cell lines with TriReagent (Sigma-Aldrich, St. Louis, MO) as described [17]. The RNA was quantified by measuring the absorption at 260 and 280 nm in a UV-spectrophotometer. The integrity of the RNA was assessed by standard agarose gel-electrophoresis and using Bioanalyzer 2100. Complementary RNA preparation and array hybridization were performed by the Functional Genomics Center (Zurich, Switzerland) using Affymetrix Human Genome U133 Plus 2.0 (54675 probe sets) and Affymetrix Mouse Genome 430 2.0 (45101 probe sets) arrays. The gene expression signals ranged from 5–22000 and 6–31000 in the four human and two mouse systems, respectively. The distribution of gene expression levels ($\log_2$) was similar in the two array types as exemplified for the SAOS/LM5 and Dunn/LM8 systems (Supplementary Figure 1 of the Supplementary Material available at doi:10.1155/2012/937506). Gene expression levels were arbitrarily set as low, intermediate, and high when values were <50, 50–300, and >300, respectively. By this criterion approximately 60% of the genes were expressed at a low level, 20% were expressed at intermediate, and the remaining 20% at high levels in both types of arrays. Quality control, RMA normalization of raw data, and statistical analysis were performed using RACE (http://race.unil.ch/). Gene ontology (GO) analysis was performed using GOEAST (http://omicslab.genetics.ac.cn/GOEAST/). We used Ingenuity Pathway Analysis (IPA) version 12710793, build 162830. In the first step of a so-called core analysis, the genes (molecules) that belong to the regulated probe sets are identified. Next, the cutoff fold-change was adjusted to select around 800 regulated molecules (to minimize noise, Ingenuity recommends that approximately 800 molecules, or less, are analyzed). These molecules are eligible for generating networks, where (in)direct and relationships between molecules are shown based on literature findings. The networks are limited to 35 molecules each in order to keep them to a usable size.

2.3. cDNA Synthesis and Real-Time PCR Analysis. cDNA was reverse transcribed from 1 μg of total RNA with a high-capacity RNA-to-cDNA kit (Applied Biosystems, Foster City, CA) and the protocol provided by the manufacturer. Three independent RNA extracts from individual cell lines were reverse transcribed in a final volume of 20 μL. Real-time PCR was carried out in a StepOnePlus Real-Time PCR System (Applied Biosystems) in 96-well plates. Intron-spanning primers were designed with NCBI Primer blast (http://www.ncbi.nlm.nih.gov/tools/primer-blast/) software (Supplementary Table 1) for amplification of cDNA sequences derived from selected genes. Five genes that were found upregulated and five genes that were found down-regulated by microarray analysis in LM5 compared SAOS cells and GAPDH as a reference gene were analyzed. PCR from individual RT reactions was carried out in triplicates. cDNA equivalent to 30 ng of RNA and appropriate primers were added to Power SYBR Green PCR Master Mix (Applied Biosystems) and the samples preincubated at 50°C for 2 min and at 95°C for 10 min and then subjected to 40 cycles of incubation at 95°C for 15 s and at 60°C for 1 min. The threshold for Ct values was set to 0.325 and the obtained values were analyzed with the delta Ct (ΔCt) method. Mean Ct values calculated from triplicate PCR were normalized to mean Ct values determined for GAPDH gene transcripts

as a measure for cDNA input. The presence of nonspecific amplification products in any of the PCR reactions was excluded by inspection of the melting curves of final PCR products. The data presented in Supplementary Figure 2 confirmed the upregulation of four and the downregulation of five genes as revealed by the microarray analysis.

2.4. Alkaline Phosphatase Activity, cAMP Stimulation, and Alizarin Red S Staining. Cell extraction and measurements of alkaline phosphatase (ALPL) activity, cAMP production stimulated by chicken parathyroid hormone-related peptide, the induction of extracellular matrix mineralization, and its visualization by Alizarin Red S staining were performed as described [14].

3. Results

3.1. Gene Expression Analysis Reveals Heterogeneity among Different Cell Line Systems and Differential Gene Expression in Low and High Metastatic Cell Lines. Four human and two mouse osteosarcoma cell lines with low metastatic potential were compared to their high-metastatic derivatives for differential gene expression by microarray analysis. The four human systems with low and upregulated metastatic activity included the SAOS/LM5, HUO9/M132, HOS/143B, and MG63/M8 cells. The two mouse systems consisted of the Dunn/LM8 and K12/K7M2 cells. A comparison of gene expression levels in the four human systems revealed that each system clustered together, although the expression levels clearly differed in low versus high metastatic cell lines (Figure 1(a)). Interestingly, the two cell line systems that underwent *in vivo* selection of the cell line with increased metastatic potential (SAOS/LM5 and HUO9/M132) were clearly different from the cluster of the HOS/143B (Ki-ras transformation of HOS) system and the MG63/M8 system obtained by *in vitro* selection of M8 from MG63. Clustering of the two mouse systems with distinct gene expression levels in low and high metastatic cell lines was also observed (Figure 1(b)). The number of differently expressed genes (i.e., up- or downregulated >2-fold with a false discovery rate (fdr) of <0.01) in low versus high metastatic cell lines was highest in HOS/143B and K12/K7M2, lower in SAOS/LM5, HUO9/M132, and Dunn/LM8, and lowest in MG63/M8. Only 1% of total probe sets were differentially regulated in MG63/M8 whereas 2.5–3.6% (SAOS/LM5, HUO9/M132, and Dunn/LM8) and 6.7–8.3% were differentially regulated in the HOS/143B and K12/K7M2 systems, respectively. These findings are summarized in Table 1. Taken together, the results indicate remarkable heterogeneity among the different OS cell line systems and also variability in the number of genes potentially involved in malignancy progression in the different cell lines.

3.2. Plasma Membrane and Extracellular Matrix Proteins Involved in Binding, Cell Migration, Angiogenesis, and Apoptosis Are Differentially Expressed in Tumor Progression. A gene ontology (GO) analysis of metastasis-regulated (>2-fold; fdr < 0.01) genes in all six cell systems revealed an enrichment (fdr < 0.00001) at the most general level 1 (Table 2). Here, 5 out of 18 "cellular component," 5 out of 20 "molecular function", and 18 out of 32 "biological process" GO terms were significantly enriched, again with a large variability among the different cell systems. For the term "cellular component," genes belonging to the terms "cell" and "extracellular region" were enriched in all cell systems, followed by "extracellular matrix" (4/6) and "membrane" (3/6). For the term "molecular function" only genes belonging to the term "binding" were enriched in all cell systems. The greatest variability was observed in the term "biological process." Here, enrichment was observed in all cell systems in terms of "biological regulation," "multicellular organismal process", "developmental process," and "biological adhesion," followed by "cellular process" (5/6), "response to stimulus" (4/6), and "signaling" (4/6). In eleven additional terms enrichment was observed to different degrees in the six cell line systems. Despite the observed heterogeneity, the results imply that aberrantly expressed binding proteins in the plasma membrane and the extracellular matrix that control the regulation of developmental processes and cellular adhesion are involved in tumor progression in mice and humans.

A GO analysis at higher and more specific levels, and with significant nodes between levels and down to the level 1, revealed an aberrant regulation of diverse biological processes in the different cell systems (Supplementary Table 2). In the SAOS/LM5 cell line system, genes involved in cardiovascular development and neurogenesis were aberrantly expressed. In the HUO9/M132 system, heart development was also affected together with ureteric bud morphogenesis and genes involved in angiogenesis and cell migration were highly regulated. In the HOS/143B system, angiogenesis and cell migration were also deregulated. In addition, apoptosis and integrin-mediated cell-cell adhesion were affected. Genes involved in ERK1 and -2 kinase, MAP kinase, SMAD, and TGFβ signaling and in ureteric bud, prostate gland, blood vessel and lung alveolus development, neurogenesis, and blood coagulation were also significantly enriched in respective GO terms. In the MG63/M8 system only genes involved in axon regeneration, cell surface receptor signaling, and intracellular protein kinase activity were differentially regulated. In the Dunn/LM8 system, genes involved in the

Table 1: Number of regulated (>2-fold; fdr < 0.01) probe sets in human and mouse OS cell line systems.

System	Total (%)[a]	Up (%)[b]	Down (%)[b]
Human			
SAOS/LM5	1351 (2.5)	668 (49)	683 (51)
HUO9/M132	1975 (3.6)	1001 (51)	974 (49)
HOS/143B	3652 (6.7)	1690 (46)	1962 (54)
MG63/M8	521 (1.0)	292 (56)	229 (44)
Mouse			
Dunn/LM8	1217 (2.7)	494 (41)	723 (59)
K12/K7M2	3749 (8.3)	1769 (47)	1980 (53)

[a] Percent of the total number of probe sets represented by the human (54675) and mouse arrays (45101); [b] percent of the total number of regulated probe sets.

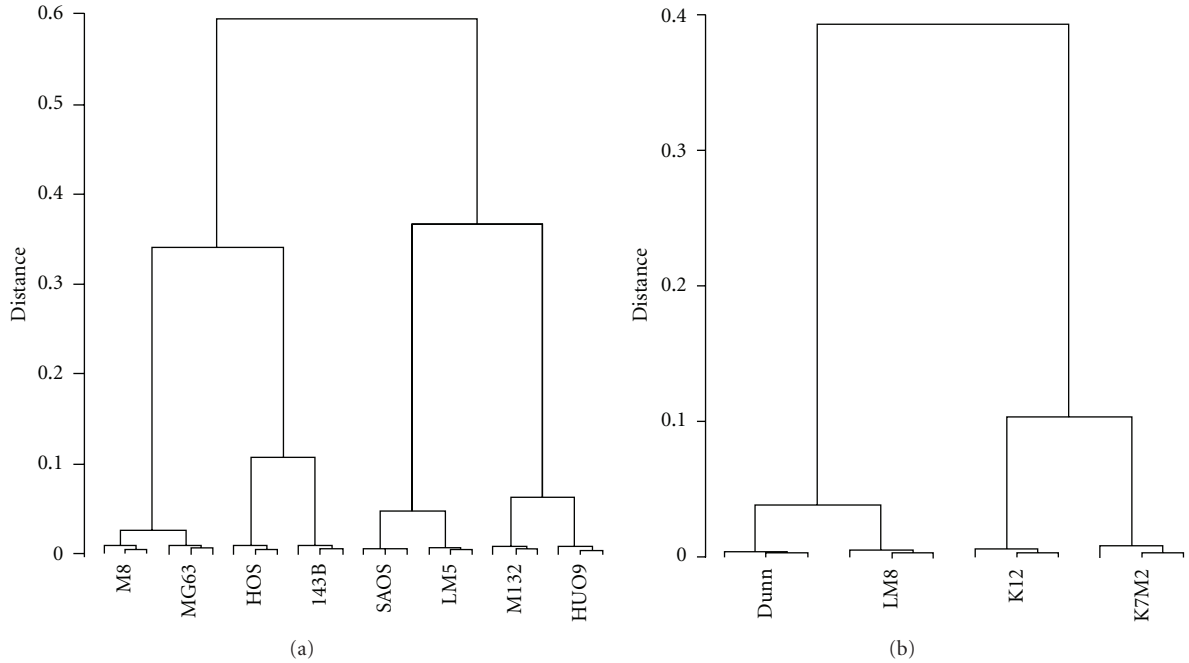

Figure 1: (a) Dendrogram of gene expression levels in the four human OS cell line systems. (b) Dendrogram of gene expression levels in the two mouse OS cell line systems. All probe sets on the arrays were included in the analysis.

regulation of cell migration and apoptosis and extracellular matrix organization together with epithelium, neuron, blood vessel, and chondrocyte differentiation were enriched in respective GO terms. Migration and angiogenesis were affected in the K12/K7M2 system together with altered ovarian follicle, mammary gland duct and salivary gland morphogenesis, and axonogenesis. Taken together, although no common biological processes were revealed in the six cell line systems, deregulation of cell migration (4/6), angiogenesis (3/6) and apoptosis (2/6) may contribute to tumor progression. The affected developmental processes were mainly neurogenesis (5/6), cardiovascular (4/6), and the reproductive system development.

In addition to GO, we also analyzed these data through the use of Ingenuity Pathways Analysis (IPA; Ingenuity Systems, http://www.ingenuity.com). The analysis confirmed all cell systems to be associated with cancerous processes (ranked as nr. 1 bio function "diseases and disorders" for all cell systems) (Supplementary Table 3). Also pathways involved in cellular movement (ranked nr. 1 in all cell systems, except for LM5) and cardiovascular development and function (ranked nr. 1 in 5 out of 6 cell systems, ranked nr. 3 in LM5), with vasculogenesis/angiogenesis pathways prominently activated, were found to be enriched. These results therefore confirm the results obtained in the GO analysis.

3.3. The SAOS/LM5 and Dunn/LM8 Cell Line Systems Are Representative for Osteoblastic OS. In humans, approximately two thirds of OS patients present with an osteoblastic tumor phenotype. We therefore searched for osteoblastic marker gene expression in our microarray data (Table 3) (for review see [18]). The transcription factor SOX9, a marker for osteoblast progenitor cells but not of mature osteoblasts, was expressed at low to intermediate levels in all cell lines, except in 143B, where it was upregulated 20-fold in comparison to HOS cells. RUNX2 (Runt-related transcription factor 2, also known as CBAF1), an early osteoblast differentiation transcription factor which is also required at lower levels for proper mature osteoblast function, was expressed at high levels in the Dunn/LM8, SAOS/LM5, HUO9/M132, and K12/K7M2 systems and at intermediate levels in the HOS/143B system. In the MG63/M8 system it was upregulated 4-fold from low to intermediate levels in M8 compared to MG63. OSX (osterix), a transcription factor that acts downstream of RUNX2, was expressed at intermediate to high levels in Dunn/LM8, SAOS/LM5, and HUO9/M132 cells. Low expression was observed in K12/K7M2, HOS/143B and MG63/M8 cells. COL1A1 (collagen 1), SPP1 (osteopontin, bone sialoprotein 1), and IBSP (bone sialoprotein 2) are produced by maturing and mature osteoblasts. COL1A1 was expressed at high levels in all cell lines except in 143B, where it was downregulated 145-fold compared to HOS. SPP1 was expressed at high levels in the Dunn/LM8, HUO9/M132, and K12/K7M2 systems and at low levels in the SAOS/LM5 and MG63/M8 systems. In HOS/143B it was upregulated 17-fold from low to intermediate levels in 143B compared to HOS cells. IBSP was only expressed at high levels in the Dunn/LM8 and SAOS/LM5 systems and was low in all other cell line systems. ALPL (liver/bone/kidney alkaline phosphatase) and PTH1R (parathyroid hormone receptor 1) are expressed by late osteoblast-like cells and mature osteoblasts. ALPL was expressed at high levels only in the Dunn/LM8 and SAOS/LM5 systems and was low in all other cell lines, except

Table 2: Number of regulated (>2-fold; fdr < 0.01) probe sets enriched (fdr < 0.00001) in GO terms level 1.

	SAOS/LM5	HU09/M132	HOS/143B	MG63/M8	Dunn/LM8	K12/K7M2
Cellular component						
Cell	884	1244	2519	362	780	2423
Membrane	486			206	475	
Extracellular region	196	266	403	96	218	365
Extracellular matrix	78		143		88	134
Synapse			112			
Molecular function						
Binding	850	1219	2435	343	805	2391
Molecular transducer activity		189	302			
Nucleic acid binding transcription factor activity		138	249			
Receptor activity		206				
Catalytic activity						1062
Biological process						
Cellular process	716	1017	2028		638	1858
Biological regulation	517	793	1537	250	522	1378
Response to stimulus		589	1074		376	1010
Multicellular organismal process	400	562	1055	186	369	846
Developmental process	345	490	931	159	351	768
Signaling		399		139	227	567
Biological adhesion	110	145	260	53	70	193
Growth	43		78			85
Locomotion		107				148
Cellular component organization or biogenesis			642			558
Localization			643			
Cell proliferation			133			
Rhythmic process			57			
Reproduction					83	
Immune system process					92	
Multiorganism process						129
Metabolic process						1132
Death						168

Table 3: Microarray mRNA expression levels of osteoblastic marker genes.

	SOX9	RUNX2	OSX	COL1A1	SPP1	IBSP	ALPL	PTH1R
Dunn	274	4306	1589	5931	15287	717	5284	2525
LM8	278	7496	2199	7235	8836	631	4306	2304
SAOS	147	2836	288	6824	12	2666	1612	124
LM5	214	2707	638	8584	29[a]	5163	2489	110
HUO9	8	2767	1397	9635	2514	11	18	439
M132	7	2702	819	10809	350	7	37	117[a]
K12	50	2097	34	6556	6994	6	29	20
K7M2	60	957[a]	38	5504	6874	6	29	22
HOS	22	175	14	5950	14	6	135	63
143B	434[a]	143	14	41[a]	242[a]	6	14[a]	24[a]
MG63	220	32	14	7473	10	6	15	24
M8	216	126[a]	13	6665	10	6	15	25

Results are means of the probe sets listed below and analyzed in triplicates. [a] >2-fold ($P < 0.05$) versus parental cell line. White, low expression (<50): yellow, intermediate expression (50–300); green, high expression (>300). Probe sets (human/mouse): SOX9 (202935_s_at/1451538_at) RUNX2 (232231_at/1424704_at); OSX (1552340_at/1418425_at); COL1A1 (1556499_s_at/1423669_at); SPP1 (209875_s_at/1449254_at); IBSP (236028_at/1417484_at); ALPL (215783_s_at/1423611_at); PTH1R (205911_at/1417092_at).

in the HOS/143B system where it was upregulated 10-fold from low to intermediate levels in HOS compared to 143B cells. PTH1R was expressed at intermediate to high levels in the Dunn/LM8, SAOS/LM5, and HUO9/M132 cell lines and at low levels in the K12/K7M2 and MG63/M8 cell lines. Similar to ALPL, PTH1R was upregulated 3-fold from low to intermediate levels in HOS compared to 143B. In summary, only the Dunn/LM8 and SAOS/LM5 cell lines exhibited gene expression characteristics of osteoblast-like cells. HUO9/M132 and K12/K7M2 cell lines appear to be osteoblastic precursors that were stalled in the osteoblastic differentiation process at an intermediate step, whereas the HOS/143B and MG63/M8 lines were stalled at an early stage.

The high ALPL gene expression in Dunn/LM8 and SAOS/LM5 was confirmed by measuring the enzyme activity in cell extracts (Figure 2). Although minimal enzyme activity was detectable in HUO9, M132, and HOS cells, it was 25-fold lower compared to Dunn/LM8 and SAOS/LM5, whereas no enzyme activity was measurable in the other cell lines. The osteoblast-like phenotype of SAOS/LM5 cells, including PTH (parathyroid hormone) stimulated cAMP production and the formation of mineralized extracellular matrix has already been described [14]. In the present study, PTH stimulated cAMP production also in Dunn (129 ± 27-fold; $n = 4$, $P < 0.02$) and LM8 cells (111 ± 17-fold; $n = 3$, $P < 0.03$) and mineralization of extracellular matrix upon induction with ascorbic acid, beta-glycerophosphate, and dexamethasone was also observed (not shown). In summary, the enzyme activity profile of the Dunn/LM8 and SAOS/LM5 cell lines paralleled the expression profile obtained with gene expression analysis, confirming their osteoblast-like properties at a functional level.

3.4. The Osteoblastic OS Cell Line Systems Present with an Enriched Set of Commonly Regulated Genes as Potential Targets for OS Treatment. In face of a similar number of regulated metastasis-related genes in Dunn/LM8 and SAOS/LM5 cell line systems (Table 1) and a similar enrichment pattern in GO terms (Table 2), we investigated if both systems had commonly regulated genes that might contribute to tumor progression and metastasis specific for osteoblastic OS. First, regulated (>2-fold; fdr < 0.01) probe set lists in both systems were separated in up- and downregulated probe set lists in metastatic versus parental cell lines. Second, separated up- and downregulated probe set lists were analyzed in GO for commonly enriched GO terms at the levels indicated in Supplementary Table 4. Upregulated probe sets were enriched in both systems in four GO terms and downregulated probe sets in seven GO terms. The GO probe set lists were then analyzed for commonly regulated genes (average of approximately 1.4 probe sets/gene) in both cell line systems and the results are summarized in Table 4. Using this strategy, we found 48 genes to be unidirectionally regulated in both Dunn/LM8 and SAOS/LM5 cell line systems, of which 17 genes were upregulated and 31 genes were downregulated. Real-time PCR analysis confirmed the upregulation of 4 out of 5 and the downregulation of 5 out of 5 genes that were selected based on the results of the microarray analysis of the SAOS/LM5 cell line system (Supplementary Figure 2). This is well within the range we previously observed by PCR and/or Western blot analysis for other gene products in this and other cell line systems (not shown).

From the relative frequencies given in Table 1, we can calculate the number of genes to be up- or downregulated in both systems by chance to be between 4 to 6, when analyzing the total datasets. As we have restricted our analysis to genes only enriched in some common GO terms in both cell line systems, the number of commonly regulated genes (48) by far exceeds the number of genes that would be selected by chance. Therefore, these genes can be considered to be relevant in osteoblastic OS metastasis. In the remaining four cell line systems, we found that of the 17 upregulated genes in our osteoblastic gene panel 1, 4, 4, and 0 genes were also upregulated in M132, K7M2, 143B, and M8, respectively, but similar numbers of genes were found to be regulated in the opposite direction as well. Likewise, of the 31 genes found downregulated 3, 5, 9, and 0 genes were also downregulated in M132, K7M2, 143B, and M8, respectively, but again similar numbers of genes were regulated in the opposite direction. Given the fact that in 143B, and K7M2 the total number of regulated genes was double the number found in M132, LM5, and LM8 cells, whereas compared to M8 cells the total number was only half (Table 1), it is likely that these genes may be commonly regulated by chance and do not necessarily contribute to tumor progression in these preosteoblast or nonosteoblastic systems.

We next looked in IPA if the 48 genes in our selected osteoblastic panel belonged to a specific pathway. This analysis revealed that half of the selected genes (24 out of 48) are related to inhibition of cell death, making it the top molecular and cellular function. Pathways related to cellular growth and proliferation were also stimulated, with the functions "proliferation of cells" and "proliferation of tumor cell lines" significantly enriched. The function "colony formation of (tumor) cells" was inhibited. Surprisingly, we also found the function "migration of cells" to be inhibited, most notably by inhibition of SERPINE2, although the expression of PAX3 (included in the same function and associated with increased migration) was found to be increased, indicating some variability in this function.

Three networks were found to be significantly regulated, of which "cell morphology, cellular assembly and organization, cellular function and maintenance" obtained the highest score with 21 regulated molecules of a total of 35 (Supplementary Figure 3), followed by "cell death, cell morphology, cell-to-cell signaling and interaction" (13 regulated out of 35) and "free radical scavenging, small molecule biochemistry, nervous system development and function" (12 regulated out of 35). These last two networks were found to be overlapping.

One interesting feature of IPA is to identify upstream regulators, such as transcription factors, that may not show an expressional change (and are therefore not included in the analyzed gene list), but are nevertheless likely to be activated based on a change in target gene expression. Using this approach, RUNX2 was identified as one of the top activated transcription factors, because its direct targets COL24A1,

Table 4: Commonly up- and downregulated genes in metastasis.

Gene name	Swiss-Prot	LM5	LM8	M132	K7M2	143B	M8	Expected OS outcome
Up-regulated in LM5 and LM8								
SERPINE2	P07093	3.2	3	4.1	−240	2.2	n.s.	Regression [25]
FHOD3	Q2V2M9	3.1	2.9	−2.8	18.9	5.5	n.s.	
PAX6	P26367	2.2	2.7	1.9	7.5	−19.6	n.s.	
EMILIN2	Q9BXX0	2.8	4.1	n.s.	3.1	−2.1	n.s.	
ZDHHC21	Q8IVQ6	2.6	2.5	−1.8	n.s.	2.6	n.s.	
GALNT3	Q14435	2.4	2.6	n.s.	n.s.	5.1	n.s.	
DLX4	Q92988	3	3.2	n.s.	3.6	−5.7	n.s.	
FOXQ1	Q9C009	3.8	2.3	n.s.	n.s.	1.6	n.s.	
LOX	P28300	5.8	6.5	−2.5	−3.3	−1.9	n.s.	Progression [54]
PAX3	P23760	2.3	2.1	n.s.	n.s.	n.s.	n.s.	Progression [39, 40]
COL24A1	Q17RW2	24.3	4.2	n.s.	n.s.	n.s.	n.s.	
MAMDC2	Q7Z304	14.8	6.3	n.s.	n.s.	−129	n.s.	
PCBD1	P61457	3.1	4.2	n.s.	n.s.	n.s.	n.s.	
PCDHB7	Q9Y5E2	7.6	3	n.s.	−1.5	n.s.	n.s.	
PHOSPHO1	Q8TCT1	4	2.2	n.s.	n.s.	n.s.	n.s.	
APCDD1	Q8J025	2.6	7.7	n.s.	n.s.	n.s.	n.s.	
EHF	Q9NZC4	2.6	10.8	n.s.	n.s.	n.s.	n.s.	
Down-regulated in LM5 and LM8								
CCDC80	Q76M96	−4.4	−2.6	−2.1	−2.2	−3.4	n.s.	
DAB2	P98082	−2.7	−2.1	−2.2	2	−15.3	n.s.	
TGFB2	P61812	−2.6	−2.4	1.9	−3.3	−10.9	n.s.	Progression [72]
SLC1A3	P43003	−2.1	−4	3.1	−5.8	−6.5	n.s.	Regression [73]
OSMR	Q99650	−6.8	−2.2	n.s.	−2.5	−2	n.s.	Progression [15, 76, 77]
CTSH	P09668	−2.1	−2.8	−1.6	n.s.	−2.6	n.s.	
AGPAT3	Q9NRZ7	−2.5	−10.7	1.8	−1.9	−1.4	n.s.	
ACTA2	P62736	−5.9	−6.8	4.7	1.5	−107	n.s.	
TPM1	P09493	−2.7	−2.3	4.5	n.s.	−5.4	n.s.	
FOXC2	Q99958	−3.1	−2.1	−3.1	n.s.	n.s.	n.s.	
TPD52L1	Q16890	−2.1	−8.7	2.3	39	−40.7	n.s.	
PRUNE2	Q8WUY3	−7.9	−8.8	n.s.	n.s.	−2.1	n.s.	
SH3RF3	Q8TEJ3	−2.3	−2.1	2.4	−12.9	2.8	2	
DEPDC6	Q8TB45	−3	−2.5	−1.9	8	n.s.	n.s.	
OGN	P20774	−2.4	−2.6	n.s.	−1.9	n.s.	n.s.	
STRBP	Q96SI9	−2.1	−2.4	n.s.	−1.5	n.s.	n.s.	
DNAJC12	Q9UKB3	−2.3	−3.4	n.s.	−1.3	n.s.	n.s.	
NACC2	Q96BF6	−2.2	−2.6	n.s.	1.4	−2	n.s.	
SLC40A1	Q9NP59	−2.7	−7.3	n.s.	n.s.	−2	n.s.	
SNCA	P37840	−2.2	−2.2	n.s.	n.s.	3.1	n.s.	
IGFBP4	P22692	−2.3	−2.8	2.2	2.5	n.s.	n.s.	
RAC3	P60763	−2.7	−2.4	n.s.	n.s.	1.9	n.s.	
AMIGO2	Q86SJ2	−2.9	−2.5	n.s.	2.8	n.s.	n.s.	
ETV1	P50549	−8.4	−3.5	n.s.	11.4	2.8	n.s.	
PLXNA2	O75051	−3.2	−3.4	n.s.	3.5	1.8	2.9	
HAPLN1	P10915	−2.8	−10.1	1.5	n.s.	n.s.	n.s.	
PHLDA1	Q8WV24	−2.1	−9	n.s.	2	48.2	n.s.	Progression [88, 89]
PPP1R13B	Q96KQ4	−2.2	−2.2	1.8	n.s.	n.s.	n.s.	
TBC1D8	O95759	−2.2	−3.6	n.s.	n.s.	5.3	n.s.	
ABCC4	O15439	−2.8	−6.7	n.s.	1.7	n.s.	n.s.	
SYNGR1	O43759	−2.9	−2.9	n.s.	n.s.	n.s.	n.s.	

Positive numbers are upregulated genes and negative numbers downregulated genes in metastatic versus parental cell lines. For LM5 and LM8: $>\pm 2$-fold (fdr < 0.01). For M132, K7M2, 143B, and M8: yellow ($>\pm 2$-fold (fdr < 0.01) in the same direction as LM5 and LM8; white (fdr < 0.01); red ($>\pm 2$-fold (fdr < 0.01) in the opposite direction as LM5 and LM8; n.s., not significant (fdr > 0.01). Gene names and Swiss-Prot (http://www.expasy.org/) numbers refer to human proteins.

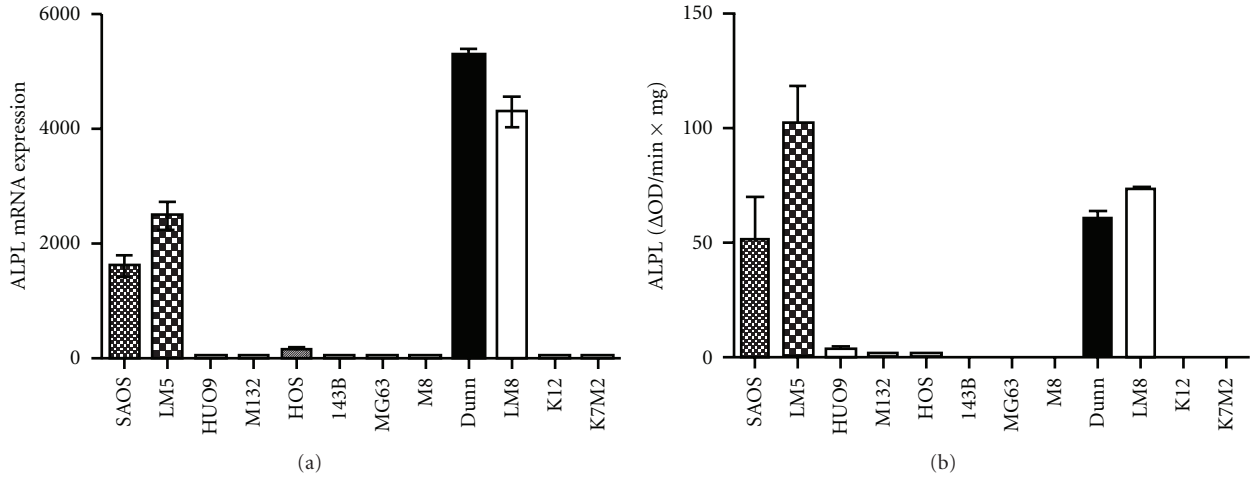

Figure 2: (a) RMA normalized ALPL (human: 215783_s_at; mouse: 1423611_at) mRNA expression. (b) ALPL enzyme activity.

TPM1, HAPLN1, and ACTA2 were present among the common regulated genes. Likewise, we identified MEIS2 (targets ETV1, PAX3, PAX6) to be significantly active. This transcription factor has not been associated to OS metastasis before, but was earlier found to be regulated in lung cancer [29], ovarian cancer [30], thyroid cancer [31], and prostate cancer [32].

4. Discussion

Metastasis-related microarray analyses have been performed using parental low metastatic HUO9, K12; HOS and SAOS cells and metastatic derivatives thereof [7–9]. Seven metastasis-related genes were described for the HUO9/M132 system and we found all these genes also differentially regulated in the same direction in our array. From the eleven genes described to be metastasis related in the K12/K7M2 system we found an overlap of 70%. This was also seen for the ten top upregulated genes in the HOS/143B cell line system. A 50% overlap was also observed when we compared our SAOS/LM5 system with the SAOS/LM7 system [9]. Generally, a high overlap in differentially regulated genes was observed when different microarray analyses were compared.

Several biological processes involved in tumor progression, such as proliferation, motility, invasion, immune surveillance, adhesion, and angiogenesis, have been identified in the K12/K7M2 system [8]. We have also found enrichment in the GO terms "proliferation," "motility," "adhesion," and "angiogenesis" although at lower levels than those listed in Supplementary Table 2. This again confirms a high overlap between the two independent analyses of this system. The former study identified ezrin as the most prominent protein involved in OS progression. We therefore looked for ezrin expression in our six cell line systems. Indeed, ezrin was overexpressed 70-fold in K7M2 compared to K12 cells. However, in LM8 and 143B cells, ezrin was downregulated 1.8- and 2.7-fold compared to the respective parental cells and in the MG63/M8 system it was not regulated. In LM5 and M132 cells it was found only minimally upregulated (<2 fold) compared to levels in corresponding parental cells. Thus, based on these *in vitro* gene expression analyses, ezrin may only play a role in OS progression in a subgroup of OS tumors.

The comparison of gene expression levels in six cell line systems revealed a high heterogeneity, illustrated by the more than 7-fold difference in the total number of differentially expressed probe sets. The enrichment in common GO terms was also low. This indicates that the cellular mechanisms involved in tumor progression differ in each system. This is in line with the hypothesis that genomic instability (chromothripsis) arising at different steps of osteoblastic commitment is a cause of OS oncogenesis [12]. In the SAOS/LM5 and Dunn/LM8 cell line systems, in which we confirmed the osteoblast-like nature, the still high RUNX2 expression makes it likely that chromothripsis took place at an early-osteoblast stage [11]. In addition, these two osteoblast-like cell line systems had the highest overlap in the number of regulated metastasis relevant genes and in GO enrichment. An analysis of a subset of differentially expressed genes that were enriched in common GO terms revealed common regulation of 48 genes in the osteoblastic cell line systems, exceeding the gene number expected from probability calculations. Thus, these genes are likely to contribute to tumor progression or chromothripsis survival in osteoblastic OS. According to the chromothripsis hypothesis, different sets of proteins are then likely to contribute to survival in different cancer cell types or in osteoprogenitor cells at different developmental stages as observed in this study.

Seventeen genes were commonly upregulated in the two metastatic osteoblastic cell lines LM5 and LM8 compared to the corresponding parental cell lines. The relevance of some of these genes is now discussed with reference to published literature on cancer in general and on OS in particular.

SERPINE2 (protease nexin 1) is a secreted serine protease inhibitor that inhibits among others the blood coagulation factors Xa and XIa, thrombin, tPA and uPA [33]. Here, SERPINE2 was upregulated in metastasis in four out of six cell line systems and remarkably downregulated in one system. Increased expression of a protease inhibitor would rather be expected to reduce invasiveness and hence malignant

progression, which is also indicated by our IPA analysis. Indeed, overexpression of SERPINE2 in prostate cancer cells reduces their invasion capacity [34], and in experimental OS, inhibition of uPAR pathway resulted in decreased lung metastasis [19]. In pancreatic tumors, on the other hand, SERPINE2 promotes extracellular matrix production and local invasion *in vivo* [35]. SERPINE2 expression is elevated in colorectal cancer, correlates with tumor grade and its silencing reduces anchorage-independent growth, migration, and tumor formation [36, 37]. SERPINE2 expression is also increased in breast cancer [38]. SERPINE2 promotes lymph node metastasis of testicular cancer [39] and SERPINE2 expression also correlates with selective lung metastasis in breast cancer [40] and lymph node metastasis of oral squamous cell carcinoma [41]. Metastasis of lung cancer cells towards bone is also associated with increased SERPINE2 expression [42]. Thus, SERPINE2 has a dual role in cancer progression and its role in OS progression, probably uPA/uPAR independent, may be further investigated.

FHOD3 (formin homolog overexpressed in spleen 2) is a member of a family of proteins involved in actin assembly and located in the cytoplasm. FHOD3 is predominantly expressed in heart and regulates sarcomere organization in striated muscles [43]. Although there is no evidence yet for a role of FHOD3 in other cancer types, the downregulation of FHOD1 (Swiss-Prot Q9Y613), another member of the family, reduces migration and invasion of breast cancer cells *in vitro* [44]. Interestingly, in the present study, FHOD3 was found upregulated in four metastatic cell lines.

PAX3 (paired box protein Pax-3) and PAX6 (paired box protein Pax-6) are nuclear transcription factors involved in the development of many tissues and the role of PAX3 in rhabdomyosarcoma and malignant melanoma is discussed [45, 46]. PAX3 is also expressed in most Ewing's sarcoma samples [47]. PAX3 was exclusively found overexpressed in the present study in metastatic osteoblastic OS, whereas PAX6 was overexpressed in four cell line systems. PAX3 overexpression in SAOS *in vitro* induces mesenchymal-epithelial transition (MET) and increases cell motility (IPA analysis of LM5–LM8 common regulated genes and [21, 22]), and therefore PAX3 expression analysis during osteoblastic tumor progression *in vivo* deserves further examination.

DLX4 (homeobox protein DLX-4) is a nuclear transcription factor that is overexpressed in several cancer types [48–51]. DLX4 suppresses the antiproliferative effect of TGF-β [52] and has an antiapoptotic function [53]. Upregulation of DLX4 increases the metastatic potential of breast cancer cells *in vitro* and *in vivo* [49, 54] and of prostate adenocarcinoma [51], and its expression correlates with advanced disease stage in ovarian cancer [50]. Here, DLX4 was also found upregulated in three cell line systems, but it was downregulated in 143B cells. To this end, downregulation of DLX4 correlates with increased metastatic potential *in vitro* and *in vivo* in lung cancer [55].

FOXQ1 (forkhead box protein Q19) is a nuclear transcription factor involved in mammary epithelial cell differentiation and in epithelial-mesenchymal transition (EMT) in breast cancer cells [56–58]. Its expression correlates with cancer cell aggressiveness *in vitro* and with lung metastasis *in vivo* in mice. FOXQ1 is also overexpressed in colorectal cancer where it increases tumorigenicity by its angiogenic and antiapoptotic effects [59]. Here, FOXQ1 was also found overexpressed in metastatic osteoblastic OS cells. Interestingly, factors that control EMT, such as FOXQ1, and mesenchymal-epithelial transition (MET), such as PAX3 were overexpressed in OS metastasis *in vitro*.

LOX (lysyl oxidase; EC 1.4.3.13) is a secreted enzyme that is involved in extracellular matrix (collagen and elastin) crosslinking and is also produced by mature osteoblasts [60]. Here, LOX expression was high in all cell lines investigated *in vitro* except in SAOS/LM5 cells (not shown). Previously we showed increased LOX expression in MG63 cells compared to fetal osteoblasts indicating that LOX might be related to OS formation [20]. Despite the fact that LOX expression did not correlate here with the osteoblastic phenotype, LOX expression was upregulated during metastatic progression in the two osteoblastic cell line systems, but downregulated in three out of four nonosteoblastic cell line systems. Tumor suppressor as well as metastasis promoting functions of LOX have been described in several cancer types [61]. Analyzing LOX protein expression in OS patients should answer the question whether LOX expression has a dual role in OS progression depending on the cellular background.

PCBD1 (pterin carbinolamine dehydratase or dimerization cofactor of hepatocyte nuclear factor (HNF) 1-alpha; EC = 4.2.1.96) is involved in tetrahydrobiopterin recycling, a cofactor used in the degradation of the amino acid phenylalanine. It regulates the transcriptional activity (i.e., homodimerization) of HNF and is located in the cytoplasm and inside the nucleus. It is overexpressed in colon cancer and in melanoma [62, 63] but to our knowledge has so far not been described in tumor progression. Here PCBD1 was exclusively overexpressed in osteoblastic metastatic OS cells.

EHF (epithelium-specific Ets transcription factor 3) is a nuclear transcription factor involved in breast cancer tumorigenesis [64] and is a marker for poor survival in ovarian carcinoma [65]. Here, EHF was exclusively overexpressed in the two osteoblastic metastatic cell lines.

Thirty-one genes were commonly downregulated in metastatic osteoblastic OS cell lines. The relevance of some of the genes in OS progression is now discussed.

CCDC80 (downregulated by oncogenes protein 1) is a secreted tumor suppressor protein that facilitates the apoptotic cascade [66] and mediates growth inhibition in colon and pancreatic cancer [67]. CCDC80 was the gene that was commonly regulated in all cell systems investigated except MG63/M8. Downregulation of this tumor suppressor gene deserves further investigation in OS.

DAB2 (disabled homolog 2), a protein of clathrin coated pits, is a negative regulator of the Wnt/β-catenin pathway and therefore a putative tumor suppressor [68]. DAB2 is underexpressed in tumors compared to normal tissue and correlates with the malignant phenotype of lung cancer, urothelial carcinoma, squamous cell carcinoma, nasopharyngeal carcinoma, and esophageal squamous carcinoma [69–73]. DAB2 expression is also reduced in breast cancer, which results in up-regulation of TGFβ2 that promotes EMT transition [74, 75]. In ovarian cancer low DAB2 levels

correlate with poor outcome, but very low levels that inhibit EMT correlate with a better prognosis [76]. Here, DAB2 was downregulated in four metastatic OS cell lines.

TGFB2 (transforming growth factor beta-2) is a secreted protein that can act as a tumor suppressor in early stages of tumorigenesis or as a metastasis promoting factor in advanced cancers (for review see [77]). In OS, elevated TGFB3 expression correlates with poor survival [23]. In the same study with only 25 patients TGFB2 was not predictive, but low TGFB2 showed a trend towards poor survival. The here observed downregulation of TGFB2 in 4 metastatic cell lines should therefore be investigated further.

SLC1A3 (excitatory amino acid transporter 1) was found downregulated in metastasis in four cell line systems contained in this study. This is in contrast with findings in tumors of OS patients, where high expression of SLC1A3 was associated with a poor prognosis [24].

OSMR (oncostatin-M-specific receptor subunit beta or interleukin-31 receptor subunit beta) is a receptor for oncostatin M (OSM; Swiss-Prot P13725), a member of the interleukin-6 cytokine family. OSM inhibits cell proliferation via the JAK/STAT pathway in a number of tumor cells (for review see [78]), including OS [15] and chondrosarcoma [79]. In OS, OSM sensitizes cells to apoptosis [25], and its overexpression was found to reduce primary tumor growth and lung metastasis formation *in vivo* in mice [26]. These data, and the loss of OSMR in metastatic cell lines as observed in this study in four of the six analyzed cell line systems, point to an important role of OSM and OSMR in inhibition of OS tumor progression. On the other hand, OSM enhanced the *in vitro* metastatic activity in a subset of canine and human OS cells [80]. To this end, it is interesting to note that OSM had different effects on osteoblastic differentiation, depending on the maturation stage [15].

TPM1 (tropomyosin alpha-1 chain) is an actin filament-binding protein with diverse biological actions including malignant transformation (for review see [81]), and it is considered as a tumor suppressor gene. TPM1 was found downregulated in colorectal cancer compared to normal tissue [82]. In breast cancer cells, loss of TPM1 conferred anoikis resistance [83] and overexpression of TPM1 suppressed anchorage-independent growth [84]. In this study, TPM1 was found downregulated in three metastatic OS cell lines.

DEPDC6 (DEP domain-containing mTOR-interacting protein or DEPTOR) is a negative regulator of mTOR signaling and is therefore expected to be a tumor suppressor [85]. However, high DEPDC6 levels have been correlated with poor prognosis in myeloma and hepatocellular carcinoma [86, 87], indicating an oncogenic role. The here observed downregulation in three metastatic OS cell lines deserves therefore further examination.

PHLDA1 (pleckstrin homology-like domain family A member 1 or apoptosis-associated nuclear protein or TSSC3) is an apoptosis regulator. Downregulation of this protein is associated with metastasis progression in breast cancer and in melanoma [88, 89]. In OS, overexpression of TSSC3 induced apoptosis *in vitro* and reduced tumor growth *in vivo* in mice [27, 28]. The results are consistent with downregulation of PHLDA1 in metastatic LM5 and LM8 cells.

Interestingly, some of the discussed proteins are involved in EMT and MET (PAX3, FOXQ1, and DAB2), TGF/Wnt/β-catenin signaling (DLX4, DAB2, and TGFB2), JAK/STAT (OSMR) or mTOR (DEPDC6) pathways. In another microarray study, the TGF/Wnt/β-catenin pathway has also been associated with increased OS metastatic activity [9].

In conclusion, we have identified a significant number of differentially expressed genes in low and highly metastatic osteoblastic OS cell lines. These genes should be considered for further evaluation as key players in tumor progression in osteoblastic OS, the predominant phenotype of the disease.

Conflict of Interests

The authors state no conflict of interests.

Acknowledgments

The authors thank all the persons that provided them with cell lines as described in Section 2. They also thank Bettina Langsam for the preparation of total RNA. This work was supported by the Swiss National Science Foundation (SNF Grant no. 31003A-120403), a Grant from the Zurcher Krebsliga (Zurich, Switzerland), the University of Zurich, and the Schweizerischer Verein Balgrist (Zurich, Switzerland), the Walter L. & Johanna Wolf Foundation (Zurich, Switzerland) and the Program for Highly Specialized Medicine (HSM) of the Kanton Zurich, Switzerland.

References

[1] S. F. Jia, L. L. Worth, and E. S. Kleinerman, "A nude mouse model of human osteosarcoma lung metastases for evaluating new therapeutic strategies," *Clinical and Experimental Metastasis*, vol. 17, no. 6, pp. 501–506, 1999.

[2] K. Kimura, T. Nakano, Y. B. Park et al., "Establishment of human osteosarcoma cell lines with high metastatic potential to lungs and their utilities for therapeutic studies on metastatic osteosarcoma," *Clinical and Experimental Metastasis*, vol. 19, no. 6, pp. 477–485, 2002.

[3] J. S. Rhim, H. Y. Cho, and R. J. Huebner, "Non producer human cells induced by murine sarcoma virus," *International Journal of Cancer*, vol. 15, no. 1, pp. 23–29, 1975.

[4] X. B. Shi, A. M. Chen, X. H. Cai, F. J. Guo, G. N. Liao, and D. Ma, "Establishment and characterization of cell sublines with high and low metastatic potential derived from human osteosarcoma," *Chinese Medical Journal*, vol. 118, no. 8, pp. 687–690, 2005.

[5] T. Asai, T. Ueda, K. Itoh et al., "Establishment and characterization of a murine osteosarcoma cell line (LM8) with high metastatic potential to the lung," *International Journal of Cancer*, vol. 76, no. 3, pp. 418–422, 1998.

[6] C. Khanna, J. Prehn, C. Yeung, J. Caylor, M. Tsokos, and L. Helman, "An orthotopic model of murine osteosarcoma with clonally related variants differing in pulmonary metastatic potential," *Clinical and Experimental Metastasis*, vol. 18, no. 3, pp. 261–271, 2000.

[7] T. Nakano, M. Tani, Y. Ishibashi et al., "Biological properties and gene expression associated with metastatic potential of human osteosarcoma," *Clinical and Experimental Metastasis*, vol. 20, no. 7, pp. 665–674, 2003.

[8] C. Khanna, J. Khan, P. Nguyen et al., "Metastasis-associated differences in gene expression in a murine model of osteosarcoma," *Cancer Research*, vol. 61, no. 9, pp. 3750–3759, 2001.

[9] R. J. Flores, Y. Li, A. Yu et al., "A systems biology approach reveals common metastatic pathways in osteosarcoma," *BMC Systems Biology*, vol. 6, no. 1, p. 50, 2012.

[10] M. Curto and A. I. McClatchey, "Ezrin... A metastatic detERMinant?" *Cancer Cell*, vol. 5, no. 2, pp. 113–114, 2004.

[11] J. W. Martin, M. Zielenska, G. S. Stein, J. A. Squire, and A. J. van Wijnen, "The role of RUNX2 in osteosarcoma oncogenesis," *Sarcoma*, vol. 2011, Article ID 282745, 13 pages, 2011.

[12] P. J. Stephens, C. D. Greenman, B. Fu et al., "Massive genomic rearrangement acquired in a single catastrophic event during cancer development," *Cell*, vol. 144, no. 1, pp. 27–40, 2011.

[13] G. Bacci, F. Bertoni, A. Longhi et al., "Neoadjuvant chemotherapy for high-grade central osteosarcoma of the extremity: histologic response to preoperative chemotherapy correlates with histologic subtype of the tumor," *Cancer*, vol. 97, no. 12, pp. 3068–3075, 2003.

[14] R. Muff, N. Nigg, P. Gruber, D. Walters, W. Born, and B. Fuchs, "Altered morphology, nuclear stability and adhesion of highly metastatic derivatives of osteoblast-like SAOS-2 osteosarcoma cells," *Anticancer Research*, vol. 27, no. 6, pp. 3973–3979, 2007.

[15] C. Chipoy, M. Berreur, S. Couillaud et al., "Downregulation of osteoblast markers and induction of the glial fibrillary acidic protein by oncostatin M in osteosarcoma cells require PKCdelta and STAT3," *Journal of Bone and Mineral Research*, vol. 19, no. 11, pp. 1850–1861, 2004.

[16] J. Schmidt, G. P. Strauss, A. Schon et al., "Establishement and characterization of osteogenic cell lines from a spontaneous murine osteosarcoma," *Differentiation*, vol. 39, no. 3, pp. 151–160, 1988.

[17] K. Husmann, R. Muff, M. E. Bolander, G. Sarkar, W. Born, and B. Fuchs, "Cathepsins and osteosarcoma: expression analysis identifies cathepsin K as an indicator of metastasis," *Molecular Carcinogenesis*, vol. 47, no. 1, pp. 66–73, 2008.

[18] F. Long, "Building strong bones: molecular regulation of the osteoblast lineage," *Nature Reviews Molecular Cell Biology*, vol. 13, no. 1, pp. 27–38, 2012.

[19] C. R. Dass, A. P. W. Nadesapillai, D. Robin et al., "Downregulation of uPAR confirms link in growth and metastasis of osteosarcoma," *Clinical and Experimental Metastasis*, vol. 22, no. 8, pp. 643–652, 2005.

[20] B. Fuchs, K. Zhang, M. E. Bolander, and G. Sarkar, "Identification of differentially expressed genes by mutually subtracted RNA fingerprinting," *Analytical Biochemistry*, vol. 286, no. 1, pp. 91–98, 2000.

[21] O. Wiggan and P. A. Hamel, "Pax3 regulates morphogenetic cell behavior in vitro coincident with activation of a PCP/non-canonical Wnt-signaling cascade," *Journal of Cell Science*, vol. 115, no. 3, pp. 531–541, 2002.

[22] O. Wiggan, M. P. Fadel, and P. A. Hamel, "Pax3 induces cell aggregation and regulates phenotypic mesenchymal-epithelial interconversion," *Journal of Cell Science*, vol. 115, no. 3, pp. 517–529, 2002.

[23] P. Kloen, M. C. Gebhardt, A. Perez-Atayde et al., "Expression of transforming growth factor-beta (TGF-beta) isoforms in osteosarcomas: TGF-beta3 is related to disease progression," *Cancer*, vol. 80, no. 12, pp. 2230–2239, 1997.

[24] M. Paoloni, S. Davis, S. Lana et al., "Canine tumor cross-species genomics uncovers targets linked to osteosarcoma progression," *BMC Genomics*, vol. 10, article 625, 2009.

[25] C. Chipoy, B. Brounais, V. Trichet et al., "Sensitization of osteosarcoma cells to apoptosis by oncostatin M depends on STAT5 and p53," *Oncogene*, vol. 26, no. 46, pp. 6653–6664, 2007.

[26] B. Brounais, C. Chipoy, K. Mori et al., "Oncostatin M induces bone loss and sensitizes rat osteosarcoma to the antitumor effect of midostaurin in vivo," *Clinical Cancer Research*, vol. 14, no. 17, pp. 5400–5409, 2008.

[27] Y. Huang, H. Dai, and Q. N. Guo, "TSSC3 overexpression reduces stemness and induces apoptosis of osteosarcoma tumor-initiating cells," *Apoptosis*, vol. 17, no. 8, pp. 749–761, 2012.

[28] H. Dai, Y. Huang, Y. Li, G. Meng, Y. Wang, and Q. N. Guo, "TSSC3 overexpression associates with growth inhibition, apoptosis induction and enhances chemotherapeutic effects in human osteosarcoma," *Carcinogenesis*, vol. 33, no. 1, pp. 30–40, 2012.

[29] S. K. Halder, Y. J. Cho, A. Datta et al., "Elucidating the mechanism of regulation of transforming growth factor beta Type II receptor expression in human lung cancer cell lines," *Neoplasia*, vol. 13, no. 10, pp. 912–922, 2011.

[30] A. P. G. Crijns, P. de Graeff, D. Geerts et al., "MEIS and PBX homeobox proteins in ovarian cancer," *European Journal of Cancer*, vol. 43, no. 17, pp. 2495–2505, 2007.

[31] M. R. Vriens, W. Moses, J. Weng et al., "Clinical and molecular features of papillary thyroid cancer in adolescents and young adults," *Cancer*, vol. 117, no. 2, pp. 259–267, 2011.

[32] J. L. Chen, J. Li, K. Kiriluk et al., "Deregulation of a hox protein regulatory network spanning prostate cancer initiation and progression," *Clinical Cancer Research*, vol. 18, no. 16, pp. 4291–4302, 2012.

[33] M. C. Bouton, Y. Boulaftali, B. Richard, V. Arocas, J. B. Michel, and M. Jandrot-Perrus, "Emerging role of serpinE2/protease nexin-1 in hemostasis and vascular biology," *Blood*, vol. 119, no. 11, pp. 2452–2457, 2012.

[34] D. Xu, C. M. McKee, Y. Cao, Y. Ding, B. M. Kessler, and R. J. Muschel, "Matrix metalloproteinase-9 regulates tumor cell invasion through cleavage of protease nexin-1," *Cancer Research*, vol. 70, no. 17, pp. 6988–6998, 2010.

[35] M. Buchholz, A. Biebl, A. Neeße et al., "SERPINE2 (protease nexin I) promotes extracellular matrix production and local invasion of pancreatic tumors in vivo," *Cancer Research*, vol. 63, no. 16, pp. 4945–4951, 2003.

[36] S. Bergeron, E. Lemieux, V. Durand et al., "The serine protease inhibitor serpinE2 is a novel target of ERK signaling involved in human colorectal tumorigenesis," *Molecular Cancer*, vol. 9, article 271, 2010.

[37] J. Selzer-Plon, J. Bornholdt, S. Friis et al., "Expression of prostasin and its inhibitors during colorectal cancer carcinogenesis," *BMC Cancer*, vol. 9, article 201, 2009.

[38] B. J. Candia, W. C. Hines, C. M. Heaphy, J. K. Griffith, and R. A. Orlando, "Protease nexin-1 expression is altered in human breast cancer," *Cancer Cell International*, vol. 6, article 16, 2006.

[39] A. Nagahara, M. Nakayama, D. Oka et al., "SERPINE2 is a possible candidate promotor for lymph node metastasis in testicular cancer," *Biochemical and Biophysical Research Communications*, vol. 391, no. 4, pp. 1641–1646, 2010.

[40] B. Fayard, F. Bianchi, J. Dey et al., "The serine protease inhibitor protease nexin-1 controls mammary cancer metastasis through LRP-1-mediated MMP-9 expression," *Cancer Research*, vol. 69, no. 14, pp. 5690–5698, 2009.

[41] S. Gao, A. Krogdahl, J. A. Sørensen, T. M. Kousted, E. Dabelsteen, and P. A. Andreasen, "Overexpression of protease nexin-1 mRNA and protein in oral squamous cell carcinomas," *Oral Oncology*, vol. 44, no. 3, pp. 309–313, 2008.

[42] S. Yang, Q. Dong, M. Yao et al., "Establishment of an experimental human lung adenocarcinoma cell line SPC-A-1BM with high bone metastases potency by 99mTc-MDP bone scintigraphy," *Nuclear Medicine and Biology*, vol. 36, no. 3, pp. 313–321, 2009.

[43] K. Taniguchi, R. Takeya, S. Suetsugu et al., "Mammalian formin Fhod3 regulates actin assembly and sarcomere organization in striated muscles," *Journal of Biological Chemistry*, vol. 284, no. 43, pp. 29873–29881, 2009.

[44] S. Jurmeister, M. Baumann, A. Balwierz et al., "MicroRNA-200c represses migration and invasion of breast cancer cells by targeting actin-regulatory proteins FHOD1 and PPM1F," *Molecular and Cellular Biology*, vol. 32, no. 3, pp. 633–651, 2012.

[45] J. Blake and M. R. Ziman, "Aberrant PAX3 and PAX7 expression. A link to the metastatic potential of embryonal rhabdomyosarcoma and cutaneous malignant melanoma?" *Histology and Histopathology*, vol. 18, no. 2, pp. 529–539, 2003.

[46] J. D. Kubic, K. P. Young, R. S. Plummer, A. E. Ludvik, and D. Lang, "Pigmentation PAX-ways: the role of Pax3 in melanogenesis, melanocyte stem cell maintenance, and disease," *Pigment Cell and Melanoma Research*, vol. 21, no. 6, pp. 627–645, 2008.

[47] T. W. Schulte, J. A. Toretsky, E. Ress, L. Helman, and L. M. Neckers, "Expression of PAX3 in Ewing's sarcoma family of tumors," *Biochemical and Molecular Medicine*, vol. 60, no. 2, pp. 121–126, 1997.

[48] S. B. Haga, S. Fu, J. E. Karp et al., "BP1, a new homeobox gene, is frequently expressed in acute leukemias," *Leukemia*, vol. 14, no. 11, pp. 1867–1875, 2000.

[49] Y. G. Man, S. W. Fu, A. Schwartz, J. J. Pinzone, S. J. Simmens, and P. E. Berg, "Expression of BP1, a novel homeobox gene, correlates with breast cancer progression and invasion," *Breast Cancer Research and Treatment*, vol. 90, no. 3, pp. 241–247, 2005.

[50] F. Hara, S. Samuel, J. Liu, D. Rosen, R. R. Langley, and H. Naora, "A homeobox gene related to Drosophila distal-less promotes ovarian tumorigenicity by inducing expression of vascular endothelial growth factor and fibroblast growth factor-2," *American Journal of Pathology*, vol. 170, no. 5, pp. 1594–1606, 2007.

[51] A. M. Schwartz, Y. G. Man, M. K. Rezaei, S. J. Simmens, and P. E. Berg, "BP1, a homeoprotein, is significantly expressed in prostate adenocarcinoma and is concordant with prostatic intraepithelial neoplasia," *Modern Pathology*, vol. 22, no. 1, pp. 1–6, 2009.

[52] B. Q. Trinh, N. Barengo, and H. Naora, "Homeodomain protein DLX4 counteracts key transcriptional control mechanisms of the TGF-β cytostatic program and blocks the antiproliferative effect of TGF-β," *Oncogene*, vol. 30, no. 24, pp. 2718–2729, 2011.

[53] Y. Sun, X. Lu, L. Yin, F. Zhao, and Y. Feng, "Inhibition of DLX4 promotes apoptosis in choriocarcinoma cell lines," *Placenta*, vol. 27, no. 4-5, pp. 375–383, 2006.

[54] Y. Fu, Y. Lian, K. S. Kim et al., "BP1 homeoprotein enhances metastatic potential in ER-negative breast cancer," *Journal of Cancer*, vol. 1, pp. 54–62, 2010.

[55] S. Tomida, K. Yanagisawa, K. Koshikawa et al., "Identification of a metastasis signature and the DLX4 homeobox protein as a regulator of metastasis by combined transcriptome approach," *Oncogene*, vol. 26, no. 31, pp. 4600–4608, 2007.

[56] Y. Qiao, X. Jiang, S. T. Lee, R. K. M. Karuturi, S. C. Hooi, and Q. Yu, "FOXQ1 regulates epithelial-mesenchymal transition in human cancers," *Cancer Research*, vol. 71, no. 8, pp. 3076–3086, 2011.

[57] H. Zhang, F. Meng, G. Liu et al., "Forkhead transcription factor Foxq1 promotes epithelial-mesenchymal transition and breast cancer metastasis," *Cancer Research*, vol. 71, no. 4, pp. 1292–1301, 2011.

[58] A. Feuerborn, P. K. Srivastava, S. Küffer et al., "The Forkhead factor FoxQ1 influences epithelial differentiation," *Journal of Cellular Physiology*, vol. 226, no. 3, pp. 710–719, 2011.

[59] H. Kaneda, T. Arao, K. Tanaka et al., "FOXQ1 is overexpressed in colorectal cancer and enhances tumorigenicity and tumor growth," *Cancer Research*, vol. 70, no. 5, pp. 2053–2063, 2010.

[60] N. Pischon, J. M. Mäki, P. Weisshaupt et al., "Lysyl oxidase (Lox) gene deficiency affects osteoblastic phenotype," *Calcified Tissue International*, vol. 85, no. 2, pp. 119–126, 2009.

[61] Siddikuzzaman, V. M. Grace, and C. Guruvayoorappan, "Lysyl oxidase: a potential target for cancer therapy," *Inflammopharmacology*, vol. 19, no. 3, pp. 117–129, 2010.

[62] E. P. von Strandmann, S. Senkel, G. Ryffel, and U. R. Hengge, "Dimerization co-factor of hepatocyte nuclear factor 1/pterin-4α-carbinolamine dehydratase is necessary for pigmentation in Xenopus and overexpressed in primary human melanoma lesions," *American Journal of Pathology*, vol. 158, no. 6, pp. 2021–2029, 2001.

[63] R. Eskinazi, B. Thöny, M. Svoboda et al., "Overexpression of Pterin-4a-carbinolamine dehydratase/dimerization cofactor of hepatocyte nuclear factor 1 in human colon cancer," *American Journal of Pathology*, vol. 155, no. 4, pp. 1105–1113, 1999.

[64] J. He, Y. Pan, J. Hu, C. Albarracin, Y. Wu, and L. D. Jia, "Profile of Ets gene expression in human breast carcinoma," *Cancer Biology and Therapy*, vol. 6, no. 1, pp. 76–82, 2007.

[65] K. Brenne, D. A. Nymoen, T. E. Hetland, C. G. Trope, and B. Davidson, "Expression of the Ets transcription factor EHF in serous ovarian carcinoma effusions is a marker of poor survival," *Human Pathology*, vol. 43, no. 4, pp. 496–505, 2012.

[66] J. Ferragud, A. Avivar-Valderas, A. Pla, J. De Las Rivas, and J. F. de Mora, "Transcriptional repression of the tumor suppressor DRO1 by AIB1," *FEBS Letters*, vol. 585, no. 19, pp. 3041–3046, 2011.

[67] G. T. Bommer, C. Jäger, E. M. Dürr et al., "DRO1, a gene down-regulated by oncogenes, mediates growth inhibition in colon and pancreatic cancer cells," *Journal of Biological Chemistry*, vol. 280, no. 9, pp. 7962–7975, 2005.

[68] C. Prunier, B. A. Hocevar, and P. H. Howe, "Wnt signaling: physiology and pathology," *Growth Factors*, vol. 22, no. 3, pp. 141–150, 2004.

[69] H. T. Xu, L. H. Yang, Q. C. Li et al., "Disabled-2 and Axin are concurrently colocalized and underexpressed in lung cancers," *Human Pathology*, vol. 42, no. 10, pp. 1491–1498, 2011.

[70] J. A. Karam, S. F. Shariat, H. Y. Huang et al., "Decreased DOC-2/DAB2 expression in urothelial carcinoma of the bladder," *Clinical Cancer Research*, vol. 13, no. 15, part 1, pp. 4400–4406, 2007.

[71] A. Hannigan, P. Smith, G. Kalna et al., "Epigenetic downregulation of human disabled homolog 2 switches TGF-β from a tumor suppressor to a tumor promoter," *Journal of Clinical Investigation*, vol. 120, no. 8, pp. 2842–2857, 2010.

[72] J. H. Tong, D. C. Ng, S. L. Chau et al., "Putative tumour-suppressor gene DAB2 is frequently down regulated by promoter hypermethylation in nasopharyngeal carcinoma," *BMC Cancer*, vol. 10, article 253, 2010.

[73] K. Anupam, C. Tusharkant, S. D. Gupta, and R. Ranju, "Loss of disabled-2 expression is an early event in esophageal squamous tumorigenesis," *World Journal of Gastroenterology*, vol. 12, no. 37, pp. 6041–6045, 2006.

[74] J. C. Martin, B. S. Herbert, and B. A. Hocevar, "Disabled-2 downregulation promotes epithelial-to-mesenchymal transition," *British Journal of Cancer*, vol. 103, no. 11, pp. 1716–1723, 2010.

[75] S. A. R. Bagadi, C. P. Prasad, A. Srivastava, R. Prashad, S. D. Gupta, and R. Ralhan, "Frequent loss of Dab2 protein and infrequent promoter hypermethylation in breast cancer," *Breast Cancer Research and Treatment*, vol. 104, no. 3, pp. 277–286, 2007.

[76] A. Chao, C. Y. Lin, Y. S. Lee et al., "Regulation of ovarian cancer progression by microRNA-187 through targeting Disabled homolog-2," *Oncogene*, vol. 31, pp. 764–775, 2011.

[77] P. M. Siegel and J. Massagué, "Cytostatic and apoptotic actions of TGF-β in homeostasis and cancer," *Nature Reviews Cancer*, vol. 3, no. 11, pp. 807–820, 2003.

[78] S. L. Grant and C. G. Begley, "The oncostatin M signalling pathway: reversing the neoplastic phenotype?" *Molecular Medicine Today*, vol. 5, no. 9, pp. 406–412, 1999.

[79] E. David, P. Guihard, B. Brounais et al., "Direct anti-cancer effect of oncostatin M on chondrosarcoma," *International Journal of Cancer*, vol. 128, no. 8, pp. 1822–1835, 2011.

[80] S. L. Fossey, M. D. Bear, W. C. Kisseberth, M. Pennell, and C. A. London, "Oncostatin M promotes STAT3 activation, VEGF production, and invasion in osteosarcoma cell lines," *BMC Cancer*, vol. 11, article 125, 2011.

[81] C. Choi, D. Kim, S. Kim, S. Jeong, E. Song, and D. M. Helfman, "From skeletal muscle to cancer: insights learned elucidating the function of tropomyosin," *Journal of Structurl Biology*, vol. 177, no. 1, pp. 63–69, 2012.

[82] V. Mlakar, G. Berginc, M. Volavšek, Z. Štor, M. Rems, and D. Glavač, "Presence of activating KRAS mutations correlates significantly with expression of tumour suppressor genes DCN and TPM1 in colorectal cancer," *BMC Cancer*, vol. 9, article 282, 2009.

[83] G. N. Raval, S. Bharadwaj, E. A. Levine et al., "Loss of expression of tropomyosin-1, a novel class II tumor suppressor that induces anoikis, in primary breast tumors," *Oncogene*, vol. 22, no. 40, pp. 6194–6203, 2003.

[84] S. Zhu, M. L. Si, H. Wu, and Y. Y. Mo, "MicroRNA-21 targets the tumor suppressor gene tropomyosin 1 (TPM1)," *Journal of Biological Chemistry*, vol. 282, no. 19, pp. 14328–14336, 2007.

[85] Y. Zhao, X. Xiong, and Y. Sun, "DEPTOR, an mTOR inhibitor, is a physiological substrate of SCF(betaTrCP) E3 ubiquitin ligase and regulates survival and autophagy," *Molecular Cell*, vol. 44, no. 2, pp. 304–316, 2011.

[86] T. R. Peterson, M. Laplante, C. C. Thoreen et al., "DEPTOR is an mTOR inhibitor frequently overexpressed in multiple myeloma cells and required for their survival," *Cell*, vol. 137, no. 5, pp. 873–886, 2009.

[87] C. H. Yen, Y. C. Lu, C. H. Li et al., "Functional characterization of glycine N-methyltransferase and its interactive protein DEPDC6/DEPTOR in hepatocellular carcinoma," *Molecular Medicine*, vol. 18, no. 1, pp. 286–296, 2012.

[88] M. A. Nagai, J. H. T. G. Fregnani, M. M. Netto, M. M. Brentani, and F. A. Soares, "Down-regulation of PHLDA1 gene expression is associated with breast cancer progression," *Breast Cancer Research and Treatment*, vol. 106, no. 1, pp. 49–56, 2007.

[89] R. Neef, M. A. Kuske, E. Pröls, and J. P. Johnson, "Identification of the human PHLDA1/TDAG51 gene: down-regulation in metastatic melanoma contributes to apoptosis resistance and growth deregulation," *Cancer Research*, vol. 62, no. 20, pp. 5920–5929, 2002.

Hindawi Publishing Corporation
Sarcoma
Volume 2012, Article ID 164803, 10 pages
doi:10.1155/2012/164803

Research Article

β-Catenin Does Not Confer Tumorigenicity When Introduced into Partially Transformed Human Mesenchymal Stem Cells

Sajida Piperdi,[1] Lukas Austin-Page,[2] David Geller,[1,3] Manpreet Ahluwalia,[1,4] Sarah Gorlick,[4] Jonathan Gill,[1,4] Amy Park,[1] Wendong Zhang,[1] Nan Li,[5] So Hak Chung,[6] and Richard Gorlick[1,4,7,8]

[1] *The Department of Pediatrics, Albert Einstein College of Medicine, Yeshiva University, Bronx, NY 10461, USA*
[2] *The Department of Pediatrics, Children's Hospital Los Angeles, Los Angeles, CA 90027, USA*
[3] *The Department of Orthopaedic Surgery, Montefiore Medical Center, Bronx, NY 10467, USA*
[4] *Division Hematology/Oncology, Department of Pediatrics, The Children's Hospital at Montefiore, Room 300, Rosenthal Building, 3415 Bainbridge Avenue, Bronx, NY 10467, USA*
[5] *Oncology Section, The Department of Orthopedics Surgery, First Affiliated Hospital of PLA General Hospital, Beijing 100037, China*
[6] *The Department of Orthopedics Surgery, College of Medicine, Kosin University Gospel Hospital, Busan 602-702, Republic of Korea*
[7] *Department of Pediatrics and Molecular Pharmacology, Albert Einstein College of Medicine, Yeshiva University, Bronx, NY 10461, USA*
[8] *Division of Hematology/Oncology, Department of Pediatrics, The Children's Hospital at Montefiore, Room 300, Rosenthal Building, 3415 Bainbridge Avenue, Bronx, NY 10467, USA*

Correspondence should be addressed to Richard Gorlick, rgorlick@montefiore.org

Received 5 July 2012; Revised 23 September 2012; Accepted 23 September 2012

Academic Editor: H. Gelderblom

Although osteosarcoma is the most common primary malignant bone tumor in children and adolescents, its cell of origin and the genetic alterations are unclear. Previous studies have shown that serially introducing hTERT, SV40 large TAg, and H-Ras transforms human mesenchymal stem cells into two distinct sarcomas cell populations, but they do not form osteoid. In this study, β-catenin was introduced into mesenchymal stem cells already containing hTERT and SV40 large TAg to analyze if this resulted in a model which more closely recapitulated osteosarcoma. *Results*. Regardless of the level of induced β-catenin expression in the stable transfectants, there were no marked differences induced in their phenotype or invasion and migration capacity. Perhaps more importantly, none of them formed tumors when injected into immunocompromised mice. Moreover, the resulting transformed cells could be induced to osteogenic and chondrogenic differentiation but not to adipogenic differentiation. *Conclusions*. β-catenin, although fostering osteogenic differentiation, does not induce the malignant features and tumorigenicity conveyed by oncogenic H-RAS when introduced into partly transformed mesenchymal stem cells. This may have implications for the role of β-catenin in osteosarcoma pathogenesis. It also may suggest that adipogenesis is an earlier branch point than osteogenesis and chondrogenesis in normal mesenchymal differentiation.

1. Introduction

Osteosarcoma is the most common primary malignant bone tumor in children and young adults [1, 2]. The lack of a precursor lesion combined with the genetic complexity of osteosarcoma has limited understanding the etiology of this disease. Microscopically, osteosarcoma is defined as a malignant spindle cell tumor that produces osteoid. The presence of this bony matrix has led to the traditional viewpoint that the tumor is derived from the osteoblast. However, depending on the type of the predominant matrix, histological subtypes of osteosarcoma including chondroblastic, fibroblastic, and osteoblastic subtypes are defined [3, 4]. The existence of these histologic subtypes suggests the tumors have a multilineage differentiation capacity and suggest that the cell of origin is more pluripotent than an osteoblast [5]. To date, the factors associated with an osteosarcoma having a particular histological appearance

are poorly understood. Osteosarcoma could arise from a cell anywhere from a mesenchymal stem cell (MSC) to an osteoblast and originate from various cellular pools existing in the bone marrow, the growth plates, or the periosteum [6]. Identifying the cell of origin and the molecular basis of osteosarcoma may be of critical clinical importance [7].

The extremely complex Wnt pathway encodes highly conserved genes and secreted proteins, which modulate cell fate and cell proliferation during embryonic development and carcinogenesis through activation of receptor-mediated signaling pathways [8–10]. In the most well-known and highly conserved canonical Wnt pathway, the presence of Wnt triggers the cascade of receptor activation causing the inactivation of the intracellular enzyme GSK3 and the tumor suppressor APC, key factors that promote the degradation of cytoplasmic pool of β-catenin, the key downstream mediator of Wnt-signaling pathway, allowing the translocation of β-catenin to the nucleus resulting in transcriptional activation of downstream targets, many of which are involved in embryonic development and oncogenesis. The activation of Wnt pathway and β-catenin has been implicated in the pathogenesis and progression of an increasingly number of human malignancies, including colorectal cancer, melanoma, myeloma, and lung cancer [11–13]. It has been reported that in osteosarcoma, there are overexpressions of numerous Wnt components [14, 15] as well as the epigenetic silencing of Wnt inhibitory factor 1 and frizzled related protein 3 [16, 17]. In addition, β-catenin mutation and elevated levels of nuclear β-catenin have been also noted in osteosarcoma and associated with lung metastasis [18–21], highlighting the potential association between the Wnt-β-catenin signaling in the development and progression of osteosarcoma.

In order to better understand osteosarcomas genetic complexity, our efforts have been directed towards developing a tumor which recapitulates osteosarcomas phenotype by introducing defined genetic elements into human mesenchymal stem cells (hMSCs). Initially, hMSCs were transformed by the serial introduction of hTERT, SV40 TAg and H-Ras as had been described previously for transformation of other normal cell types [22, 23]. The resulting cells were oncogenic, capable of producing tumors in mice, but histologically they were a malignant spindle cell tumor which did not produce osteoid, hence they were not osteosarcoma [23]. It was hypothesized that introducing a genetic alteration inducing osteogenic differentiation may result in the desired phenotype. Based on the aforementioned involvement of β-catenin in both tumor development and osteogenic differentiation, β-catenin was introduced into hMSC already transformed by hTERT and SV40 TAg. In this paper, the creation of these cells along with their characterization is reported, providing insights into the potential role of β-catenin in osteosarcoma pathogenesis.

2. Materials and Methods

2.1. Cell Culture. hMSCs and their transformed derivatives, transfected with hTERT and SV40 TAg, named, MSC-TS, were obtained, produced, and cultured as previously described [23] in MSC medium (Lonza, Walkersville, MD, USA) at 37′C with 5% CO_2. Cell morphologies were observed and pictures were taken using a Nikon Inverted Microscope ECLIPSE TE200 attached to a cooled charge coupled device (Diagnostic Instruments, Sterling Heights, MI, USA). HT1080, HOS, and NIH 3T3 cells were purchased from American Tissue Type Culture Collection (Manassas, VA, USA) and cultured as per their instructions.

2.2. Viral Transfection, Creating Stably Transfected Cell Lines and Immunoblotting. A full length cDNA clone of β-catenin constructed in pCMV6-XL5 vector was purchased from OriGene (Rockville, MD, USA). The lentiviral plasmid pLenti-β-catenin-blast was constructed by subcloning the above β-catenin entry clone using pLenti6.2/V5-DEST Gateway Vector Kit and ViralPower Lentiviral Expression Systems (Invitrogen, Carlsbad, CA, USA). PLenti-β-catenin-blast was transiently transfected into the 293FT packaging cell line (Invitrogen, CA, USA). Viral stock was harvested at 30 hours and MSC-TS cells were infected with 6 μg/mL polybrene when they were at 50% confluence. Following 24 hours of coculture, drug selection of infected cells was performed using 3 μg per mL blasticidin. Ten drug resistant colonies were picked up after 6 weeks and were separately subcultured. Expression of β-catenin was measured by immunoblotting 15 μg total protein with β-catenin monoclonal antibody, 6B3 (Cell Signaling Technology, Beverly, MA, USA), according to the manufacturer's instructions. Clones which had the highest, lowest, and intermediate β-catenin level were selected for further analysis.

2.3. Immunocytochemical Analysis. Immunocytochemical staining of β-catenin in cultured cells was carried out using immunofluorescence staining methods. Cells were plated and cultured to 30–40% confluence on four-well chamber slides. Cells were then washed with PBS, fixed in ice-cold methanol for 5 min, washed, permeabilized with 0.25% Triton X-100 in PBS, and washed again. Nonspecific sites were blocked with 10% normal serum in 1% BSA in PBS for 1 h at RT. Cells were then incubated with 2 ug/mL rabbit polyclonal anti-β-catenin antibody (Millipore, Billerica, MA, USA) or purified IgG for isotype controls overnight at 4′. The next day, cells were incubated with a 1 : 250 dilution of goat anti-rabbit IgG secondary antibody conjugated to Alexa-488 green fluorescence (Life Technologies, Grand Island, NY, USA) for 1 h at RT. Cells were then washed and counterstained with prolong gold antifade reagent with DAPI (Life Technologies, Grand Island, NY). Immunostaining was visualized by Zeiss Axio Observer inverted microscope at 63X magnification.

2.4. Subcutaneous and Orthotopic Tumorigenicity Assays. Six-to-eight-week-old CB-17 SCID mice (Taconic, Germantown, NY, USA) were injected with the MSC-TS and now also transfected with β-catenin, which were named MSC-TSB, as described previously [23]. Parallel subcutaneous injections of MSC-TS and a subline of MSC-TS transfected with

activated H-Ras and previously named MSC-TSR6 were performed as negative and positive controls, respectively. Twelve mice were used for each cell line, regularly checked for tumor formation, and all experiments were performed in accordance with protocols approved by the Institutional Animal Care and Use Committee of the Albert Einstein College of Medicine.

2.5. Motility/Migration and Invasion Assays. Motility (random migration) was measured by the wound healing assay as previously described [23]. Cells were cultured in serum-free media overnight before creating wounds. Photos were taken every 12 hours until 72 hours at the same region. The width of the scratch wounds was measured in Image J Software, and relative change in scratch wound width was calculated for 0 and 12 hr. Migration (haptotaxis) was measured using the Chemicon QCM Quantitative Cell Migration Assay (Millipore, Billerica, MA, USA). Again, cells were serum-starved overnight before being seeded into Boyden chambers. Cells that migrated to the outside of the chamber were stained and extracted in 300 μL of extraction buffer. Absorbance at 562 nm was measured using a microplate reader (Bio-Rad, Hercules, CA, USA).

Invasion was measured using the Chemicon Cell Invasion Assay (Millipore, Billerica, MA, USA). Serum-starved cells were plated in the invasion chambers which have 8 μm pore size polycarbonate membrane, over which a thin layer of extracellular matrix (ECM) is applied. The invasive cells which migrate through the matrix layer become attached to the bottom of the polycarbonate membrane, which is then stained and extracted.

2.6. Differentiation Assays. The osteogenic, adipogenic and chondrogenic differentiation capacity were measured according to manufacturer's instructions using an MSC osteogenesis kit, mesenchymal adipogenesis kit, and chondrogenic differentiation media with transforming growth factor (TGF-β3) (Lonza, Walkersville, MD, USA), respectively. Cells were cultured in differentiation induction medium for 4–8 weeks. Differentiated cells were stained with Alizarin Red, Oil Red O, and immunohistochemical staining of type II collagen using antibody collagen type II 003-02 (Santa Cruz, Santa Cruz, CA, USA), which can stain calcium, fat, and type II collagen, respectively, to verify formation of osteocytes, adipocytes, and chondrocytes, respectively. Chondrogenesis was also performed using a StemPro chondrogenesis differentiation kit (Invitrogen, Carlsbad, CA, USA) and was subsequently stained with alcian blue (Sigma-Aldrich, St. Louis, MO, USA) for proteoglycans produced by chondrocytes. Pictures were taken using a Nikon Inverted Microscope ECLIPSE TE200 attached to a CCD (Diagnostic Instruments, Sterling Heights, MI, USA).

2.7. Statistical Analysis. Student's t test was used to compare the difference between means. $P < 0.05$ was considered statistically significant. All of the data were analyzed using a statistical software package (SPSS 20.0, Chicago, IL, USA).

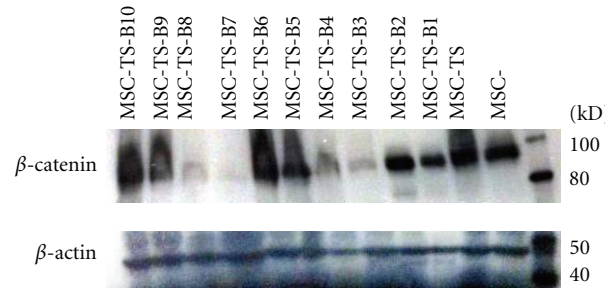

Figure 1: β-catenin protein expression was confirmed by western blot, with β-actin serving as a loading control. Lane 1: hMSC. Lane 2: hMSC-TS. Lane 3–12: hMSC-TSB clones 1 through 10.

3. Results

3.1. Generation of Stably Transformed Human Mesenchymal Stem Cell Lines. Stably transformed MSC-TS cell lines had been developed previously using neomycin and puromycin as the selectable markers [23]. β-catenin was introduced into the MSC-TS cells using blasticidin as the selectable marker. This new stably transfected MSC derived line was named MSC-TSB with T representing hTERT, S representing SV40 Tag, and B representing β-catenin, respectively. The levels of β-catenin expression were confirmed by western blot (Figure 1). β-catenin was expressed at varying levels in the ten clones that were selected after transfection, and also to some extent, in the parental cell lines, MSC, and MSC-TS. Clones that had the highest level of β-catenin, MSC-TSB-H1 and MSC-TSB-H2, lowest or null β-catenin level, MSC-TSB-L3 and MSC-TSB-L7, and intermediate level, MSC-TSB-I9 and MSC-TSB-I10, were selected for further analysis of the impact of β-catenin on their behavior.

No distinguishable changes in cellular localization of β-catenin (Figure 2), morphology, growth rate, and growth pattern were observed between these different colonies. The proliferation rate was markedly increased after β-catenin transfection, compared to MSC-TS with a population doubling time of less than 24 hours. Consistent with the behavior of the MSC-TSR cell line, the MSC-TSB cell lines also showed immortalization with the cells proliferating beyond 50 passages in culture.

3.2. Motility and Invasion. Two different kinds of motility were measured: random migration by wound healing assay (Figure 3(a)) and haptotaxis, a cell movement towards an immobilized ECM protein gradient as measured in the Boyden chamber system (Figure 3(b)). In these experiments, there were no major differences among the clones with differing β-catenin levels and the parental MSC-TS with P values > 0.05, statistically insignificant.

Upon measuring the cellular invasiveness into the ECM, again, MSC-TSB clones did not show much variability between clones with differing β-catenin levels with the degree of invasion similar to that of MSC-TS, P values > 0.05. Their invasion capacity was far less than that of HT1080 which was used as the positive control. The noninvasive cell line 3T3

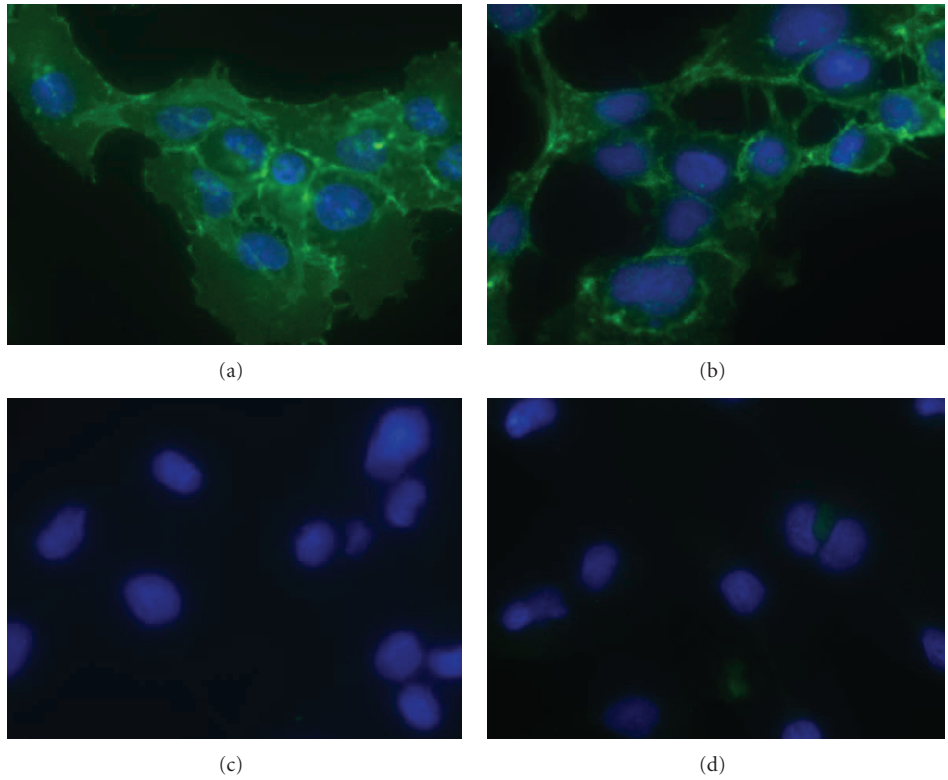

Figure 2: Representative pictures of immunofluorescence staining of β-catenin in tramsformed MSC-TSB cell lines. ((a)-(b)) β-catenin signal (green) was detected in both the cytoplasm and nucleus. ((c)-(d)) Their isotype control counterparts, respectively (63x original magnification).

was used as the negative control (Figure 4). MSC-TSB-L3 was excluded due to a technical error.

3.3. Formation of Tumors in CB-17 SCID Mice. In tumorigenicity assays, no palpable tumor was found with any of the MSC-TSB clones in both subcutaneous and orthotopic-injected mice 6 weeks after the implantation. As a positive control, we used MSC-TSR6 which formed tumors in 7 out of 8 mice subcutaneously, and 4 out of 4 orthotopically. The parental MSC-TS also did not form tumors.

3.4. Changes in Multilineage Differentiation Capacity of Transformed hMSCs. Osteogenic differentiation capacity was more rapid in MSC-TSB cell lines, once again independent of β-catenin expression level, as compared to MSC-TS. Strong intensity staining with Alizarin Red could be detected as early as 3 weeks in differentiation media (Figure 5). With the introduction of β-catenin, the cells lost the capacity for adipogenic differentiation as demonstrated by the lack of Oil Red O staining after being in differentiation media 8 weeks (Figure 6). For the chondrogenic differentiation assay, some MSC-TSB clones were found to stain weakly for collagen type II after 8 weeks of culture in chondrogenic induction media (Figure 7), whereas they were negative for proteoglycan by Alcian Blue staining (data not shown).

4. Discussion

In summary, β-catenin was successfully introduced into MSC-TS cells with the resulting cells being proliferative and immortalized, but without marked changes in motility or invasion and unable to produce orthotopic or heterotopic tumors in immunodeficient mice. Additionally these cells more rapidly underwent osteogenic differentiation but were unable to undergo adipogenic differentiation. Although these experiments did not produce an experimental model of osteosarcoma, some insights into the role of β-catenin in mesenchymal stem cell differentiation may be inferred. In addition, some implications may exist for intermediate stages of MSC differentiation.

There have been several reports indicating that murine mesenchymal stem cells could be transformed into malignant phenotype due to spontaneous mutations after many passages in culture, and therefore MSC could be a potential cell of origin of many sarcomas [24–26]. In addition, our previous study has been reported that the malignant transformation of hMSCs by serially introducing hTERT, SV40 Tag, and H-Ras produces a high-grade spindle cell sarcoma [23]. This led the current study to determine if an osteosarcoma phenotype could be produced by the introduction of β-catenin instead of H-Ras into the MSC-TS cells. Some of the resulting clones showed lower level of β-catenin than the parental MSC-TS on the western

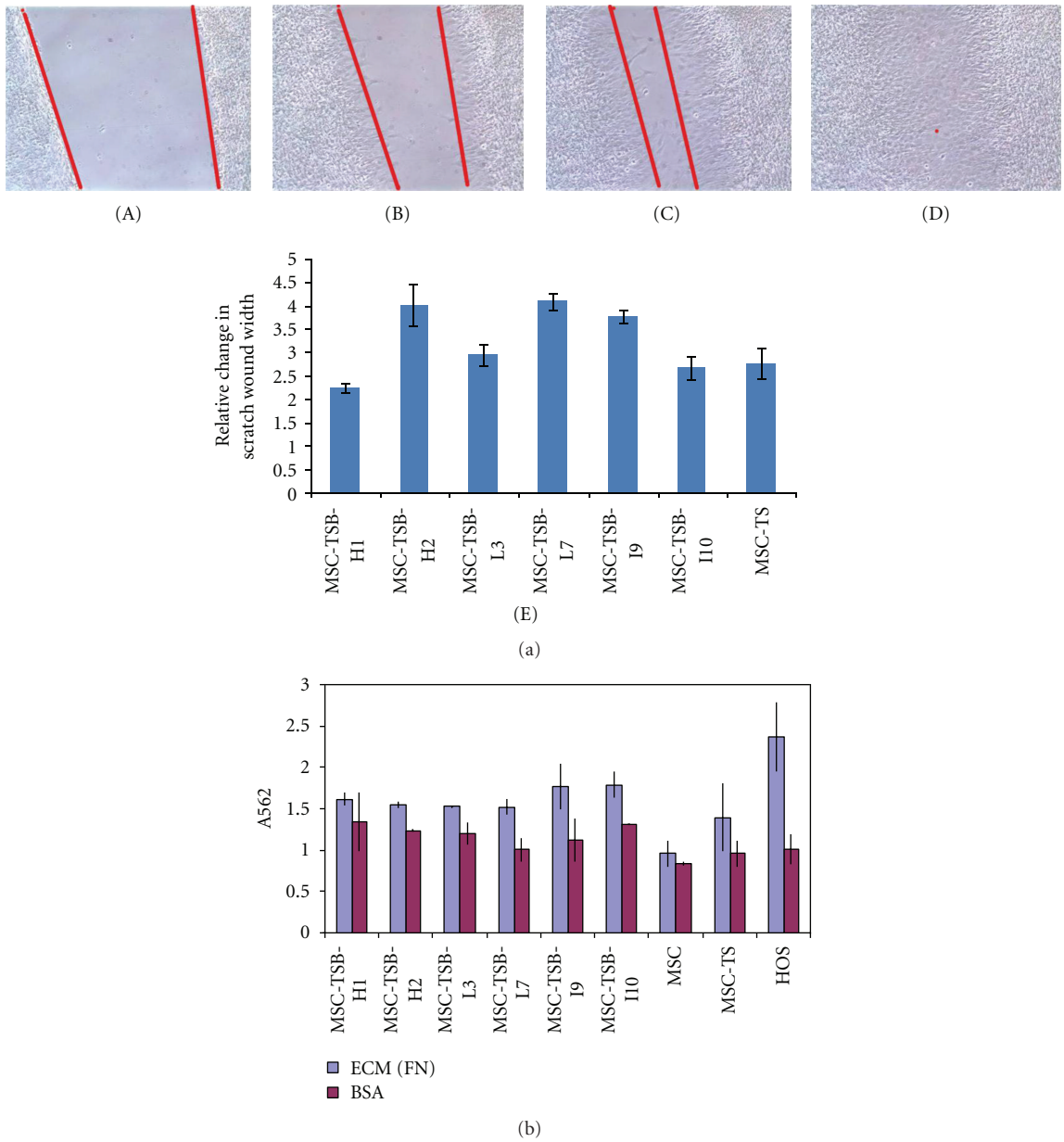

Figure 3: Migration assay. (a) A single representative wound healing assay (10x magnification), which showed no significant differences, $P > 0.05$, between the variants and the parental cell line MSC-TS at (A) 0 hour, (B) 12 hours, (C) 24 hours, and (D) 48 hours. (E) Quantitative measurement of wound gap by Image J software also showed no statistical significance between clones and the parental line. (b) A summary of the Boyden chamber experiment results; BSA coated wells serve as control along with HOS cells. Bars, standard deviation (SD). Experiments were replicated three times.

blot. In this context, it is unclear why these clones have lower protein levels; however, possible explanations include either posttranslational modification or negative feedback regulation of β-catenin/Tcf pathway in which increased β-catenin signalings induce Tcf-dependent βTrCP protein expression resulting in a rapid degradation of wild-type β-catenin [27]. The presence and subsequent use of multiple clones makes random events such as insertional mutagenesis less likely. As the resulting cells did not produce tumors in mice, these efforts were not successful in producing an osteosarcoma model system. Creation of a model system was intended to address questions of the cell of origin as well as the critical genetic steps in osteosarcoma development. In the context of these experiments, it is not possible to address these questions, as the failure to produce osteosarcoma could reflect once again an inappropriate use of hMSC as the starting point or an inappropriate selection of a gene for cellular transformation.

The rationale for the use of β-catenin to transform these cells has been discussed previously but the involvement of

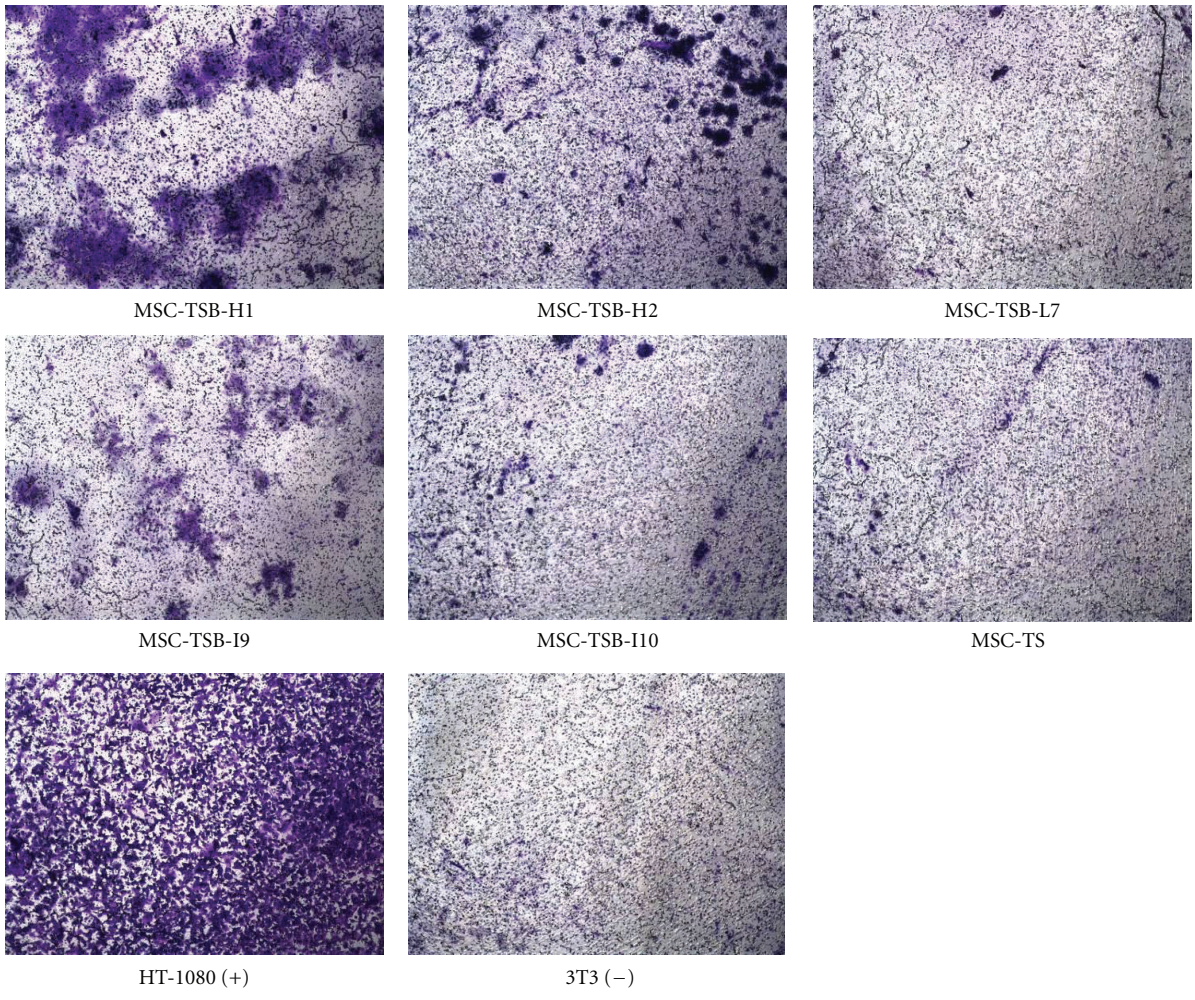

Figure 4: Cell invasion assay. (a) Pictures taken under microscope after staining (10x magnifications) to visualize the invasive cells across the polycarbonate membrane. (b) A summary of the invasion assay results after staining and extracting the cells outside the membrane. The highly invasive HT-1080 cell lines served as a positive control, and the noninvasive NIH-3T3 (3T3) cells served as a negative control. There is no statistically significant difference between the transformed clones with different β-catenin level and the parental MSC-TS, all P values are greater than 0.05.

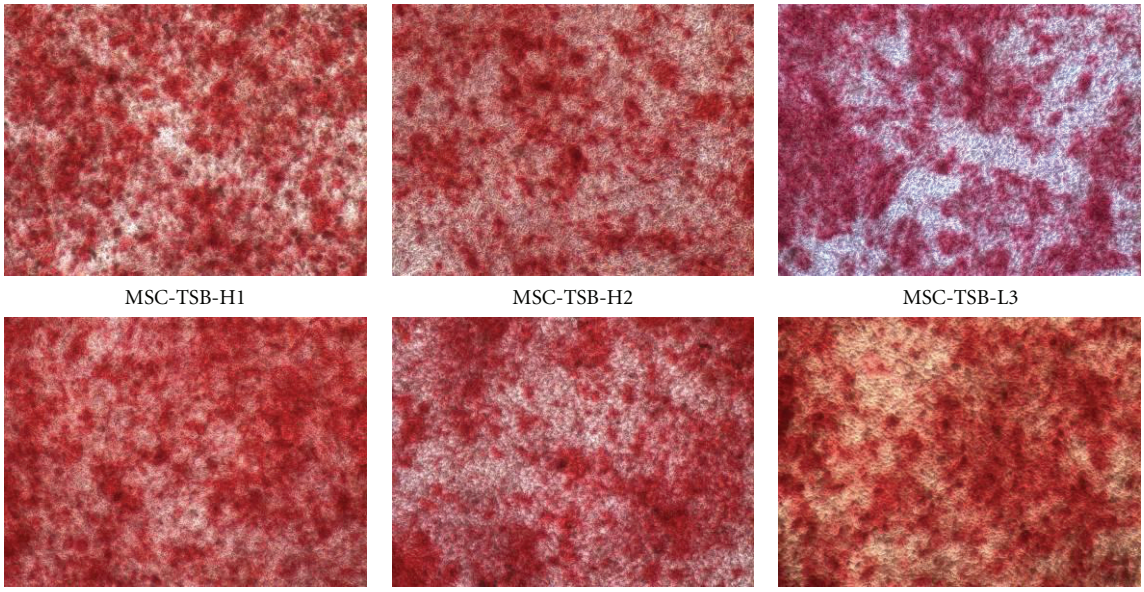

Figure 5: Osteogenic differentiation as demonstrated by staining with Alizarin Red 21 days after induction, 10x magnifications.

the Wnt pathway in osteosarcoma pathogenesis and progression is somewhat controversial [28]. Numerous studies have demonstrated an involvement of the Wnt pathway, including thorough expression of LRP5 as involved in osteosarcoma disease progression [16, 18, 19, 29, 30]. More specifically, previous studies have shown that downregulating the Wnt pathway by transfecting Dkk-3 and dominant-negative LRP5 into osteosarcoma cells significantly reduced invasion capacity and cell motility potentially by recruiting β-catenin to the cell surface to promote cell-cell adhesion [20]. This is supported by other studies in which the Wnt pathway was downregulated by genetic or drug-treatment approaches in osteosarcoma cells, and as a result the decreased invasion and motility were observed, with the related clinical observations being an antitumor and antimetastasis effect [18, 29, 31, 32]. Furthermore, the activation of Wnt pathway and increased nuclear β-catenin localization has been detected in the majority of osteosarcomas and may correlate with metastasis [14, 33]. This is recapitulated in canine osteosarcoma which is very similar to the human disease [34]. Interestingly, on the other hand, a group has performed expression profiling of high-grade osteosarcoma, MSCs, and the same MSCs differentiated into osteoblasts, and osteoblastomas and has suggested that downregulation of Wnt signaling has an important role in osteosarcoma pathogenesis [35]. That same group has also reported the loss of Wnt/β-catenin pathway activity in osteosarcoma cells by measuring the nuclear β-catenin level, and using a GSK3β inhibitor [36]. Although the authors discussed these results as being contradictory with other reported studies, factors involved in pathogenesis and progression are frequently not the same. In this study, after transfecting β-catenin into MSC-TS, clones with different β-catenin level were deliberately picked to detect the effects of β-catenin on pathogenesis. No significant changes were detected among clones both phenotypically and functionally. Moreover, no tumor formation was observed in mice. These findings support the view that the expression of β-catenin alone is not involved in osteosarcoma pathogenesis regardless of the activity of the Wnt-signaling pathway. Frequent β-catenin accumulation in osteosarcoma may relate to the stage at which most cases become clinically apparent rather than reflecting events early in pathogenesis [14]. The other possibility could be generating a model with active canonical Wnt signaling, for example, transfection with constitutively active LRP5/6. An additional explanation which needs to be considered is the tested genetic manipulations and tumor-specific alterations which have utilized and tested different components of this complicated signaling pathway, which complicates the interpretation of results. As an example, manipulation of Dkk-3 may be either context-dependent or may potentially produce some affects independent of β-catenin or other selected Wnt pathway components [17, 32].

A potentially important observation is that after β-catenin transfection into MSC-TS cell lines, the full multilineage differentiation capacity of the parental MSCs was lost. When MSC-TSBs were induced to osteoblasts, adipocytes, and chondrocytes via the respective induction media, osteogenesis was favored. No adipogenic differentiation was observed and chondrogenesis was delayed. This finding is also supported by previous studies in which inactivating mutations in LRP-5, Wnt coreceptor, are associated with decreased bone mass, as a consequence of reduced osteoblast differentiation and vice versa [37–40]. Loss of adipogenicity of MSC-TSB cells upon induction is worth noting here because osteosarcoma does not have an adipocytic subtype variant, while osteoblastic, chondroblastic, and fibroblastic osteosarcoma subtypes do exit [3, 4]. Osteosarcoma may therefore derive from such an intermediate stage

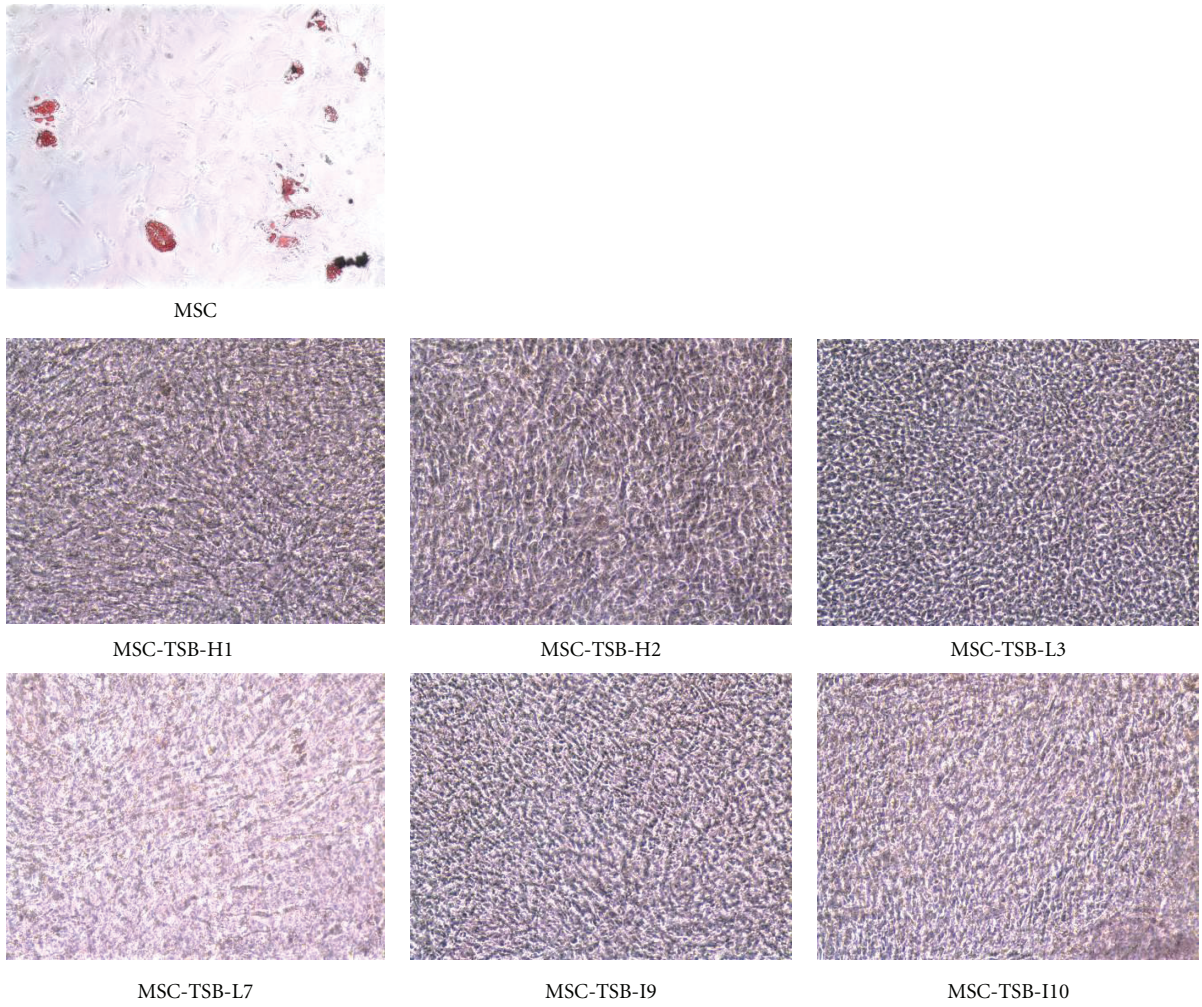

Figure 6: Adipogenic differentiation is not present as determined by staining with Oil Red O in the various MSC-TSB clones after 8 weeks in differentiation media. hMSC demonstrates adipogenic differentiation by Oil Red O staining after 4 weeks in differentiation media as a positive control (10x magnification).

of differentiated MSCs. Current descriptions of mesenchymal stem cell do not describe intermediate stages of differentiation in which cells have become committed to a restricted set of final lineages. Comparable to hematopoiesis, it is quite likely that intermediate stages of differentiation exist. These results suggest that adipogenesis may be an early branch point in mesenchymal differentiation. It is possible in normal mesenchymal stem cell differentiation that a stem cell which has the capacity to differentiate into chondrogenic and osteogenic but not adipogenic lineages may exist. A caveat of this suggestion is that these results were obtained with transformed cells and may not reflect what occurs with normal mesenchymal stem cell differentiation.

In conclusion, this study demonstrated the addition of β-catenin to MSC-TS cells did not result in cells with tumorigenic properties. This suggests that β-catenin may not have a role in osteosarcoma pathogenesis; however, this does not rule out its potential involvement in osteosarcoma progression. The generation of cells with the capacity to differentiate into selected but not all mesenchymal stem cell lineages suggests that intermediate stages may exist. Further studies will be necessary to clarify the role of other components of the Wnt-signaling pathway in osteosarcoma pathogenesis and progression.

Abbreviations

MSC:	Mesenchymal stem cells
hMSC:	Human mesenchymal stem cells
MSC-TS:	Human mesenchymal stem cells transfected with hTERT and SV40 large T antigen
MSC-TSB:	MSC-TS transfected with β-catenin
MSC-TSR6:	An MSC-TS subline transfected with activated H-Ras
ECM:	Extracellular matrix.

Conflict of Interests

The authors declare that there is no conflict of interest in this paper.

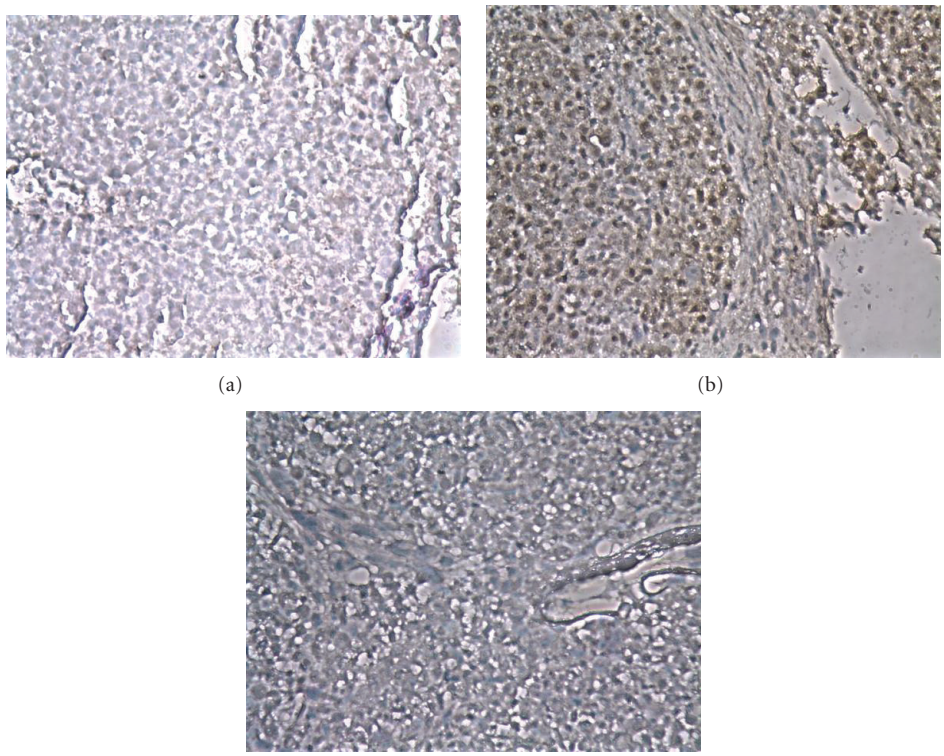

(a) (b)

(c)

Figure 7: Representative pictures of staining of collagen type II after induction in chondrogenic differentiation media for 8 weeks. (a) Weakly positive, (b) positive for collagen, and (c) isotype control (10x magnification).

Acknowledgments

The authors thank the Albert Einstein College of Medicine Histopathology Core Facility and Analytical Imaging Facility for assistance in performing histological preparations/interpretations and taking images. This work was supported by Swim Across America Inc., and the FOSTER Foundations.

References

[1] L. Mirabello, R. J. Troisi, and S. A. Savage, "Osteosarcoma incidence and survival rates from 1973 to 2004: data from the surveillance, epidemiology, and end results program," *Cancer*, vol. 115, no. 7, pp. 1531–1543, 2009.

[2] G. Ottaviani and N. Jaffe, "The epidemiology of osteosarcoma," *Cancer Treatment and Research*, vol. 152, pp. 3–13, 2009.

[3] R. Gorlick BS, L. Teot, J. Meyer, L. Randall, and N. Marina, "Osteosarcoma: biology, diagnosis, treatment and remaining challengings," in *Principles and Practice of Pediatric Oncology*, P. A. Pizzo and D. G. Poplack, Eds., pp. 1015–1044, Lippincott Williams & Wilkins, Philadelphia, Pa, USA, 2011.

[4] C. D. M. Fletcher, K. K. Unni, and F. Mertens, Eds., *Pathology and Genetics of Tumors of Soft Tissue and Bone, WHO Classification of Tumors*, IARC Press, Lyon, France, 2002.

[5] M. Kansara and D. M. Thomas, "Molecular pathogenesis of osteosarcoma," *DNA and Cell Biology*, vol. 26, no. 1, pp. 1–18, 2007.

[6] A. B. Mohseny and P. C. W. Hogendoorn, "Concise review: mesenchymal tumors: when stem cells go mad," *Stem Cells*, vol. 29, no. 3, pp. 397–403, 2011.

[7] R. Ricafort and R. Gorlick, "Molecularly targeted therapy in osteosarcoma," in *Molecularly Targeted Therapy for Childhood Cancer*, R. Arceci and P. J. Houghton, Eds., pp. 459–498, Springer, New York, NY, USA, 2010.

[8] T. Reya and H. Clevers, "Wnt signalling in stem cells and cancer," *Nature*, vol. 434, no. 7035, pp. 843–850, 2005.

[9] N. Barker and H. C. Catenins, "Wnt signaling and cancer," *Bioessays*, vol. 22, no. 11, pp. 961–965, 2000.

[10] K. M. Cadigan and R. Nusse, "Wnt signaling: a common theme in animal development," *Genes and Development*, vol. 11, no. 24, pp. 3286–3305, 1997.

[11] J. Deng, S. A. Miller, H. Y. Wang et al., "β-catenin interacts with and inhibits NF-κB in human colon and breast cancer," *Cancer Cell*, vol. 2, no. 4, pp. 323–334, 2002.

[12] Y. W. Qiang, Y. Endo, J. S. Rubin, and S. Rudikoff, "Wnt signaling in B-cell neoplasia," *Oncogene*, vol. 22, no. 10, pp. 1536–1545, 2003.

[13] A. T. Weeraratna, Y. Jiang, G. Hostetter et al., "Wnt5a signaling directly affects cell motility and invasion of metastatic melanoma," *Cancer Cell*, vol. 1, no. 3, pp. 279–288, 2002.

[14] R. C. Haydon, A. Deyrup, A. Ishikawa et al., "Cytoplasmic and/or nuclear accumulation of the β-catenin protein is a frequent event in human osteosarcoma," *International Journal of Cancer*, vol. 102, no. 4, pp. 338–342, 2002.

[15] D. Mandal, A. Srivastava, E. Mahlum et al., "Severe suppression of Frzb/sFRP3 transcription in osteogenic sarcoma," *Gene*, vol. 386, no. 1-2, pp. 131–138, 2007.

[16] B. H. Hoang, T. Kubo, J. H. Healey et al., "Expression of LDL receptor-related protein 5 (LRP5) as a novel marker for disease progression in high-grade osteosarcoma," *International Journal of Cancer*, vol. 109, no. 1, pp. 106–111, 2004.

[17] M. Kansara, M. Tsang, L. Kodjabachian et al., "Wnt inhibitory factor 1 is epigenetically silenced in human osteosarcoma, and targeted disruption accelerates osteosarcomagenesis in mice," *Journal of Clinical Investigation*, vol. 119, no. 4, pp. 837–851, 2009.

[18] K. Chen, S. Fallen, H. O. Abaan et al., "Wnt10b induces chemotaxis of osteosarcoma and correlates with reduced survival," *Pediatric Blood and Cancer*, vol. 51, no. 3, pp. 349–355, 2008.

[19] M. Enomoto, S. Hayakawa, S. Itsukushima et al., "Autonomous regulation of osteosarcoma cell invasiveness by Wnt5a/Ror2 signaling," *Oncogene*, vol. 28, no. 36, pp. 3197–3208, 2009.

[20] B. H. Hoang, T. Kubo, J. H. Healey et al., "Dickkopf 3 inhibits invasion and motility of Saos-2 osteosarcoma cells by modulating the Wnt-β-catenin pathway," *Cancer Research*, vol. 64, no. 8, pp. 2734–2739, 2004.

[21] E. M. Rubin, Y. Guo, K. Tu, J. Xie, X. Zi, and B. H. Hoang, "Wnt inhibitory factor 1 decreases tumorigenesis and metastasis in osteosarcoma," *Molecular Cancer Therapeutics*, vol. 9, no. 3, pp. 731–741, 2010.

[22] W. C. Hahn, C. M. Counter, A. S. Lundberg, R. L. Beijersbergen, M. W. Brooks, and R. A. Weinberg, "Creation of human tumour cells with defined genetic elements," *Nature*, vol. 400, no. 6743, pp. 464–468, 1999.

[23] N. Li, R. Yang, W. Zhang, H. Dorfman, P. Rao, and R. Gorlick, "Genetically transforming human mesenchymal stem cells to sarcomas: changes in cellular phenotype and multilineage differentiation potential," *Cancer*, vol. 115, no. 20, pp. 4795–4806, 2009.

[24] M. Miura, Y. Miura, H. M. Padilla-Nash et al., "Accumulated chromosomal instability in murine bone marrow mesenchymal stem cells leads to malignant transformation," *Stem Cells*, vol. 24, no. 4, pp. 1095–1103, 2006.

[25] J. Tolar, A. J. Nauta, M. J. Osborn et al., "Sarcoma derived from cultured mesenchymal stem cells," *Stem Cells*, vol. 25, no. 2, pp. 371–379, 2007.

[26] A. B. Mohseny, K. Szuhai, S. Romeo et al., "Osteosarcoma originates from mesenchymal stem cells in consequence of aneuploidization and genomic loss of Cdkn2," *Journal of Pathology*, vol. 219, no. 3, pp. 294–305, 2009.

[27] V. S. Spiegelman, T. J. Slaga, M. Pagano, T. Minamoto, Z. Ronai, and S. Y. Fuchs, "Wnt/β-catenin signaling induces the expression and activity of βTrCP ubiquitin ligase receptor," *Molecular Cell*, vol. 5, no. 5, pp. 877–882, 2000.

[28] D. M. Thomas, "Wnts, bone and cancer," *Journal of Pathology*, vol. 220, no. 1, pp. 1–4, 2010.

[29] Y. Guo, E. M. Rubin, J. Xie, X. Zi, and B. H. Hoang, "Dominant negative LRP5 decreases tumorigenicity and metastasis of osteosarcoma in an animal model," *Clinical Orthopaedics and Related Research*, vol. 466, no. 9, pp. 2039–2045, 2008.

[30] Y. Guo, X. Zi, Z. Koontz et al., "Blocking Wnt/LRP5 signaling by a soluble receptor modulates the epithelial to mesenchymal transition and suppresses met and metalloproteinases in osteosarcoma Saos-2 cells," *Journal of Orthopaedic Research*, vol. 25, no. 7, pp. 964–971, 2007.

[31] P. C. Leow, Q. Tian, Z. Y. Ong, Z. Yang, and P. L. R. Ee, "Antitumor activity of natural compounds, curcumin and PKF118-310, as Wnt/β-catenin antagonists against human osteosarcoma cells," *Investigational New Drugs*, vol. 28, no. 6, pp. 766–782, 2010.

[32] N. Lee, A. J. Smolarz, S. Olson et al., "A potential role for Dkk-1 in the pathogenesis of osteosarcoma predicts novel diagnostic and treatment strategies," *British Journal of Cancer*, vol. 97, no. 11, pp. 1552–1559, 2007.

[33] K. Iwaya, H. Ogawa, M. Kuroda, M. Izumi, T. Ishida, and K. Mukai, "Cytoplasmic and/or nuclear staining of beta-catenin is associated with lung metastasis," *Clinical and Experimental Metastasis*, vol. 20, no. 6, pp. 525–529, 2003.

[34] T. J. Stein, K. E. Holmes, A. Muthuswamy, V. Thompson, and M. K. Huelsmeyer, "Characterization of β-catenin expression in canine osteosarcoma," *Veterinary and Comparative Oncology*, vol. 9, no. 1, pp. 65–73, 2011.

[35] A. M. Cleton-Jansen, J. K. Anninga, I. H. Briaire-de Bruijn et al., "Profiling of high-grade central osteosarcoma and its putative progenitor cells identifies tumourigenic pathways.," *British Journal of Cancer*, vol. 101, no. 12, article 2064, 2009.

[36] Y. Cai, A. B. Mohseny, M. Karperien, P. C. W. Hogendoorn, G. Zhou, and A. M. Cleton-Jansen, "Inactive Wnt/β-catenin pathway in conventional high-grade osteosarcoma," *Journal of Pathology*, vol. 220, no. 1, pp. 24–33, 2010.

[37] Y. Gong, R. B. Slee, N. Fukai et al., "LDL receptor-related protein 5 (LRP5) affects bone accrual and eye development," *Cell*, vol. 107, no. 4, pp. 513–523, 2001.

[38] L. M. Boyden, J. Mao, J. Belsky et al., "High bone density due to a mutation in LDL-receptor-related protein 5," *The New England Journal of Medicine*, vol. 346, no. 20, pp. 1513–1521, 2002.

[39] L. van Wesenbeeck, E. Cleiren, J. Gram et al., "Six novel missense mutations in the LDL receptor-related protein 5 (LRP5) gene in different conditions with an increased bone density," *American Journal of Human Genetics*, vol. 72, no. 3, pp. 763–771, 2003.

[40] N. Tang, W. X. Song, J. Luo, R. C. Haydon, and T. C. He, "Osteosarcoma development and stem cell differentiation," *Clinical Orthopaedics and Related Research*, vol. 466, no. 9, pp. 2114–2130, 2008.

Hindawi Publishing Corporation
Sarcoma
Volume 2012, Article ID 126906, 11 pages
doi:10.1155/2012/126906

Research Article

Enhanced Growth Inhibition of Osteosarcoma by Cytotoxic Polymerized Liposomal Nanoparticles Targeting the Alcam Cell Surface Receptor

Noah Federman,[1] Jason Chan,[1] Jon O. Nagy,[2] Elliot M. Landaw,[3] Katelyn McCabe,[4] Anna M. Wu,[4] Timothy Triche,[5] HyungGyoo Kang,[5] Bin Liu,[6] James D. Marks,[6] and Christopher T. Denny[1]

[1] *Division of Pediatric Hematology/Oncology, Department of Pediatrics, Mattel Children's Hospital and Gwynne Hazen Cherry Memorial Laboratories, UCLA Jonsson Comprehensive Cancer Center, Los Angeles, CA 90095-1781, USA*
[2] *NanoValent Pharmaceuticals Inc., Bozeman, MT 59718-4012, USA*
[3] *Department of Biomathematics, David Geffen School of Medicine, UCLA, Los Angeles, CA 90095-1766, USA*
[4] *Department of Molecular and Medical Pharmacology, Crump Institute for Molecular Imaging, UCLA, Los Angeles, CA 90095-1770, USA*
[5] *Department of Pathology and Laboratory Medicine, Children's Hospital Los Angeles, University of Southern California, Los Angeles, CA 90027, USA*
[6] *Department of Anesthesia and Perioperative Cave, Helen Diller Family Comprehensive Cancer Center, University of California, San Francisco, CA 94110, USA*

Correspondence should be addressed to Noah Federman, nfederman@mednet.ucla.edu

Received 5 June 2012; Accepted 3 July 2012

Academic Editor: Norman Jaffe

Osteosarcoma is the most common primary malignancy of bone in children, adolescents, and adults. Despite extensive surgery and adjuvant aggressive high-dose systemic chemotherapy with potentially severe bystander side effects, cure is attainable in about 70% of patients with localized disease and only 20%–30% of those patients with metastatic disease. Targeted therapies clearly are warranted in improving our treatment of this adolescent killer. However, a lack of osteosarcoma-associated/specific markers has hindered development of targeted therapeutics. We describe a novel osteosarcoma-associated cell surface antigen, ALCAM. We, then, create an engineered anti-ALCAM-hybrid polymerized liposomal nanoparticle immunoconjugate (α-AL-HPLN) to specifically target osteosarcoma cells and deliver a cytotoxic chemotherapeutic agent, doxorubicin. We have demonstrated that α-AL-HPLNs have significantly enhanced cytotoxicity over untargeted HPLNs and over a conventional liposomal doxorubicin formulation. In this way, α-AL-HPLNs are a promising new strategy to specifically deliver cytotoxic agents in osteosarcoma.

1. Introduction

Osteosarcoma is the most common primary malignant neoplasm of bone in children and adolescents and is characterized by unregulated proliferation of primitive osteoid-producing mesenchymal cells [1]. Prior to 1970, the prognosis for patients with osteosarcoma who were treated with surgery alone was a dismal 10%–20% overall survival. Though aggressive surgeries would render most patients grossly tumor-free, the vast majority would develop progressively fatal metastatic disease within two years. This suggested that at the time of their initial diagnosis clinically undetectable tumor had already spread to distant sites in most patients and that effective systemic anticancer therapy was needed [2].

The development of neoadjuvant cytotoxic chemotherapy regimens over the past three decades has dramatically improved the fate of osteosarcoma patients. The addition of multiagent regimens plus refinement in surgical resection

has resulted in a 65%–75% long-term survival rate in patients presenting with localized disease [3]. While this is a substantial improvement, current multimodality therapy still has significant shortcomings. First, the outlook remains poor for patients with radiographically detectable metastases at diagnosis or for those in whom the cancer recurs. Second, while the currently utilized chemotherapy regimens are effective against osteosarcoma, they also wreak havoc on normal cells that can result in acute and potentially life-threatening complications. It is also now appreciated that exposure of pediatric cancer patients to cytotoxic chemotherapy can lead to secondary malignancies and other medical maladies, decades after their tumor has been eradicated [4].

The long-sought goal of being able to preferentially deliver anticancer therapy to tumors while sparing normal cells could have a significant impact on the deficiencies of current osteosarcoma treatment regimens. In this regard, the use of nanoparticles as delivery vehicles appears promising. Liposomes, unilamellar vesicles composed of natural and/or synthetic lipids, have been a particularly intensively studied system [5]. The problem of containment versus controlled release of anti-cancer agents has been a challenge for liposomal drug delivery. On the one hand, liposomes need to be formulated to allow for efficient packaging of therapeutic agents and stable containment of drug in a normal extracellular environment. On the other hand, liposomes that have localized to tumors need to be able to release their payload in order to have a therapeutic effect. This latter attribute has been particularly difficult to program into standard liposome formulations [6, 7].

Many nanoparticle anti-cancer targeting strategies require identification of a marker that is expressed on the surface of the tumor cell. In particular, tumor-associated molecules that are expressed at higher levels than in normal tissues are sought since nanoparticles coated with antibodies recognizing these markers can preferentially bind to tumor cells. Finally from a potential therapeutic delivery perspective, it is best when candidate tumor markers are internalized when bound by ligands or proteins at the cell surface [8]. By exploiting this interaction, targeted nanoparticles can deliver therapeutic payloads into tumor cells through receptor-mediated endocytosis.

With these criteria in mind, the cell surface receptor activated leukocyte adhesion molecule (ALCAM, CD166) is an attractive candidate to target osteosarcoma. This glycoprotein is a member of the immunoglobulin superfamily and is thought to mediate important cell-cell interactions involved in cell migration, neurogenesis, hematopoiesis, and the immune response [9]. More recently, increased ALCAM expression has been linked to a variety of cancers including pancreatic, breast, prostate, and colorectal carcinomas and melanoma [10–12]. Furthermore, others have found that immunoliposomes coated with a recombinant anti-ALCAM monoclonal antibody were taken up by prostate cancer cell lines expressing this antigen [13].

In this paper, we demonstrate that ALCAM is overexpressed in both osteosarcoma tumor-derived cell lines and primary biopsy specimens. We show that this cell surface molecule can be exploited to enhance binding and uptake of nanoparticles by osteosarcoma cells. We present a new polymerized liposome formulation consisting of a mixture of lipids with saturated and diacetylene containing acyl chains that when loaded with doxorubicin displays enhanced cytotoxicity to osteosarcoma cells. Finally, we find that coating these hybrid liposomes with recombinant anti-ALCAM antibody further improves cytotoxic killing of osteosarcoma cell lines.

2. Methods

2.1. Materials. Conventional and polymerized liposomal nanoparticles (PLNs and HPLNs) were obtained from NanoValent Pharmaceuticals, Inc. (Bozeman, MT, USA). The components comprising the conventional liposomes are L-α-phosphatidylcholine hydrogenated soy, (hydrogenated soy PC), cholesterol and 1,2-distearoyl-*sn*-glycero-3-phosphoethanolamine-N-[methoxy(polyethylene glycol)-2000] (m-PEG_{2000}-DSPE), (Avanti Polar Lipids, Alabaster, AL, USA). The PLNs are comprised of (5′-hydroxy-3′-oxypentyl)-10-12-pentacosadiynamide (h-PEG_1-PCDA), (5′-sulfo-3′-oxypentyl)-10-12-pentacosadiynamide (sulfo-PEG_1-PCDA), N-[(methoxy(polyethylene glycol)-750]-10-12-pentacosadiynamide (m-PEG_{750}-PCDA) and N-[(maleimide(polyethylene glycol)-1500]-10-12-pentacosadiynamide (mal-PEG_{1500}-PCDA) (NanoValent Pharmaceuticals, Inc. Bozeman, MT, USA) and the HPLNs are comprised h-PEG_1-PCDA, hydrogenated soy PC, m-PEG_{2000}-DSPE, 1,2-distearoyl-*sn*-glycero-3-phosphoethanolamine-N-[maleimide(polyethylene glycol)-2000] (mal-PEG_{2000}-DSPE) (Avanti Polar Lipids, Alabaster, AL, USA), and cholesterol.

2.2. Preparation of Conventional Liposomes and HPLNs. Conventional liposomes were prepared from hydrogenated soy PC, cholesterol, and m-PEG_{2000}-DSPE in molar proportions of 57.5 : 37.5 : 5, nontargetable HPLNs prepared from h-PEG_1PCDA, hydrogenated soy PC, cholesterol, and m-PEG_{2000}-DSPE at a molar proportion of 15 : 47 : 32 : 6, and targetable HPLNs prepared from h-PEG_1PCDA, hydrogenated soy PC, cholesterol, mal-PEG_{2000}-DSPE, and m-PEG_{2000}-DSPE at a molar proportion of 15 : 47 : 32 : 4.5 : 1.5, and the PLNs prepared from h-PEG_1-PCDA, m-PEG_{750}-PCDA, sulfo-PEG_1-PCDA and mal-PEG_{1500}-PCDA at a molar proportion of 65 : 25 : 5 : 5, according to the method previously described [14]. Briefly, lipids were mixed and evaporated *in vacuo,* to a film. Deionized water or 300 mM ammonium sulfate was added to the films so as to give a 25 mM (total lipid and cholesterol) suspension. The suspension was heated via sonication between 70 and 80°C with a probe-tip sonicator (Fisher sonic dismembrator model 300) for 5 min. The resulting milky solution was then passed through a stacked polycarbonate membrane (100 nm), eleven times, with a dual syringe extruder (LiposoFast-Basic, Avestin, Inc., Ottawa, ON, Canada), heated to 65°C. The nearly clear liposome solutions were cooled to 5°C for 12 hours. After warming to ambient temperature, the water-filled liposomes that contain PCDA lipids were polymerized by UV light irradiation (254 nm) with a Spectrolinker

XL-1000 UV Crosslinker (Spectronics Corp.) for 10 minutes. The resulting blue PLNs and HPLNs were heated to 65°C for 5 min to convert them to the red (fluorescent) form. The colored solutions were syringe filtered through 0.2 μm cellulose acetate filters in order to remove trace insoluble contaminants.

2.3. Doxorubicin Loading. The ammonium sulfate-containing conventional and polymerizable (HPLN) liposomes was passed over a G50 Sephadex column (washed with 20 mM HEPES) to exchange the external buffer. The liposomes were then incubated with doxorubicin HCl (Shandong Tianyu Fine Chemical Co., Ltd.) at a concentration of 1 μM of Dox to 3.2 μM of lipid while heating to 65°C for 20 min. The unencapsulated doxorubicin was removed by shaking with anionic exchange resin (Bio-Rex 70, Bio-Rad Inc) in a ratio of 7 μg of doxorubicin to 1 μL of packed resin, for 5 min. Liposomes were separated from resin by filtering through Pierce Spin Cups. The average particle size measurements were obtained on a Zetasizer Nano S (Malvern Inst.), in a solution of 10 mM sodium chloride.

2.4. Preparation of ALCAM-Antibody-Conjugated PLNs and HPLNs. An anti-ALCAM antibody was previously engineered into a cys-diabody (cross-paired dimer of single-chain antibody fragments, with C-terminal cysteine residues) as described [19]. PLNs and non-crossslinked, dox-loaded HPLNs, were incubated with anti-ALCAM cys-diabody was conjugated to the particle surface. TCEP (500 mM) that became added to cys-diabody (1–4 μg/μL) solution to a final concentration of 10 mM and incubated at room temperature for 30 minutes to reduce the diabody's terminal cysteine residues. Reduced α-ALCAM cys-diabody was then added to the liposome mixture (2.5–10 μg/μL lipid) at a diabody/lipid ratio of 1 μg diabody : 7.5 μg total lipid and incubated at room temperature for 2 hours to allow for conjugation to maleimide residues on either the PLN or HPLNs. Unbound maleimide residues were quenched with 20 mM cysteine solution for 30 minutes. Unbound diabody, free cysteine, and TCEP were removed using filtration through Amicon Ultra-0.5 mL 100 K Centrifugal Filters (Millipore). Samples were diluted 1 : 2 with HEPES-buffered saline and centrifuged at 6000 rpm for 10 minutes to concentrate the ALCAM diabody conjugated sample. After purification the antibody-conjugated, dox-loaded, non-crosslinked HPLNs were photopolymerized by UV irradiation as described in Section 2.1. The untargeted PLNs were prepared as controls by quenching the maleimide residues with 20 mM cysteine.

2.5. Quantification of Entrapped Liposomal Doxorubicin. Doxorubicin was quantified spectrophotometrically based on the molar extinction coefficient of 12,500. Unencapsulated Dox was removed using Bio-Rex 70. Dox-loaded particles were disrupted using diluted a 1 : 20 isopropanol with 0.075 M HCl solution and then vortexed for at least 30 seconds to ensure complete membrane rupture. Absorbance was read at 480 nm on a Beckman Coulter DU800 spectrophotometer.

2.6. Quantification of Total Lipid. Total lipid content of HPLN samples was measured using a colorimetric assay. A 4 μL aliquot of HPLN sample was vacuum dried and resuspended in an ammonium ferrothiocyanate/chloroform solution consisting of 0.1 M Ferric chloride mixed with 0.4 M ammonium thiocyanate and 200 ul of chloroform. Absorbance at 488 nm of the organic phase was then measured in a Beckman Coulter DU800 spectrophotometer. OD488 of the sample was then compared to a standard curve of known lipid concentration values.

2.7. Stability of Liposomal Doxorubicin Containment. The ability of nanoparticles (both HPLN and conventional liposome formulation) to hold on to entrapped doxorubicin was measured using a postload time course study. Nanoparticles were loaded with doxorubicin using the procedure previously described. After loading, several conditions of nanoparticle storage were altered to simulate neutral pH of intracellular environment and early and late endosome cellular compartments. Nanoparticles were stored at a pH of 4.5, 6, or 7.4 and at temperature of either 4°C or 37°C giving a total of six different storage conditions. The concentrations of doxorubicin inside the nanoparticles were measured at 0 hr, 0.5 hr, 4 hr, 24 hr, 48 hr, and 144 hr using the method described previously. Before each measurement, any extraliposomal doxorubicin was removed by incubation with BioRex 70 resin (Bio-Rad, Inc.). Each measurement was then normalized to the time-zero measurement of the respective sample to obtain a "percent-contained" doxorubicin measurement in order to assess the stability of the particles. Analysis of variance using log transformed data and blocking on experiment day was used to assess the effect of vehicle, pH, and temperature on doxorubicin leakage, to test for interactions among factors, and to construct 95% confidence intervals for geometric mean fold changes in leakage.

2.8. MTT Assay. Osteosarcoma cell lines KHOS 240S, HOS, or MNNG-HOS were grown in Dulbecco's Modified Eagle Medium (HyClone Cat no. SH30022.01) with 10% fetal bovine serum (Gemini Bioproducts). Cells were seeded in a 96-well format at a concentration of 5×10^3 cells/well at a volume of 100 μL media with penicillin/streptomycin and incubated overnight. The following day, wells were treated with doxorubicin-loaded targeted HPLNs, untargeted HPLNs, conventional liposomes, or free doxorubicin for a four-hour period then washed with fresh media. Doses were added based on doxorubicin concentrations ranging on a log scale from 0.01 to 100 μM and at 0 nM. The 0 nM well was treated with HEPES-buffered saline. Each treatment was performed in triplicate. Cells were incubated under standard CO_2 conditions for 72 hrs at 37°C. At 72 hrs, all wells are treated with 10 μL of thiazolyl blue tetrazolium bromide (Sigma) solution at an initial concentration of 5 μg/μL in phosphate buffered saline and incubated for 4 hrs. Reaction was ceased and cells lysed by adding 100 μL of 15% sodium dodecyl sulfate/15 mM HCl solution and incubated overnight in the dark at room temperature. Plate absorbance was read using Bio-Rad microplate reader at 570 nm. To account for background absorbance, the arithmetic mean

of the OD570 of the blank wells was subtracted from the OD570 readings of all treated wells. The arithmetic mean of each plate was calculated and considered as 100% viability. The remaining wells were then divided by this mean to obtain nominal percent viability within each well. Viability was plotted against log drug concentration, and unweighted nonlinear regression was used to estimate log (IC50) for each treatment using a four-parameter sigmoid dose-response model (Prism Software, GraphPad). Fixing the bottom parameter to zero yielded better residual patterns and more stable Hill slope estimates than analyses allowing a variable bottom. For each cell line experiment, a run comparing the four treatment vehicles was repeated 3 to 7 times on different days. Within each cell line, a linear mixed effects model revealed day-to-day variability as a much greater source of variation in log (IC50) than batch variability, and blocking on experiment day improved the precision of estimated differences between treatments. In assessing IC50 results across cell lines, a significant cell line by treatment interaction was detected that could be fully accounted for by modeling a shift in conventional liposome potency (relative to the other 3 treatments) just in the MNNG-HOS cell line.

2.9. PLN Binding Fluorescent Microscopy Assay. Osteosarcoma cell lines were seeded onto 4-well Lab-Tek II Chamber Slides (Thermo Scientific) to reach 80% confluence overnight. Cells were treated with anti-ALCAM diabody conjugated PLN at 50 μg/mL per well. Cells were incubated for 4 hrs at 37°C. Media were removed, and wells were washed with 1 mL fresh media. Cell fixation was with 3.7% formaldehyde in Phosphate buffered saline for 15 minutes at 4°C. Cells were mounted using VECTASHIELD mounting medium with DAPI (Vector Laboratories). Positive and negative control cell lines were pancreatic cell lines HPAF and MiaPaca, respectively. Cells were viewed using a Carl Zeiss Axio Imager D1 fluorescence microscope. Cells were viewed at 20x magnification. DAPI was visualized through blue/cyan filter. Bound nanoparticles were visualized using the rhodamine filter at a 1 second exposure.

2.10. Western Immunoblot. Antibodies used for immunoblot were monoclonal mouse anti-CD166 (Vector Laboratories, Cat no. VP-C375) at a concentration of 1 : 400 and anti-Actin C-11 (Santa Cruz Biotechnology, Cat no. sc-1615) at a concentration of 1 : 3000.

2.11. Immunohistochemistry. Deidentified human patient osteosarcoma paraffin-embedded samples were obtained from the UCLA Tissue Procurement Core Laboratory (IRB Exempt). Four-micrometer sections were cut and placed onto slides. Samples were then deparaffinized, rehydrated, and subjected to heat-induced epitope retrieval. Slides were incubated with a 1 : 50 dilution of anti-CD166 mouse monoclonal antibody (Vector) for 2 h at room temperature, and signal was detected using the mouse EnVision+ System-HRP (DAB) kit (Dako). Sections were counterstained with hematoxylin. Images were viewed and obtained using Zeiss AxioImager at 20x magnification.

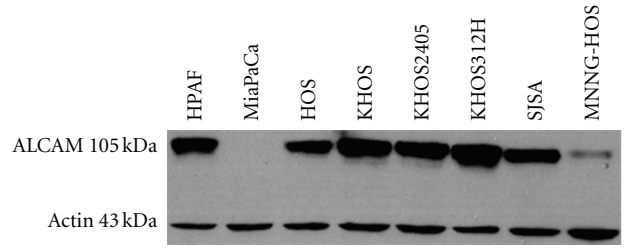

Figure 1: ALCAM/CD166 is highly expressed in osteosarcoma cell lines. Western immunoblot analysis of osteosarcoma cell lines probed with α-ALCAM antisera. There is high total cell expression of ALCAM in HOS, KHOS, KHOS240s, and SJSA with moderate expression in the MNNG-HOS cell line. A pancreatic cancer cell line, HPAF, with known high levels of ALCAM expression was used as a positive control. MiaPaCa, a pancreatic cancer cell line with known lack of ALCAM expression served as a negative control. Membrane-localized ALCAM isoform is present at 105 kDa. β-Actin was used as an internal loading control.

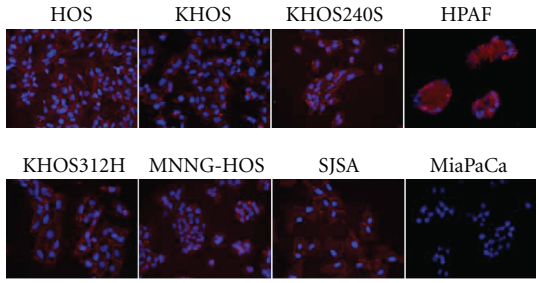

Figure 2: Surface ALCAM expression in osteosarcoma cell lines. Fluorescent immunohistochemistry showing membranous ALCAM expression in osteosarcoma cell lines in comparison to a known ALCAM expressing pancreatic cancer cell line, HPAF (positive control), and ALCAM negative cell line, MiaPaCa. ALCAM binding shown in red (Alexa Fluor 564) and nuclei counterstained with DAPI (20x magnification).

3. Results

3.1. ALCAM Is Highly Expressed in Both Primary Osteosarcoma Specimens and Tumor-Derived Cell Lines. A molecular survey of the osteosarcoma cell line U2-OS demonstrated expression of ALCAM on the surface of these cells [15]. These observations prompted a more in-depth investigation of ALCAM expression in human osteosarcoma. Evaluation of ALCAM expression in a collection of 6 tumor-derived cell lines was used as an initial platform. Cell lysates were harvested from subconfluent adherent cultures grown in tissue culture and analyzed by immunoblot using anti-ALCAM antisera. Pancreatic cancer cell lines with high (HPAF) and no (MiaPaCa) ALCAM expression were used as controls. All 6 osteosarcoma cell lines expressed ALCAM, and 5 of 6 demonstrated elevated expression at the level seen in the HPAF control (Figure 1). The quality of ALCAM expression was further confirmed in fluorescent immunohistochemistry showing primarily a membranous, surface component to the ALCAM expression in osteosarcoma cell lines (Figure 2).

Though there was a high frequency of ALCAM expression in our cell line collection, there is always a concern that

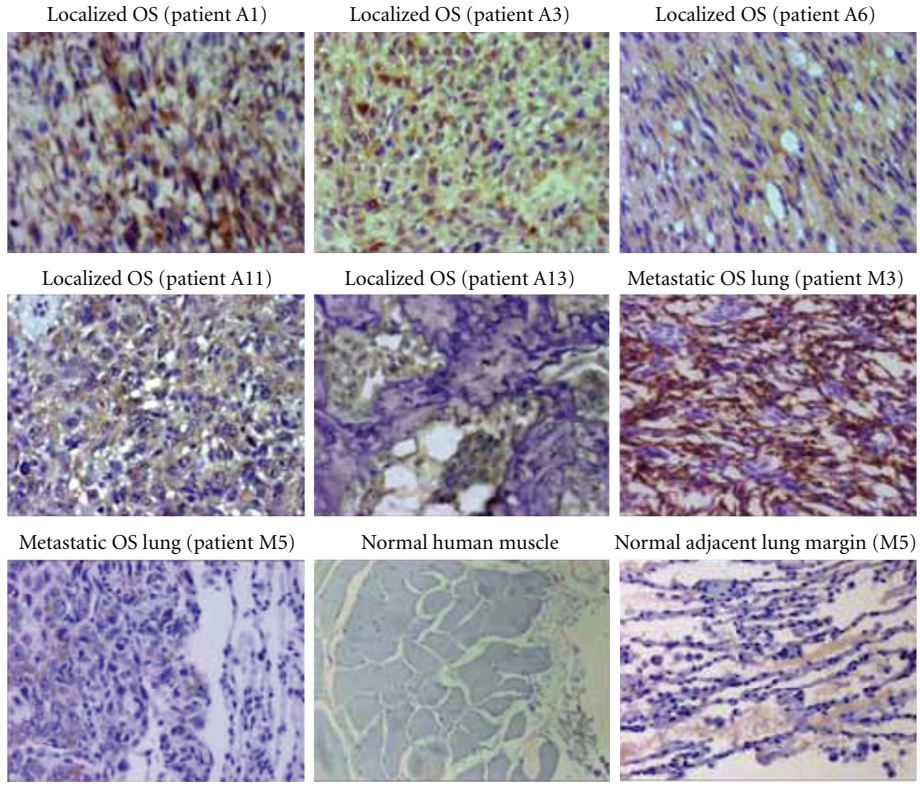

Figure 3: ALCAM expression in human osteosarcoma patient tumor samples. Immunohistochemistry studies in human paraffin-embedded localized and pulmonary metastatic osteosarcoma samples show mild to strong expression of ALCAM (brown) both membranous and cytoplasmic in appearance in comparison to normal human muscle and human lung. Tissues were counterstained with hematoxylin (magnification 20x).

it may be due to a selection process inherent in creating tumor-derived cell lines. In addition, differences in growth conditions between in vivo in osteosarcoma patients and in vitro in tissue culture may be responsible for changes in ALCAM expression.

To address these concerns, human osteosarcoma tumor samples both from primary and metastatic sites were assayed for ALCAM expression by immunocytochemistry. Banked anonymized patient specimens were fixed, sectioned, and incubated with anti-ALCAM antisera. After washing, in situ ALCAM expression was detected using a colorimetric assay and evaluated by light microscopy. Tissues were graded as strongly positive (+++), moderately positive (++), weakly positive (+), or negative (−). All OS tumor samples stained positively for ALCAM. Of 10 localized and metastatic OS samples, 5 of the localized OS tissues stained weakly to strongly positive for ALCAM and 5 of the metastatic OS samples also had moderate to strong IHC staining. Osteosarcoma cells demonstrated both cytoplasmic and membranous ALCAM expression (representative IHC images are shown in Figure 3).

3.2. Anti-ALCAM Coupled Polymerized Liposomal Nanoparticles Avidly Bind to Osteosarcoma Cell Lines. Polymerized liposomes and hybrid polymerized liposomal nanoparticles (PLNs and HPLNs) were evaluated as a potential therapeutic delivery vehicle that could be targeted to osteosarcoma cells expressing ALCAM. PLNs and HPLNs share many structural attributes of conventional liposomes. They are self-assembling unilamellar spheres whose surfaces can be modified using the same chemical coupling strategies as employed for liposomes. Unlike liposomes, PLNs and HPLNs can be manufactured to be intrinsically fluorescent. Ultraviolet irradiation leads to cross-linking of diacetylene residues present in their acyl chains, leading to highly colored blue particles, and heat treatment of the PLNs and HPLN vesicles leads to color change and fluorophore formation [16, 17]. The fluorescence emission spectrum is centered at 635 nm with a broad and complex excitation spectrum from 480 to 580 nm. As a result, PLNs and HPLNs converted into their fluorescent form can be readily traced from the time they bind to target cells until they are deposited and compartmentalized into subcellular structures.

Targeted PLNs and HPLNs were created by chemically coupling a recombinant anti-ALCAM antibody fragment to its surface. PLNs and HPLNs were synthesized containing maleimide reactive groups at the distal end of surface polyethylene glycol (PEG) molecules. A bivalent anti-ALCAM diabody, derived from a previously described scFv [18], was genetically engineered to contain a C-terminal cysteine [19]. The resulting cys-diabody is bivalent, compact (one-third the size of an intact antibody) and enables site-specific oriented coupling of the antibody variable regions to the surface of nanoparticles [20]. Mixing these two

components induced a condensation reaction between the thiol of the cysteine and the maleimide moiety, resulting in the anti-ALCAM diabody being covalently coupled to the PLN or HPLN surface. As a negative control, untargeted HPLNs where prepared without maleimide lipid and untargeted PLNs were made by coupling free cysteine to nanoparticles.

Binding studies were performed comparing the relative affinities of anti-ALCAM coupled PLNs (α-AL-PLN) versus untargeted PLNs towards osteosarcoma cell lines. After a 4-hour incubation, cells were washed and (α-AL-PLN) binding was detected by fluorescence microscopy. α-AL-PLNs bound to all of the osteosarcoma cell lines in our panel, much more efficiently than untargeted negative controls (Figure 4). This interaction was dependent on cellular ALCAM expression. Both targeted and untargeted PLNs bound equally to MiaPaCa cells that do not express cell surface ALCAM.

To gauge the rapidity of the interaction between α-AL-PLNs and osteosarcoma cells, a time course study was performed. Osteosarcoma cells were incubated with α-AL-PLNs for varying time periods up to 4 hours, washed, and then evaluated by fluorescence microscopy.

α-AL-PLNs binding was detected as early as 30 minutes and reached a maximum by 4 hours (Figure 5). The presence of a strong perinuclear fluorescence signal suggested that the targeted nanoparticles were rapidly internalized into the endosome compartment of the cell. To further evaluate this, binding studies were performed at 4°C, which would inhibit cellular endocytosis. Under these conditions, a strong membrane fluorescence signal was detected without perinuclear nuclear localization consistent with α-AL-PLNs being bound to the cell surface but not internalized (Figure 6).

3.3. Hybrid PLNs Were Formulated to Function as Potential Therapeutic Delivery Vehicles. Our initial PLN formulation was composed entirely of 10,12-pentacosadiynoic acid (PCDA) derivatives and when polymerized formed a very fluorescent particle that could easily be detected. However, these nanoparticles proved to be problematic when trying to adapt them for delivery of therapeutics. Attempts at effectively loading them with cytotoxic chemotherapeutic agents, either through encapsulation during vesicle formation or across ion gradients using the prepolymerized liposomes, failed at multiple levels. For this reason, hybrid PLNs were created which composed of PCDA lipids mixed with saturated phospholipids found in many liposome formulations.

To approach this problem, we started with a standard liposomal formulation consisting of hydrogenated soy PC (where the major component is distearoylphosphatidylcholine (DSPC)), cholesterol, and polyethylene glycol-distearoylphosphatidyl ethanolamine (m-PEG_{2000}-DSPE) in molar proportions of 57.5 : 37.5 : 5. Increasing amounts of unsaturated PCDA lipids were then added. We chose a very short PEG chain PCDA derivative, h-PEG_1-PCDA, because it is an extremely reactive cross-linking lipid, has good aqueous dispersion properties when mixed with charged lipids, and is in itself uncharged so it will not alter the overall surface charge, and the small polar head will not interfere with the conjugation of targeting agents. After sonication and

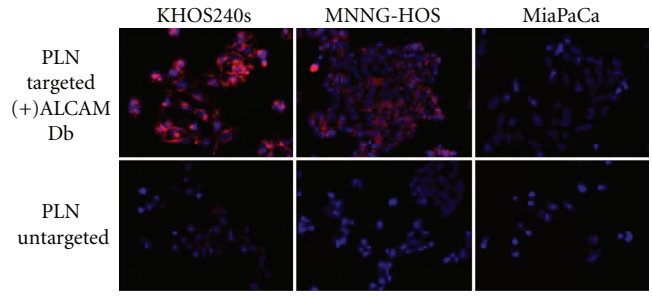

Figure 4: α-ALCAM-targeted PLNs bind specifically to osteosarcoma cell lines. α-ALCAM cys-diabody conjugated PLNs show specific binding (red) to two osteosarcoma cell lines expressing ALCAM, KHOS240s and MNNG-HOS. There was no binding to a cell line that does not express ALCAM, MiaPaCa. Fluorescence microscopy of PLNs is shown in red and DAPI nuclear counterstaining in blue (magnification 20x).

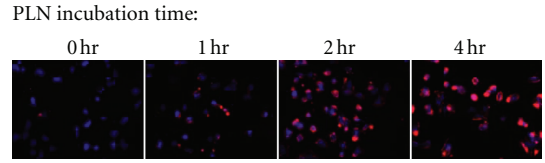

Figure 5: α-ALCAM-conjugated PLNs show cell-specific targeting in a time-dependent manner. α-ALCAM-conjugated PLNs were incubated with osteosarcoma cells for 0, 1, 2, and 4 hours then washed off. α-ALCAM targeted PLNs bind specifically to the ALCAM expressing osteosarcoma cell line KHOS240s at one hour and reach a maximum binding at 4 hours of incubation. Fluorescence microscopy of PLNs (shown in red) with DAPI (blue) nuclear counterstaining (magnification 20x).

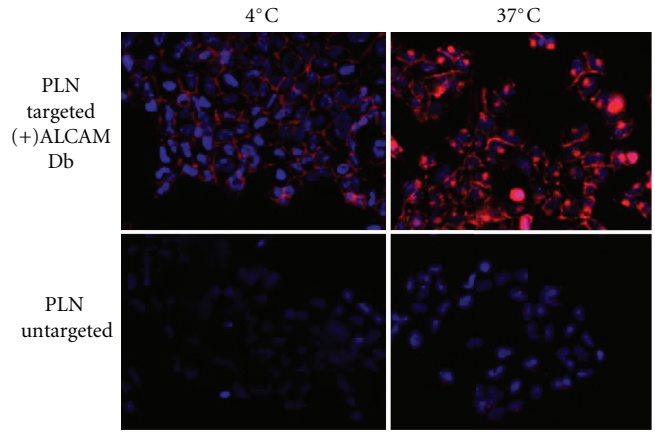

Figure 6: α-ALCAM-conjugated PLNs are internalized via receptor-mediated endocytosis. α-ALCAM-targeted PLNs incubated with the osteosarcoma cell line KHOS240s at 4 degrees and at 37 degrees Celsius show inhibition of receptor-mediated endocytosis at 4°C and rapid internalization of targeted PLNs at 37°C versus untargeted PLNs that do not bind under either circumstance. Fluorescence microscopy of PLNs (shown in red) with DAPI (blue) nuclear counterstaining (magnification 20x).

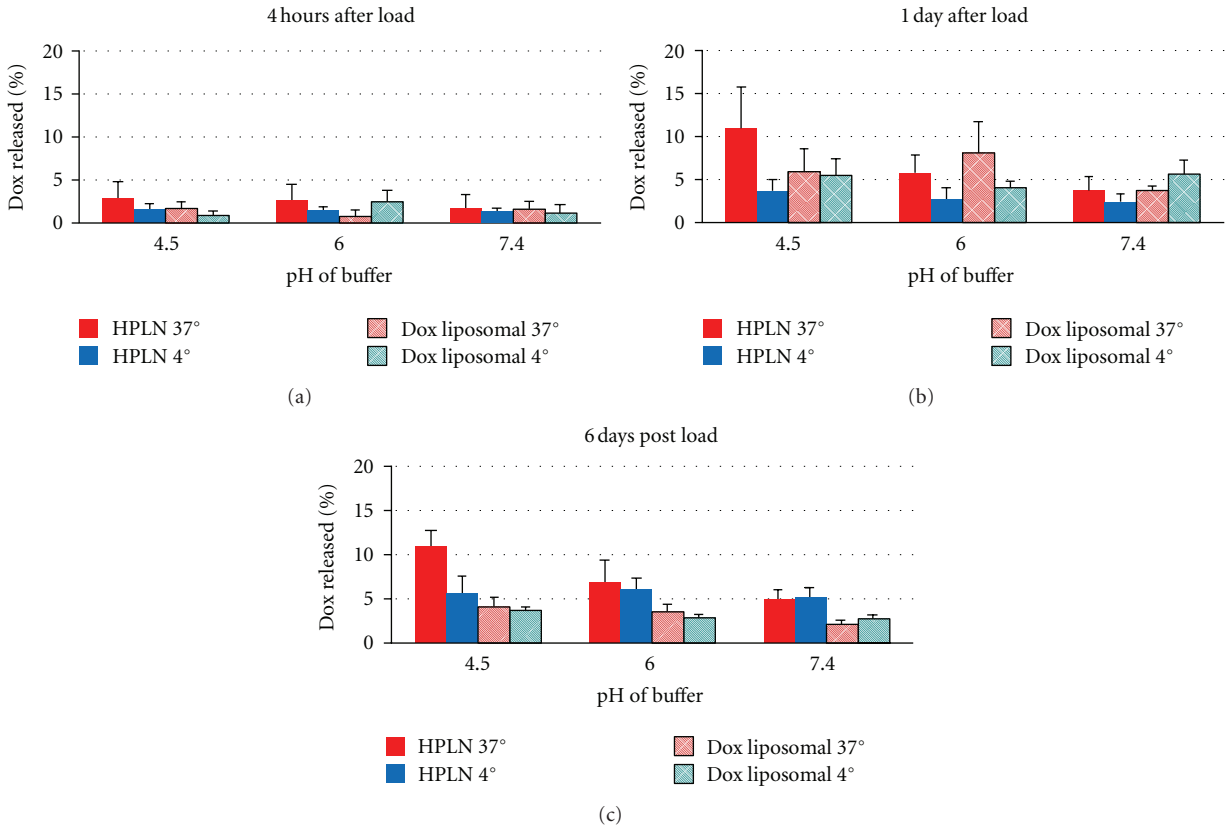

Figure 7: Containment of doxorubicin over time in drug-loaded liposomal vehicles. Containment studies of loaded HPLNs versus conventional PEG-liposomes showed that leakage increased significantly with time ($P < 0.0001$), with geometric means at 4 hours, 1 day, and 6 days being, respectively, 0.9%, 4.6%, and 3.1% for conventional doxorubicin-loaded PEG-liposomes and 1.2%, 3.2%, and 5.9% for HPLN. There were no significant differences between the vehicles or the effects of pH or temperature that could be detected at 4 hours or 1 day. However, at 6 days HPLN had 1.9-fold greater overall leakage than DOX ($P < 0.001$; 95% C.I. 1.6- to 2.4-fold). Lowering pH from 7.4 to 4.5 increased leakage by a factor of 1.5 ($P = 0.01$; 95% C.I. 1.1- to 2.1-fold) with enhanced leakage at 37 degrees compared to 4 degrees ($P = 0.03$).

extrusion, vesicles were evaluated for size by dynamic light scattering and the ability to form fluorescent particles when treated with UV irradiation and heat. After overnight cooling to 5°C, we found that inclusion of as little as 15 mole% h-PEG_1-PCDA resulted in brightly blue-colored particles but that this color became progressively attenuated with decreasing h-PEG_1-PCDA proportions.

Considering that our HPLNs were a heterogeneous mix of lipids with two very different acyl chain structures, stability in solution was a major concern. Certain hybrid formulations formed insoluble aggregates within hours after extrusion. Overnight cooling at 5°C immediately after extrusion, but prior to polymerization, proved to be critical in creating stable HPLNs. Particles treated this way were stable for weeks either refrigerated or at room temperature. Hybrid PLNs of the same lipid composition constructed without this cooling step were irretrievably unstable.

From these studies, an optimized HPLN formulation was empirically derived consisting of h-PEG_1-PCDA, hydrogenated soy phosphatidylcholine, DSPC, cholesterol, and m-PEG_{2000}-DSPE at a molar proportion of 15 : 47 : 32 : 6. Using this formulation, HPLNs were fabricated and their ability to be actively loaded with doxorubicin through generation of an ion gradient was assessed [21]. Using this method, doxorubicin could be loaded into HPLNs to an average final drug/lipid molar ratio of 0.15 (range 0.13–0.18) in comparison to conventional PEG-liposomes lacking PCDA lipids which could be loaded to an average molar ratio of 0.44 (range 0.35 to 0.49).

Containment studies of loaded HPLNs versus conventional PEG-liposomes showed that leakage increased significantly with time ($P < 0.0001$), with geometric means at 4 hours, 1 day, and 6 days being, respectively, 0.9%, 4.6%, and 3.1% for conventional doxorubicin-loaded PEG-liposomes and 1.2%, 3.2%, and 5.9% for HPLN (Figure 7). No significant differences between the liposomal vehicles or the effects of pH or temperature could be detected at 4 hours or 1 day. However, at 6 days at 37 degrees HPLN had 1.9-fold greater overall leakage than DOX liposome at either 4 or 37 degrees ($P < 0.001$; 95% C.I. 1.6- to 2.4-fold). In addition, lowering pH from 7.4 to 4.5 increased drug release in HPLN by a factor of 1.5 ($P = 0.01$; 95% C.I. 1.1- to 2.1-fold) with evidence that this effect was enhanced at 37 degrees compared to 4 degrees ($P = 0.03$).

3.4. Untargeted Doxorubicin-Loaded HPLNs Are More Cytotoxic to Osteosarcoma Cells Than Liposomal Doxorubicin Formulations. Since doxorubicin is a mainstay in the current treatment of osteosarcoma, it was chosen as our initial payload to test whether HPLNs could serve as therapeutic delivery vehicles. HPLNs and conventional liposomes were fabricated by the same procedure of hydration of dried lipid films by brief sonication followed by extrusion through 100 nm polycarbonate filters. The sizes of HPLNs and liposomes were approximately the same varying from batch to batch from 90 to 110 nm with a typical polydispersity index of about 0.1. Both particles were loaded with doxorubicin using ammonium sulfate gradients. Prior to dosing cells, loaded nanoparticles were incubated briefly with an anionic exchange resin (BioRex 70, BioRad Inc) to scavenge any nonencapsulated (free) doxorubicin. This ensured that cells were not exposed to free drug that may have leaked out while particles were in storage. Nonconfluent osteosarcoma cell lines were then incubated for 4 hours with varying concentrations of doxorubicin-loaded HPLNs or liposomes in triplicate. Cells exposed to free doxorubicin (DOX) served as positive controls. After dosing, cells were washed with fresh media and incubated for a total of 72 hours. Cell viability was then quantified by MTT assay, and 50% inhibitory concentrations (IC50s) were estimated. For each osteosarcoma cell line, this experiment was performed 3–7 times using at least two different batches of HPLNs and liposomes.

Absolute IC50 values for each doxorubicin preparation varied according to osteosarcoma cell line (Figure 8). However, the trend reflecting the relative potency of these preparations was consistent across all cell lines tested. As has been seen previously in other cell models, free doxorubicin was approximately 38- to 82-fold more potent than conventional liposomal doxorubicin [22]. Loaded HPLNs without targeting (HPLN/Dox) showed intermediate potency that was about 6-fold greater than the conventional PEGylated liposomal preparation.

Follow-up experiments were performed to determine whether the increased growth inhibition mediated by loaded HPLN/Dox was related to the amount of PCDA lipid in this formulation. HPLN/Dox with reduced PCDA were fabricated, loaded, and incubated with the KHOS240S osteosarcoma cell line. Though these variant HPLN/Dox formulations were of similar size and loaded equally well with doxorubicin, decreasing the PCDA lipid composition resulted in nanoparticles with decreased growth inhibitory potency (data not shown).

3.5. ALCAM Targeting Enhances the Growth Inhibitory Effect of Doxorubicin-Loaded PLNs. We have shown that coupling anti-ALCAM diabodies to the surface of PLNs increases their binding affinity for osteosarcoma cell lines (Figure 4). This same effect was found using α-AL-HPLNs (data not shown). Experiments were then performed to determine whether this targeting function improved the ability of doxorubicin-loaded HPLNs to inhibit growth of osteosarcoma cell lines. Targetable HPLNs were fabricated using h-PEG$_1$-PCDA, hydrogenated soy phosphatidylcholine, cholesterol, Mal-PEG$_{2000}$-DSPE, and m-PEG$_{2000}$-DSPE at a molar ratio of 15 : 47 : 32 : 4.5 : 1.5. The proportion of maleimide DSPE was empirically determined as the lowest amount that when coupled to anti-ALCAM diabody would result in enhanced binding to osteosarcoma cells (data not shown). After loading with doxorubicin, HPLNs were coupled to anti-ALCAM diabody as before giving α-AL-HPLN/Dox. Osteosarcoma cells were then incubated with α-AL-HPLN/Dox as previously described.

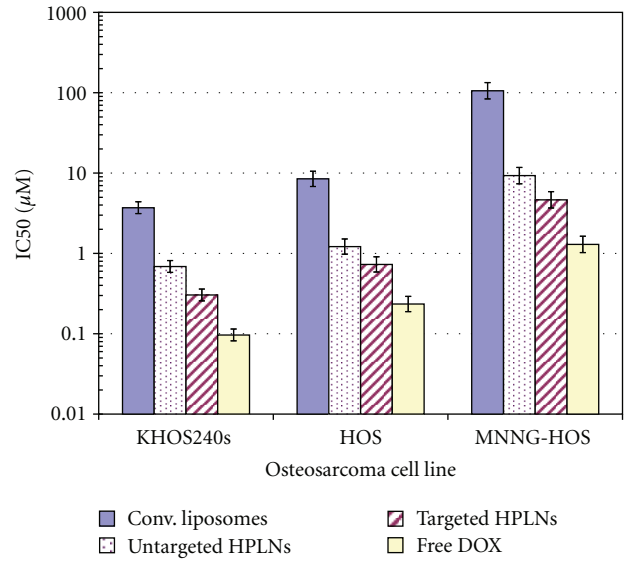

Figure 8: Cytotoxicity IC50s for doxorubicin-loaded vehicles and free DOX. Targeted and untargeted hybrid PLNs were incubated with osteosarcoma cell lines in comparison to free doxorubicin and conventional PEG-liposomal doxorubicin. Mean log IC50 for osteosarcoma cell lines shows that untargeted hybrid PLNs have a 6-fold increase in cytotoxicity over conventional liposomal formulation. ALCAM targeted hybrid PLNs (HPLN) show an additional 2-fold increase over untargeted HPLNS and 12-fold increase in cytotoxicity over conventional PEG-liposomal doxorubicin. Geometric mean IC50s were derived from seven, five, and three sets of MTT assay experiments in, respectively, the KHOS240s, HOS, and MNNG-HOS cell lines. Error bars correspond to 1 standard error for mean log (IC50). Within each cell line, differences among vehicles are highly significant ($P < 0.0001$). Confidence intervals for pairwise ratios of IC50s, corrected for multiple comparisons, are summarized in Table 1.

As seen with untargeted hybrids, the absolute sensitivity to α-AL-HPLN/Dox varied across different osteosarcoma cell lines (Table 1). However, in all cases, the targeted HPLNs demonstrated an additional growth inhibitory potency over untargeted HPLN counterparts of approximately 2-fold in all cell lines (Figure 8). Taken together, α-AL-HPLN/Dox had a log order (12-fold) increase in cytotoxicity over the conventional untargeted PEG-liposomal doxorubicin formulation in KHOS240s and HOS cell lines while having a 23-fold increase in the chemoresistant MNNG-HOS cell line. This implies that α-AL-HPLN/Dox can both specifically bind cells and deliver doxorubicin to achieve greater cytotoxicity over a conventional untargeted liposomal nanoparticle formulation.

Table 1: Relative cytotoxic potency of doxorubicin-loaded vehicles: ratio of $(IC50)^{-1}$ between vehicles summarized by geometric mean (95% confidence interval)[a].

Osteosarcoma cell line	Untargeted HPLNs over conventional liposomes	Targeted HPLNs over untargeted HPLNs	Targeted HPLNs over conventional liposomes	Free Dox over targeted HPLNs
KHOS240s	5.4 (3.7–8.0)	2.3 (1.5–3.3)	12.2 (8.3–18.0)	3.1 (2.1–4.6)
HOS	7.0 (4.8–10.1)	1.7 (1.1–2.4)	11.6 (8.0–16.8)	3.1 (2.1–4.5)
MNNG-HOS	11.4 (5.4–23.9)	2.0 (0.95–4.2)	22.8 (10.8–47.8)	3.6 (1.7–7.5)
Summary of all 3 lines[b,c]	5.9[c] (4.6–7.6)	2.0 (1.6–2.5)	11.8[c] (9.2–15.2)	3.2 (2.6–4.1)

[a]Tukey HSD 95% confidence intervals for multiple comparisons in each cell line.
[b]Based on linear mixed effects model for log IC50 as a function of cell line and vehicle.
[c]Indicated potency ratio is 2.0-fold greater (95% CI: 1.4–2.8) in MNNG-HOS cell line, consistent with significant cell line by vehicle interaction ($P = 0.015$).

4. Discussion

Our data clearly demonstrate an increase in ALCAM expression in osteosarcoma though the biologic consequences of this are difficult to gauge. The normal physiologic roles of ALCAM are still coming to light, but its molecular structure and clustering at tight junctions suggest that it could be involved in cell adhesion and migration [23]. In this context, it is tempting to think that modulating ALCAM expression could potentiate the invasive and metastatic behaviors found in high-grade malignancies such as osteosarcoma. However, there is no consistent correlation between ALCAM expression level and patient survival across all cancers. For example, an increase in ALCAM expression is found in higher-stage more aggressive malignant melanoma [24]. By contrast, high ALCAM is correlated with low-grade less aggressive cases of prostate cancer [11]. Considering the high frequency of elevated ALCAM expression in even our small cohort of osteosarcomas, it may not be able to discriminate between high- and low-risk patients with this disease.

Though ALCAM may be a limited prognostic biomarker in osteosarcoma, it has potential to serve as a molecule through which to therapeutically target this tumor. Fluorescent nanoparticles coated with anti-ALCAM diabodies preferentially bind to osteosarcoma cell lines, even those that express ALCAM at relatively low levels. As seen in prostate cancer cells, ALCAM-targeted nanoparticles were rapidly internalized by osteosarcoma cells suggesting a strategy for intracellular delivery of anticancer agents.

The use of diacetylene containing lipids to create polymerizable films and vesicles has been intensively studied for creating biosensors [25] and have been explored as cancer diagnostic and delivery vehicles [26]. When these membranes are treated with ultraviolet irradiation the resulting intralipid cross-links form an intensely blue chromophore. When exposed to physiochemical perturbations such as heat, shear, or pH stress, these membranes shift from a blue nonfluorescent state to a red fluorescent state [17]. A distinct advantage to the HPLN fluorescence is that little or no photobleaching occurs. Taking advantage of these properties, we were able to track binding and internalization of red, fluorescent ALCAM-targeted PLNs (α-AL-PLN) that had been treated with UV irradiation and heat. Interestingly, we obtained the same results using a similar preparation of α-AL-PLN that received only UV irradiation and were therefore blue and nonfluorescent in solution (data not shown). It appears that the interaction between the coupled diabody molecules and the cell surface ALCAM proteins exerted sufficient stress to shift the bound α-AL-PLN into a fluorescent state.

Though vesicles composed entirely of diacetylene containing lipids had excellent detection properties, they had limited capability as therapeutic delivery vehicles. We were unable to stably load these liposomes with doxorubicin either by passive encapsulation during vesicle formation or actively across ion gradients in formed vesicles. Others have been able to passively load hybrid liposomes composed of a 1 : 1 mixture of a phosphatidylcholine derivative with a dichain diacetylene lipid and another phospholipid [27]. However, loading efficiencies were low and this strategy may be limited to hydrophobic payloads. We have found that for amphiphilic molecules such as doxorubicin, in HPLNs, with single-chain, neutral PCDA lipids the polymerizable lipid concentration needs to be 20 mole percent or less for efficient loading to occur (data not shown).

Though our HPLNs were initially formulated for their stable drug loading characteristics, they surprisingly also proved to be more therapeutically potent in in vitro testing. The IC50 concentrations of untargeted doxorubicin-loaded hybrid PLNs in three independent osteosarcoma tumor-derived cell lines were at least 6-fold lower than conventional liposomal doxorubicin composed of PEGylated saturated phospholipid. This boost in potency appears to depend on PCDA lipid content since it is progressively lost as the PCDA concentration is titrated down from an optimum of 15–20 mole percent (data not shown). From this point, the lower the PCDA lipid concentration is in our HPLNs, the higher the IC50 becomes in our osteosarcoma model. Recently, others have used mixtures of diacetylene lipids and phospholipids to create liposomes that could be selectively destabilized either by photochemical means or by thermal shock [28, 29]. The goal here was to create a therapeutic vehicle that would release its payload in a temporal spatially controlled fashion.

We have found that even without applying an external destabilizing stimulus, HPLNs can be more effective therapeutic delivery vehicles than standard liposomal formulations. The mechanisms underlying this effect are unclear and

require further investigation. The presence of PCDA in our hybrid formulations could be having an effect at multiple steps in our in vitro assay from (i) nanoparticle binding to cells to (ii) cellular uptake to (iii) intracellular release of cytotoxic payload. This last step in particular may be rate limiting. The roughly 50-fold difference in IC50 between free doxorubicin and conventional liposomal doxorubicin seen in our osteosarcoma cell lines is consistent with that found in previously published model systems [22]. Others have shown that this is primarily due to delayed release of free drug from the endocytic compartment of cells that have taken up liposomal doxorubicin [30].

Evaluating the stability of doxorubicin drug containment within the HPLN versus conventional PEG-liposomes showed that there was a statistically significant increase in doxorubicin release from the HPLN over time. Furthermore, this enhanced drug release was accentuated under acidic conditions mimicking the receptor-mediated endocytic environmental conditions of late endosomes and lysosomes. It is tempting to hypothesize that the PCDA lipids may enhance the release of doxorubicin from HPLNs that have been taken up by osteosarcoma cells. Given their differences in molecular structure, it is highly likely that microsegregation occurs between PCDA lipids and phospholipid molecules on the surface of HPLNs. Evidence found in published studies with similar mixtures of longer chain diacetylene lipids and shorter chain phosphatidylcholine lipids suggests that a phase separation occurs between the lipid types [31]. It is possible that these PCDA lipid islands could serve as destabilization points that could enhance drug release when exposed to intracellular environments.

The creation of an osteosarcoma-targeted doxorubicin loaded HPLN (α-AL-HPLN/Dox) resulted in a 2-fold increase in cytotoxicity over the untargeted HPLN/Dox and a 12-fold increase in cytotoxicity over the conventional PEG-liposomal formulation in the HOS and KHOS240s osteosarcoma cell lines. These results suggest that ALCAM targeting in osteosarcoma adds an incremental therapeutic effect. Interestingly, in the MNNG-HOS cell line the α-AL-HPLN/Dox had an even greater increase (23-fold) in cytotoxicity over the PEG-liposomal formulation. The MNNG-HOS cell line has high expression levels of the multidrug resistant protein 1 (MDR1) conferring chemotherapeutic resistance to doxorubicin [32]. The increased sensitivity of the MNNG-HOS chemoresistant cell line to the α-AL-HPLN/Dox formulation over the conventional formulation points to a therapeutic effect that may overcome multidrug resistance. We can hypothesize that the targeting and improved sustained drug release characteristics of our α-AL-HPLN/Dox formulation may help to bypass or overwhelm the drug efflux proteins mediating chemoresistance thereby improving cytotoxicity.

In conclusion, we have found a novel surface marker in human osteosarcoma, ALCAM, which we have used to specifically target osteosarcoma cells with a novel engineered drug-loaded hybrid PLN formulation anti-ALCAM immunoconjugate. These α-AL-HPLN/Dox particles show improved cytotoxicity over a conventional untargeted PEG-liposomal doxorubicin formulation and show promise as a potential therapeutic delivery platform in osteosarcoma. This new liposomal nanoparticle formulation is particularly attractive for its potential therapeutic application in resistant, refractory, and metastatic osteosarcoma where current standard systemic untargeted chemotherapy is generally not efficacious and prognosis is dismal. Furthermore, the bystander and dose-limiting side effects of systemic chemotherapy are substantial. Thus far this formulation has only been tested in tissue culture based assays, so further assessment in tumorigenic animal models is a crucial next step to validate these findings. These experiments are currently under way.

Acknowledgments

Dr. N. Federman is supported by a St. Baldrick's Career Development Award and STOP Cancer Research Development Award. Dr. C. T. Denny and Dr. N. Federman are supported by a Hyundai Hope on Wheels Grant. Funding was also provided by NIH Grants U54 CA19367, P50 CA092131, and P30 CA016042. Dr. J. Nagy is supported by a National Science Foundation SBIR Phase I Grant IIP-1143342.

References

[1] A. G. Huvos, *Bone Tumors: Diagnosis, Treatment, and Prognosis*, WB Saunders, Philadelphia, Pa, USA, 1991.

[2] D. C. Dahlin and K. K. Unni, "Osteosarcoma of bone and its important recognizable varieties," *American Journal of Surgical Pathology*, vol. 1, no. 1, pp. 61–72, 1977.

[3] J. G. Gurney, A. R. Swensen, and M. Bulterys, "Malignant bone tumors," in *Cancer Incidence and Survival Among Children and Adolescents: United States SEER Program 1975–1995*, pp. 99–110, SEER program, National Cancer Institute, Bethesda, Md, USA, 1999.

[4] K. A. Janeway and H. E. Grier, "Sequelae of osteosarcoma medical therapy: a review of rare acute toxicities and late effects," *The Lancet Oncology*, vol. 11, no. 7, pp. 670–678, 2010.

[5] A. Puri, K. Loomis, B. Smith et al., "Lipid-based nanoparticles as pharmaceutical drug carriers: from concepts to clinic," *Critical Reviews in Therapeutic Drug Carrier Systems*, vol. 26, no. 6, pp. 523–580, 2009.

[6] L. H. Lindner and M. Hossann, "Factors affecting drug release from liposomes," *Current Opinion in Drug Discovery and Development*, vol. 13, no. 1, pp. 111–123, 2010.

[7] T. L. Andresen, S. S. Jensen, and K. Jørgensen, "Advanced strategies in liposomal cancer therapy: problems and prospects of active and tumor specific drug release," *Progress in Lipid Research*, vol. 44, no. 1, pp. 68–97, 2005.

[8] T. M. Allen, "Ligand-targeted therapeutics in anticancer therapy," *Nature Reviews Cancer*, vol. 2, no. 10, pp. 750–763, 2002.

[9] G. W. M. Swart, "Activated leukocyte cell adhesion molecule (CD166/ALCAM): developmental and mechanistic aspects of cell clustering and cell migration," *European Journal of Cell Biology*, vol. 81, no. 6, pp. 313–321, 2002.

[10] S. F. Ofori-Acquah and J. A. King, "Activated leukocyte cell adhesion molecule: a new paradox in cancer," *Translational Research*, vol. 151, no. 3, pp. 122–128, 2008.

[11] G. Kristiansen, C. Pilarsky, C. Wissmann et al., "ALCAM/CD166 is up-regulated in low-grade prostate cancer and progressively lost in high-grade lesions," *Prostate*, vol. 54, no. 1, pp. 34–43, 2003.

[12] J. A. King, S. F. Ofori-Acquah, T. Stevens, A. B. Al-Mehdi, O. Fodstad, and W. G. Jiang, "Activated leukocyte cell adhesion molecule in breast cancer: prognostic indicator," *Breast Cancer Research*, vol. 6, no. 5, pp. R478–R487, 2004.

[13] B. Liu, A. Roth, D. C. Drummond et al., "Anti-CD166 single chain antibody-mediated intracellular delivery of liposomal drugs to prostate cancer cells," *Molecular Cancer Therapeutics*, vol. 6, no. 10, pp. 2737–2746, 2007.

[14] R. E. Bruehl, F. Dasgupta, T. R. Katsumoto et al., "Polymerized liposome assemblies: bifunctional macromolecular selectin inhibitors mimicking physiological selectin ligands," *Biochemistry*, vol. 40, no. 20, pp. 5964–5974, 2001.

[15] J. M. D. T. Nelissen, R. Torensma, M. Pluyter et al., "Molecular analysis of the hematopoiesis supporting osteoblastic cell line U2-OS," *Experimental Hematology*, vol. 28, no. 4, pp. 422–432, 2000.

[16] J. Olmsted and M. Strand, "Fluorescence of polymerized diacetylene bilayer films," *Journal of Physical Chemistry*, vol. 87, no. 24, pp. 4790–4792, 1983.

[17] H. Eckhardt, D. S. Boudreaux, and R. R. Chance, "Effects of substituent-induced strain on the electronic structure of polydiacetylenes," *The Journal of Chemical Physics*, vol. 85, no. 7, pp. 4116–4119, 1986.

[18] B. Liu, F. Conrad, A. Roth, D. C. Drummond, J. P. Simko, and J. D. Marks, "Recombinant full-length human IgG1s targeting hormone-refractory prostate cancer," *Journal of Molecular Medicine*, vol. 85, no. 10, pp. 1113–1123, 2007.

[19] K. E. McCabe, B. Liu, J. D. Marks, J. S. Tomlinson, H. Wu, and A. M. Wu, "An engineered cysteine-modified diabody for imaging activated leukocyte cell adhesion molecule (ALCAM)-positive tumors," *Molecular Imaging and Biology*, vol. 14, no. 3, pp. 336–347, 2012.

[20] B. Barat, S. J. Sirk, K. E. McCabe et al., "Cys-diabody quantum dot conjugates (ImmunoQdots) for cancer marker detection," *Bioconjugate Chemistry*, vol. 20, no. 8, pp. 1474–1481, 2009.

[21] G. Haran, R. Cohen, L. K. Bar, and Y. Barenholz, "Transmembrane ammonium sulfate gradients in liposomes produce efficient and stable entrapment of amphipathic weak bases," *Biochimica et Biophysica Acta*, vol. 1151, no. 2, pp. 201–215, 1993.

[22] T. Ishida, M. J. Kirchmeier, E. H. Moase, S. Zalipsky, and T. M. Allen, "Targeted delivery and triggered release of liposomal doxorubicin enhances cytotoxicity against human B lymphoma cells," *Biochimica et Biophysica Acta*, vol. 1515, no. 2, pp. 144–158, 2001.

[23] M. A. Bowen and A. Aruffo, "Adhesion molecules, their receptors, and their regulation: analysis of CD6-activated leukocyte cell adhesion molecule (ALCAM/CD166) interactions," *Transplantation Proceedings*, vol. 31, no. 1-2, pp. 795–796, 1999.

[24] L. C. L. T. van Kempen, J. J. van den Oord, G. N. P. van Muijen, U. H. Weidle, H. P. J. Bloemers, and G. W. M. Swart, "Activated leukocyte cell adhesion molecule/CD166, a marker of tumor progression in primary malignant melanoma of the skin," *American Journal of Pathology*, vol. 156, no. 3, pp. 769–774, 2000.

[25] E. C. M. Cabral, P. T. Hennies, C. R. D. Correia, R. L. Zollner, and M. H. A. Santana, "Preparation and characterization of diacetylene polymerized liposomes for detection of autoantibodies," *Journal of Liposome Research*, vol. 13, no. 3-4, pp. 199–211, 2003.

[26] D. A. Sipkins, D. A. Cheresh, M. R. Kazemi, L. M. Nevin, M. D. Bednarski, and K. C. P. Li, "Detection of tumor angiogenesis in vivo by $\alpha(v)\beta 3$-targeted magnetic resonance imaging," *Nature Medicine*, vol. 4, no. 5, pp. 623–626, 1998.

[27] C. Guo, S. Liu, Z. Dai, C. Jiang, and W. Y. Li, "Polydiacetylene vesicles as a novel drug sustained-release system," *Colloids and Surfaces B*, vol. 76, no. 1, pp. 362–365, 2010.

[28] A. Puri, A. Yavlovich, A. Singh, and R. Blumenthal, "A novel class of photo-triggerable liposomes containing DPPC:DC 8,9PC as vehicles for delivery of doxorubcin to cells," *Biochimica et Biophysica Acta*, vol. 1808, no. 1, pp. 117–126, 2011.

[29] Z. Li, G. T. Qin, R. M. Xia et al., "Partially polymerized liposomes: stable against leakage yet capable of instantaneous release for remote controlled drug delivery," *Nanotechnology*, vol. 22, no. 15, Article ID 155605, 2011.

[30] D. E. L. de Menezes, M. J. Kirchmeier, J. F. Gagne, L. M. Pilarski, and T. M. Allen, "Cellular trafficking and cytotoxicity of anti-CD19-targeted liposomal doxorubicin in B lymphoma cells," *Journal of Liposome Research*, vol. 9, no. 2, pp. 199–228, 1999.

[31] J. M. Moran-Mirabal, D. M. Aubrecht, and H. G. Craighead, "Phase separation and fractal domain formation in phospholipid/diacetylene-supported lipid bilayers," *Langmuir*, vol. 23, no. 21, pp. 10661–10671, 2007.

[32] C. M. F. Gomes, H. van Paassen, S. Romeo et al., "Multidrug resistance mediated by ABC transporters in osteosarcoma cell lines: mRNA analysis and functional radiotracer studies," *Nuclear Medicine and Biology*, vol. 33, no. 7, pp. 831–840, 2006.

Hindawi Publishing Corporation
Sarcoma
Volume 2012, Article ID 764796, 7 pages
doi:10.1155/2012/764796

Research Article

Low-Grade Central Osteosarcoma: A Difficult Condition to Diagnose

A. M. Malhas, V. P. Sumathi, S. L. James, C. Menna, S. R. Carter, R. M. Tillman, L. Jeys, and R. J. Grimer

The Royal Orthopaedic Hospital Oncology Service, Royal Orthopaedic Hospital, Bristol Road South, Birmingham B31 2AP, UK

Correspondence should be addressed to A. M. Malhas, amarmalhas@hotmail.com

Received 13 March 2012; Accepted 23 May 2012

Academic Editor: H. Gelderblom

Low-grade central osteosarcoma (LGCO) is a rare variant of osteosarcoma which is difficult to diagnose. If not treated appropriately, the tumour can recur with higher-grade disease. We reviewed our experience of this condition to try and identify factors that could improve both diagnosis and outcome. 18 patients out of 1540 osteosarcoma cases (over 25 years) had LGCO (1.2%). Only 11 patients (61%) were direct primary referrals. Almost 40% (7 of 18) cases were referred after treatment elsewhere when the diagnosis had not been made initially and all presented with local recurrence. Of the 11 who presented primarily, the first biopsy was diagnostic in only 6 (55%) cases. Of the remaining cases, up to three separate biopsies were required before a definitive diagnosis was made. Overall survivorship at 5 years was 90%. 17 patients were treated with limb salvage procedures, and one patient had an amputation. The diagnosis of LGCO remains challenging due to the relatively nonspecific radiological and histological findings. Since treatment of LGCO is so different to a benign lesion, accurate diagnosis is essential. Any difficult or nondiagnostic biopsies of solitary bone lesions should be referred to specialist tumour units for a second opinion.

1. Introduction

Osteosarcoma is the most common nonhaematological malignant primary bone tumour [1]. Low-grade central osteosarcoma (LGCO), or intraosseous well-differentiated osteosarcoma, is a rare intramedullary bone producing tumour [2]. It accounts for only 1-2% of all osteosarcomas and has an equal gender distribution [2, 3]. The majority of cases occur in the second and third decades [3].

The difficulty in the management of patients with LGCO is diagnosing the disease. Radiologically, the appearance of LGCO is often confused with that of fibrous dysplasia [4–8]. On histological examination, LGCO consists of fibroblastic stroma of variable cellularity and variable amounts of osteoid productions that are characteristically arranged in parallel seams resembling the pattern seen in parosteal osteosarcoma. The cytologic atypia is minimal, and occasional mitotic figures are always present [9]. There are some overlapping features with benign lesions such as fibrous dysplasia and desmoplastic fibroma [7, 9, 10]. The key feature to distinguish LGCO from the benign mimics is to identify permeative growth pattern [9]. Diagnosis is difficult on biopsy samples particularly when only the fibroblastic stroma devoid of cytologic atypia is represented and when permeation of the host trabecular bone cannot be demonstrated. LGCO can be confused radiologically with fibrous dysplasia, desmoplastic fibroma, nonossifying fibroma, osteoblastoma, and aneurysmal bone cysts [3–9, 11]. It is therefore vital to combine both radiological and histological findings to raise the suspicion of LGCO.

In a large case series of 80 patients from the Mayo clinic, the type of surgical management was found to strongly influence the prognosis [3]. Treatment by curettage or marginal excision was found to almost always result in local-recurrence. In those that recurred, 15% returned as a high-grade osteosarcoma with a worse subsequent prognosis. However, wide local resection with clear margins was found to have a much better prognosis [3]. The prognosis for LGCO has been reported to be over 90% at both 5 and 10 years [11, 12].

LGCO is therefore an eminently treatable malignant condition with a high chance of cure with appropriate

treatment. If the diagnosis is not made in an accurate and timely fashion, then the prognosis is significantly worse, with a high chance of recurrence, often of higher-grade disease. The aim of this study was to review our experience of diagnosis and treatment of LGCO and highlight features that may lead to earlier diagnosis and, subsequently, better treatment and outcomes.

2. Methods

A retrospective review was performed of the orthopaedic oncology unit's database covering all patients referred from 1986 to the present (25 years). Inclusion criteria were a definitive histological diagnosis of LGCO at some stage in the patient's management. The identified cohort was then reviewed for age, gender, site, biopsy type, initial diagnosis, definitive diagnosis, treatment, outcome, and morbidity. All available radiographs, MRI, and bone scintigraphy were then reviewed by a dedicated musculoskeletal radiologist and the histological features reviewed by an experienced musculoskeletal pathologist.

All needle and open biopsy samples were fixed in formalin and decalcified in 5% nitric acid as per local guidelines. The diagnosis of LGCOS was made on histological examination of haematoxylin and eosin-stained sections. Diagnosis was made on the presence of lesional tissue consisting of spindle cell proliferation, presence of cytologic atypia, presence of mitotic figures, and well-formed matrix production. Identification of permeative growth pattern was helpful in making a definitive diagnosis.

Survival time was analysed using the Kaplan-Meier survival method, and statistical significance was tested with the Mantel-Cox log-rank test.

3. Results

A total of 18 patients were identified with a definitive diagnosis of LGCO from a total of 1540 patients with osteosarcoma. LGCO therefore constituted a 1.2% subset of osteosarcoma. The gender distribution was equal with 9 males and 9 females and a mean age of 37 years at diagnosis (range 11 to 72 years) (Table 1).

The majority of the tumours occurred in the lower limb (15 cases: 10 femur, 4 tibia, 1 os calcis). There were two cases in the pelvis and one in the upper limb. The most common presentation was that of pain in the affected limb, usually described more as a background ache than as a severe pain. The average duration of symptoms prior to presentation was over 2 years (range 4 weeks to 10 years).

A review of the available radiographic imaging studies revealed that the mean length of the tumour at presentation was 9.9 cm (range 8–14). The appearance was predominantly mixed, sclerotic, and lytic, with well-defined margins. Two lesions were found to be lytic lesions with internal trabeculations. The majority of lesions were central although 3 were subarticular and 1 lesion was diaphyseal (final lesion was in the pelvis). Seven of the cases demonstrated a clear cortical breach, 2 were expansile, and only two lesions were contained. All but three demonstrated extraosseous masses on radiographs.

On review of the MRI investigations, the tumour predominantly showed intermediate signal on T1 with one case being of low signal. All cases demonstrated an extraosseous mass and cortical disruption on MRI. Cystic areas were present centrally within the tumour in 4 cases with a single tumour showing fluid levels. All of the bone scans available for review demonstrated that the lesions gave a "hot" signal.

Eleven of the patients were referred directly to the unit for full diagnostic evaluation. The remaining 7 patients were investigated and treated elsewhere prior to referral.

Of the 11 patients referred directly to the unit, a primary diagnosis of LGCO was made in only 6 of the cases at the initial biopsy (3 open biopsy and 3 needle biopsy). A further 5 patients required multiple biopsies (2-3) to make the correct diagnosis. Three patients required 3 or more biopsies before the final diagnosis was made. In all three cases, the initial samples lacked cytologic atypia and a permeative pattern and the lesions appeared benign. In one case, the definitive diagnosis was made on the final resection sample. In the other two cases, the radiological studies were highly suggestive of a malignant lesion and so only after repeated sampling did the histology demonstrate enough cell atypia and infiltration to confirm a diagnosis of LGCO.

In one case, a diagnosis of fibrous dysplasia was given by a nonspecialist histopathologist and the patient was referred to the unit for curettage. The curetted material then gave a diagnosis of LGCO. In another case, an initial biopsy suggested atypical fibrous dysplasia which was treated with bisphosphonates. When the pain did not improve, he underwent curettage and again the histology showed atypical fibrous dysplasia. The lesion healed and the pain resolved, but within 15 months the pain recurred and he underwent a further curettage with a fibula strut graft and DHS fixation of the femoral neck. Histology, again, did not give a diagnosis of LGCO but rather fibrous dysplasia and osteofibrous dysplasia. The pain never resolved after this operation and gradually the fibula graft was resorbed. At that stage, a proximal femoral replacement was carried, removing all of the previous abnormal area. Analysis of the whole specimen confirmed the diagnosis of LGCO but with some areas now showing progression to intermediate grade.

Of the 7 patients who were initially treated elsewhere, all had an initial diagnosis other than LGCO. These included fibrous lesion (benign and malignant), giant cell tumour, and simple bone cyst. Seven patients had undergone prior curettage (with or without bone graft or cement), and one had a local excision (see Figure 1 for an example). All of these patients presented with local recurrence, with two cases revealing a higher-grade osteosarcoma, but review of the original histology confirmed the retrospective diagnosis of LGCO.

Four patients sustained a pathological fracture. Only one occurred prior to biopsy, the rest occurred prior to definitive surgery.

For definitive treatment, 14 patients underwent wide local excision and endoprosthetic replacement, 3 patients

Table 1: Patients within the case series.

Gender	Age at diagnosis	Site	Primary or secondary referral	Previous diagnosis	Previous treatment	Definitive treatment	Chemotherapy	Followup (months)	Outcome
M	11	Mid tibia	Secondary	Osteoma	Excision "osteoma," recurred after 1 year	Resection and fibula graft		186	No evident disease
F	14	Distal femur	Primary		None	EPR	Thought to be high grade	48	No evident disease
M	18	Distal femur	Secondary	Mesenchymoma	Curettage, LR after 4 yrs, recuretted, further LR 3yrs	EPR	90	No evident disease	
M	19	Distal femur	Secondary	Cyst	Curettage and bone graft of fracture through cyst, LR 9 months	EPR	170	No evident disease	
F	19	Distal femur	Secondary	Desmoplastic fibroma	Curettage and fixation of fracture through cyst, LR 3 yrs, recuretted and bone grafted, slowly progressive lesion for 4 years	EPR	24	No evident disease	
M	29	Proximal femur	Primary	Atypical fibrous dysplasia	Curettage, then curettage and bone graft	EPR	As higher grade on LR	4	No evident disease
M	32	Distal femur	Secondary	Cyst	Curettage of cyst, uncertain diagnosis, post op RT, recurrence after 7 yrs as high grade tumour, lung met	EPR and thoracotomy	As higher grade on LR	7	No evident disease
F	33	Ilium	Primary		None	Excision		10	No evident disease
M	37	Proximal humerus	Secondary	Giant cell tumour	Curettage, LR 9 months with high-grade areas	EPR	As higher grade on LR	212	No evident disease
F	38	Ilium	Primary	Atypical fibrous dysplasia	Biopsy x3	Resection and fibula graft	As higher grade on LR	57	LR 14 months, high grade, chemo and amputation, alive with metastases
F	43	Distal femur	Primary		None	EPR		64	No evident disease
F	45	Proximal tibia	Primary	MFH	None	EPR	As initially thought be MFH	109	LR and metastatic disease at 102 months died 109 months
F	47	Distal femur	Primary	Fibroosseous lesion	Biopsy x2, curettage and cementation	EPR	Thought to be high grade after curettage	16	No evident disease
M	48	Calcaneum	Primary		None	Amputation	60	No evident disease	
M	51	Distal femur	Primary		None	EPR	156	No evident disease	
F	54	Distal femur	Primary		None	EPR	171	No evident disease	
M	55	Proximal tibia	Primary	Fibrous dysplasia	Biopsy suggested fibrous dysplasia, curettage led to diagnosis	EPR	144	No evident disease	
F	72	Proximal tibia	Secondary	Cyst? malignant	Curettage and bone graft of cyst, recurred 40 yrs later as LGCO	EPR	52	No evident disease	

Key: RT: radiotherapy, CT: chemotherapy, LR: local recurrence, EPR: endoprosthesis, MFH: malignant fibrous histiocytoma, LGCO: low-grade central osteosarcoma.

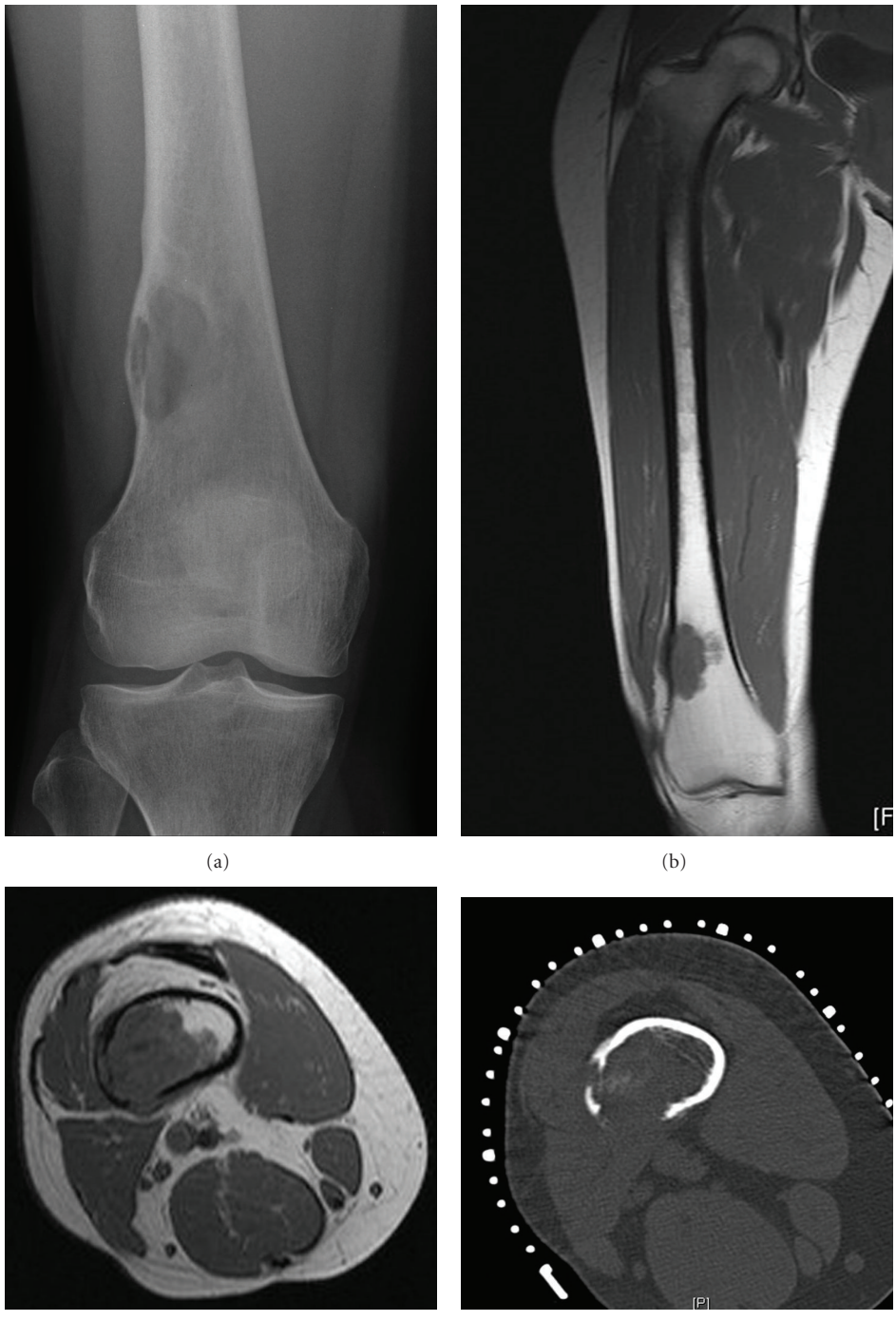

Figure 1: Radiological appearance of LGCO: a patient presented with a solitary bone lesion (a). MRI demonstrated an intermediate signal intraosseous lesion relative to skeletal muscle on T1 (b) and (c). CT-guided biopsy was undertaken (d). The lesion had marked cortical involvement with extraosseous expansion.

underwent wide local excision and fibular grafting, and one patient underwent an amputation. The patient requiring an amputation was referred for initial investigation of a calcaneal lesion and only required one biopsy.

A total of seven patients received chemotherapy. Of the seven, four had chemotherapy when they presented with high-grade recurrence and three patients received it as they were thought to have higher-grade tumours but had the diagnosis revised to LGCO following the histology of the resection specimen.

Of the 7 patients who presented with local recurrence, two had high grade tumours (one probably radiation

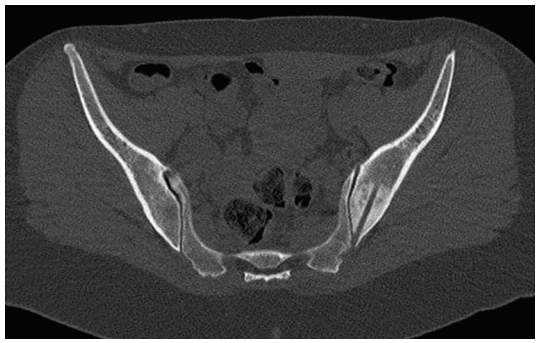

Figure 2: CT scan of the pelvis of a 33-year-old lady with low back pain. X-rays were normal as was an MRI of the lumbar spine. A bone scan showed increased activity in the ilium adjacent to the sacroiliac joint, and a CT showed a dense sclerotic lesion. This would have been typical for fibrous dysplasia radiologically, but this did not explain the pain. CT-guided needle biopsy confirmed the diagnosis. This CT image clearly shows the lesion and the path of the biopsy.

induced). All of these patients remain alive and well following further treatment.

Of the 9 patients treated primarily at our unit, there were two recurrences, both as higher-grade tumours. One patient developed local recurrence and lung metastases 102 months following wide resection and a tibial endoprosthetic replacement. Histology confirmed high-grade recurrence, and the patient had palliative treatment, surviving for 7 months. The second patient presented with a pelvic lesion after 18 months of hip pain. Two CT-guided biopsies were inconclusive, suggestive of fibrous dysplasia or a low-grade sarcoma (Figure 2). Surgery was undertaken in the form of an en bloc excision of the ilium and reconstruction with fibula grafts. The specimen confirmed a 15×11 cm LGCO. The patient made a good recovery. At 15 months, two small nodules were noted in the scar. Excision revealed a locally recurrent high-grade osteosarcoma. Despite chemotherapy and a hindquarter amputation (giving clear margins with 60% necrosis), the patient developed lung metastasis and further local recurrence at 1 year. The patient was then treated with palliative radiotherapy for symptomatic relief.

As mentioned above, a total of four of the nine patients who developed recurrence of the tumour had reoccurred with a higher grade to tumour (44%) and three of the nine patients developed metastases (33%).

Disease-free survival for all patients was found to be over 90% at 5 years and 80% at 10 years. When the survival rates were compared between patients referred directly and those treated elsewhere, the survival curves were not statistically significant.

4. Discussion

This study demonstrates that several biopsies may be required to make the diagnosis of LGCO, even in a primary referral. This case series demonstrates that only 6 of the 11 patients treated primarily had a clear diagnosis of LGCO after the first biopsy. Seven patients presented with local recurrence of a LGCO that was not initially identified. Even in a specialist tumour centre, biopsy yielded an initial diagnostic rate of only 55% (6 out of 12). Five patients required multiple biopsies before the definitive diagnosis was made. The literature is in agreement with our findings, demonstrating the difficulty in recognising such a rare variant of osteosarcoma [11, 12]. Any unit seeing and treating patients with bone abnormalities must be aware of this potential diagnosis and have a high level of suspicion in any case where the clinical appearances, the radiology, and the histology do not match.

The classical case is therefore a patient in the 2nd or 3rd decade with a long history of mild-to-moderate pain who is found to have a fibroosseous lesion, frequently with a cystic component and in whom the histology is similar to but not typical of fibrous dysplasia.

Larger biopsies and second opinions may then clarify the diagnosis and ensure that appropriate treatment is carried out.

The radiological features are variable, as reported in the literature and confirmed in this series, demonstrating a mixed lytic and blastic appearance. Andresen et al. [13] described four radiographic patterns of low-grade central osteosarcomas (in 70 cases): (1) lytic with varying amounts of thick and coarse trabeculation (31%); (2) predominantly lytic with few thin, incomplete trabecula (30%); (3) densely sclerotic (24%); (4) mixed lytic and sclerotic (14%) [14]. By contrast, in this series, the majority of radiographic patterns were in keeping with mixed lytic and sclerotic lesions (80% type 4). Only two cases were found to be lytic with trabecular patterning (type 1 and 2).

Histologically, LGCO is a malignant intramedullary bone forming neoplasm in which the tumour is so well differentiated that it is difficult to make a diagnosis of malignancy on limited biopsy samples [7, 10] (see Figure 3). These tumours are usually well-demarcated firm whitish masses that have a fibrous whorled appearance, typically centred in the medullary cavity of metaphysis or meta-diaphyseal region. Microscopically, the tumours are hypo-cellular consisting of interlacing fascicles of spindle cells. These spindle cells show mild cytological atypia, and mitotic activity is low. The tumour typically has a permeative growth pattern entrapping native bony trabeculae. There may be an associated soft tissue mass. The matrix produced is variable and well differentiated. On a biopsy material, LGCOS can be indistinguishable from benign fibrous lesions such as desmoplastic fibroma and fibrous dysplasia. LGCO is distinguished from benign tumours by virtue of its infiltrative growth pattern. Desmoplastic fibroma lack matrix production and fibrous dysplasia does not exhibit a permeative growth pattern. Histologically LGCO has morphological similarities with parosteal osteosarcoma which is a surface tumour. Therefore, close clinical radiological correlation is necessary in distinguishing these entities.

Immunohistochemical stains murine double-minute type 2 (MDM2) and cyclin-dependent kinase 4 (CDK4) are presenting viable solutions to aid the histological diagnosis of LGCO. Because these patients were treated prior to

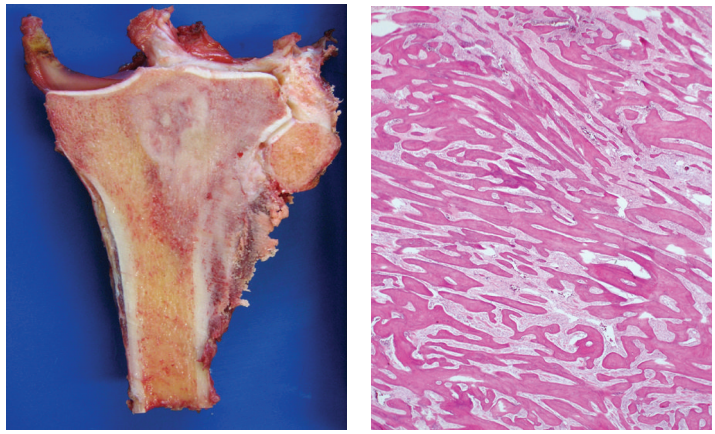

(a) (b)

Figure 3: A histological example of LGCO: macroscopically, this greyish white tumour shows extramedullary extension (a). Microscopic review (haematoxylin and eosin stain, ×10) demonstrates (b): low-grade intramedullary osteosarcoma, which consists of parallel seams surrounded by spindle cell stroma which exhibits very minimal cytological atypia. The appearances are similar to parosteal osteosarcoma or fibrous dysplasia, for which it can be mistaken.

the availability of these recent advances, none of the patients in this study underwent these immunohistochemical tests. Cyclin-dependent kinase 4 (CDK4) and murine double-minute type 2 (MDM2) genes (found on chromosome 12 q13–15) are genetic markers with a reported sensitivity of 89–100% and a specificity of 97–100% (when either one or both genes are present) in various studies [15, 16]. However, given the rarity of LGCO [2, 3], the clinical, radiological, and histological picture is still vital in raising the suspicion of LGCO in order to apply these tests.

The imaging appearance of LGCO can often be indistinguishable from fibrous dysplasia or parosteal osteosarcoma [3, 9, 17]. Even in the setting of an experienced multidisciplinary meeting, the diagnosis is often difficult to make but should be considered if atypical "fibrous dysplasia" is encountered.

It is generally accepted that management is with surgical excision with wide margins and that chemotherapy and radiotherapy are not routinely required. The main risk is from local recurrence which may be delayed (5 to 10 years or more) and is related to inadequate excision margins [3, 11, 12]. The literature suggests that 15% of recurrences will be high grade [3], but in this series four of the nine patients with recurrence had higher grade tumours (44%) and three of these four patients developed metastases, although only one patient has died thus far.

Although this series contains only 18 patients, the sample size reflects the rarity of the disease. Patients referred secondarily to our centre may also suffer from a selection bias for inclusion. Despite these limitations, the study does demonstrate clearly the difficulty in arriving at the correct diagnosis and it also demonstrates the relatively good long-term prognosis when treated appropriately. When compared to other survivorship series within the literature, the study size is comparable. The largest historical series was published by Kurt et al. [3] over 20 years ago. Although it encompassed 80 cases, only 15 of those patients had follow-up data. The largest survivorship series was published by Choong et al. [11] in 1996 reporting on 20 patients. There are many smaller case reports within the literature dealing with a handful of patients [4–8].

This study has highlighted the problems previously reported by others of difficulty in obtaining the diagnosis and has confirmed that wide excision and limb salvage in most cases have a high chance of cure. We strongly recommend that any bone lesion proving difficult to diagnose should be referred to a specialist centre for evaluation. If a needle biopsy is not diagnostic, then a generous open biopsy has been found to be invaluable. It is important to take part of the lesion and, most importantly, a part of the margin with the adjacent, normal bone to offer the best chance of obtaining a diagnosis. As demonstrated, even a negative biopsy result should be treated with caution and referred to a tertiary sarcoma centre (with an experienced specialist pathologist). Once diagnosed, treatment is relatively easy with complete excision. The prognosis once treated appropriately is excellent.

References

[1] G. A. Marulanda, E. R. Henderson, D. A. Johnson, G. D. Letson, and D. Cheong, "Orthopedic surgery options for the treatment of primary osteosarcoma," *Cancer Control*, vol. 15, no. 1, pp. 13–20, 2008.

[2] B. T. Rougraff, "Variants of osteosarcoma," *Current Opinion in Orthopaedics*, vol. 10, no. 6, pp. 485–490, 1999.

[3] A. M. Kurt, K. K. Unni, R. A. McLeod, and D. J. Pritchard, "Low-grade intraosseous osteosarcoma," *Cancer*, vol. 65, no. 6, pp. 1418–1428, 1990.

[4] S. Kenan, D. T. Ginat, and G. C. Steiner, "Dedifferentiated high-grade osteosarcoma originating from low-grade central osteosarcoma of the fibula," *Skeletal Radiology*, vol. 36, no. 4, pp. 347–351, 2007.

[5] M. J. Franceschina, R. C. Hankin, and R. B. Irwin, "Low-grade central osteosarcoma resembling fibrous dysplasia. A report of

two cases," *American Journal of Orthopedics*, vol. 26, no. 6, pp. 432–440, 1997.

[6] H. R. Park, W. W. Jung, P. Bacchini, F. Bertoni, Y. W. Kim, and Y. K. Park, "Ezrin in osteosarcoma: comparison between conventional high-grade and central low-grade osteosarcoma," *Pathology Research and Practice*, vol. 202, no. 7, pp. 509–515, 2006.

[7] A. Kumar, M. K. Varshney, S. A. Khan, S. Rastogi, and R. Safaya, "Low grade central osteosarcoma—a diagnostic dilemma," *Joint Bone Spine*, vol. 75, no. 5, pp. 613–615, 2008.

[8] K. Muramatsu, T. Hashimoto, S. Seto, T. Gondo, K. Ihara, and T. Taguchi, "Low-grade central osteosarcoma mimicking fibrous dysplasia: a report of two cases," *Archives of Orthopaedic and Trauma Surgery*, vol. 128, no. 1, pp. 11–15, 2008.

[9] F. Bertoni, P. Bacchini, N. Fabbri et al., "Osteosarcoma. Low-grade intraosseous-type osteosarcoma, histologically resembling parosteal osteosarcoma, fibrous dysplasia, and desmoplastic fibroma," *Cancer*, vol. 71, no. 2, pp. 338–345, 1993.

[10] K. K. Unni, D. C. Dahlin, R. A. McLeod, and D. J. Pritchard, "Intraosseous well differentiated osteosarcoma," *Cancer*, vol. 40, no. 3, pp. 1337–1347, 1977.

[11] P. F. M. Choong, D. J. Pritchard, M. G. Rock, F. H. Sim, R. A. McLeod, and K. K. Unni, "Low grade central osteogenic sarcoma. A long-term followup of 20 patients," *Clinical Orthopaedics and Related Research*, no. 322, pp. 198–206, 1996.

[12] R. M. Wilkins, J. W. Cullen, L. Odom et al., "Superior survival in treatment of primary nonmetastatic pediatric osteosarcoma of the extremity," *Annals of Surgical Oncology*, vol. 10, no. 5, pp. 498–507, 2003.

[13] K. J. Andresen, M. Sundaram, K. K. Unni, and F. H. Sim, "Imaging features of low-grade central osteosarcoma of the long bones and pelvis," *Skeletal Radiology*, vol. 33, no. 7, pp. 373–379, 2004.

[14] W. F. Enneking, "Endosteal osteosarcoma," in *Musculoskeletal Tumor Surgery*, vol. 2, pp. 1080–1090, Churchill Livingstone, New York, NY, USA, 1983.

[15] F. Dujardin, M. B. N. Binh, C. Bouvier et al., "MDM2 and CDK4 immunohistochemistry is a valuable tool in the differential diagnosis of low-grade osteosarcomas and other primary fibro-osseous lesions of the bone," *Modern Pathology*, vol. 24, no. 5, pp. 624–637, 2011.

[16] A. Yoshida, T. Ushiku, T. Motoi et al., "Immunohistochemical analysis of MDM2 and CDK4 distinguishes low-grade osteosarcoma from benign mimics," *Modern Pathology*, vol. 23, no. 9, pp. 1279–1288, 2010.

[17] M. Campanacci, F. Bertoni, R. Capanna, and C. Cervellati, "Central osteosarcoma of low grade malignancy," *Italian Journal of Orthopaedics and Traumatology*, vol. 7, no. 1, pp. 71–78, 1981.